TRANSCRIPTS FROM THE CIRCADIAN CLOCK

Telling Time and Season

Karl Brand

TRANSCRIPTS FROM THE CIRCADIAN CLOCK

Telling Time and Season

TRANSCRIPTEN VAN DE CIRCADIANE KLOK

Vertellen Tijd en Seizoen

PROEFSHRIFT

ter verkrijging van de graad van doctor aan de
Erasmus Universiteit Rotterdam
op gezag van de rector magnificus
Prof.dr. H.G. Schmidt
en volgens besluit van het College voor Promoties.

De openbare verdediging zal plaatsvinden op
woensdag 22 june 2011 om 9.30 uur

DOOR

Karl Brand
geboren te Hanover, Canada

PROMOTIECOMMISSIE

Promotoren: Prof.dr. G.T.J. van der Horst
                  Prof.dr. J.H.J. Hoeijmakers

Overige leden: Prof.dr. F.G. Grosveld
                  Prof.dr. S. Philipsen
                  Prof.dr. P.J. van der Spek

CONTENTS

"The Days Run Away Like Wild Horses Over The Hills" Charles Bukowski, 1969

I

INTRODUCTION

TABLE OF CONTENTS

1 BIOLOGICAL RHYTHMS

We all know it when we wake mere moments before an alarm clock is scheduled to wake us: our body clock made the alarm clock redundant. This phenomenon is driven by an endogenous timer known as the biological, or *circadian* clock. Each revolution of the Earth about its own axis produces periods of light and dark which define what we all experience as a 'day'. This profound cyclic variation in solar energy is responsible for driving the evolution of adaptive responses as early as 3.8 billion years ago (Ditty et al., 2003), as identified in the ancient freshwater cyanobacterium *Synechococcus elongatus* (Kondo et al., 1993). Since this time the circadian clock appears to have arisen independently in prokaryota and eukaryota (Young and Kay, 2001) underscoring the importance of the circadian clock for reproductive fitness under daily rhythmic environments (Woelfle et al., 2004; Johnson et al., 2008). In theory, a time keeper might have been needed to temporally segregate incompatible processes such as nitrogen fixation and photosynthesis which both occur in the same cell, e.g. in *Oscillatoria* (Stal and Krumbein, 1987). Or to hide cellular processes vulnerable to disruption by solar (i.e. UV) radiation like DNA replication in the night- to 'escape from light' (Darwin, 1868; Pittendrigh, 1993; Crosthwaite et al., 1997). Whatever the reason, their ubiquity within cells and across taxa suggests a clear advantage for life able to anticipate and coordinate internal biological processes to the daily light-dark cycle. 'Circadian' derives from the Latin *circa dies*, roughly translating to, 'approximately a day'. Careful consideration was given creating this term (Halberg et al., 1959): since daily endogenous rhythms are typically precise to the minute (Richter, 1968), but rarely exactly 24 hours. More often the internal or 'subjective day' of an organism is slightly faster or slower than 24 hours. In essence, circadian rhythms have been defined thus (Pittendrigh, 1960):

1. repeat once a day,
2. persist in the absence of environmental timing cues,
3. persist irrespective of temperature or temperature fluctuations, and
4. synchronize to local environmental timing cues.

The day is not the only cyclic variation in environmental conditions. Seasonal variation arises from the 23.44° tilt of the Earths axis from the plane of its rotation around the Sun combined with its annual solar orbit. This seasonal, or *circannual*, variation in day length and temperature brings with it a profound variation in resources needed to sustain life which is proportional to the distance biota are from the equator. As a circadian clock evolved to anticipate and adapt to daily changes, to segregate opposing or incompatible biological process like energy capture and energy expenditure, so too a circannual timer which is dependent on the circadian timer evolved to temporally segregate processes like reproduction to specific times of the year which maximizes reproductive success (Cooke, 1984; Bradshaw et al., 2004). The principles of the circadian clock defined above also apply to the circannual clock, namely self-sustainability and entrainment (Johnston, 2005). Under constant photoperiodic conditions circannual rhythms persist with a period of 9 – 15 months (Dawson, 2002). As such circannual rhythms are analogous in many ways

to circadian rhythms including their prevalence throughout nature, found in diverse taxa from rotifers, through plants to animals.

1.1 The history of circadian rhythms

The study of circadian rhythms is as old as science itself: Androsthenes of Thasos recorded the diurnal behavior of the Tamarind tree (*Tamarindus indica*) circa 4th century BC (Bretzl and Bretzl, H., 1903), but it was the French astronomer Jean-Jacques d'Ortous de Mairan who was credited with the first circadian experiment, wresting his gaze from the heavens briefly to observe heliotropes (*Mimosa pudica*) diurnally opening and closing their leaves in his basement, in constant darkness (De Mairan, 1729). The taxonomist Carolus Linnaeus designed the first biological clock based, naturally, on flowers to create the Horologium Florae or 'flower clock' which cycled by the daily opening and closing times for different flower species (Figure 1; Linnaeus, 1751) and whilst botanists recapitulated de Mairan's observations in plants (Duhamel du Monceau, 1758; Candolle, 1832). The evolutionary relevance of a circadian clock did not escape the notice of Charles Darwin and his son Sir Francis who found the internal daily rhythms of plants were heritable and perhaps selected for to avoid harmful solar radiation (Darwin, 1868). The Cold Spring Harbor Symposium of 1960 on 'Biological Clocks' was a defining moment in the study of circadian rhythms. Organized and attended by those pioneering the field, a blueprint was drawn up, carefully delineating circadian rhythms and distilled by Colin Pittendrigh (Pittendrigh,

Figure 1. Floral clock, *Horologium Florae*. Carolus Linnaeus recorded the flower opening and closing times of local flowering plants at different times throughout the day. Using this knowledge he designed a clock based on the sequential flower opening times with a precision of half an hour (1751).

1960) into a reference which remains in use today and summarized in the aforementioned four-point definition.

At the time two questions tantamount to progress remained unanswered - where is this 'clock' and what are its cogs made of? Discrete, central 'pacemakers' responsible for generating and synchronizing daily rhythms in behavior to local time were identified first in the pineal gland of birds (Gaston and Menaker, 1968) and the optic lobes of cockroaches (Nishiitsutsuji-Uwo and Pittendrigh, 1968) and finally, in the suprachiasmatic nuclei (SCN) of the mammal brain (Stephan and Zucker, 1972; Moore and Eichler, 1972). As to the cogs which compose the clock: a model positing gene expression as the basis of rhythm generation (Ehret and Trucco, 1967) was convincingly demonstrated in fruit flies, *Drosophila melanogaster*, harboring a *period* (*Per*) gene mutation (Reddy et al., 1984; Hardin et al., 1990) which became the darling model organism for unraveling the workings of the clock in organisms with complex behavior. Orthologous genes were subsequently identified in SCN neurons of hamsters (Ralph and Menaker, 1988) and ultimately across much of the animal kingdom (reviewed in (Dunlap, 1999).

1.2 Circadian Phenotypes

The study of circadian rhythms in mammals runs on rodents. With the invention of the wheel , specifically the *running wheel* (Richter, 1922), rodents provided free access to these devices display 'spontaneous running wheel activity', i.e. a propensity to engage the running wheel during most waking moments. When housed with rodents thus, and in combination with a device measuring the number of revolutions in time, they provide a precise assay of circadian locomotor activity; the essence of behavioral rhythms. Recorded over days, weeks or months, these daily recordings comprise an *actogram* (Figure 2A), which is typically 'double plotted' for clarity of complex rhythmic phenotypes. With a small logistic overhead, rodents in running wheels propelled the study of the mammalian clock forward, quickly hammering out the fundamentals of mammalian circadian behavior (Pittendrigh and Daan, 1976a; Daan and Pittendrigh, 1976a; Pittendrigh and Daan, 1976b, 1976c). Timing cues, or *zeitgebers* (German for 'time giver') are used by circadian clocks to synchronize, or *entrain* internal rhythms to external environmental time. Light is the primary zeitgeber in most mammals, although food (Richter, 1922; Stephan, 2002), temperature (Barrett and Takahashi, 1995) and social cues (Aschoff et al., 1971) are also effective, and occasionally dominant zeitgebers. As zeitgebers effectively 'set' the clock, this is used to define time within controlled circadian studies, eg. *zeitgeber time 0* (ZT0), refers to initiation of a time cue, which for light is the moment an animal is exposed to first daily light, analogous to dawn in 'real-life'. For nocturnal rodents, ZT0 or 'lights on' is a cue for activity cessation and sleep (*activity offset*), and 'lights off', typically ZT12 in a 12 hour light, 12 hour dark (LD 12:12) light regime commonly used, the daily cue for *activity onset*. Various light schedules, intensities and brief pulses were used extensively to impinge on the central pacemaker to understand SCN functioning, which until its genetic interrogation, was the most effective tool available to probe this 'black box'. In the absence of light, or any other daily time cues (*constant conditions)*, an animal's daily rhythm is determined solely by the endogenous
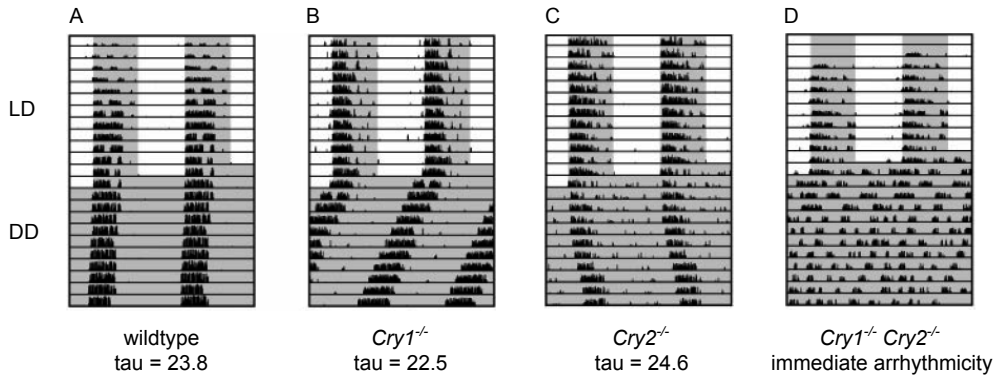
A   B   C   D

LD

DD

| wildtype | Cry1^-/- | Cry2^-/- | Cry1^-/- Cry2^-/- |

wildtype
tau = 23.8

Cry1^-/-
tau = 22.5

Cry2^-/-
tau = 24.6

Cry1^-/- Cry2^-/-
immediate arrhythmicity

Figure 2. Actograms of wildtype and Cryptochrome deficient mice. A wild type animal shows normal daily running period with slightly less than 24 hour endogenous rhythms (A). *Cry1^-/-* mutant animals show faster than normal endogenous daily rhythms (B). *Cry2^-/-* mutants conversely display a slower than normal endogenous rhythm (C). *Cry1^-/-* and *Cry2^-/-* double knockout mutant animals immediately lose behavioral rhythms under constant conditions where running wheel rhythms under LD likely arise solely as a result of 'masking' by light. LD refers to a daily light regime of 12 hours light, 12 hours dark. DD refers to a light regime of constant darkness. Grey shading indicates periods of darkness. Vertical lines represent number of wheel rotations per two minutes, i.e. periods of activity.

clock c.q. its *circadian time* (CT); referred to as 'free-running'. By convention (Winfree, 2001), when free running under constant conditions, activity offset corresponds to CT0 or *subjective dawn,* and CT12 to activity onset or *subjective dusk*. Obviously in studies where photoperiod is altered this convention breaks down. To this end an alternative nomenclature, *external time* (ExT) and *internal time* (InT)*,* was proposed (Daan et al., 2002) and is defined by ExT0 corresponding to mid-night, and ExT12 to mid-day.

Constant conditions provide a unique window into an animal's characteristic endogenous rhythm, determined by genes alone. The endogenous rhythm of the popular lab mouse (*Mus musculus*) in constant darkness cycles with ~23.5 hour period, golden hamsters (*Mesocricetus auratus*) ~24.0 hours (Daan and Pittendrigh, 1976b) and humans, by comparison, ~24.2 hours (Czeisler et al., 1999). This is also the gold standard for identifying a role for a gene in the core clock from which self-sustained daily rhythms arise. Mutations affecting core clock genes typically alter free-running rhythms. For example, faster rhythms are observed in mice deficient for the *Cryptochrome, Cry1*, slower rhythms in *Cry2* deficient mice (Figures 2B and C), and no daily rhythms at all in animals lacking both *Cry1* and *Cry2* genes (Figure 2D). The latter observation well demonstrates that CRY proteins are indispensable for circadian rhythms (Horst et al., 1999; Yagita et al., 2001). Observing running wheel behavior during transition to altered light regimes (akin to transmeridian jet travel), or with the even more exotic protocols employing pulses of light characterized the fundamental properties of entrainment (Daan and Pittendrigh, 1976a; Schwartz and Zimmerman, 1990). Exposure to light in the late evening, around ZT/CT22 induces an advance in subsequent cycles, thus referred to as a *phase advance* (Figure 3A). Conversely, exposure in the early evening, around ZT/CT14 induces a *phase delay,* with an animal's internal cycle delaying in the following days (Figure 3B). Plotting the quantitative

A

B
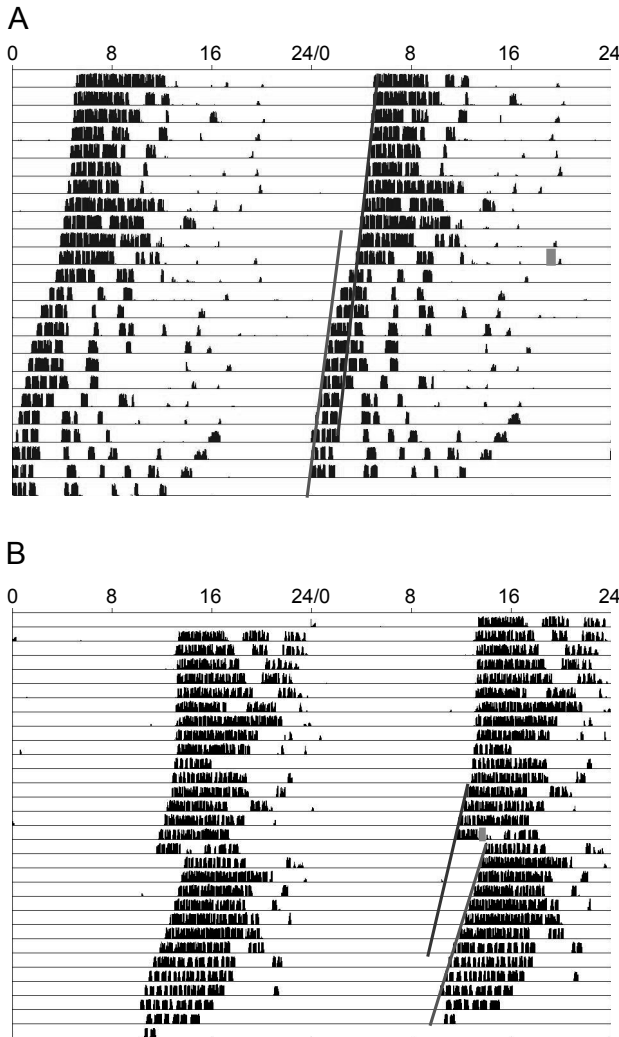
Figure 3. Daily locomotor rhythms for mice exposed to phase-shift inducing light pulse. Representative activity record (actogram) for a mouse exposed to a light pulse delivered during the late subjective evening (CT22), indicated by grey rectangle. Subsequent daily rhythms begin earlier, indicated by light grey line, compared to daily rhythms before the dark pulse, indicated by light grey line. This is referred to as a phase advance (A). Conversely, a light pulse delivered during the early subjective evening (CT14) results in a phase delay. Subsequent onset of activity commences later in the subsequent days compared to rhythms prior to the light pulse (B). Black lines indicate the number of running wheel rotations per 2 minutes, i.e. periods of activity.

phase response, advances and delays, against the time of day the light pulse is delivered yields a *phase response curve* (PRC; Figure 4; Nelson and Takahashi, 1991; Pittendrigh, 1981). This sensitivity of the central pacemaker to light around dawn and dusk allows the fine tuning in anticipatory behavior, indeed entrainment under non-laboratory conditions, needed in a photoperiodically variable environment such as Earths.

1.3 Self-sustained oscillator

Circadian rhythms in cellular life as diverse as mold, insects and mammals arise from a self-sustaining molecular oscillator based on the 'central dogma' of molecular biology: DNA, transcribed to RNA, is translated to protein. Thus composed of sub-cellular components, it remained uncharacterized until the acceleration of molecular biology in the

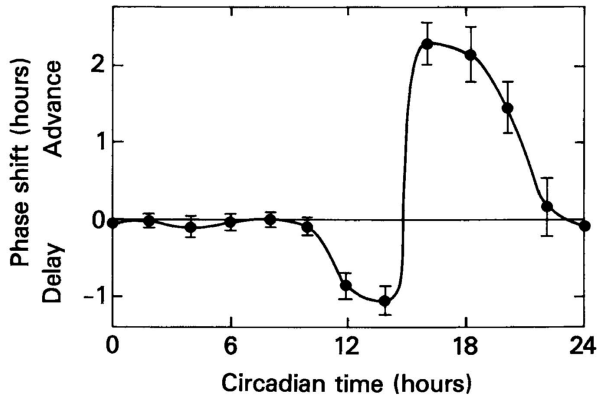**Figure 4. Phase response curve (PRC) to light for hamsters.** Animals were housed in constant conditions and received a single light pulse at indicated circadian times (CT) over the course of the subjective day. Light pulse received at CT14 elicit the maximum delay in internal rhythms of ~1hour, whilst light pulses received at CT16 produce the maximum phase advance (~2 hours). Although specific times of the day that elicit maximum phase responses vary, ±4 hours, and the extent of the response also varies, ±1 hour between organisms, the paradigm remains constant: light pulses delivered during early evening induce phase delays and when given during late evening a phase advance is effected. Reproduced with permission from Lowrey and Takahashi et al., 2004.

1970's when, armed with new understanding and tools to interrogate living cells, ushered in the 'transcription-translation feed-back loop' (TTFL) model now accepted as the basis of virtually all daily rhythms. This model describes an auto-regulatory feed-back loop beginning with the transcription of core clock genes, which, when translated to protein, 'feed-back' and directly regulate the expression of their own or other core clock genes thus closing the loop which takes about 24 hours (Dunlap, 1999; Bell-Pedersen et al., 2005).

The concept of a genetic basis of circadian timing was first seeded in plant (*Phaseolus coccineus*) studies (Bünning, 1936) but experimental support only emerged with the identification of fruit flies harboring a mutant copy of the *period* (*per*) gene. This remarkable work (Konopka and Benzer, 1971) identified three strains of flies with long (28 hours), short (19 hours) or no endogenous rhythms at all (arrhythmic), each induced by a mutation traced to the same X chromosomal locus they named *period* given its affect on the period length of the circadian clock- the first core clock gene identified. Similar observations made in mutant screens of red bread mold (*Neurospora crassa*) mapped mutant circadian phenotypes to the aptly named frequency (*frq*) locus (Feldman and Hoyle, 1973) further supported this, then radical, notion of a genetically based timing system. Years later, the wild type *period* gene was cloned and used to restore normal (24 hour) rhythmicity in *per* mutant flies (Bargiello et al., 1984; Reddy et al., 1984; Zehring et al., 1984). In 1990 Hardin et al. closed the loop for circadian rhythms by showing that the *D. melanogaster* PER protein is responsible for the cycling of its own *per* mRNA levels. This finding was swiftly recapitulated in *N. crassa* for *frq* (Aronson et al., 1994). The rapid advances made using these simple, fast-living genetic model organisms to uncover the mechanisms of a living circadian clock paved the way (and stole a little glory) for circadian research in mammals. The first core clock gene serendipitously identified in this class was named τ (*tau*), circadian jargon for period, given

that golden hamsters harboring the naturally occurring mutation at this locus showed a shortened endogenous period (Ralph and Menaker, 1988). In fact the gene responsible for this mutation, c̲asein k̲inase 1̲ epsilon (*CK1ε*), remained uncharacterized until Lowrey et al. (2000) confirmed mutations in this gene cause the *tau* phenotype. In this time a forward genetics screen using the mutagenic compound N-e̲thyl-N-n̲itroso̲urea (ENU) to induce mutations in populations of several inbred laboratory mouse strains (*Mus musculus*) was undertaken and the progeny systematically screened for altered circadian phenotypes (Vitaterna et al., 1994). This heroic effort identified the ostentatiously named c̲ircadian l̲ocomotor o̲utput c̲ycles k̲aput or *Clock* gene, wherein mutations result in a lengthened period of more than 24.5 hours in both heterozygous and homozygous mice, and arhythmicity in homozygous mutant mice under constant conditions. Characterization of *Clock* revealed that it is a basic helix-loop-helix (bHLH)-containing transcription factor, whose mRNA and protein are constitutively expressed (Antoch et al., 1997; King et al., 1997), and, along with the rhythmically expressed b̲rain and m̲uscle A̲rnt-l̲ike protein-1 (*Bmal1*; also known as *Arntl*, *Mop3* or *Arnt3*) whose levels peak mid to late evening, participates directly in activating the expression of other core clock genes *Cryptochrome*, *Period* and others, thus constituting a 'positive limb' of the core clock TTFL. The first naturally occurring clock gene variant identified in humans, *hPer2*, orthologous to the fruit fly *period* gene arrived late (Toh et al., 2001). A cohort of individuals with familial advanced sleep phase syndrome (FASPS), characterized by a 4-hour advance in their sleep-wake cycle and referred to as 'morning larks' given their propensity to rise earlier than most people (Jones et al., 1999), were used to pinpoint the *hPer2* loci.

More genes (described below) were subsequently identified in the core clock loop and also in secondary loops which modulate the core clock function (reviewed in Lowrey and Takahashi, 2004) reinforcing and expanding the TTFL model for self-sustained rhythm generation at its simplest, as in the cyanobacterium *Synechococcus elongatus* (Nakajima et al., 2005) to the most complex so far characterized- in mouse (reviewed in Bell-Pedersen et al., 2005; see Figure 5). Currently this model describes a core 'postive limb' composed of the above described CLOCK and BMAL1 proteins that heterodimerize via their P̲eriod A̲rnt S̲ingleminded (PAS) protein-protein interacting domains in the cytoplasm, translocate to the nucleus and bind cis-regulatory E-box enhancer sequences upstream of genes resulting in transcription of the respective gene (Gekakis et al., 1998; Hogenesch et al., 1998; Bunger et al., 2000). Core clock genes regulated by E-box elements include the *Period* (*Per1* and *Per2*) and *Cryptocrome* (*Cry1* and *Cry2*) genes (Albrecht et al., 1997; Horst et al., 1999) whose rhythmic mRNA and protein products peak around mid to late day, in antiphase with *Bmal1*. CLOCK/BMAL1 activate expression of *Cry1/2* and *Per1/2*, increasing mRNA levels and consequently protein levels in the cytoplasm. After posttranslational modifications including phosphorylation, CRY1/2 and PER1/2 dimerize, translocate into the nucleus and inhibit the transcriptional activity of CLOCK/BMAL1 bound to E-box elements present in *Per* and *Cry* (and other promoters) annulling the activation of *Cry1/2* and *Per1/2* expression and forming a negative feedback-loop, or the 'negative limb' of the core clock. This interference in turn relaxes the activation and expression of *Cry1/2* and *Per1/2*
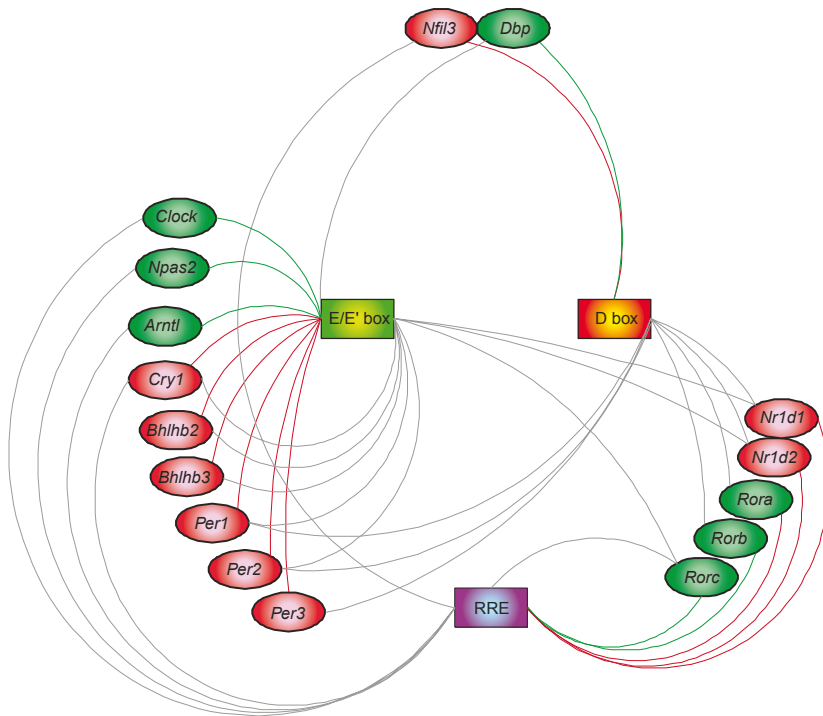
Figure 5. Core clock. This mechanism depends on a transcription-translation feedback loop to generate cell autonomous, approximate 24-hour rhythms. Shown here are the circuits composed of core clock transcriptional activators (green) and transcriptional repressors (red). Colored lines indicate binding to target regulatory elements for activation (green lines) or repression (red lines). Grey lines link regulatory elements (E/E' box, D box and RRE) to the genes regulated by them. E.g. *Cry1* contains both E/E' boxes and RRE elements and is a transcriptional repressor of genes containing E/E' box elements. Reprinted with permission from Ueda et al., 2005.

resulting in a reduction of mRNA and protein levels as the existing pools are degraded. As PER and CRY protein levels dwindle, regulated by ubiquitin ligase degradation complexes β-TrCP1 and FBXL3 (Busino et al., 2007; Godinho et al., 2007; Reischl et al., 2007; Siepka et al., 2007), so too the inhibition of CLOCK/BMAL1 subsides, thus allowing the cycle to restart with a periodicity of ~24 hours. Disruption of any one of these core clock genes alters circadian rhythms and/or entrainment and can result in complete loss of rhythmicity under constant conditions, as in the case of *Bmal1* knockout, *Per1/Per2* double knockout and *Cry1/Cry2* double knockout mice (Okamura et al., 1999; Horst et al., 1999; Vitaterna et al., 1999; Zheng et al., 1999; Bunger et al., 2000; Bae et al., 2001). A secondary negative feedback loop mediated by the orphan nuclear receptor *Rev-erbα*, also known as <u>n</u>uclear <u>r</u>eceptor <u>s</u>ubfamily <u>1</u>, group <u>D</u>, member <u>1</u> (*Nr1d1*), connects the 'positive limb' with the 'negative limb'. *Rev-erbα* expression is activated by CLOCK/BMAL1 heterodimers binding to E-box elements in its promoter. REV-ERBα binds another clock enhancer element, <u>r</u>etinoic acid related <u>o</u>rphan receptor <u>r</u>esponse <u>e</u>lement (RORE), in the *Bmal1* (and also *Cry1* and *Clock*) promoter(s) inhibiting the activation of expression of *Bmal1* by other

transcription factors, thus suppressing *Bmal1* expression (Preitner et al., 2002; Ueda et al., 2002b, 2005). Whilst *Rev-erbα* is not required for behavioral rhythms, it increases precision and stability of molecular rhythms and provides a second means of circadian regulation besides E-boxes via ROREs. Post translational modification of core clock proteins plays an important modulatory role in clock performance. All core clock proteins undergo phosphorylation at some point which contributes to either protein stability, degradation or nuclear retention, or even a combination of these as in the case of PER2 (Vanselow et al., 2006). Several of the <u>c</u>asein <u>k</u>inase <u>I</u> (*CKI*) family members, including CKIε and CKIδ, phosphorylate PER and CRY proteins and probably BMAL1 (Keesler et al., 2000; Vielhaber et al., 2000; Camacho et al., 2001; Lee et al., 2001; Akashi et al., 2002; Eide et al., 2002).

Although it was assumed for some time after the localization of the SCN that only SCN neurons were intrinsically rhythmic, it wasn't until the demonstration in cultured fibroblasts that the mechanism described above for rhythm generation was found in peripheral tissues to depend on the same core clock genes and proteins (Balsalobre et al., 1998; Yagita et al., 2001). In rat-1 fibroblasts a serum shock induces rhythmic output from the cell population in the core clock genes *Rev-Erbα*, <u>D</u> *site albumin promoter* <u>b</u>*inding* <u>p</u>*rotein* (*DBP*) and *rPer2*. With the power of single cell resolution, it was later established that a serum shock synchronizes the population of asynchronous cells rather than 'kick-starting' a non-ticking molecular oscillator (Nagoshi et al., 2004). Besides its convenient use in studying the molecular oscillator, these findings spurred research into peripheral oscillators. They are phase delayed compared to the SCN by 3 – 9 hours, depending on the peripheral tissue (Zylka et al., 1998) and although initially were not believed capable of sustaining rhythms for more than several days in *ex vivo* organ culture, they do in fact sustain rhythms for more than 20 days (Yamazaki et al., 2000; Abe et al., 2002; Yoo et al., 2004). Furthermore, these rhythms are sustained *in vivo* in behaviorally arrhythmic, SCN ablated animals, redefining the SCN as a coordinator of internal phase with the external environment, as opposed to the sole source of self-sustained rhythms (Yoo et al., 2004). For the large part the above described core clock mechanism utilizes the same genes for rhythm generation in peripheral tissues, although homologous genes fulfill tissue specific roles beyond the SCN. For example, <u>n</u>*euronal* <u>PAS</u> *domain protein 2* (*Npas2*) was observed to fulfill *Clock's* role in most brain regions and tissues beyond the central pacemaker (Reick et al., 2001). And whilst the TTFL model for rhythm generation, dependent on transcription and translation, is believed to be responsible for generating self-sustained rhythms in the majority of cell types in virtually all organisms, an alternative mechanism was unexpectedly identified in human erythrocytes (O'Neill and Reddy, 2011; O'Neill et al., 2011), in which peroxiredoxins demonstrate a ~24-hour redox cycle, which persist at least several days under constant conditions. These rhythms are entrainable by environmental stimuli and are temperature compensated, thus fulfilling the rules for a basic clock (O'Neill and Reddy, 2011).

1.4 Input

A circadian system, at its simplest consists of: (a) an input pathway for light or other time cues to (b), a self-sustained oscillator which generates and synchronizes rhythms to

the input signal, and (c) an output pathway coupling the synchronized rhythm to time dependent biochemical, physiological and behavioral processes (reviewed in Moore and Silver, 1998; Lowrey and Takahashi, 2004). In mammals, the structures which fulfill these functions are (a), the retina and retinohypothalamic tract (RHT), (b) the SCN and, (c) efferent and peptidergic signaling to other brain regions and peripheral organs and together constitute the central pacemaker responsible for adaptive circadian behavior in mammals.

As light is the primary zeitgeber in most mammals, unsurprisingly the eye was found to be the sole light sensing tissue reporting to the central pacemaker (Nelson and Zucker, 1981; Foster et al., 1991; Yamazaki et al., 1999). Intrinsically photosensitive retinal ganglion cells (ipRGC) of the inner plexiform layer (IPL) of the retina, which contain the photopigment melanopsin probably responsible for transducing luminescence information, directly impinge on the central pacemaker (Provencio et al., 2000; Berson et al., 2002; Hattar et al., 2002) and measure light brightness (Brown et al., 2011). Notably, there appears to be some functional redundancy between ipRGCs and the image forming cells of the retina, rods and cones, in resetting the clock (Hattar et al., 2003; Panda et al., 2003), and in image formation (Zaidi et al., 2007; Ecker et al., 2010). ipRGC efferents, comprising the RHT, carrying luminescence information by action potential, terminate directly on SCN neurons (Moore and Lenn, 1972), and other brain regions depending on such information (reviewed in Miller et al., 1996).

Action potentials of ipRGC's efferents induce the release of the neurotransmitters glutamate, sufficient alone to affect circadian rhythms (Hannibal, 2002), and also pituitary adenylyl cyclase activating peptide (PACAP) and substance P (SP), which modulate and augment glutamatergic signaling (Kim et al., 2001; Michel et al., 2006) across the synaptic cleft to retino-recipient neurons of the SCN. Post-synaptic N-methyl D-aspartate (NMDA) and α-amino-3-hydroxy-5-methyl-4-isoxazolepropionic acid (AMPA) receptors on SCN neurons, activated by glutamate, depolarize the membrane invoking a cascade of activity in SCN neurons analogous to long term potentiation (LTP) occurring in the hippocampus during learning and new memory formation (reviewed in Kandel, 2001): an influx of Ca^{2+} which activates kinases including calcium/calmodulin dependent protein kinase (CaMK), mitogen activated protein kinase (MAPK) and protein kinase A (PKA) that in turn activate cAMP response element binding (CREB) via phosphorylation. Activated CREB binds cAMP response elements (CREs) present in the promoter sequences of the *Period* clock genes, *Per1* and *Per2*, responsible for regulating expression (Travnickova-Bendova et al., 2002). Given that expression of *Per1* and *Per2* constitutes part of the temporal fabric that is the circadian clock, this pathway of zeitgeber (light) to the self-sustained oscillator (SCN neurons) has been ostensibly accepted as the input pathway to the clock and core mechanism by which the clock synchronizes to local time (Shigeyoshi et al., 1997; Shearman et al., 1997; Albrecht et al., 1997; Akiyama et al., 1999; Travnickova-Bendova et al., 2002).

1.5 Suprachiasmatic Nuclei

A pacemaker critical to maintaining behavioral rhythms was localized within the anterior hypothalamus of rodents (Richter, 1965) where autoradiographic tracing in rats

demonstrated direct projections to this region from the retina (Moore and Lenn, 1972; Hendrickson et al., 1972). These projections terminated at the SCN which was found to be responsible for maintenance of rhythms in key ablation studies (Stephan and Zucker, 1972; Moore and Eichler, 1972). The SCN demonstrate intrinsic rhythms in electrical firing rate both *in vivo*, and in *in vitro* organotypic slice cultures (Green and Gillette, 1982; Groos and Hendriks, 1982; Shibata et al., 1982) confirming its function as a pacemaker. The SCN were ultimately proven to be the source of behavioral rhythm generation in an extraordinary transplantation study: hamsters rendered arrhythmic by SCN ablation received a donor SCN which reinstated the same behavioral rhythm as that of the donor hamster (Ralph et al., 1990). This was later attributed to a diffusible signal reinstated by the donor SCN (Silver et al., 1996). Unequivocal isolation of the source of rhythms provided a focal point for circadian studies in mammals: intracellular dissection of the molecular oscillator and functional characterization of SCN physiology.

Mindful that the core clock genes underpinning rhythm generation were only beginning to emerge in fruit flies and fungi at the end of the previous millennium, the source of rhythm generation in mammals remained unclear. An important question thus confronted researchers as this point: do rhythms from the SCN arise as a function of the interaction between its neurons or collectively from its individual neurons (Moore and Silver, 1998)? Whilst a rhythm in membrane conductance observed in isolated neurons of the sea slug (*Bulla gouldiana*) central pacemaker provided compelling support for a cellular basis of rhythmicity in higher organisms (Michel et al., 1993), the finding that individual, dispersed SCN neurons were capable of self-sustained oscillation in culture (Welsh et al., 1995) advanced the question: to what degree do individual, self-sustained oscillators of the SCN interact to produce the rhythmic output of the SCN? A clue to approaching this question was provided by the unexpected finding that cultured fibroblasts are capable of rhythmic gene expression similar to SCN neurons and which later found to be self-sustained (Balsalobre et al., 1998; Yagita et al., 2001; Nagoshi et al., 2004; Welsh et al., 2004). If cultured fibroblasts show the same asynchronous, rhythmic behavior as cultured SCN neurons, then the distinguishing properties of pacemaker cells include (Welsh et al., 2010), (a) being retino-recipient, i.e. receive light, (input), (b) directly and indirectly coupled by gap junctions and synapses respectively (synchrony), and (c) produce a daily rhythm in firing rate (output). Whilst non-pacemaker cells receive an analogous circadian input, and deliver a circadian output, there is no evidence showing direct coupling between non-SCN cells. It is this property, coupling, that distinguishes the SCN as the pacemaker. Supported by simulation studies (Beersma et al., 2008), coupling is believed to underpin the SCN being (a) eminently entrainable (b) highly precise and (c) fault tolerant to boot (Liu et al., 2007).

1.5.1 Structure

The mouse SCN is embedded dorsally in the o̲ptic c̲hiasm (OC) and is composed of two oviform nuclei, each ~10,000 densely packed neurons, between which is the third ventricle (3V). Distinct subregions had already been implicated by the selective innervation of RHT afferents to the ventral SCN characterized during the pursuit of the central pacemaker's location (Hendrickson et al., 1972; Moore and Lenn, 1972). Immunohistochemistry, a then

new technique for visualizing specific cell contents or structures, immediately revealed an astonishing heterogeneity of neuropeptide content distribution in the SCN, generally recapitulated across rodent species (van den Pol and Tsujimoto, 1985; Cassone et al., 1988; Antle and Silver, 2005). Arginine vasopressin (AVP) expression was seen to be restricted to the dorsal/dorsal-medial SCN; vasoactive intestinal polypeptide (VIP) expression enriched in neurons of the ventral / ventral-lateral SCN and also evident at lower levels throughout the rat (*Rattus norvegicus*) SCN especially in fibers; and gastrin releasing peptide (GRP), mostly co-localized with VIP in rat and hamster but sandwiched between the VIP and AVP immunoreactive regions in mouse central SCN (Vandesande et al., 1975; Samson et al., 1979). These findings have been recapitulated and expanded to a plethora of other neuropeptides in rat, hamster, mouse and human SCN, by Robert Moore, Rae Silver and Lawrence Morin, cartographers of the mammalian pacemaker. They include gamma hydroxy butyric acid (GABA), calbindin (CALB), angiotensin II (ATII), met-enkephalin (mENK), galanin (GAL), calretinin (CALR), neurotensin (NT), neuropeptide Y (NPY), and 5-hydroxytryptamine (5HT; Card and Moore, 1984; Moore, 1992; Moga and Moore, 1997; LeSauter and Silver, 1998, 1999; Silver et al., 1999; Abrahamson and Moore, 2001; Morin et al., 2006; Morin, 2007). GABA in particular is expressed almost homogenously through the entire SCN (Strecker et al., 1997).

The regions delineated by neuropeptides, observed first in rat for VIP and AVP, prompted their naming as 'core' and 'shell' respectively (Moore, 1996), which becomes ambiguous when applied across species and for this reason some, including this thesis, avoid in preference for explicitly referring to a region by neuropetide content or by using anatomic terms, i.e., ventral and dorsal. Neuropeptide content generally reflects the functional difference between subregions given (a) the role of VIP in coupling between SCN neurons (Piggins et al., 1995; Harmar et al., 2002), (b) the innervation of these regions to other brain regions (Abrahamson and Moore, 2001), and (c) oscillator behavior (Yamaguchi et al., 2003; Quintero et al., 2003; Butler and Silver, 2009). However, resulting from a combination of oversimplification, terminology misuse- especially between species, and a lack of temporal and rostro-caudal neuropeptide content characterization, the value of investigating and inferring function based on neuropetide content alone has been diminished (reviewed in Morin, 2007). Keeping this in mind and focusing on the mid-rostro/caudal plane of the mouse SCN, AVP, VIP and GRP hitherto remain the most commonly used neuropeptides to subdivide the SCN into functionally different regions. These account for at least 20%, 10% and 5%, respectively, of the total neurons (Abrahamson and Moore, 2001), which combined is only 35% of the total; but at least in the mid-rostro/caudal plane they are clearly distributed across almost the entire SCN in near discrete expression patterns.

1.5.2 Function

Early attempts to characterize the basis of rhythms arising from the SCN employed electrophysiological techniques. *In vivo* studies in rats demonstrated spontaneous activity of individual SCN neurons with a consistent increase in activity upon retinal photic stimulation, which simultaneously validated RHT function in photic input (Mason and Lincoln, 1976; Nishino et al., 1976; Sawaki, 1977). These findings were extended in showing

a monotonic response of SCN electrical discharge to photic input (Groos and Mason, 1978) and most critically, by demonstrating a circadian rhythm in multi-unit SCN electrical discharge under constant conditions (Inouye and Kawamura, 1979). Recapitulation of these findings *in vitro* by recording SCN output from hypothalamic slices in culture convincingly demonstrated the innate rhythm generation by the SCN where multi-unit extracellular recordings of populations of neurons showed a peak in electrical discharge over the subjective night, and a trough throughout subjecting evening (Groos and Hendriks, 1982; Shibata et al., 1982). Although behavioral rhythms remain rhythmic in rodents where efferents have been severed or otherwise isolated (Silver et al., 1996; LeSauter and Silver, 1998), electrical output remains in use as a reliable readout of SCN function both *in vivo* and *in vitro* given its dependence on core clock gene expression (Albus et al., 2002; Nakamura et al., 2002). In particular, the flexibility to measure output from any number of neurons, from one to thousands deepened understanding how the SCN encodes day length by showing that electrical discharge from a large population of neurons reflects day length, but single unit discharge does not (VanderLeest et al., 2007). Intriguingly, these observations indicate coupling between neurons is altered between different photoperiods, as opposed to individual neuron discharge.

Elucidation of the molecular oscillator in mammals also yielded powerful new techniques for interrogating SCN function. Having discovered that individual SCN neurons in culture were capable of self-sustained rhythms in electrical discharge (Welsh et al., 1995) the field sought to understand how ~20,000 oscillators might integrate self-sustained rhythms with the afferent photic signal and other inputs to the SCN. Analysis of the molecular clock in the SCN *in vivo* revealed differences in core clock behavior between SCN subregions delineated by AVP, VIP and GRP neuropeptide content, in particular during re-entrainment and in response to phase resetting in early and late subjective evening. Studies in mice employing *in situ* hybridization (ISH) and immunohistochemistry (IHC) to visualize *Per1* mRNA and protein levels show immediate induction of mRNA and protein in the VIP enriched ventral subregion in response to light pulses given in early, mid or late subjective evening (Yan and Silver, 2002; Kuhlman et al., 2003) outpacing shifting behavioral rhythms in the case of early and late evening light pulses (Reddy et al., 2002). Intriguingly *Per2* shows a differential response to phase advance and phase delays with immediate induction in VIP enriched SCN in response to phase delay but not phase advance inducing light pulses. Surprisingly, neurons of the VIP enriched ventral region do not show robust rhythms, at least *in vivo* where *Per1/2* mRNA and protein show reduced amplitude in the absence of light (Yan et al., 1999; Karatsoreos et al., 2004). Rhythmic electrical output of the ventral SCN driven by the core clock and in phase with *Per* oscillations of the molecular oscillator, accelerates firing in response to phase advances and delays firing during phase delaying in light regimes (Albus et al., 2005). This sub-region, often referred to as the 'core' region of the SCN, appears to play a role in light reception. In targeted microlesions of the retino-recipient ventral region in hamsters, this region was found to be required for rhythm maintenance in constant darkness (Kriegsfeld et al., 2004).

Neurons of the dorsal-lateral region of the SCN, defined by AVP expression, are functionally distinguished from the 'core' region by (a) intrinsic rhythmicity of the *Period*

genes (Hamada et al., 2001, 2004), (b) sparse retinal innervation (Abrahamson and Moore, 2001), and (c) a delayed electrical (Albus et al., 2005) and transcriptional (Yan and Silver, 2002) response to phase shifting light pulses, especially phase advances. These observations indicate a rhythm maintenance role for the dorsal-lateral or 'shell' region, underscored by the finding that an animal's locomotor rhythms follow, *pari passu*, its mRNA rhythms of *Per1*, *Per2* and *Cry1* gene expression in the dorsal-medial, but not the ventral sub-region after phase advances and delays (Reddy et al., 2002).

The GRP specific expression of the central SCN region, although overlapping with VIP localization in ventral SCN, may be considered a third SCN 'sub-region' in its own right (Morin, 2007). Studies demonstrate a critical role for this subregion in the communication and gating of photic stimulus from ventral to dorsal subregions (Hamada et al., 2001; Karatsoreos et al., 2004). Mutant mice deficient for the *gastrin-releasing peptide receptor* (*Grpr*, also known as *bombesin receptor*) fail to phase delay upon administration of GRP in either early of late subjective evening in contrast to wild type mice which show a normal phase shift response (Aida et al., 2002). Furthermore, induction of *Per1/2* and *c-fos* was attenuated in GRP-R deficient animals whereas wild type mice show an immediate induction after GRP application in early and late evening akin to phase shifting light pulses. When the analogous region in hamsters, immunoreactive for CalB, is lesioned, but sparing the remainder of the (dorsal) SCN, animals lose overt rhythms under constant conditions (Kriegsfeld et al., 2004), suggesting a critical role for this region in pacemaker function besides entrainment.

The spatial overlap of GRP with VIP in the dorsal SCN is mirrored by a functional redundancy between these neuropeptides in signaling between SCN neurons: like GRP, VIP is rhythmically expressed, induces photic like phase shifts and binds cognate receptors within the SCN (reviewed in Vosko et al., 2007). Unlike GRP, the lack of its receptor, vasoactive intestinal peptide receptor 2 (VIPR2; also known as VPAC2) or the VIP neuropetide itself, results in near total loss of locomotor rhythms (Harmar et al., 2002; Colwell et al., 2003). VIPR2 expression is also more widespread in the SCN than GRP-R expression, present to a large degree in both VIP and AVP expressing SCN regions. This indicates VIP/VPAC2 contributes to coupling both within and between ventral and dorsal SCN (Kalló et al., 2004) and underscore its greater contribution to intra SCN signaling than that of GRP. Finally, that some SCN neurons of *Vip* and *Vipr2* deficient mice remain rhythmic and that a daily application of a VPAC2 agonist reinstated electrical rhythms of VIP deficient neurons, but not to *Vipr2* deficient neurons, demonstrates a critical role for VIP in synchronizing pacemaker neurons (Aton et al., 2005; Brown et al., 2005; Brown and Piggins, 2007; Hughes et al., 2008).

The ability to continuously monitor core clock behavior in the intact SCN over several days revolutionized the understanding of SCN function. Cultured SCN slices obtained from transgenic reporter mice expressing the luminescent fire fly protein luciferase (LUC) from the *Per1* promoter (Yamaguchi et al., 2003), or as a functional PER2-LUC fusion protein (Yan et al., 2007) allowed monitoring circadian clock performance with single cell resolution. Expression first peaks in the dorsomedial, periventricular region of the SCN and spreads, wave-like, ventrolaterally across the entire dorsal SCN, i.e., the 'shell'/

AVP expressing region; repeating every ~24 hours. Maintaining this coordination and spontaneous network oscillation is dependent on the neuronal action potential; blockade with tetrodotoxin (TTX, Yamaguchi et al., 2003) causes an overall loss of synchrony between neurons although individual neurons continue to oscillate.

1.6 Entrainment

The mechanism by which the central pacemaker synchronises or entrains to local time, at both the physiological and molecular level remains poorly understood. Although the pathway taken by photons into the core clock has been shown to occur via the glutamatergic mechanism described above, which directly regulates E-box containing genes including the core clock genes *Per1* and *Per2* (Doi et al., 2007), what is lacking is a thorough explanation of the phase response curve (Antle et al., 2007). GRP positive cells have been proposed to play a role in gating and GRP itself advanced as the signal mediating the output of these cells, conveying the rhythm tuning message in response to environmental time information received by the retino-recipient, VIP enriched dorsal SCN (Karatsoreos et al., 2004; Gamble et al., 2007). Strikingly similar to GRP in both localization and function, neuropeptide little SAAS (derived from ProSAAS and encoded by *Pcsk1n*) was identified in a mass-spectrometry screen of SCN neuropeptide content (Mzhavia et al., 2001; Atkins et al., 2010). Litte SAAS is implicated in downstream gating of light/glutamatergic signaling and mediating the effects of photic stimulus in early and late evening via a GRP and VIP independent circuit (Atkins et al., 2010).

1.7 Output

Communication of environmentally synchronized temporal information to every peripheral cell is part of the central pacemaker's function in coordinating internal rhythms (Yoo et al., 2004). This is achieved by direct efferent innervation of target brain nuclei and peripheral organs as well as peptidergically. In confirming the SCN as the locus of the central pacemaker (Silver et al., 1996), SCN grafts isolated by a membrane preventing fiber re-innervations with the host, but allowing diffusible molecules to pass was sufficient to drive locomotor and other rhythms, but not in endocrine systems, including gonad function or daily cortisol secretion (Lehman et al., 1987; Meyer-Bernstein et al., 1999). The humoral factors responsible for re-instating rhythms in membrane isolated SCN recipients are TGF-alpha, prokineticin-2 and cardiotrophin-like cytokine (CLC; Kramer et al., 2001; Cheng et al., 2002; Kraves and Weitz, 2006). These humoral factors are expressed by clock controlled genes (CCGs), genes with regulatory elements which are targets of the core clock proteins (Kumaki et al., 2008). Specifically, E/E'-box, D-box and ROREs regulatory sequences which are components of the core clock (Ueda et al., 2005) also present three distinct output options of the clock. AVP, VIP and GRP also represent CCGs given their function in intra-SCN synchrony and distal circadian control in the digestive system (Jin et al., 1999).

Autonomous output by SCN efferents primarily project to the paraventricular nuclei, via both the sympathetic and parasympathetic autonomous nervous system, which acts as an intermediary relay, projecting to the nucleus tractus solitarius and intermediolateral

column of the spinal cord. These nuclei in turn incorporate the circadian signal with other physiological input and project to and regulate liver and adrenal function which in turn regulate hormonal signals governing physiology (Kalsbeek et al., 2006). The regulation of melatonin is particularly relevant in circadian studies given that it is responsible for regulating the sleep-wake cycle and circadian behavioral rhythms (Bartness et al., 1993). The SCN conveys timing information to the pineal gland which in turn secretes melatonin directly in response to photic input received by the SCN, commencing around dusk (peak blood concentrations) and ending around dawn (Buijs and Kalsbeek, 2001).

1.8 Photoperiod

The number of hours of daylight experienced during a day, or *photoperiod* at any given position on Earth is a precise indicator of season. The capability of circadian timers to anticipate dawn and dusk implies the ability to encode photoperiod, which was proposed as a cue for plants and animals to synchronize their circannual clocks via the circadian machinery (Bünning, 1936; Pittendrigh and Minis, 1964). The photoperiodic cue alone is sufficient to time seasonal adaptive responses in most arthropods and short lived vertebrates (< 1 year), and is required for entrainment of an endogenous circannual timer in longer lived (> 1 year) deuterostomes (Gwinner, 1996). From their observations of entrainment and free-running under various light regimes in the white-footed mouse (*Peromyscus leucopus*), Pittendrigh and Daan, (1976) advanced a model which explained circadian phenomena and incorporated a mechanism co-opting photoperiod as a seasonal cue: two independent circadian oscillators, morning (*M*) and evening (*E*), which were 'mutually interacting but coupled separately to sunrise and sunset'. In golden hamsters SCN ablation results in complete loss of circannual rhythms (Stetson and Watson-Whitmyre, 1976; Rusak and Morin, 1976) suggesting a critical role for the SCN in the circannual clock. This raises the question whether the circadian timer doubles as the circannual timer.

There are studies implying the contra, that the SCN plays little role in encoding/decoding photoperiod or driving seasonal adaption. In animal models beyond the laboratory subject to strong, continuous seasonal pressure, there is evidence of co-evolution of the circannual timer with the circadian pacemaker. Here the circannual timer is dependent on the daily timer for day-length information, but with selection independently driven by seasonal and not daily pressure (reviewed in Bradshaw and Holzapfel, 2007). Studies in the domestic duck (decendants of *Anas platyrhynchos*) and starlings (*Sturnus vulgaris*) identified a central role for the hypothalamic-pituitary axis in which thyroid hormone plays a key role in decoding annual time and driving adaptive responses advantageous for reproduction (reviewed in Hanon et al., 2008). This has since been recapitulated for mammals in sheep, hamsters and mice (Reiter and Hester, 1966; Nicholls et al., 1988; Masumoto et al., 2010). In this classic scheme the SCN plays no larger role than the retina and RHT, i.e., relegated to a temporal luminescence recorder merely conveying the photoperiod message. The day length signal travels autonomically via the PVN of the hindbrain to the IML column of the spinal chord superior and cervical ganglion. Then peptidergically via norepinephrine to the pituitary where activated α and β-adrenergic receptors on the surface of pinealocytes

increase cytoplasmic cAMP. This in turn increases the catalytic activity of aralkylamine N-acetyltransferase, essential to melatonin synthesis (Arendt, 1998). This pathway yields a melatonin signal precisely reflecting the photoperiod, which the pituitary pars tuberalis (PT) uses as an input signal (Klosen et al., 2002) to decode photoperiod and drive adaptive responses. Here, melatonin synchronises expression of _eyes absent 3_ (_Eya3_) which together with _thyrotroph embryonic factor_ (_Tef_) activate expression of _thyroid stimulating hormone β_ (_TSHβ_) via the known circadian D-box regulatory element. _TSHβ_, required for photoperiodic adaptation (Nakao et al., 2008b, 2008a) as TSH, regulates type II and type III _deiodinase_ (_DIO2_ and _DIO3_) expression, the levels of which directly regulate the concentration of the active form of thyroid hormone, tri-iodothyronine, which drives the observed phenotypic seasonal changes, for example in gonads (T3, Nakao et al., 2008a; Dardente et al., 2010; Dupré et al., 2010; Masumoto et al., 2010).

Concerted attempts to clarify the extent to which the central pacemaker encodes and/or decodes photoperiod were in fact treasure hunts for _E_ and _M_ oscillators. The hunt found golden hamsters with a compelling demonstration of bimodal electrical discharge specifically around dawn and dusk from cultured _horizontally_ sliced SCN preparations (Jagota et al., 2000). Moreover these _E_ and _M_ like peaks were independently entrainable by the light pulse mimetic of glutamate application. The authors suggested this was probably due to the unconventional horizontal preparation isolating rostral and caudal SCN sub-regions from which the _E_ and _M_ oscillations might be generated. At this time, with a brand new molecular clock to re-consider existing circadian hypotheses, (Daan et al., 2001) advanced the proposition that the core clock molecular components, _Cry1_ and _Per1_, and _Cry2_ and _Per2_, might form the basis of _M_ and _E_ oscillators, respectively, rather than groups of SCN neurons. Studies recapitulating Jagota et al., (2000) intriguing findings failed to materialize. However, simulations of photoperiodic encoding by the SCN, as a consequence of the 'plasticity in its neuronal network' (Schaap et al., 2003) reignited a potential role for the SCN. The neuronal basis of photoperiod encoding via the _M_ and _E_ model was vindicated in fruit flies (Stoleru et al., 2004, 2005, 2007) and finally in mammals: _Per2_ showed differential phasing in the SCN under a long photoperiod between the rostral, peaking at dusk, and caudal hemisphere, peaking at dawn (Hazlerigg et al., 2005). More persuasive yet was the observation of electrical discharge from multiunit recordings of the SCN, under constant conditions which precisely reflected the prior photoperiod (VanderLeest et al., 2007) in the melatonin deficient C57BL6/J lab mouse. That this appeared to be a network phenomenon and not encoded by individual neurons, was compatible with the observations of (Hazlerigg et al., 2005). In combining _Per1_ with luciferase, (Inagaki et al., 2007; Naito et al., 2008) impressively demonstrated dusk and dawn phasing of _Per1_ in sub-populations of neurons within the rostral and caudal SCN. This single neuron resolution within the central pacemaker provides the strongest support to date for the _E_ and _M_ model of Daan and Pittendrigh (1973, reviewed in Meijer et al., 2010). That this was observed in melatonin deficient mice suggests there may be a prominent role for the SCN in encoding and driving seasonal responses besides or in addition to the established pathway via the PT.

2 TECHNOLOGY TO INTERROGATE THE MAMMALIAN CLOCK

2.1 Microarrays

The 2000's heralded the arrival of 'omics' technologies. The field of genomics, born with the completion of the draft sequence of the human genome (Venter et al., 2001; Lander et al., 2001), is concerned with the study of an orgasm's entire hereditary information, in contrast to the study of single or groups of related genes. Publication of the draft human genome coincided with the maturation of microarray technology (Velculescu et al., 1995; Schena et al., 1995; Lockhart et al., 1996; Eisen et al., 1998). Microarrays allow the simultaneous measurement of the expression of virtually every gene in the genome, which for humans, rodents and most mammals is ~30,000 (Blake et al., 2010). This technology, more than any other, accelerated the development of 'omics' methodologies, and drove the development of new tools to help scientists deal with the avalanche of data generated in genomics (global DNA in cells and tissue), transcriptomics (mRNA), proteomics (protein), metabalomics (metabolites) and more.

Given the source of circadian rhythms is dependent on transcription, the field was as quick as any to hop on the genomics bandwagon (Reviewed in Sato et al., 2003). Studies in plants and flies emerged first. In *Arabidopsis thaliana* about 2 – 6% of the genome is circadianly expressed, which mainly involves energy capture and protection from the Sun (Harmer et al., 2000; Schaffer et al., 2001) whilst in *D. melanogaster*, the ~2% of the genome showing daily expression in heads collected at time points over several days is associated with metabolism, immune response, proteolysis and photoreception (Claridge-Chang et al., 2001; Lin et al., 2002; McDonald and Rosbash, 2001; Ueda et al., 2002a). Importantly, these first studies were pioneering statistical methods to identify rhythmicity *en masse* for a large portion of the genome which depended mainly on classical time series statistics with methods to correct estimates of significance needed when iteratively repeating tests gene by gene, i.e. ~10,000 times. An algorithm developed specifically for circadian applications, CORCOS, based on goodness-of-fit of a temporal expression profile to a Sinus curve was a leap in circadian analytic power and was further refined in the seminal analysis of the mouse SCN and liver transcriptome by Panda et al., 2002. The powerful COSOPT algorithm efficiently uncovered ~330 daily cycling transcripts in each of the SCN and liver of which 28 were found to be common to both and assumed to play a role in the core clock oscillator and cell cycle. From these results the authors conclude that about 10% of the mammalian genome is circadianly expressed and that rate limiting, tissue specific biochemistry is controlled by the circadian clock. Despite the pivotal role of the SCN in synchronizing and coordinating circadian rhythms only one other circadian microarray study of the SCN has since been performed, finding 101 rhythmically expressed transcripts in the central pacemaker, of which only ~36 are common to both studies, although a similar proportion of genome was estimated to be rhythmic (Ueda et al., 2002a). A number of transcriptome studies have been performed since, examining various tissues including heart, lung, kidney, colon, adrenal, blood and bone (Kita et al., 2002; Storch et al., 2002; Oster et al., 2006; Zvonic et al., 2007; Hoogerwerf et al., 2008; Keller et al., 2009; Vasu et al., 2009) which deploy ever more sensitive statistical methods to

identify cycling transcripts from genomic data, including GeneCycle, CircWaveBatch and JTK_CYCLE amongst others (Wichert et al., 2004; Oster et al., 2006; Hughes et al., 2010).

2.2 Laser pressure catapult microscopy

The small size of the SCN presents the same challenge today for those who wish to study its inner workings as biologists have faced since ground glass was first focused on cells in 1665 (Hooke, 1665): to see is not necessarily to understand. And although current microscopes allow insight into structures smaller even than lights 400 nm wavelength, not only do we need a method to isolate sub-sets of SCN cells, but also a sufficiently sensitive assay for studying aspects of interest about the cells having attained them. Several methods have proven successful isolating specific cell subsets, such as 'laser capture microscopy' or LCM and 'flow cytometry'. LCM has several practical advantages over flow cytometry for the direct isolation of cells, obviating the need for time and resource intensive development of biological tools before isolation of cells of interest can begin. This approach combines the magnification power and resolution of modern microscopes with the precision of a laser to 'cut' and/or 'shoot' specimens from a surface, e.g. microscope slide, securely into a tube allowing the direct, rapid acquisition of virtually any biological structure observable under a microscope, including SCN subregions (Emmert-Buck et al., 1996). A more flexible and refined variant, 'laser pressure catapulting' (LPC), utilizes an ultrathin membrane to support tissue throughout the capture process (Böhm et al., 1997; Schuitze and Lahr, 1998). Having first prepared the tissue appropriately, e.g. using haematoxylin stained cryosections, the laser 'cuts' through both the tissue and supporting membrane without detectable heating or tissue damage and 'catapults' the free tissue into a tube for subsequent analyses (Micke et al., 2005; Liu, 2010). Given the need for a researcher to select the tissue of interest for isolation, no matter how clear the selection criteria (cellular morphology, fluorescence-tagged antibodies etc.) or precise the acquisition by laser, it is likely some tissue of interest will be missed and perhaps more problematic, tissue not intended for collection is acquired in error thus contaminating the sample. However the impracticality of generating transgenic mice or antibodies combined with the relative ease distinguishing these tissues by morphology made LPC the obvious choice for isolating SCN subregions by us and others (Porterfield et al., 2007).

3 SCOPE OF THIS THESIS

Enormous strides have been made in our comprehension of circadian clocks in mammals over the past two decades, particularly in the core clock molecular oscillator. And whilst the rhythmic behavior of the molecular oscillator in the SCN has been thoroughly examined under normal, long and short photoperiods, there remains a gap in our understanding of how the central pacemaker encodes and adjusts to different photoperiods. In this thesis we attempt to address this lack of knowledge by developing a method to examine the transcriptome of small populations of neurons within the SCN. We demonstrate its value by recapitulating previously identified biological markers whilst presenting novel makers for these SCN subregions. This technology was also used in a preliminary investigation of

light-resetting, to confirm transgene expression in a genetically engineered mouse, and to investigate differentially regulated biological themes in response to fasting and long term caloric restriction. Most prominently, we applied this technology to characterize the role rostral and caudal SCN play in encoding photoperiod. Our results show new insight into regulation of the SCN transcriptome by photoperiod.

BIBLIOGRAPHY

Abe, M., Herzog, E. D., Yamazaki, S., Straume, M., Tei, H., Sakaki, Y., Menaker, M., and Block, G. D. (2002). Circadian Rhythms in Isolated Brain Regions. The Journal of Neuroscience *22*, 350 -356.

Abrahamson, E. E., and Moore, R. Y. (2001). Suprachiasmatic nucleus in the mouse: retinal innervation, intrinsic organization and efferent projections. Brain Research *916*, 172-191.

Aida, R., Moriya, T., Araki, M., Akiyama, M., Wada, K., Wada, E., and Shibata, S. (2002). Gastrin-Releasing Peptide Mediates Photic Entrainable Signals to Dorsal Subsets of Suprachiasmatic Nucleus via Induction of Period Gene in Mice. Mol Pharmacol *61*, 26-34.

Akashi, M., Tsuchiya, Y., Yoshino, T., and Nishida, E. (2002). Control of intracellular dynamics of mammalian period proteins by casein kinase I epsilon (CKIepsilon) and CKIdelta in cultured cells. Mol. Cell. Biol *22*, 1693-1703.

Akiyama, M., Kouzu, Y., Takahashi, S., Wakamatsu, H., Moriya, T., Maetani, M., Watanabe, S., Tei, H., Sakaki, Y., and Shibata, S. (1999). Inhibition of Light- or Glutamate-Induced mPer1Expression Represses the Phase Shifts into the Mouse Circadian Locomotor and Suprachiasmatic Firing Rhythms. The Journal of Neuroscience *19*, 1115 -1121.

Albrecht, U., Sun, Z. S., Eichele, G., and Lee, C. C. (1997). A Differential Response of Two Putative Mammalian Circadian Regulators, mper1and mper2, to Light. Cell *91*, 1055-1064.

Albus, H., Bonnefont, X., Chaves, I., Yasui, A., Doczy, J., van der Horst, G. T. J., and Meijer, J. H. (2002). Cryptochrome-deficient mice lack circadian electrical activity in the suprachiasmatic nuclei. Curr. Biol *12*, 1130-1133.

Albus, H., Vansteensel, M. J., Michel, S., Block, G. D., and Meijer, J. H. (2005). A GABAergic Mechanism Is Necessary for Coupling Dissociable Ventral and Dorsal Regional Oscillators within the Circadian Clock. Current Biology *15*, 886-893.

Antle, M. C., and Silver, R. (2005). Orchestrating time: arrangements of the brain circadian clock. Trends in Neurosciences *28*, 145-151.

Antle, M. C., Foley, N. C., Foley, D. K., and Silver, R. (2007). Gates and Oscillators II: Zeitgebers and the Network Model of the Brain Clock. J Biol Rhythms *22*, 14-25.

Antoch, M. P., Song, E. J., Chang, A. M., Vitaterna, M. H., Zhao, Y., Wilsbacher, L. D., Sangoram, A. M., King, D. P., Pinto, L. H., and Takahashi, J. S. (1997). Functional identification of the mouse circadian Clock gene by transgenic BAC rescue. Cell *89*, 655-667.

Arendt, J. (1998). Melatonin and the pineal gland: influence on mammalian seasonal and circadian physiology. Rev Reprod *3*, 13-22.

Aronson, B. D., Johnson, K. A., Loros, J. J., and Dunlap, J. C. (1994). Negative feedback defining a circadian clock: autoregulation of the clock gene frequency. Science *263*, 1578-1584.

Aschoff, J., Fatranska, M., Giedke, H., Doerr, P., Stamm, D., and Wisser, H. (1971). Human Circadian Rhythms in Continuous Darkness: Entrainment by Social Cues. Science *171*, 213 -215.

Atkins, N., Mitchell, J. W., Romanova, E. V., Morgan, D. J., Cominski, T. P., Ecker, J. L., Pintar, J. E., Sweedler, J. V., and Gillette, M. U. (2010). Circadian Integration of Glutamatergic Signals by Little SAAS in Novel Suprachiasmatic Circuits. PLoS ONE *5*, e12612.

Aton, S. J., Colwell, C. S., Harmar, A. J., Waschek, J., and Herzog, E. D. (2005). Vasoactive intestinal polypeptide mediates circadian rhythmicity and synchrony in mammalian clock neurons. Nat Neurosci *8*, 476-483.

Bae, K., Jin, X., Maywood, E. S., Hastings, M. H., Reppert, S. M., and Weaver, D. R. (2001). Differential functions of mPer1, mPer2, and mPer3 in the SCN circadian clock. Neuron *30*, 525–536.

Balsalobre, A., Damiola, F., and Schibler, U. (1998). A Serum Shock Induces Circadian Gene Expression in Mammalian Tissue Culture Cells. Cell *93*, 929-937.

Bargiello, T. A., Jackson, F. R., and Young, M. W. (1984). Restoration of circadian behavioural rhythms by gene transfer in Drosophila. Nature *312*, 752-754.

Barrett, R. K., and Takahashi, J. S. (1995). Temperature compensation and temperature entrainment of the chick pineal cell circadian clock. The Journal of neuroscience *15*, 5681.

Bartness, T. J., Powers, J. B., Hastings, M. H., Bittman, E. L., and Goldman, B. D. (1993). The timed infusion paradigm for melatonin delivery: what has it taught us about the melatonin signal, its reception, and the photoperiodic control of seasonal responses? J. Pineal Res *15*, 161-190.

Beersma, D. G. M., van Bunnik, B. A. D., Hut, R. A., and Daan, S. (2008). Emergence of circadian and photoperiodic system level properties from interactions among pacemaker cells. J. Biol. Rhythms *23*, 362-373.

Bell-Pedersen, D., Cassone, V. M., Earnest, D. J., Golden, S. S., Hardin, P. E., Thomas, T. L., and Zoran, M. J. (2005). Circadian rhythms from multiple oscillators: lessons from diverse organisms. Nat Rev Genet *6*, 544-556.

Berson, D. M., Dunn, F. A., and Takao, M. (2002). Phototransduction by Retinal Ganglion Cells That Set the Circadian Clock. Science *295*, 1070 -1073.

Blake, J. A., Bult, C. J., Kadin, J. A., Richardson, J. E., Eppig, J. T., and the Mouse Genome Database Group (2010). The Mouse Genome Database (MGD): premier model organism resource for mammalian genomics and genetics. Nucleic Acids Research *39*, D842-D848.

Böhm, M., Wieland, I., Schütze, K., and Rübben, H. (1997). Microbeam MOMeNT: non-contact laser microdissection of membrane-mounted native tissue. Am J Pathol *151*, 63-67.

Bradshaw, W. E., Zani, P. A., and Holzapfel, C. M. (2004). Adaptation to temperate climates. Evolution *58*, 1748-1762.

Bradshaw, W. E., and Holzapfel, C. M. (2007). Evolution of Animal Photoperiodism. Annu. Rev. Ecol. Evol. Syst. *38*, 1-25.

Bretzl, H., and Bretzl, H. (1903). Botanische Forschungen des Alexanderzuges (Leipzig: Teubner).

Brown, T. M., Wynne, J., Piggins, H. D., and Lucas, R. J. (2011). Multiple hypothalamic cell populations encoding distinct visual information. J. Physiol. (Lond.) *589*, 1173-1194.

Brown, T. M., and Piggins, H. D. (2007). Electrophysiology of the suprachiasmatic circadian clock. Progress in Neurobiology *82*, 229-255.

Brown, T. M., Hughes, A. T., and Piggins, H. D. (2005). Gastrin-Releasing Peptide Promotes Suprachiasmatic Nuclei Cellular Rhythmicity in the Absence of Vasoactive Intestinal Polypeptide-VPAC2 Receptor Signaling. The Journal of Neuroscience *25*, 11155 -11164.

Buijs, R. M., and Kalsbeek, A. (2001). Hypothalamic integration of central and peripheral clocks. Nat Rev Neurosci *2*, 521-526.

Bunger, M. K., Wilsbacher, L. D., Moran, S. M., Clendenin, C., Radcliffe, L. A., Hogenesch, J. B., Simon, M. C., Takahashi, J. S., and Bradfield, C. A. (2000). Mop3 Is an Essential Component of the Master Circadian Pacemaker in Mammals. Cell *103*, 1009-1017.

Bünning, E. (1936). Die endogene Tagesrhythmik als Grundlage der photoperiodischen Reaktion. Ber. dtsch. bot. Ges *54*, 35.

Busino, L., Bassermann, F., Maiolica, A., Lee, C., Nolan, P. M., Godinho, S. I. H., Draetta, G. F., and Pagano, M. (2007). SCFFbxl3 controls the oscillation of the circadian clock by directing the degradation of cryptochrome proteins. Science *316*, 900.

Butler, M. P., and Silver, R. (2009). Basis of Robustness and Resilience in the Suprachiasmatic Nucleus: Individual Neurons Form Nodes in Circuits that Cycle Daily. J Biol Rhythms *24*, 340-352.

Camacho, F., Cilio, M., Guo, Y., Virshup, D. M., Patel, K., Khorkova, O., Styren, S., Morse, B., Yao, Z., and Keesler, G. A. (2001). Human casein kinase I[delta] phosphorylation of human circadian clock proteins period 1 and 2. FEBS Letters *489*, 159-165.

Candolle, A. P. de (1832). Physiologie végétale ou exposition des forces et des fonctions vitales des végétaux: pour servir de suite a lòrganographie végétale et dìntroduction a la botanique géographique et agricole (Béchet Jeune).

Card, J. P., and Moore, R. Y. (1984). The suprachiasmatic nucleus of the golden hamster: Immunohistochemical analysis of cell and fiber distribution. Neuroscience *13*, 415-431.

Cassone, V. M., Speh, J. C., Card, J. P., and Moore, R. Y. (1988). Comparative Anatomy of the Mammalian Hypothalamic Suprachiasmatic Nucleus. Journal of Biological Rhythms *3*, 71 -91.

Cheng, M. Y., Bullock, C. M., Li, C., Lee, A. G., Bermak, J. C., Belluzzi, J., Weaver, D. R., Leslie, F. M., and Zhou, Q.-Y. (2002). Prokineticin 2 transmits the behavioural circadian rhythm of the suprachiasmatic nucleus. Nature *417*, 405-410.

Claridge-Chang, A., Wijnen, H., Naef, F., Boothroyd, C., Rajewsky, N., and Young, M. W. (2001). Circadian regulation of gene expression systems in the Drosophila head. Neuron *32*, 657-671.

Colwell, C. S., Michel, S., Itri, J., Rodriguez, W., Tam, J., Lelievre, V., Hu, Z., Liu, X., and Waschek, J. A. (2003). Disrupted circadian rhythms in VIP- and PHI-deficient mice. Am J Physiol Regul Integr Comp Physiol *285*, R939-949.

Cooke, B. (1984). Factors Limiting the Distribution of the European Rabbit Flea, Spilopsyllus Cuniculi (Dale) (Siphonaptera), in Inland South Australia. Aust. J. Zool. *32*, 493-506.

Crosthwaite, S. K., Dunlap, J. C., and Loros, J. J. (1997). Neurospora wc-1 and wc-2: Transcription, Photoresponses, and the Origins of Circadian Rhythmicity. Science *276*, 763 -769.

Czeisler, C. A., Duffy, J. F., Shanahan, T. L., Brown, E. N., Mitchell, J. F., Rimmer, D. W., Ronda, J. M., Silva, E. J., Allan, J. S., Emens, J. S., et al. (1999). Stability, Precision, and Near-24-Hour Period of the Human Circadian Pacemaker. Science *284*, 2177 -2181.

Daan, S., Albrecht, U., Van der Horst, G. T. J., Illnerová, H., Roenneberg, T., Wehr, T. A., and Schwartz, W. J. (2001). Assembling a Clock for All Seasons: Are There M and E Oscillators in the Genes? Journal of Biological Rhythms *16*, 105 -116.

Daan, S., and Pittendrigh, C. S. (1976a). A Functional analysis of circadian pacemakers in nocturnal rodents II. The Variability of Phase Response Curves. Journal of Comparative Physiology A: Neuroethology, Sensory, Neural, and Behavioral Physiology *106*, 253-266.

Daan, S., and Pittendrigh, C. S. (1976b). A functional analysis of circadian pacemakers in nocturnal rodents III. Heavy Water and Constant Light: Homeostasis of Frequency ? J. Comp. Physiol. *106*, 267-290.

Daan, S., Merrow, M., and Roenneberg, T. (2002). External time--internal time. J. Biol. Rhythms *17*, 107-109.

Dardente, H., Wyse, C. A., Birnie, M. J., Dupré, S. M., Loudon, A. S. I., Lincoln, G. A., and Hazlerigg, D. G. (2010). A Molecular Switch for Photoperiod Responsiveness in Mammals. Current Biology *20*, 2193-2198.

Darwin, C. (1868). The Power of Movement in Plants. Physiologie Végétale, 199–205.

Dawson, A. (2002). Photoperiodic control of the annual cycle in birds and comparison with mammals. Ardea *90*, 355–367.

Ditty, J. L., Williams, S. B., and Golden, S. S. (2003). A CYANOBACTERIAL CIRCADIAN TIMING MECHANISM. Annu. Rev. Genet. *37*, 513-543.

Doi, M., Cho, S., Yujnovsky, I., Hirayama, J., Cermakian, N., Cato, A. C. B., and Sassone-Corsi, P. (2007). Light-Inducible and Clock-Controlled Expression of MAP Kinase Phosphatase 1 in Mouse Central Pacemaker Neurons. Journal of Biological Rhythms *22*, 127-139.

Duhamel du Monceau, M. (1758). La physique des arbres: où il est traité de l'anatomie des plantes et de l'économie végétale: pour servir d'introduction au traité complet des bois & des forests: avec une dissertation sur l'utilité des méthodes de botanique ... (H.L. Guerin & L.F. Delatour).

Dunlap, J. C. (1999). Molecular Bases for Circadian Clocks. Cell *96*, 271-290.

Dupré, S. M., Miedzinska, K., Duval, C. V., Yu, L., Goodman, R. L., Lincoln, G. A., Davis, J. R. E., McNeilly, A. S., Burt, D. D., and Loudon, A. S. I. (2010). Identification of Eya3 and TAC1 as Long-Day Signals in the Sheep Pituitary. Current Biology *20*, 829-835.

Ecker, J. L., Dumitrescu, O. N., Wong, K. Y., Alam, N. M., Chen, S.-K., LeGates, T., Renna, J. M., Prusky, G. T., Berson, D. M., and Hattar, S. (2010). Melanopsin-expressing retinal ganglion-cell photoreceptors: cellular diversity and role in pattern vision. Neuron *67*, 49-60.

Ehret, C. F., and Trucco, E. (1967). Molecular models for the circadian clock : I. The chronon concept. Journal of Theoretical Biology *15*, 240-262.

Eide, E. J., Vielhaber, E. L., Hinz, W. A., and Virshup, D. M. (2002). The circadian regulatory proteins BMAL1 and cryptochromes are substrates of casein kinase Iepsilon. J. Biol. Chem *277*, 17248-17254.

Eisen, M. B., Spellman, P. T., Brown, P. O., and Botstein, D. (1998). Cluster analysis and display of genome-wide expression patterns. Proceedings of the National Academy of Sciences of the United States of America *95*, 14863-14868.

Emmert-Buck, M. R., Bonner, R. F., Smith, P. D., Chuaqui, R. F., Zhuang, Z., Goldstein, S. R., Weiss, R. A., and Liotta, L. A. (1996). Laser Capture Microdissection. Science *274*, 998 -1001.

Feldman, J. F., and Hoyle, M. N. (1973). Isolation of circadian clock mutants of Neurospora crassa. Genetics *75*, 605-613.

Foster, R. G., Provencio, I., Hudson, D., Fiske, S., De Grip, W., and Menaker, M. (1991). Circadian photoreception in the retinally degenerate mouse (rd/rd). J. Comp. Physiol. A *169*, 39-50.

Gamble, K. L., Allen, G. C., Zhou, T., and McMahon, D. G. (2007). Gastrin-Releasing Peptide Mediates Light-Like Resetting of the Suprachiasmatic Nucleus Circadian Pacemaker through cAMP Response Element-Binding Protein and Per1 Activation. The Journal of Neuroscience *27*, 12078 -12087.

Gaston, S., and Menaker, M. (1968). Pineal Function: The Biological Clock in the Sparrow? Science *160*, 1125 -1127.

Gekakis, N., Staknis, D., Nguyen, H. B., Davis, F. C., Wilsbacher, L. D., King, D. P., Takahashi, J. S., and Weitz, C. J. (1998). Role of the CLOCK protein in the mammalian circadian mechanism. Science *280*, 1564-1569.

Godinho, S. I. H., Maywood, E. S., Shaw, L., Tucci, V., Barnard, A. R., Busino, L., Pagano, M., Kendall, R., Quwailid, M. M., Romero, M. R., et al. (2007). The after-hours mutant reveals a role for Fbxl3 in determining mammalian circadian period. Science *316*, 897.

Green, D. J., and Gillette, R. (1982). Circadian rhythm of firing rate recorded from single cells in the rat suprachiasmatic brain slice. Brain Res *245*, 198-200.

Groos, G., and Hendriks, J. (1982). Circadian rhythms in electrical discharge of rat suprachiasmatic neurones recorded in vitro. Neurosci. Lett *34*, 283-288.

Groos, G., and Mason, R. (1978). Maintained discharge of rat suprachiasmatic neurons at different adaptation levels. Neuroscience Letters *8*, 59-64.

Halberg, F., Halberg, E., Barnum, C. P., and Bittner, J. J. (1959). Physiologic 24-hour periodicity in human beings and mice, the lighting regimen and daily routine. Photoperiodism and related phenomena in plants and animals, 803–878.

Hamada, T., Antle, M. C., and Silver, R. (2004). Temporal and spatial expression patterns of canonical clock genes and clock-controlled genes in the suprachiasmatic nucleus. European Journal of Neuroscience *19*, 1741-1748.

Hamada, T., LeSauter, J., Venuti, J. M., and Silver, R. (2001). Expression of Period Genes: Rhythmic and Nonrhythmic Compartments of the Suprachiasmatic Nucleus Pacemaker. The Journal of Neuroscience *21*, 7742-7750.

Hannibal, J. (2002). Neurotransmitters of the retino-hypothalamic tract. Cell Tissue Res *309*, 73-88.

Hanon, E. A., Lincoln, G. A., Fustin, J.-M., Dardente, H., Masson-Pévet, M., Morgan, P. J., and Hazlerigg, D. G. (2008). Ancestral TSH mechanism signals summer in a photoperiodic mammal. Curr. Biol *18*, 1147-1152.

Hardin, P. E., Hall, J. C., and Rosbash, M. (1990). Feedback of the Drosophila period gene product on circadian cycling of its messenger RNA levels. Nature *343*, 536-540.

Harmar, A. J., Marston, H. M., Shen, S., Spratt, C., West, K. M., Sheward, W. J., Morrison, C. F., Dorin, J. R., Piggins, H. D., Reubi, J.-C., et al. (2002). The VPAC2 Receptor Is Essential for Circadian Function in the Mouse Suprachiasmatic Nuclei. Cell *109*, 497-508.

Harmer, S. L., Hogenesch, J. B., Straume, M., Chang, H. S., Han, B., Zhu, T., Wang, X., Kreps, J. A., and Kay, S. A. (2000). Orchestrated transcription of key pathways in Arabidopsis by the circadian clock. Science *290*, 2110-2113.

Hattar, S., Liao, H.-W., Takao, M., Berson, D. M., and Yau, K.-W. (2002). Melanopsin-Containing Retinal Ganglion Cells: Architecture, Projections, and Intrinsic Photosensitivity. Science *295*, 1065-1070.

Hattar, S., Lucas, R. J., Mrosovsky, N., Thompson, S., Douglas, R. H., Hankins, M. W., Lem, J., Biel, M., Hofmann, F., Foster, R. G., et al. (2003). Melanopsin and rod-cone photoreceptive systems account for all major accessory visual functions in mice. Nature *424*, 75-81.

Hazlerigg, D. G., Ebling, F. J. P., and Johnston, J. D. (2005). Photoperiod differentially regulates gene expression rhythms in the rostral and caudal SCN. Current Biology *15*, R449-R450.

Hendrickson, A. E., Wagoner, N., and Cowan, W. M. (1972). An autoradiographic and electron microscopic study of retino-hypothalamic connections. Z Zellforsch Mikrosk Anat *135*, 1-26.

Hogenesch, J. B., Gu, Y. Z., Jain, S., and Bradfield, C. A. (1998). The basic-helix-loop-helix-PAS orphan MOP3 forms transcriptionally active complexes with circadian and hypoxia factors. Proc. Natl. Acad. Sci. U.S.A *95*, 5474-5479.

Hoogerwerf, W. A., Sinha, M., Conesa, A., Luxon, B. A., Shahinian, V. B., Cornélissen, G., Halberg, F., Bostwick, J., Timm, J., and Cassone, V. M. (2008). Transcriptional profiling of mRNA expression in the mouse distal colon. Gastroenterology *135*, 2019-2029.

Hooke, R. (1665). Micrographia, or, Some physiological descriptions of minute bodies made by magnifying glasses (London: John Martin & James Allestry).

Horst, G. T. J. van der, Muijtjens, M., Kobayashi, K., Takano, R., Kanno, S.-ichiro, Takao, M., Wit, J. de, Verkerk, A., Eker, A. P. M., Leenen, D. van, et al. (1999). Mammalian Cry1 and Cry2 are essential for maintenance of circadian rhythms. Nature *398*, 627-630.

Hughes, A. T. L., Guilding, C., Lennox, L., Samuels, R. E., McMahon, D. G., and Piggins, H. D. (2008). Live imaging of altered period1 expression in the suprachiasmatic nuclei of Vipr2−/− mice1. Journal of Neurochemistry *106*, 1646-1657.

Hughes, M. E., Hogenesch, J. B., and Kornacker, K. (2010). JTK_CYCLE: an efficient nonparametric algorithm for detecting rhythmic components in genome-scale data sets. J. Biol. Rhythms *25*, 372-380.

Inagaki, N., Honma, S., Ono, D., Tanahashi, Y., and Honma, K.-ichi (2007). Separate oscillating cell groups in mouse suprachiasmatic nucleus couple photoperiodically to the onset and end of daily activity. Proc Natl Acad Sci U S A. *104*, 7664–7669.

Inouye, S. T., and Kawamura, H. (1979). Persistence of circadian rhythmicity in a mammalian hypothalamic "island" containing the suprachiasmatic nucleus. Proceedings of the National Academy of Sciences *76*, 5962-5966.

Jagota, A., de la Iglesia, H. O., and Schwartz, W. J. (2000). Morning and evening circadian oscillations in the suprachiasmatic nucleus in vitro. Nat Neurosci *3*, 372-376.

Jin, X., Shearman, L. P., Weaver, D. R., Zylka, M. J., de Vries, G. J., and Reppert, S. M. (1999). A molecular mechanism regulating rhythmic output from the suprachiasmatic circadian clock. Cell *96*, 57-68.

Johnson, C. H., Egli, M., and Stewart, P. L. (2008). Structural Insights into a Circadian Oscillator. Science *322*, 697 -701.

Johnston, J. D. (2005). Measuring Seasonal Time within the Circadian System: Regulation of the Suprachiasmatic Nuclei by Photoperiod. J Neuroendocrinol *17*, 459-465.

Jones, C. R., Campbell, S. S., Zone, S. E., Cooper, F., DeSano, A., Murphy, P. J., Jones, B., Czajkowski, L., and Ptácek, L. J. (1999). Familial advanced sleep-phase syndrome: A short-period circadian rhythm variant in humans. Nat. Med *5*, 1062-1065.

Kalló, I., Kalamatianos, T., Wiltshire, N., Shen, S., Sheward, W. J., Harmar, A. J., and Coen, C. W. (2004). Transgenic approach reveals expression of the VPAC2 receptor in phenotypically defined neurons in the mouse suprachiasmatic nucleus and in its efferent target sites. European Journal of Neuroscience *19*, 2201-2211.

Kalsbeek, A., Palm, I. F., La Fleur, S. E., Scheer, F. A. J. L., Perreau-Lenz, S., Ruiter, M., Kreier, F., Cailotto, C., and Buijs, R. M. (2006). SCN Outputs and the Hypothalamic Balance of Life. Journal of Biological Rhythms *21*, 458 -469.

Kandel, E. R. (2001). The Molecular Biology of Memory Storage: A Dialogue Between Genes and Synapses. Science *294*, 1030 -1038.

Karatsoreos, I. N., Yan, L., LeSauter, J., and Silver, R. (2004). Phenotype Matters: Identification of Light-Responsive Cells in the Mouse Suprachiasmatic Nucleus. J. Neurosci. *24*, 68-75.

Keesler, G. A., Camacho, F., Guo, Y., Virshup, D., Mondadori, C., and Yao, Z. (2000). Phosphorylation and destabilization of human period I clock protein by human casein kinase I [epsilon]. Neuroreport *11*, 951.

Keller, M., Mazuch, J., Abraham, U., Eom, G. D., Herzog, E. D., Volk, H.-D., Kramer, A., and Maier, B. (2009). A circadian clock in macrophages controls inflammatory immune responses. Proceedings of the National Academy of Sciences *106*, 21407-21412.

Kim, D. Y., Kang, H. C., Shin, H. C., Lee, K. J., Yoon, Y. W., Han, H. C., Na, H. S., Hong, S. K., and Kim, Y. I. (2001). Substance p plays a critical role in photic resetting of the circadian pacemaker in the rat hypothalamus. J. Neurosci *21*, 4026-4031.

King, D. P., Zhao, Y., Sangoram, A. M., Wilsbacher, L. D., Tanaka, M., Antoch, M. P., Steeves, T. D., Vitaterna, M. H., Kornhauser, J. M., Lowrey, P. L., et al. (1997). Positional cloning of the mouse circadian clock gene. Cell *89*, 641-653.

Kita, Y., Shiozawa, M., Jin, W., Majewski, R. R., Besharse, J. C., Greene, A. S., and Jacob, H. J. (2002). Implications of circadian gene expression in kidney, liver and the effects of fasting on pharmacogenomic studies. Pharmacogenetics *12*, 55-65.

Klosen, P., Bienvenu, C., Demarteau, O., Dardente, H., Guerrero, H., Pévet, P., and Masson-Pévet, M. (2002). The mt1 Melatonin Receptor and RORβ Receptor Are Co-localized in Specific TSH-immunoreactive Cells in the Pars Tuberalis of the Rat Pituitary. Journal of Histochemistry & Cytochemistry *50*, 1647 -1657.

Kondo, T., Strayer, C. A., Kulkarni, R. D., Taylor, W., Ishiura, M., Golden, S. S., and Johnson, C. H. (1993). Circadian rhythms in prokaryotes: luciferase as a reporter of circadian gene expression in cyanobacteria. Proceedings of the National Academy of Sciences *90*, 5672 -5676.

Konopka, R. J., and Benzer, S. (1971). Clock Mutants of Drosophila melanogaster. Proceedings of the National Academy of Sciences *68*, 2112 -2116.

Kramer, A., Yang, F. C., Snodgrass, P., Li, X., Scammell, T. E., Davis, F. C., and Weitz, C. J. (2001). Regulation of daily locomotor activity and sleep by hypothalamic EGF receptor signaling. Science *294*, 2511-2515.

Kraves, S., and Weitz, C. J. (2006). A role for cardiotrophin-like cytokine in the circadian control of mammalian locomotor activity. Nat Neurosci *9*, 212-219.

Kriegsfeld, L. J., LeSauter, J., and Silver, R. (2004). Targeted Microlesions Reveal Novel Organization of the Hamster Suprachiasmatic Nucleus. J. Neurosci. *24*, 2449-2457.

Kuhlman, S. J., Silver, R., Le Sauter, J., Bult-Ito, A., and McMahon, D. G. (2003). Phase Resetting Light Pulses Induce Per1 and Persistent Spike Activity in a Subpopulation of Biological Clock Neurons. J. Neurosci. *23*, 1441-1450.

Kumaki, Y., Ukai-Tadenuma, M., Uno, K.-ichiro D., Nishio, J., Masumoto, K.-hei, Nagano, M., Komori, T., Shigeyoshi, Y., Hogenesch, J. B., and Ueda, H. R. (2008). Analysis and synthesis of high-amplitude Cis-elements in the mammalian circadian clock. Proc. Natl. Acad. Sci. U.S.A *105*, 14946-14951.

Lander, E. S., Linton, L. M., Birren, B., Nusbaum, C., Zody, M. C., Baldwin, J., Devon, K., Dewar, K., Doyle, M., FitzHugh, W., et al. (2001). Initial sequencing and analysis of the human genome. Nature *409*, 860–921.

Lee, C., Etchegaray, J.-P., Cagampang, F. R. A., Loudon, A. S. I., and Reppert, S. M. (2001). Posttranslational Mechanisms Regulate the Mammalian Circadian Clock. Cell *107*, 855-867.
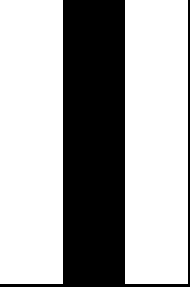
Lehman, M., Silver, R., Gladstone, W., Kahn, R., Gibson, M., and Bittman, E. (1987). Circadian rhythmicity restored by neural transplant. Immunocytochemical characterization of the graft and its integration with the host brain. The Journal of Neuroscience *7*, 1626 -1638.

LeSauter, J., and Silver, R. (1998). Output signals of the SCN. Chronobiology international *15*, 535–550.

LeSauter, J., and Silver, R. (1999). Localization of a Suprachiasmatic Nucleus Subregion Regulating Locomotor Rhythmicity. J. Neurosci. *19*, 5574-5585.

Lin, Y., Han, M., Shimada, B., Wang, L., Gibler, T. M., Amarakone, A., Awad, T. A., Stormo, G. D., Van Gelder, R. N., and Taghert, P. H. (2002). Influence of the period-dependent circadian clock on diurnal, circadian, and aperiodic gene expression in Drosophila melanogaster. Proc. Natl. Acad. Sci. U.S.A *99*, 9562-9567.

Linnaeus, C. (1751). Philosophia botanica. Stockholm: G. Kiesewetter.

Liu, A. (2010). Laser Capture Microdissection in the Tissue Biorepository. Journal of biomolecular techniques: JBT *21*, 120.

Liu, A. C., Welsh, D. K., Ko, C. H., Tran, H. G., Zhang, E. E., Priest, A. A., Buhr, E. D., Singer, O., Meeker, K., Verma, I. M., et al. (2007). Intercellular Coupling Confers Robustness against Mutations in the SCN Circadian Clock Network. Cell *129*, 605-616.

Lockhart, D. J., Dong, H., Byrne, M. C., Follettie, M. T., Gallo, M. V., Chee, M. S., Mittmann, M., Wang, C., Kobayashi, M., Norton, H., et al. (1996). Expression monitoring by hybridization to high-density oligonucleotide arrays. Nat Biotech *14*, 1675-1680.

Lowrey, P. L., and Takahashi, J. S. (2004). MAMMALIAN CIRCADIAN BIOLOGY: Elucidating Genome-Wide Levels of Temporal Organization. Annu. Rev. Genom. Human Genet. *5*, 407-441.

Lowrey, P. L., Shimomura, K., Antoch, M. P., Yamazaki, S., Zemenides, P. D., Ralph, M. R., Menaker, M., and Takahashi, J. S. (2000). Positional Syntenic Cloning and Functional Characterization of the Mammalian Circadian Mutation tau. Science *288*, 483 -491.

De Mairan, M. (1729). Observation botanique. Histoire de l'Academie Royale des Sciences, Paris *35*.

Mason, C. A., and Lincoln, D. W. (1976). Visualization of the retino-hypothalamic projection in the rat by cobalt precipitation. Cell Tissue Res *168*, 117-131.

Masumoto, K.-hei, Ukai-Tadenuma, M., Kasukawa, T., Nagano, M., Uno, K. D., Tsujino, K., Horikawa, K., Shigeyoshi, Y., and Ueda, H. R. (2010). Acute Induction of Eya3 by Late-Night Light Stimulation Triggers TSHβ Expression in Photoperiodism. Current Biology *20*, 2199-2206.

McDonald, M. J., and Rosbash, M. (2001). Microarray analysis and organization of circadian gene expression in Drosophila. Cell *107*, 567-578.

Meijer, J. H., Michel, S., VanderLeest, H. T., and Rohling, J. H. T. (2010). Daily and seasonal adaptation of the circadian clock requires plasticity of the SCN neuronal network. European Journal of Neuroscience *32*, 2143-2151.

Meyer-Bernstein, E. L., Jetton, A. E., Matsumoto, S.-ichiro, Markuns, J. F., Lehman, M. N., and Bittman, E. L. (1999). Effects of Suprachiasmatic Transplants on Circadian Rhythms of Neuroendocrine Function in Golden Hamsters. Endocrinology *140*, 207 -218.

Michel, S., Geusz, M. E., Zaritsky, J. J., and Block, G. D. (1993). Circadian rhythm in membrane conductance expressed in isolated neurons. Science *259*, 239-241.

Michel, S., Itri, J., Han, J., Gniotczynski, K., and Colwell, C. (2006). Regulation of glutamatergic signalling by PACAP in the mammalian suprachiasmatic nucleus. BMC Neuroscience *7*, 15.

Micke, P., Ostman, A., Lundeberg, J., and Ponten, F. (2005). Laser-assisted cell microdissection using the PALM system. Methods Mol Biol *293*, 151–166.

Miller, J. D., Morin, L. P., Schwartz, W. J., and Moore, R. Y. (1996). New insights into the mammalian circadian clock. Sleep *19*, 641-67.

Moga, M. M., and Moore, R. Y. (1997). Organization of neural inputs to the suprachiasmatic nucleus in the rat. The Journal of Comparative Neurology *389*, 508-534.

Moore, R. Y. (1996). Entrainment pathways and the functional organization of the circadian system. Prog. Brain Res *111*, 103-119.

Moore, R. Y. (1992). The fourth C.U. Ariëns Kappers lecture. The organization of the human circadian timing system. Prog. Brain Res *93*, 99-115; discussion 115-117.

Moore, R. Y., and Lenn, N. J. (1972). A retinohypothalamic projection in the rat. J. Comp. Neurol *146*, 1-14.

Moore, R. Y., and Eichler, V. B. (1972). Loss of a circadian adrenal corticosterone rhythm following suprachiasmatic lesions in the rat. Brain Research *42*, 201-206.

Moore, R. Y., and Silver, R. (1998). Suprachiasmatic Nucleus Organization. Chronobiology International *15*, 475.

Morin, L. P., Shivers, K.-Y., Blanchard, J. H., and Muscat, L. (2006). Complex organization of mouse and rat suprachiasmatic nucleus. Neuroscience *137*, 1285-1297.

Morin, L. P. (2007). SCN organization reconsidered. J Biol Rhythms *22*, 3-13.

Mzhavia, N., Berman, Y., Che, F. Y., Fricker, L. D., and Devi, L. A. (2001). ProSAAS processing in mouse brain and pituitary. J. Biol. Chem *276*, 6207-6213.

Nagoshi, E., Saini, C., Bauer, C., Laroche, T., Naef, F., and Schibler, U. (2004). Circadian Gene Expression in Individual Fibroblasts: Cell-Autonomous and Self-Sustained Oscillators Pass Time to Daughter Cells. Cell *119*, 693-705.

Naito, E., Watanabe, T., Tei, H., Yoshimura, T., and Ebihara, S. (2008). Reorganization of the Suprachiasmatic Nucleus Coding for Day Length. Journal of Biological Rhythms *23*, 140 -149.

Nakajima, M., Imai, K., Ito, H., Nishiwaki, T., Murayama, Y., Iwasaki, H., Oyama, T., and Kondo, T. (2005). Reconstitution of Circadian Oscillation of Cyanobacterial KaiC Phosphorylation in Vitro. Science *308*, 414 -415.

Nakamura, W., Honma, S., Shirakawa, T., and Honma, K.-ichi (2002). Clock mutation lengthens the circadian period without damping rhythms in individual SCN neurons. Nat. Neurosci *5*, 399-400.

Nakao, N., Ono, H., and Yoshimura, T. (2008a). Thyroid hormones and seasonal reproductive neuroendocrine interactions. Reproduction *136*, 1-8.

Nakao, N., Ono, H., Yamamura, T., Anraku, T., Takagi, T., Higashi, K., Yasuo, S., Katou, Y., Kageyama, S., Uno, Y., et al. (2008b). Thyrotrophin in the pars tuberalis triggers photoperiodic response. Nature *452*, 317-322.

Nelson, D. E., and Takahashi, J. S. (1991). Sensitivity and integration in a visual pathway for circadian entrainment in the hamster (Mesocricetus auratus). J. Physiol. (Lond.) *439*, 115-145.

Nelson, R. J., and Zucker, I. (1981). Photoperiodic control of reproduction in olfactory-bulbectomized rats. Neuroendocrinology *32*, 266-271.

Nicholls, T. J., Goldsmith, A. R., and Dawson, A. (1988). Photorefractoriness in birds and comparison with mammals. Physiol. Rev *68*, 133-176.

Nishiitsutsuji-Uwo, J., and Pittendrigh, C. S. (1968). Central nervous system control of circadian rhythmicity in the cockroach. Z. Vergl. Physiol. *58*, 14-46.

Nishino, H., Koizumi, K., and Brooks, C. M. (1976). The role of suprachiasmatic nuclei of the hypothalamus in the production of circadian rhythm. Brain Research *112*, 45-59.

O'Neill, J. S., and Reddy, A. B. (2011). Circadian clocks in human red blood cells. Nature *469*, 498-503.

O'Neill, J. S., van Ooijen, G., Dixon, L. E., Troein, C., Corellou, F., Bouget, F.-Y., Reddy, A. B., and Millar, A. J. (2011). Circadian rhythms persist without transcription in a eukaryote. Nature *469*, 554-558.

Okamura, H., Miyake, S., Sumi, Y., Yamaguchi, S., Yasui, A., Muijtjens, M., Hoeijmakers, J. H., and van der Horst, G. T. (1999). Photic induction of mPer1 and mPer2 in cry-deficient mice lacking a biological clock. Science *286*, 2531-2534.

Oster, H., Damerow, S., Hut, R. A., and Eichele, G. (2006). Transcriptional Profiling in the Adrenal Gland Reveals Circadian Regulation of Hormone Biosynthesis Genes and Nucleosome Assembly Genes. Journal of Biological Rhythms *21*, 350 -361.

Panda, S., Provencio, I., Tu, D. C., Pires, S. S., Rollag, M. D., Castrucci, A. M., Pletcher, M. T., Sato, T. K., Wiltshire, T., Andahazy, M., et al. (2003). Melanopsin Is Required for Non-Image-Forming Photic Responses in Blind Mice. Science *301*, 525 -527.

Piggins, H., Antle, M., and Rusak, B. (1995). Neuropeptides phase shift the mammalian circadian pacemaker. The Journal of Neuroscience *15*, 5612 -5622.

Pittendrigh, C. S. (1993). Temporal Organization: Reflections of a Darwinian Clock-Watcher. Annu. Rev. Physiol. *55*, 17-54.

Pittendrigh, C. S. (1981). Circadian systems: entrainment. Handbook of behavioral neurobiology *4*, 95–124.

Pittendrigh, C. S. (1960). Circadian Rhythms and the Circadian Organization of Living Systems. Cold Spring Harbor Symposia on Quantitative Biology *25*, 159 -184.

Pittendrigh, C. S., and Daan, S. (1976a). A functional analysis of circadian pacemakers in nocturnal rodents I. The stability and lability of spontaneous frequency. J. Comp. Physiol. *106*, 223-252.

Pittendrigh, C. S., and Daan, S. (1976b). A functional analysis of circadian pacemakers in nocturnal rodents IV. Entrainment: Pacemaker as clock. J. Comp. Physiol. *106*, 291-331.

Pittendrigh, C. S., and Daan, S. (1976c). A functional analysis of circadian pacemakers in nocturnal rodents V. Pacemaker structure: A clock for all seasons. J. Comp. Physiol. *106*, 333-355.

Pittendrigh, C. S., and Minis, D. H. (1964). The Entrainment of Circadian Oscillations by Light and Their Role as Photoperiodic Clocks. The American Naturalist *98*, 261-294.

van den Pol, A. N., and Tsujimoto, K. L. (1985). Neurotransmitters of the hypothalamic suprachiasmatic nucleus: Immunocytochemical analysis of 25 neuronal antigens. Neuroscience *15*, 1049-1086.

Porterfield, V., Piontkivska, H., and Mintz, E. (2007). Identification of novel light-induced genes in the suprachiasmatic nucleus. BMC Neuroscience *8*, 98.

Preitner, N., Damiola, F., Luis-Lopez-Molina, Zakany, J., Duboule, D., Albrecht, U., and Schibler, U. (2002). The Orphan Nuclear Receptor REV-ERB[alpha] Controls Circadian Transcription within the Positive Limb of the Mammalian Circadian Oscillator. Cell *110*, 251-260.

Provencio, I., Rodriguez, I. R., Jiang, G., Hayes, W. P., Moreira, E. F., and Rollag, M. D. (2000). A Novel Human Opsin in the Inner Retina. The Journal of Neuroscience *20*, 600 -605.

Quintero, J. E., Kuhlman, S. J., and McMahon, D. G. (2003). The Biological Clock Nucleus: A Multiphasic Oscillator Network Regulated by Light. J. Neurosci. *23*, 8070-8076.

Ralph, M., and Menaker, M. (1988). A mutation of the circadian system in golden hamsters. Science *241*, 1225 -1227.

Ralph, M., Foster, R., Davis, F., and Menaker, M. (1990). Transplanted suprachiasmatic nucleus determines circadian period. Science *247*, 975 -978.

Reddy, A. B., Field, M. D., Maywood, E. S., and Hastings, M. H. (2002). Differential Resynchronisation of Circadian Clock Gene Expression within the Suprachiasmatic Nuclei of Mice Subjected to Experimental Jet Lag. J. Neurosci. *22*, 7326-7330.

Reddy, P., Zehring, W. A., Wheeler, D. A., Pirrotta, V., Hadfield, C., Hall, J. C., and Rosbash, M. (1984). Molecular analysis of the period locus in Drosophila melanogaster and identification of a transcript involved in biological rhythms. Cell *38*, 701-710.

Reick, M., Garcia, J. A., Dudley, C., and McKnight, S. L. (2001). NPAS2: An Analog of Clock Operative in the Mammalian Forebrain. Science *293*, 506 -509.

Reischl, S., Vanselow, K., Westermark, P. O., Thierfelder, N., Maier, B., Herzel, H., and Kramer, A. (2007). β-TrCP1-Mediated Degradation of PERIOD2 Is Essential for Circadian Dynamics. Journal of Biological Rhythms *22*, 375 -386.

Reiter, R. J., and Hester, R. J. (1966). Interrelationships of the Pineal Gland, the Superior Cervical Ganglia and the Photoperiod in the Regulation of the Endocrine Systems of Hamsters. Endocrinology *79*, 1168-1170.

Richter, C. P. (1922). A Behavioristic Study of the Activity of the Rat. Comparative Psychology Monographs.

Richter, C. P. (1965). Biological clocks in medicine and psychiatry, Charles C. Thomas, Springfield, IL, 111.

Richter, C. P. (1968). Inherent 24-hour and lunar clocks of a primate—The squirrel monkey. Communications in Behavioral Biology *1*, 305–332.

Rusak, B., and Morin, L. P. (1976). Testicular Responses to Photoperiod Are Blocked by Lesions of the Suprachiasmatic Nuclei in Golden Hamsters. Biology of Reproduction *15*, 366 -374.

Samson, W. K., Said, S. I., and McCann, S. M. (1979). Radioimmunologic localization of vasoactive intestinal polypeptide in hypothalamic and extrahypothalamic sites in the rat brain. Neuroscience Letters *12*, 265-269.

Sato, T. K., Panda, S., Kay, S. A., and Hogenesch, J. B. (2003). DNA Arrays: Applications and Implications for Circadian Biology. Journal of Biological Rhythms *18*, 96 -105.

Sawaki, Y. (1977). Retinohypothalamic projection: electrophysiological evidence for the existence in female rats. Brain Res *120*, 336-341.

Schaap, J., Pennartz, C. M. A., and Meijer, J. H. (2003). Electrophysiology of the circadian pacemaker in mammals. Chronobiol. Int *20*, 171-188.

Schaffer, R., Landgraf, J., Accerbi, M., Simon, V., Larson, M., and Wisman, E. (2001). Microarray analysis of diurnal and circadian-regulated genes in Arabidopsis. Plant Cell *13*, 113-123.

Schena, M., Shalon, D., Davis, R. W., and Brown, P. O. (1995). Quantitative Monitoring of Gene Expression Patterns with a Complementary DNA Microarray. Science *270*, 467 -470.

Schuitze, K., and Lahr, G. (1998). Identification of expressed genes by laser-mediated manipulation of single cells. Nat Biotech *16*, 737-742.

Schwartz, W., and Zimmerman, P. (1990). Circadian timekeeping in BALB/c and C57BL/6 inbred mouse strains. The Journal of Neuroscience *10*, 3685 -3694.

Shearman, L. P., Zylka, M. J., Weaver, D. R., Kolakowski Jr., L. F., and Reppert, S. M. (1997). Two period Homologs: Circadian Expression and Photic Regulation in the Suprachiasmatic Nuclei. Neuron *19*, 1261-1269.

Shibata, S., Oomura, Y., Kita, H., and Hattori, K. (1982). Circadian rhythmic changes of neuronal activity in the suprachiasmatic nucleus of the rat hypothalamic slice. Brain Res *247*, 154-158.

Shigeyoshi, Y., Taguchi, K., Yamamoto, S., Takekida, S., Yan, L., Tei, H., Moriya, T., Shibata, S., Loros, J. J., Dunlap, J. C., et al. (1997). Light-Induced Resetting of a Mammalian Circadian Clock Is Associated with Rapid Induction of the mPer1 Transcript. Cell *91*, 1043-1053.

Siepka, S. M., Yoo, S.-H., Park, J., Lee, C., and Takahashi, J. S. (2007). Genetics and neurobiology of circadian clocks in mammals. Cold Spring Harb Symp Quant Biol *72*, 251-9.

Silver, R., Sookhoo, A. I., LeSauter, J., Stevens, P., Jansen, H. T., and Lehman, M. N. (1999). Multiple regulatory elements result in regional specificity in circadian rhythms of neuropeptide expression in mouse SCN. Neuroreport *10*, 3165-74.

Silver, R., LeSauter, J., Tresco, P. A., and Lehman, M. N. (1996). A diffusible coupling signal from the transplanted suprachiasmatic nucleus controlling circadian locomotor rhythms. Nature *382*, 810-813.

Stal, L. J., and Krumbein, W. E. (1987). Temporal separation of nitrogen fixation and photosynthesis in the filamentous, non-heterocystous cyanobacterium Oscillatoria sp. Arch. Microbiol. *149*, 76-80.

Stephan, F. K. (2002). The "Other" Circadian System: Food as a Zeitgeber. Journal of Biological Rhythms *17*, 284 -292.

Stephan, F. K., and Zucker, I. (1972). Circadian Rhythms in Drinking Behavior and Locomotor Activity of Rats Are Eliminated by Hypothalamic Lesions. Proc Natl Acad Sci U S A. *69*, 1583–1586.

Stetson, M. H., and Watson-Whitmyre, M. (1976). Nucleus suprachiasmaticus: the biological clock in the hamster? Science *191*, 197-9.

Stoleru, D., Nawathean, P., Fernández, M. de la P., Menet, J. S., Fern, M., Ceriani, a, and Rosbash, M. (2007). The Drosophila Circadian Network Is a Seasonal Timer. Cell *129*, 207-219.

Stoleru, D., Peng, Y., Agosto, J., and Rosbash, M. (2004). Coupled oscillators control morning and evening locomotor behaviour of Drosophila. Nature *431*, 862-868.

Stoleru, D., Peng, Y., Nawathean, P., and Rosbash, M. (2005). A resetting signal between Drosophila pacemakers synchronizes morning and evening activity. Nature *438*, 238-242.

Storch, K.-F., Lipan, O., Leykin, I., Viswanathan, N., Davis, F. C., Wong, W. H., and Weitz, C. J. (2002). Extensive and divergent circadian gene expression in liver and heart. Nature *417*, 78-83.

Strecker, G. J., Wuarin, J.-P., and Dudek, F. E. (1997). GABAA-Mediated Local Synaptic Pathways Connect Neurons in the Rat Suprachiasmatic Nucleus. Journal of Neurophysiology *78*, 2217 -2220.

Toh, K. L., Jones, C. R., He, Y., Eide, E. J., Hinz, W. A., Virshup, D. M., Ptáček, L. J., and Fu, Y.-H. (2001). An hPer2 Phosphorylation Site Mutation in Familial Advanced Sleep Phase Syndrome. Science *291*, 1040 -1043.

Travnickova-Bendova, Z., Cermakian, N., Reppert, S. M., and Sassone-Corsi, P. (2002). Bimodal regulation of mPeriod promoters by CREB-dependent signaling and CLOCK/BMAL1 activity. Proceedings of the National Academy of Sciences *99*, 7728 -7733.

Ueda, H. R., Hayashi, S., Chen, W., Sano, M., Machida, M., Shigeyoshi, Y., Iino, M., and Hashimoto, S. (2005). System-level identification of transcriptional circuits underlying mammalian circadian clocks. Nat Genet *37*, 187-192.

Ueda, H. R., Matsumoto, A., Kawamura, M., Iino, M., Tanimura, T., and Hashimoto, S. (2002a). Genome-wide transcriptional orchestration of circadian rhythms in Drosophila. J. Biol. Chem *277*, 14048-14052.

Ueda, H. R., Chen, W., Adachi, A., Wakamatsu, H., Hayashi, S., Takasugi, T., Nagano, M., Nakahama, K.-ichi, Suzuki, Y., Sugano, S., et al. (2002b). A transcription factor response element for gene expression during circadian night. Nature *418*, 534-539.

VanderLeest, H. T., Houben, T., Michel, S., Deboer, T., Albus, H., Vansteensel, M. J., Block, G. D., and Meijer, J. H. (2007). Seasonal Encoding by the Circadian Pacemaker of the SCN. Current Biology *17*, 468-473.

Vandesande, F., Dierickx, K., and Mey, J. (1975). Identification of the vasopressin-neurophysin producing neurons of the rat suprachiasmatic nuclei. Cell Tissue Res. *156*. Available at: http://www.springerlink.com/content/t4833g74v0u77613/ [Accessed April 25, 2011].

Vanselow, K., Vanselow, J. T., Westermark, P. O., Reischl, S., Maier, B., Korte, T., Herrmann, A., Herzel, H., Schlosser, A., and Kramer, A. (2006). Differential effects of PER2 phosphorylation: molecular basis for the human familial advanced sleep phase syndrome (FASPS). Genes & Development *20*, 2660 -2672.

Vasu, V. T., Cross, C. E., and Gohil, K. (2009). Nr1d1, an important circadian pathway regulatory gene, is suppressed by cigarette smoke in murine lungs. Integr Cancer Ther *8*, 321-328.

Velculescu, V. E., Zhang, L., Vogelstein, B., and Kinzler, K. W. (1995). Serial Analysis of Gene Expression. Science *270*, 484 -487.

Venter, J. C., Adams, M. D., Myers, E. W., Li, P. W., Mural, R. J., Sutton, G. G., Smith, H. O., Yandell, M., Evans, C. A., Holt, R. A., et al. (2001). The Sequence of the Human Genome. Science *291*, 1304 -1351.

Vielhaber, E., Eide, E., Rivers, A., Gao, Z.-H., and Virshup, D. M. (2000). Nuclear Entry of the Circadian Regulator mPER1 Is Controlled by Mammalian Casein Kinase I varepsilon. Mol. Cell. Biol. *20*, 4888-4899.

Vitaterna, M. H., Selby, C. P., Todo, T., Niwa, H., Thompson, C., Fruechte, E. M., Hitomi, K., Thresher, R. J., Ishikawa, T., Miyazaki, J., et al. (1999). Differential regulation of mammalian Period genes and circadian rhythmicity by cryptochromes 1 and 2. Proceedings of the National Academy of Sciences *96*, 12114 -12119.

Vitaterna, M., King, D., Chang, A., Kornhauser, J., Lowrey, P., McDonald, J., Dove, W., Pinto, L., Turek, F., and Takahashi, J. (1994). Mutagenesis and mapping of a mouse gene, Clock, essential for circadian behavior. Science *264*, 719 -725.

Vosko, A. M., Schroeder, A., Loh, D. H., and Colwell, C. S. (2007). Vasoactive intestinal peptide and the mammalian circadian system. Gen. Comp. Endocrinol *152*, 165-175.

Welsh, D. K., Logothetis, D. E., Meister, M., and Reppert, S. M. (1995). Individual neurons dissociated from rat suprachiasmatic nucleus express independently phased circadian firing rhythms. Neuron *14*, 697-706.

Welsh, D. K., Takahashi, J. S., and Kay, S. A. (2010). Suprachiasmatic Nucleus: Cell Autonomy and Network Properties. Annu. Rev. Physiol. *72*, 551-577.

Welsh, D. K., Yoo, S.-H., Liu, A. C., Takahashi, J. S., and Kay, S. A. (2004). Bioluminescence Imaging of Individual Fibroblasts Reveals Persistent, Independently Phased Circadian Rhythms of Clock Gene Expression. Current Biology *14*, 2289-2295.

Wichert, S., Fokianos, K., and Strimmer, K. (2004). Identifying periodically expressed transcripts in microarray time series data. Bioinformatics *20*, 5-20.

Winfree, A. T. (2001). The geometry of biological time (Springer).

Woelfle, M. A., Ouyang, Y., Phanvijhitsiri, K., and Johnson, C. H. (2004). The Adaptive Value of Circadian Clocks: An Experimental Assessment in Cyanobacteria. Current Biology *14*, 1481-1486.

Yagita, K., Tamanini, F., van der Horst, G. T. J., and Okamura, H. (2001). Molecular Mechanisms of the Biological Clock in Cultured Fibroblasts. Science *292*, 278 -281.

Yamaguchi, S., Isejima, H., Matsuo, T., Okura, R., Yagita, K., Kobayashi, M., and Okamura, H. (2003). Synchronization of Cellular Clocks in the Suprachiasmatic Nucleus. Science *302*, 1408-1412.

Yamazaki, S., Goto, M., and Menaker, M. (1999). No evidence for extraocular photoreceptors in the circadian system of the Syrian hamster. J. Biol. Rhythms *14*, 197-201.

Yamazaki, S., Numano, R., Abe, M., Hida, A., Takahashi, R.-ichi, Ueda, M., Block, G. D., Sakaki, Y., Menaker, M., and Tei, H. (2000). Resetting Central and Peripheral Circadian Oscillators in Transgenic Rats. Science *288*, 682 -685.

Yan, L., Karatsoreos, I., LeSauter, J., Welsh, D. K., Kay, S., Foley, D., and Silver, R. (2007). Exploring Spatio-temporal Organization of SCN Circuits. Cold Spring Harbor Symposia on Quantitative Biology *72*, 527 -541.

Yan, L., Takekida, S., Shigeyoshi, Y., and Okamura, H. (1999). Per1 and Per2 gene expression in the rat suprachiasmatic nucleus: circadian profile and the compartment-specific response to light. Neuroscience *94*, 141-150.

Yan, L., and Silver, R. (2002). Differential induction and localization of mPer1 and mPer2 during advancing and delaying phase shifts. European Journal of Neuroscience *16*, 1531-1540.

Yoo, S.-H., Yamazaki, S., Lowrey, P. L., Shimomura, K., Ko, C. H., Buhr, E. D., Siepka, S. M., Hong, H.-K., Oh, W. J., Yoo, O. J., et al. (2004). PERIOD2::LUCIFERASE real-time reporting of circadian dynamics reveals persistent circadian oscillations in mouse peripheral tissues. Proceedings of the National Academy of Sciences of the United States of America *101*, 5339 -5346.

Young, M. W., and Kay, S. A. (2001). Time zones: a comparative genetics of circadian clocks. Nat Rev Genet *2*, 702-715.

Zaidi, F. H., Hull, J. T., Peirson, S. N., Wulff, K., Aeschbach, D., Gooley, J. J., Brainard, G. C., Gregory-Evans, K., Rizzo, J. F., 3rd, Czeisler, C. A., et al. (2007). Short-wavelength light sensitivity of circadian, pupillary, and visual awareness in humans lacking an outer retina. Curr. Biol *17*, 2122-2128.

Zehring, W. A., Wheeler, D. A., Reddy, P., Konopka, R. J., Kyriacou, C. P., Rosbash, M., and Hall, J. C. (1984). P-element transformation with period locus DNA restores rhythmicity to mutant, arrhythmic drosophila melanogaster. Cell *39*, 369-376.

Zheng, B., Larkin, D. W., Albrecht, U., Sun, Z. S., Sage, M., Eichele, G., Lee, C. C., and Bradley, A. (1999). The mPer2 gene encodes a functional component of the mammalian circadian clock. Nature *400*, 169-173.

Zvonic, S., Ptitsyn, A. A., Kilroy, G., Wu, X., Conrad, S. A., Scott, L. K., Guilak, F., Pelled, G., Gazit, D., and Gimble, J. M. (2007). Circadian oscillation of gene expression in murine calvarial bone. J. Bone Miner. Res *22*, 357-365.

Zylka, M. J., Shearman, L. P., Levine, J. D., Jin, X., Weaver, D. R., and Reppert, S. M. (1998). Molecular Analysis of Mammalian Timeless. Neuron *21*, 1115-1122.

A POWERFUL AND SENSITIVE mRNA PROFILING METHOD REVEALS NOVEL TRANSCRIPTION SIGNATURES WITHIN SCN SUBREGIONS

Karl Brand[1], Filippo Tamanini[1], Malgorzata Oklejewicz[1],
Peter J. van der Spek[2], Ed Jacobs[1] and Gijsbertus T.J. van der Horst[1,*]

[1] Department of Genetics, Erasmus University Medical Center,
3000 CA Rotterdam, The Netherlands.
[2] Department of Bioinformatics, Erasmus University Medical Center,
3000 CA Rotterdam, The Netherlands.
* Corresponding author

ABSTRACT

The suprachiasmatic nuclei (SCN) in the hypothalamus is the site of the central pacemaker in mammals, using light to synchronize an animal's behavior and internal physiology in anticipation of daily environmental changes imposed by earths daily axial rotation. Sustained by an intracellular molecular 'clock' with a period of about 24 hours, SCN neurons drive rhythmic ~24 hour electrical and hormonal outputs responsible for maintaining behavioral and physiological circadian rhythms. Consisting of approximately 20,000 neurons, recent data reveal an SCN of increasing spatial and temporal heterogeneity, localizing different functions to different subregions, including dorsal and ventral SCN. As proof of principle, we present methodology developed for the purpose of broadening understanding how subregions contribute to central pacemaker function and also to unify available subregion data. By combining laser catapult microdissection with a powerful, sensitive single cycle mRNA amplification protocol, we obtained global transcription profiles for dorsal SCN, ventral SCN and central SCN during late evening and early day. Analysis yielded unique transcriptional signatures for each subregion which we present here for the first time aiding selection of novel, subregion specific makers.

II

INTRODUCTION

Life exposed to Earths daily changes have evolved mechanisms to anticipate and regulate all aspects of their biology in order to survive (Harmer et al., 2001). In mammals the suprachiasmatic nuclei (SCN) fulfill the role as the central pacemaker coordinating animal timing in response to, and anticipation of Earths daily rhythm (Stephan and Zucker, 1972; Stetson and Watson-Whitmyre, 1976). The SCN is dorsally embedded in the optic chiasm and densely innervated by intrinsically photoreceptive retinal ganglion cells (ipRGCs) which communicate photic information from the retina (Foster and Hankins, 2007; Hankins et al., 2008). SCN neurons drive a daily electrical and hormonal output responsible for maintaining behavioral and physiological circadian rhythms (Okamura, 2007). The SCN performs at least two roles thus; rhythm synchronization to the environment and coordination of internal daily synchrony. A cell autonomous molecular clock generates approximate 24-hour rhythms in SCN neurons and all peripheral cells (Reppert and Weaver, 2002; Stratmann and Schibler, 2006; Dardente and Cermakian, 2007). This depends on a transcription-translation feedback loop of core-clock genes *Clock*, *Bmal1*, *Period*, *Cryptochrome* and *Rev-erbα* for maintaining rhythms (Siepka et al., 2007). Besides the requirement for rhythmicity, the period genes (*Per1* and *Per2*) are induced by light suggesting the mechanism for adjusting and synchronizing rhythms is regulated by these genes (Shigeyoshi et al., 1997; Albrecht et al., 2001).

The SCN is composed of a heterogeneous population of neurons with accumulating evidence revealing ever greater complexity in neuropeptide content, molecular clock function, neurotransmitter distribution and electrical output (reviewed in Antle and Silver, 2005; Morin, 2007; Welsh et al., 2010). Based on pioneering studies of SCN architecture in rat and hamster, the SCN is classically divided into two subregions, 'core' and 'shell' based on neuropeptide content and retinal innervation. In this early scheme, a ventrally positioned 'core' nucleus is densely innervated by efferent ipRGCs and immunoreactive for vasoactive polypeptide (VIP) whilst the dorsally positioned 'shell' is sparsely innervated by ipRGCs and is immunoreactive for arginine vasopressin (AVP; Vandesande et al., 1975; Samson et al., 1979; Silver et al., 1999). Mouse SCN architecture is similarly described to consist of 'core' and 'shell' subregions and shows analogous localization of AVP and VIP as in hamster and rats, however the discrete localization of gastrin releasing peptide (GRP) centrally within the SCN renders this terminology less appropriate (Abrahamson and Moore, 2001; Morin et al., 2006; Morin, 2007). Here we refer to the VIP enriched ventral subregion as 'SCNv', the AVP enriched dorsal subregion as 'SCNd', and the GRP enriched central region as 'SCNce'.

Functional characterization of these neuropeptides has provided insight into their respective subregion's role in central pacemaker operation. The best characterized example, VIP, together with its cognate receptor VPAC2 is required for maintaining daily rhythms in locomotor activity. A role for VIP has been shown in coupling and maintaining stable phase relationships between SCN neurons (Harmar et al., 2002; Aton et al., 2005; Colwell et al., 2003). A similar role has been shown for GRP, in addition to a role in 'gating' the SCN's

response to photic stimuli in early and late evening which elicits phase delays and advances respectively (Brown et al., 2005; Antle et al., 2005; Maywood et al., 2006; Drouyer et al., 2009; Drouyer et al., 2010). The phasing and light responsiveness of the molecular oscillator within individual SCN neurons demonstrates similar differences between subregions that mirror the spatial subdivisions of the SCN by neuropeptide content (Yamaguchi et al., 2003; Yan et al., 2007; Noguchi and Watanabe, 2008). The tightly regulated temporal and spatial coordination of *Per1* expression in the SCNd (Yamaguchi et al., 2003) support a role in endogenous rhythm generation, particularly given its *pari parssu Per* and C*ry* gene expression with locomotor activity (Yan and Silver, 2002; Reddy et al., 2002; Yan and Silver, 2004) and sustained rhythms in constant conditions in hamsters. In contrast, *Per1* and *Per2* are immediately induced by light in SCNv but do not sustain rhythms in constant conditions (Yan and Silver, 2002; Yan and Silver, 2004; Hamada et al., 2001) suggesting a function in light receipt. Of particular interest is the differential response by SCNv and SCNd during re-entrainment. Light pulses in the early subjective evening (CT14) which elicit a phase delay in behavioral rhythms over subsequent days show a coherent response of *Per* and *Cry* peak phase of expression between SCNd, SCNv and behavioral rhythms. However, light pulses delivered in late subjective evening (CT22), eliciting a phase advance, show a differential response of *Per* and *Cry* in SCNd and SCNv: SCNv responds immediately, showing *Per1/2* and *Cry1/2* induction in phase with the 'new' light regime, whereas the SCNd does not; lagging behind with the 'old' light regime, taking several days to accelerate to the SCNv's advanced phasing (Reddy et al., 2002; Yan and Silver, 2002; Kuhlman et al., 2003). Clearly the functional differences identified between subregions of the central pacemaker also have common borders aligned with those defined by AVP, VIP and GRP localization.

Characterization of SCN function, including the roles played by subregions toward this function have proceeded along two lines: single molecular study and global analyses. Molecular studies closely scrutinize, 'bottom up', the activity of a few molecules e.g. clock mRNAs or proteins, assaying quantity, localization or interactions. These studies have revealed a heterogeneous and functionally subdivided SCN as discussed above but require unifying towards a holistic understanding of the SCN. In contrast, global analyses broadly assay, 'top down', quantities of several thousand molecules of a single species, e.g. mRNA. Transcriptional profiling has thus proven invaluable in characterizing circadian systems by revealing the circadian transcriptome of both whole SCN and peripheral organs (Panda et al., 2002; Storch et al., 2002; Ueda et al., 2002), as well as its response to a phase shifting stimulus (Morris et al., 1998; Araki et al., 2006; Porterfield et al., 2007). Although these global analyses have broadened understanding of the central pacemaker they have, so far, failed to unify existing SCN knowledge, especially for environment synchronization.

In attempting to deepen understanding of subregion functioning and to unify existing data we detail our highly specific, sensitive and robust method of transcriptional profiling of SCNv, SCNd and SCNce subregions. We demonstrate the success of our method by confirming the expression of genes known to be localized within these subregions. In addition, we present unique transcriptional signatures identified for each subregion and biological themes suggested by these signatures.

RESULTS AND DISCUSSION

SCN collection and subregion isolation

To assay global transcription levels in ventral, dorsal and central SCN subregions mice were entrained to a 12 hour light, 12 hour dark (LD 12:12) regime whilst circadian locomotor behavior was monitored with a freely available running wheel. To eliminate gene expression arising from light input, mice were subsequently held in constant darkness (DD) for 7 days before collecting brain samples at CT22 and CT2 (Figure 1). We chose these time points for two reasons: First, light pulses delivered at CT22 produce a unique, differential response from the SCNv and SCNd as described above. A snapshot of global transcriptional levels in these subregions at this time may provide insight in the mechanism underlying this differential response and aid in future studies of phase advances and re-entrainment. Second, the subregion markers *Vip* and *Avp* show peak expression mid-evening (ZT/CT20, (Takahashi et al., 1989; Glazer and Gozes, 1994; Dardente et al., 2004) and mid-day (ZT/CT6, (Tominaga et al., 1992; Smith and Carter, 1996; Jin et al., 1999) respectively. Given the use of VIP and AVP here to delineate subregion selection; for *a posteriori* estimation of the accuracy of subregion mRNA isolation methodology we needed to ensure these marker mRNAs with known circadian regulation were present in detectable quantities by collection of samples around their peak phase of expression.

For optimal SCN subregion identification and isolation we attempted a rapid staining procedure (Fend et al., 1999) to directly visualize the neuropeptides defining these regions (data not shown). Rapid staining conditions that minimize RNA degradation, including acetone or ethanol fixation, did not allow visualization of AVP or VIP content with available antisera. This is likely due to the precipitating nature of alcohols which clear free–protein, presumably including AVP and VIP. However the neuron density and morphology of these

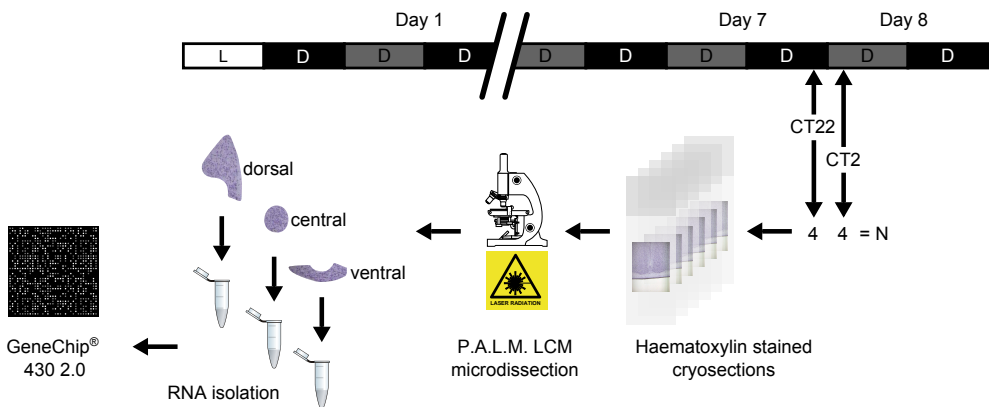**Figure 1. Work flow schema.** Mice entrained to standard LD12:12 regime were placed in constant conditions for seven days. Brain collection was performed under dim red light illumination at CT22 and CT2. Haematoxylin stained cryosections were microdissected, the RNA purified and hybridized to Affymetrix 430 2.0 GeneChips. Daily scheduling black shading indicates (subjective) evening; gray, subjective day; and white, light exposure.

SCN subregions closely parallels AVP and VIP content and is clearly discernible after rapid haematoxylin staining. During subregion microdissection we used previously prepared anti-VIP and anti-AVP stained SCN sections (Figures 2A and 2B) to guide subregion dissection of haematoxylin stained cryosections. Ventral, dorsal and central subregions were captured sequentially (Figures 2D, 2E and 2F) from six 25μm mid-rostro/caudal coronal cryosections mounted on PALM-PEN membrane slides. Captured subregions were immediately lysed and stored at -80 ºC for subsequent RNA isolation and amplification. Addition of an RNA carrier species was employed to maximize recovery of sample RNA during purification by column filtration. We used purified bacterial ribosomal RNA (20ng per sample) as a carrier species. Other commonly used carriers ie., polyinosinic acid (Winslow and Henkart, 1991) and poly-dT (2000-5000) appeared to interfere with RNA amplification and reduce yield. As co-purified genomic DNA appeared to reduce specific amplification of mRNAs, DNase digestion was employed during purification to minimize unwanted genomic DNA amplification.
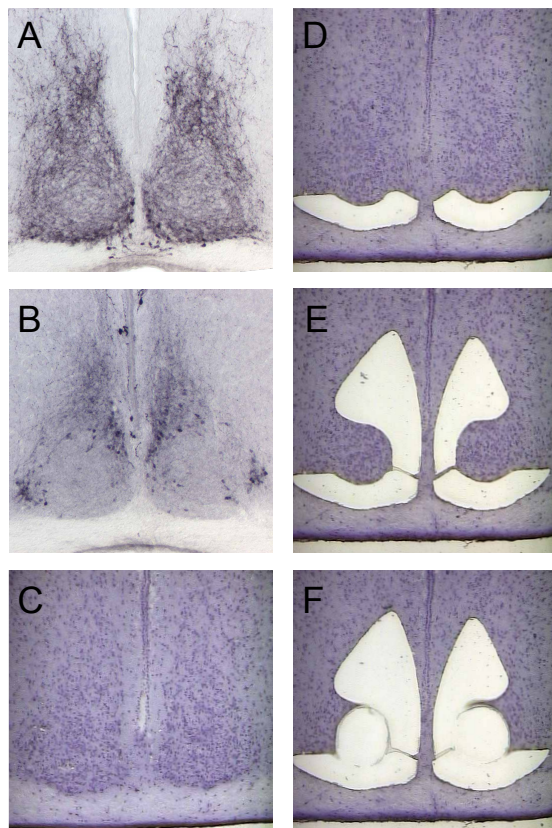

Figure 2. Laser Catapult Microdissection (LCM) of SCN subregions. Example anti-VIP (A) and anti-AVP (B) stained SCN used to aid identification of these regions in haematoxylin stained cryosections. Representative Haematoxylin stained cryosections of the SCN collected at CT22 and CT2, prior to (C) and after LCM of ventral (D), dorsal (E) and central (F) sub-regions.

Subregion quality control

Purified total RNA integrity was assayed using the Bioanalyser 'Pico' chip. Representative ventral, dorsal and central RNA Pico chip assays are shown in Figures 3A, 3B and 3C. As the amount of RNA recovered was sufficient for subsequent amplification only, determined during pilot studies to be approximately 1ng of total RNA, no further sample was used for quality control purposes, ie. quantification. Universal Mouse Reference RNA (UMR) was purified along side laser catapult microdissection (LCM) isolated subregions and used throughout sample preparation for microarray analysis as a positive control. Pico chip analysis of co-purified UMR, of which 20ng was used, was qualitatively similar to those obtained for LCM isolated subregions (Figure 3D). As RNA samples with 18S/28S ribosomal peaks evident by Pico chip analysis consistently amplified successfully, including the UMR
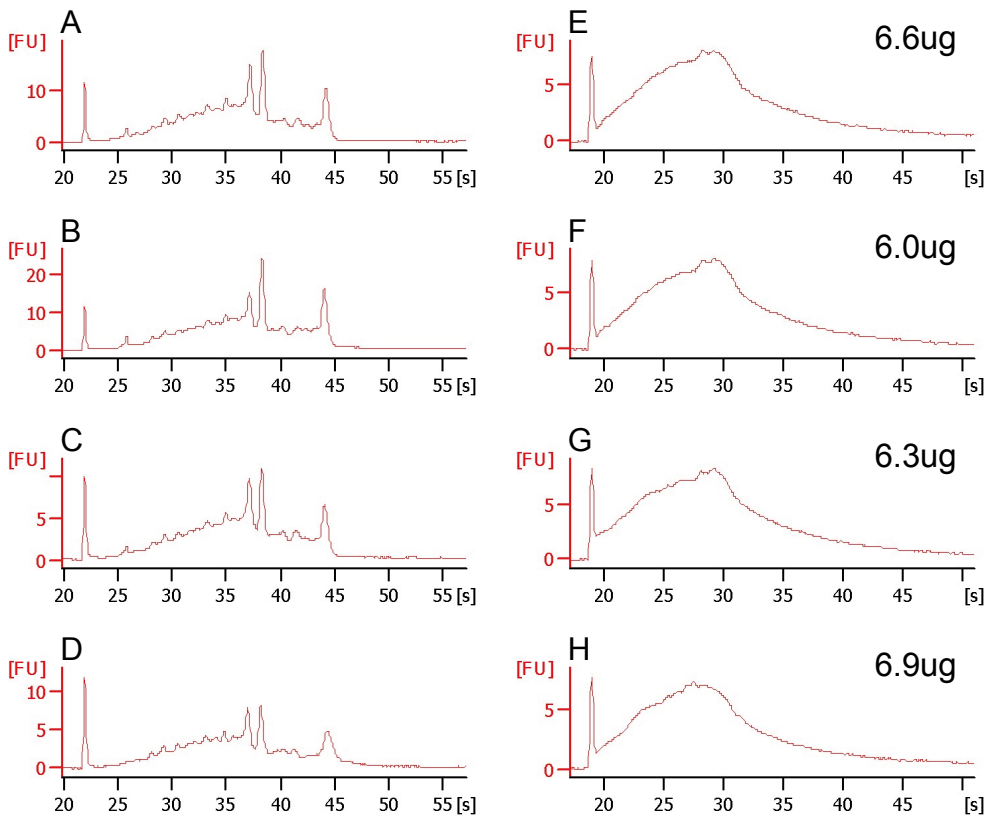
Figure 3. Bio-analsyzer assay of purified sub-region total RNA and amplified cDNA quality. Bioanalzyer RNA Pico chip profiles of purified total RNA from SCN ventral (A), dorsal (B) and central (B) sub-regions. Detectable 18S (visible at 38 seconds) and 28S (visible at 44 seconds) peaks above the 'background' bacterial rRNA demonstrate recovery of intact purified sample RNA. The 16S (lowest peak) rRNA carrier species is also visible. Bioanalyser profiles of cDNA product after single cycle Ribo-SPIA amplification from SCN ventral (E), dorsal (F) and central (G) sub-regions. Universal human reference RNA (UHR) was co-purified and used throughout RNA isolation (D) and amplification (H) procedures as a positive control. cDNA yield estimated by 260/280nm Nandrop quantification is shown for respective samples.

positive control, samples with such 18S/28S ribosomal peaks were deemed worthwhile for amplification, which was virtually all LCM samples obtained in our laboratory as described above (see also Materials and Methods).

Previous microarray analyses of the SCN were performed on samples from two or more animals obtained using a punch biopsy (Panda et al., 2002; Storch et al., 2002; Ueda et al., 2002; Araki et al., 2006; Morris et al., 1998) or from microdissected SCN (Porterfield et al., 2007). Pooling is typically required because of the paucity of RNA available from the approximate 20,000 neurons that constitute the mouse SCN. Unfortunately, pooling biological replicates has been shown to decrease sensitivity (Shih et al., 2004; Kendziorski et al., 2005). An alternative to pooling is employing additional rounds of amplification. However, as amplification is not linear, especially for oligo-dT based amplifications commonly used, each additional round doubles the bias of transcript amplification resulting in the reduction or loss of representation of moderate and low abundance mRNA species. For this reason we employed a single cycle Ribo-SPIA based protocol (Dafforn et al., 2004). This method is sufficiently powerful to generate enough cDNA for GeneChip analysis from the ~1 ng total RNA obtained from each SCN subregion, per mouse. Bioanalyser Nano chip assay of the purified cDNA product indicated an average fragment size of ~900bp for all subregions (Figures 3E, 3F and 3G) and the UHR positive control (Figure 3H). Amplification yield correlated with product length, where 5µg or more cDNA was generated from specific, efficient amplification of target mRNA's. This is consistent with the manufacturers suggested yield for specific amplification of target mRNAs. The Nanodrop quantification is shown for each sample on the respective Bioanalyser assay for all subregions and the UMR positive control (Figures 3E, 3F, 3G and 3H). Notably, the fragment profile closely resembles that of purified mRNA (Agilent compendium) suggesting amplification with minimal bias compared to T7-polymermase based amplification methods.

Verification of Avp, Vip and Grp localisation

Unpurified cDNA amplification product was assayed by SYBR green based quantitative PCR (Q-PCR) for expression of canonical SCN markers AVP, VIP and GRP. This was undertaken before hybridizing amplified cDNA to microarrays to determine our success in separating ventral, dorsal and central SCN using cDNA derived from biological replicates (n=2). To date there is limited data available for mRNA localization within the mouse SCN for these genes. *In situ* hybridization localization of AVP and VIP parallels peptide localization (Kraves and Weitz, 2006). We consider recapitulation of the relative expression differences for these markers indicative of successfully isolating these SCN subregions. Figure 4 details expression fold change of these marker genes normalized for RNA loading quantity by *hypoxanthine guanine phosphoribosyl transferase (HPRT)*. The expression differences we observed for these markers relative to the subregion for which its expression is expected to be enriched can be summarized as: VIP ventral vs dorsal shows +5.5 and ventral vs central +6.5 fold differential expression; AVP shows dorsal vs ventral +4.4 and dorsal vs central +6.2 fold differential expression; and GRP shows central vs ventral +2.9 and central vs dorsal +4.8 fold differential expression. Importantly, the relative expression differences of
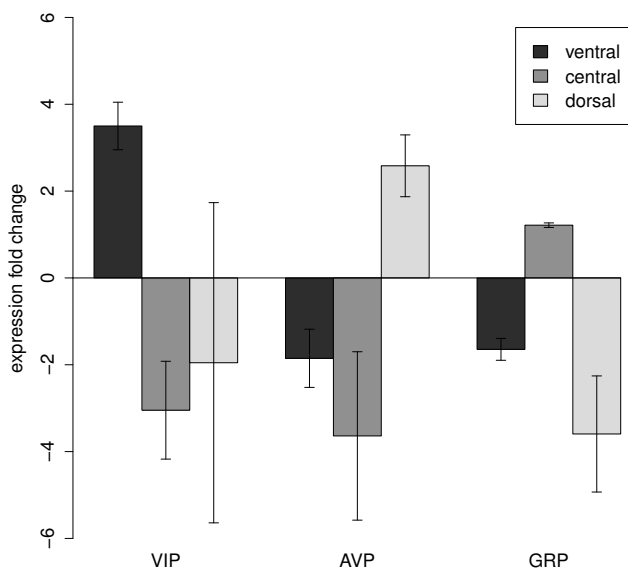
Figure 4. Q-PCR assay of marker genes. *Avp*, *Vip* and *Grp* expression fold changes relative to *HPRT* were assayed using SYBR green based RT-QPCR to confirm the successful capture of ventral, central and dorsal SCN subregions.

AVP, VIP and GRP reflect what would be expected from observed protein expression in these subregions thus validating our approach (Karatsoreos et al., 2004; Morin et al., 2006; Abrahamson and Moore, 2001).

Microarray analysis of subregions

Amplified cDNA was biotin labeled, fragmented and hybridized to Affymetrix 430 2.0 arrays according to the manufacturers protocols. Data normalization and probe set expression summarization was performed using the r̲obust m̲ulti-array a̲verage (RMA) expression measure (Irizarry et al., 2003). To identify regionally enriched gene expression during late evening/early day for each SCN subregion we combined several criteria described below. Notably, we combined data obtained from samples collected at CT22 and ~CT2 since we propose a region specific marker should remain thus, irrespective of time, exactly as canonical markers AVP, VIP and GRP do. First, to remove transcripts assumed to be of no interest in this study, that is with the lowest differential expression between subregions, probe sets with variance $S^2 < 0.55$ across all arrays were discarded as per (Bourgon et al., 2010). Second we sought to identify significant differences in probe set expression between subregions. To achieve this we combined the two replicates of each batch (four in total) for analysis to gain maximum statistical power from the greater replication (n). A linear mixed-effects (LME) model was employed to separate 'batch effect' (level 1) from 'region effect' (level 2) without assuming equal variance across, or interaction between levels. Thus expression data were RMA normalized per batch and a two level LME model fitted to determine the significance of gene expression between regions without the effect of batch. Third, to control for multiple testing the Benjamini-Hochberg method was applied at $p < 0.01$ (Benjamini and Hochberg, 1995). Finally, to enrich for differentially expressed probe sets with large differences between subregions, probe sets lacking fold changes (FCs) of >

1.8 or < -1.8 between any two subregions were discarded. In so doing we defined a total of 581 S̲CN S̲ub-region E̲nriched E̲xpression T̲ranscripts (SEETs) as having *increased* expression, ie. positive fold-change, in one subregion versus either one or both other sub-regions, where 254, 163 and 164 SEETs were identified for ventral, central and dorsal SCN subregions respectively (Online Supplementary Table 1). SEET expression profiles were hierarchically clustered by probe set and subregion according to (Eisen et al., 1998) and presented as a heat map to illustrate the unique transcription signatures determined for each subregions (Figure 5A). Probe sets for *Avp* (1450794_at), *Vip* (1428664_at) and *Grp* (1424525_at) are included in the SEETs list. These show +2.3 fold dorsal vs ventral and +4.0 fold dorsal vs central *Avp* enriched expression, i.e. dorsally enriched. *Vip* shows +8.9 fold ventral vs dorsal and +1.5 fold ventral vs central enriched expression ie., ventral enrichment. And *Grp* shows +1.8 fold central vs ventral and +4.7 central vs dorsal enriched
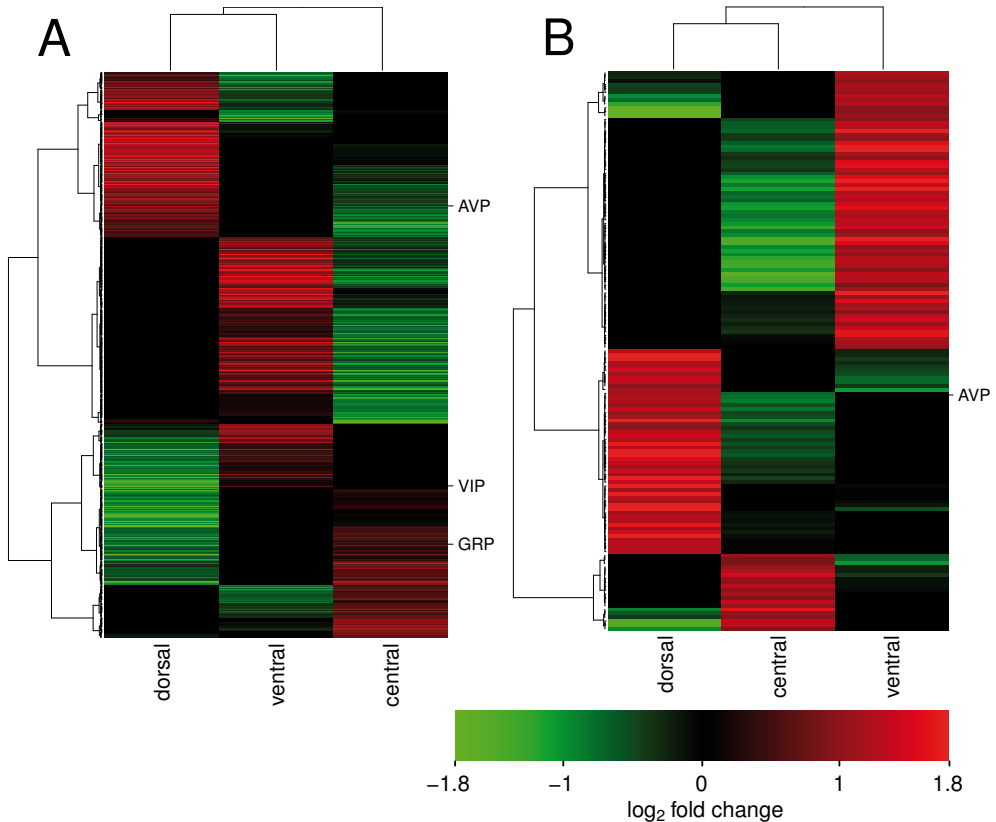
Figure 5. Heat-map visualization of transcription profiles unique for each SCN sub-region. Unsupervised hierarchical clustering of the 581 transcripts with expression difference of at least 1.8 fold in one region versus either of the two other regions (A) enabling visualization of genes with enriched expression in ventral, dorsal or central. Hierarchical clustering of the 145 transcripts with an expression difference of at least 1.8 fold in one region versus both other regions, clarifying transcripts with specific expression in either core, middle or shell (B). Expression profiles for AVP, VIP and GRP are indicated. Bright red indicates over-expression and bright green under-expression relative to mean expression levels between subregions. Black represents mean expression level across subregions.

expression, i.e., is centrally enriched. Taken together these GeneChip results correlate well with the Q-PCR assay of these transcripts with a Spearmans rho = 0.94 (p value = 0.017) and thus with respective peptide localization shown by us and others (Figure 2A and B; (Abrahamson and Moore, 2001). Besides the known subregion markers our data confirm the SCNce localization identified for the androgen receptor (AR; Karatsoreos et al., 2007), which we show has +1.9 fold central vs ventral and +3.2 fold central vs dorsal enrichment. Given the parity of our microarray and Q-PCR data described above together with the peptide localization data shown by others, these 581 transcripts may reveal new insight into the unique functioning within these SCN subregions which we investigate (below) by assessing these transcripts for overrepresentation of their respective annotation terms. To identify transcripts with *highly* enriched subregion expression we further refined these c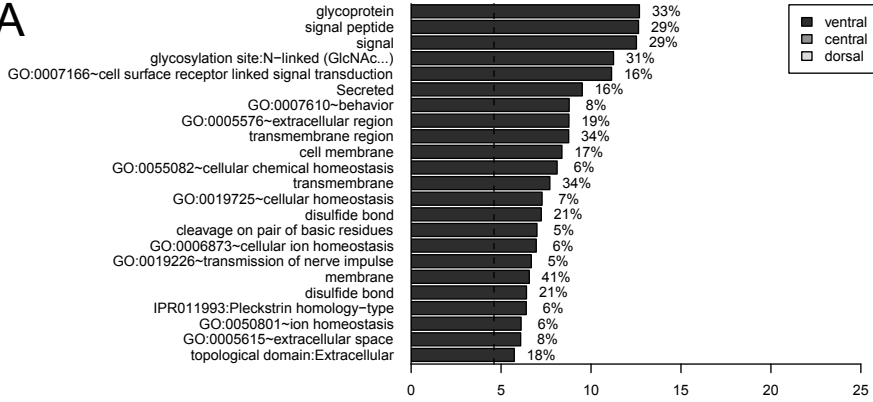riteria to include only those transcripts showing at least 1.8 fold increased expression in one region versus *both* other regions (Online Supplementary Table 2) and cluster these as we did for the SEETs (Figure 5B). Of the 72 SCNv, 20 SCNce and 53 SCNd transcripts (145 total) we define here as 'SCN subregion Highly Enriched Expression Transcripts' (SHEETs), AVP is the only known subregion marker present. This is appropriate given the virtually exclusive peptide localization in SCNd (Figure 2B) compared for example to VIP, which although enriched in SCNv, is also clearly evident in SCNd (Figure 2A). Notably, AR also fulfills this criterion thus representing an SCNce highly enriched marker. The SHEETs are ideal candidates as novel alternatives to the known subregion markers, AVP, VIP and GRP, and may improve on the specificity of these markers for subregion specific expression. Of note, there are around 50% more SEETs and SHEETs in SCNv than SCNd or SCNce.

Analysis of biological themes

To explore biological processes suggested by known and putative SEET and SHEET functions we tested which Gene Ontology (GO) and KEGG terms annotated with these probe sets were over represented using DAVID (Huang et al., 2009a, 2009b). Over-represented GO terms (q < 0.05) identified for each sub-region are shown in Figure 6A, and for SHEETs in Figure 6B. Over-represented terms for SHEETs for each subregion were clustered using the DAVID 'Annotation Clustering' tool which clusters annotation terms by similarity of function and thus over-presented terms contained therein. This effectively highlights the most prominent over-represented annotation terms. In the SCNv over-representation of the 'myelin basic protein' and 'GO:0042552 myelination' term might be expected given the dense innervation of highly myelinated RHT projections from the retina projecting to neurons of this subregion (Hartwig, 1974). In SCNce the most prominent terms identified involve signaling, membrane based receptors ie., terms 'G protein-couple receptor 83', 'poliovirus receptor-related 132C', 'signal' and 'signal peptide'. This dovetails well with SCNce putative function in relaying photic input signals from the SCNv to the SCNd-the ability to both receive humoral signals and secrete them (Piggins et al., 1995; Antle et al., 2005). Over-represented terms obtained from the SCNd subregion are more cryptic. As this regions role is primarily in rhythm generation - maintaining a coherently phased population of rhythmic oscillator - and whilst the intracellular function of the molecular

A

B

GO:0043209~myelin sheath — 7%
GO:0007272~ensheathment of neurons — 9%
GO:0008366~axon ensheathment — 9%
GO:0019228~regulation of action potential in neuron — 9%
GO:0001508~regulation of action potential — 9%
GO:0019911~structural constituent of myelin sheath — 5%
signal — 38%
signal peptide — 38%
GO:0006873~cellular ion homeostasis — 13%
GO:0055082~cellular chemical homeostasis — 13%
GO:0042552~myelination — 7%
GO:0050801~ion homeostasis — 13%
disulfide bond — 31%
cleavage on pair of basic residues — 11%
cell membrane — 25%
GO:0042391~regulation of membrane potential — 9%
disulfide bond — 31%
transmembrane protein — 13%
GO:0019725~cellular homeostasis — 13%
GO:0030247~polysaccharide binding — 9%
GO:0001871~pattern binding — 9%
GO:0048878~chemical homeostasis — 13%
Secreted — 22%
glycoprotein — 36%
GO:0030246~carbohydrate binding — 11%
GO:0033267~axon part — 5%

legend: ventral / central / dorsal

glycosylation site:N−linked (GlcNAc...) — 59%
glycoprotein — 59%
GO:0007156~homophilic cell adhesion — 18%
GO:0047238~glucuronosyl−N−acetylgalactosaminyl (abreviated) — 12%

GO:0043005~neuron projection — 18%
GO:0030425~dendrite — 14%
mmu04080:Neuroactive ligand−receptor interaction — 16%
GO:0042165~neurotransmitter binding — 11%
GO:0030594~neurotransmitter receptor activity — 11%
lipoprotein — 20%
GO:0042995~cell projection — 20%
GO:0045202~synapse — 16%
cell membrane — 30%
glycoprotein — 43%
lipid moiety~binding region:S−palmitoyl cysteine — 11%
glycosylation site:N−linked (GlcNAc...) — 41%
palmitate — 11%
GO:0046903~secretion — 11%
GO:0005886~plasma membrane — 36%
GO:0007186~G−protein coupled receptor protein signaling pathway — 16%
GO:0008188~neuropeptide receptor activity — 7%
GO:0042923~neuropeptide binding — 7%
GO:0043025~cell soma — 9%
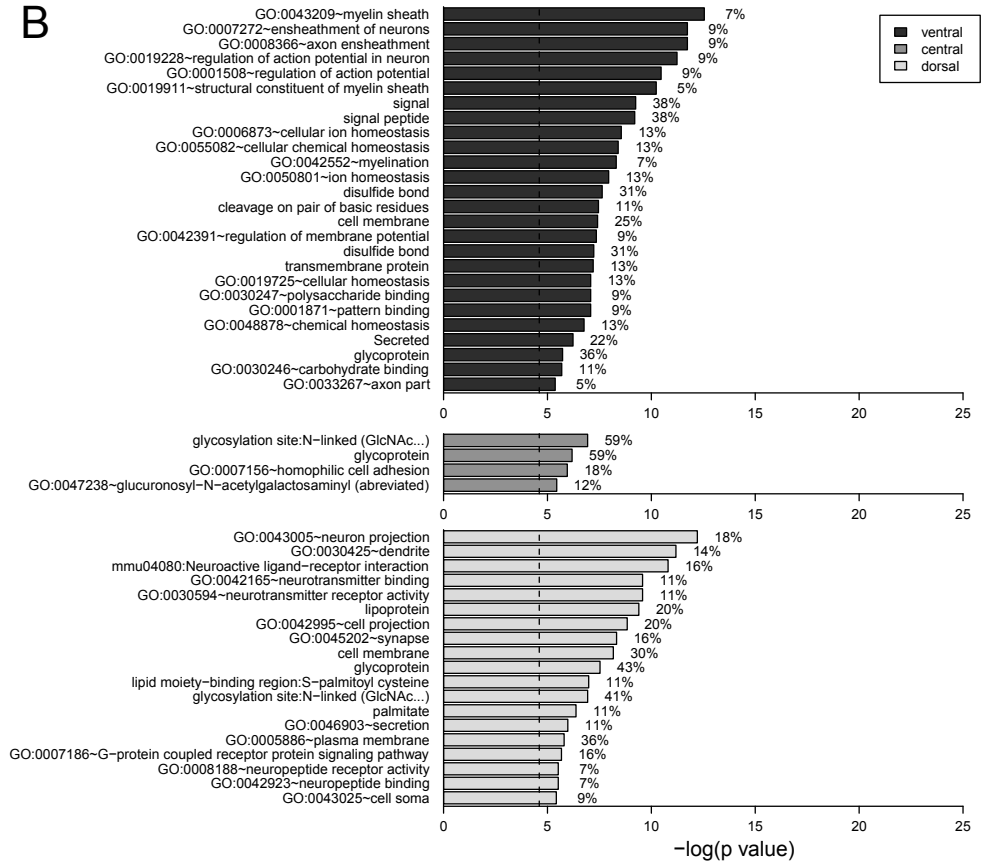
−log(p value)

Figure 6. Over representation bar-plot of biological processes in SCN sub regions. Differentially expressed gene's enriched for expression in one region versus either of the two other regions, ie., SEETs (A) or one region versus both other regions, ie., SHEETs (B) were assessed for over-representation of Gene Ontology and other annotation terms using DAVID (see Materials and Methods). Significantly over-represented annotation terms (false discovery rate < 5% and percent representation of 430 2.0 GeneChip > 5%) are plotted, most significant to least significant (Fishers Exact test), for each subregion. Dashed line corresponds to a p-value of 0.01. Percentage over-representation indicated for each annotation right side of the bar-plot.

clock has been well characterized, the physiology of the tissue has not. The majority of the terms demonstrate neuronal function as would be expected e.g., 'GO:0045202~synapse', however further study of specific genes will be required in interpreting the role they play in SCNd functioning.

CONCLUSION

Ultimately we will move to a characterization at the single cellular level as we refine this method. Until this time we present 'poly-cellular' (hundreds of cells) resolution to clarify overall function in attempting to unify the vast quantity of molecular level details.
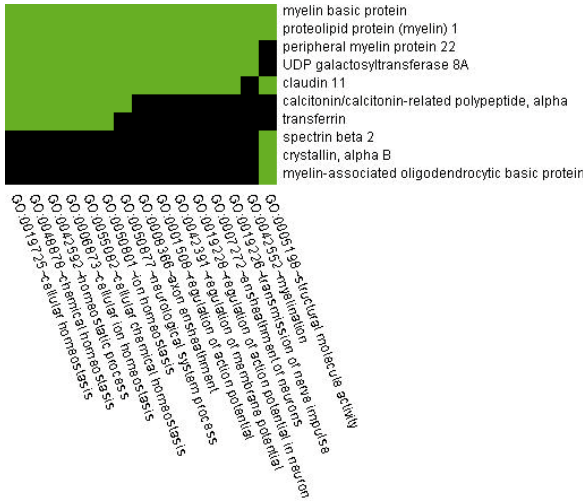
A

Figure 7. Heat-map visualization of differentially regulated processes in SCN subregions. Hierarchical clustering of over and under-represented Gene Ontology Biological Process (GO_BP) terms for SHEETs, as listed in Figure 6B, were assessed using the DAVID Annotation Clustering for SCNv (A), SCNce (B) and SCNd (C) subregions. Clustered GO_BP terms are plotted on the abscissa and significantly differentially expressed genes responsible for these terms plotted on the ordinate.

B
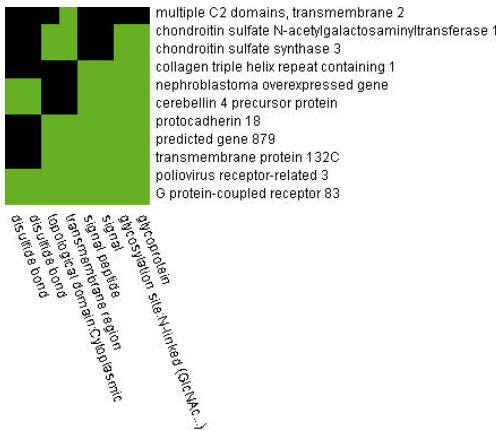
C
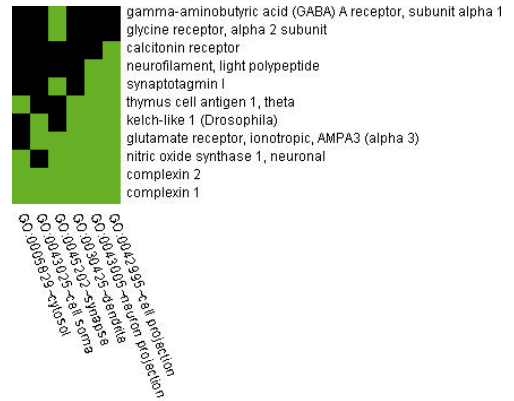
Furthermore, these data can aid in identifying novel SCN specific, or subregion specific genes for potential use in generating conditional mouse models (Gu et al., 1993; Schwenk et al., 1995).

MATERIALS AND METHODS

Animals

All procedures with animals were performed in accordance with Erasmus University Medical Center, The Netherlands, animal welfare guidelines. Eight C57BL/6JOlaHsd (Harlan, Horst, The Netherlands) male 8-week old mice were placed in cages with running wheels housed in a 12:12 light/dark cycle (12:12 LD) for at least two weeks before being transferred to constant

conditions under dim red light illumination. After 7 days in constant conditions animals were euthanized by decapitation at CT22 and CT2, the brains rapidly removed, snap frozen on dry ice and stored at -80 °C for subsequent cryosectioning. Clock Lab software (Actimetrics) was used to monitor locomotor behavior, calculate free running period and estimate CT22/2 for brain collection of each mouse. Food and water were supplied *ad libitum*.

Isolation of SCN subregions.

25µm coronal cryrosections mounted on 1 mm PALM pen-membrane slides were rapidly thawed, fixed for 30s in 70% EtOH and stained with haematoxylin for 3min. Following staining sections were rinsed in DEPC treated dH$_2$O and dehydrated by several rinses in 100% EtOH. Laser catapult microdissection (LCM) of vento-medial, dorso-lateral and mid-ventro-dorsal SCN subregions was accomplished using the PALM Microlaser system on freshly prepared sections. Isolated SCN subregions were dissolved immediately in Lysis Buffer (Qiagen) and stored at –80ºC for subsequent RNA purification. RNA was purified with the inclusion of 'on-column' DNase treatment using the Qiagen RNeasy Micro kit according the manufacturers protocol, except that 20 ng of 16s/23s bacterial ribosomal RNA (Roche) was used as carrier and an additional elution was performed in the final step to maximize RNA yield. RNA eluted with RNase free dH$_2$O was vacuum evaporated for immediate amplification and cDNA generation.

Amplification and labeling of purified RNA samples.

Quality of the freshly purified RNA was assayed using the BioAnalyzer (Agilent) in combination with the RNA 'Pico' chip. Where intact 18S/28S ribosomal RNA peaks were evident, the sample was considered worthy of amplification and labeling. Amplification and cDNA labeling with biotin was accomplished using the Ovation RNA Amplification System V2 and FL-Ovation cDNA Biotin Module V2 respectively according to the manufacturers protocols (Nugen Technologies). Efficiency of the amplification was assayed quantitatively by 260/280 nm estimation of cDNA concentration, where a yield of at least 5µg cDNA was deemed sufficient for specific amplification of the RNA template.

Hybridization of Biotin labeled cDNA samples.

Biotin labeled cDNA samples were combined with hybridization cocktail including DMSO according to the manufacturers protocol (Nugen Technologies) and hybridized to Affymetrix GeneChip 430_2.0 arrays for 18hrs. Post-hybridization washing, scanning and image analysis were performed as according to the Affymetrix fluidics protocol FS450_0004. Expression measures were exported using the MAS5.0 software suite (Affymetrix), and normalized per batch using the Robust Multichip Average (Irizarry et al., 2003) running in the R version 2.11.1 environment.

Quantitative RT-PCR

Amplification and complementary DNA strand synthesis of purified sample RNA was accomplished using the Ovation RNA Amplification System V2 according to the

manufacturer's protocol except where the final cDNA purification step was omitted. Unpurified cDNA template was assayed using a SYBR green PCR mastermix (Applied Biosystems) according to the manufacturers protocol using the following primers: VIP (F, 5'-GCA TCG CCT ATA CGT CCA TCT AG-3', R, 5'-GCG CTC TTC TAC GTC CAT CTA G-3'), AVP (F, 5'-GCA TCG CCT ATA CGT CCA TCT AG-3', R, 5'-GCA TCG GCT TAT ATA TTA G-3'), GRP (F, 5'-GCA TCG GCA TAG CTC CCT CTA G-3', R, 5'-GCG TTT TAT CGA TAC GTC CAT CTA G-3') and HPRT (F, 5'-ATC GCT AGG CTA CGT CCA TCT AG-3', R, 5'-GCA TCG CCT ACG TTT CAA CTG GC-3').

Statistical analysis

Significant expression differences between SCN subregions were identified by applying a 2-level linear mixed effects model to the individually normalized 'per batch' datasets . Level 1 assessed the effect of hybridization batch whilst level 2 assessed the effect of region. This allowed the greatest statistical power to be derived from the 4 biological replicates assayed despite the significant expression differences identified between the two sets of duplicates when level 1 (effect of hybridization batch) was excluded.

Hierarchical Clustering

Expression profiles were hierarchically clustered by subregion and probe set using Pearson's product-moment correlation coefficient as a distance metric and average linkage according to (Eisen et al., 1998).

Gene Ontology (GO) over-representation analysis.

Differentially expressed probes sets (SEETs and SHEETs, q < 0.01) with fold changes greater than 1.8 were assessed for overrepresentation of terms from the Gene Ontology database for Biological Process (GO_BP) and KEGG database using DAVID (Harris et al., 2004; Kanehisa and Goto, 2000; Kanehisa et al., 2007; Huang et al., 2009a, 2009b).

## Online Supplementary Material

Supplementary tables are available at http://bioinf-quad07.erasmusmc.nl/scn/

ACKNOWLEDGMENTS

REFERENCES

Abrahamson, E. E., and Moore, R. Y. (2001). Suprachiasmatic nucleus in the mouse: retinal innervation, intrinsic organization and efferent projections. Brain Research *916*, 172-191.

Agilent, Agilent 2100 Bioanalyzer - Application Compendium. Available at: http://www.chem.agilent.com

Albrecht, U., Zheng, B., Larkin, D., Sun, Z. S., and Lee, C. C. (2001). mPer1 and mPer2 Are Essential for Normal Resetting of the Circadian Clock. J Biol Rhythms *16*, 100-104.

Antle, M. C., Kriegsfeld, L. J., and Silver, R. (2005). Signaling within the Master Clock of the Brain: Localized Activation of Mitogen-Activated Protein Kinase by Gastrin-Releasing Peptide. The Journal of Neuroscience *25*, 2447 -2454.

Antle, M. C., and Silver, R. (2005). Orchestrating time: arrangements of the brain circadian clock. Trends in Neurosciences *28*, 145-151.

Araki, R., Nakahara, M., Fukumura, R., Takahashi, H., Mori, K., Umeda, N., Sujino, M., Inouye, S.-I. T., and Abe, M. (2006). Identification of genes that express in response to light exposure and express rhythmically in a circadian manner in the mouse suprachiasmatic nucleus. Brain Research *1098*, 9-18.

Aton, S. J., Colwell, C. S., Harmar, A. J., Waschek, J., and Herzog, E. D. (2005). Vasoactive intestinal polypeptide mediates circadian rhythmicity and synchrony in mammalian clock neurons. Nat Neurosci *8*, 476-483.

Benjamini, Y., and Hochberg, Y. (1995). Controlling the False Discovery Rate: A Practical and Powerful Approach to Multiple Testing. Journal of the Royal Statistical Society. Series B (Methodological) *57*, 289-300.

Bourgon, R., Gentleman, R., and Huber, W. (2010). Independent filtering increases detection power for high-throughput experiments. Proceedings of the National Academy of Sciences *107*, 9546 -9551.

Brown, T. M., Hughes, A. T., and Piggins, H. D. (2005). Gastrin-Releasing Peptide Promotes Suprachiasmatic Nuclei Cellular Rhythmicity in the Absence of Vasoactive Intestinal Polypeptide-VPAC2 Receptor Signaling. The Journal of Neuroscience *25*, 11155 -11164.

Colwell, C. S., Michel, S., Itri, J., Rodriguez, W., Tam, J., Lelievre, V., Hu, Z., Liu, X., and Waschek, J. A. (2003). Disrupted circadian rhythms in VIP- and PHI-deficient mice. Am J Physiol Regul Integr Comp Physiol *285*, R939-949.

Dafforn, A., Chen, P., Deng, G., Herrler, M., Iglehart, D., Koritala, S., Lato, S., Pillarisetty, S., Purohit, R., Wang, M., et al. (2004). Linear mRNA amplification from as little as 5 ng total RNA for global gene expression analysis. BioTechniques *37*, 854-857.

Dardente, H., and Cermakian, N. (2007). Molecular circadian rhythms in central and peripheral clocks in mammals. Chronobiol Int *24*, 195-213.

Dardente, H., Menet, J. S., Challet, E., Tournier, B. B., Pévet, P., and Masson-Pévet, M. (2004). Daily and circadian expression of neuropeptides in the suprachiasmatic nuclei of nocturnal and diurnal rodents. Molecular Brain Research *124*, 143-151.

Drouyer, E., LeSauter, J., Hernandez, A. L., and Silver, R. (2010). Specializations of gastrin-releasing peptide cells of the mouse suprachiasmatic nucleus. The Journal of Comparative Neurology *518*, 1249-1263.

Drouyer, E., LeSauter, J., Hernandez, A. L., and Silver, R. (2009). Specializations of gastrin releasing peptide cells of the mouse suprachiasmatic nucleus. J. Comp. Neurol., NA-NA.

Eisen, M. B., Spellman, P. T., Brown, P. O., and Botstein, D. (1998). Cluster analysis and display of genome-wide expression patterns. Proceedings of the National Academy of Sciences of the United States of America *95*, 14863-14868.

Fend, F., Emmert-Buck, M. R., Chuaqui, R., Cole, K., Lee, J., Liotta, L. A., and Raffeld, M. (1999). Immuno-LCM: Laser Capture Microdissection of Immunostained Frozen Sections for mRNA Analysis. Am J Pathol *154*, 61-66.

Foster, R. G., and Hankins, M. W. (2007). Circadian vision. Curr Biol *17*, R746-51.

Glazer, R., and Gozes, I. (1994). Diurnal oscillation in vasoactive intestinal peptide gene expression independent of environmental light entraining. Brain Res *644*, 164-167.

Gu, H., Zou, Y.-R., and Rajewsky, K. (1993). Independent control of immunoglobulin switch recombination at individual switch regions evidenced through Cre-loxP-mediated gene targeting. Cell *73*, 1155-1164.

Hamada, T., LeSauter, J., Venuti, J. M., and Silver, R. (2001). Expression of Period Genes: Rhythmic and Nonrhythmic Compartments of the Suprachiasmatic Nucleus Pacemaker. J. Neurosci. *21*, 7742-7750.

Hankins, M. W., Peirson, S. N., and Foster, R. G. (2008). Melanopsin: an exciting photopigment. Trends in Neurosciences *31*, 27-36.

Harmar, A. J., Marston, H. M., Shen, S., Spratt, C., West, K. M., Sheward, W. J., Morrison, C. F., Dorin, J. R., Piggins, H. D., Reubi, J.-C., et al. (2002). The VPAC2 Receptor Is Essential for Circadian Function in the Mouse Suprachiasmatic Nuclei. Cell *109*, 497-508.

II

Harmer, S. L., Panda, S., and Kay, S. A. (2001). Molecular bases of circadian rhythms. Annu Rev Cell Dev Biol *17*, 215-53.

Harris, M. A., Clark, J., Ireland, A., Lomax, J., Ashburner, M., Foulger, R., Eilbeck, K., Lewis, S., Marshall, B., Mungall, C., et al. (2004). The Gene Ontology (GO) database and informatics resource. Nucleic Acids Res *32*, D258-261.

Hartwig, H. G. (1974). Electron microscopic evidence for a retinohypothalamic projection to the suprachiasmatic nucleus of Passer domesticus. Cell Tissue Res *153*, 89-99.

Huang, D. W., Sherman, B. T., and Lempicki, R. A. (2009a). Bioinformatics enrichment tools: paths toward the comprehensive functional analysis of large gene lists. Nucleic Acids Res *37*, 1-13.

Huang, D. W., Sherman, B. T., and Lempicki, R. A. (2009b). Systematic and integrative analysis of large gene lists using DAVID bioinformatics resources. Nat Protoc *4*, 44-57.

Irizarry, R. A., Hobbs, B., Collin, F., Beazer-Barclay, Y. D., Antonellis, K. J., Scherf, U., and Speed, T. P. (2003). Exploration, normalization, and summaries of high density oligonucleotide array probe level data. Biostat *4*, 249-264.

Jin, X., Shearman, L. P., Weaver, D. R., Zylka, M. J., de Vries, G. J., and Reppert, S. M. (1999). A molecular mechanism regulating rhythmic output from the suprachiasmatic circadian clock. Cell *96*, 57-68.

Kanehisa, M., Araki, M., Goto, S., Hattori, M., Hirakawa, M., Itoh, M., Katayama, T., Kawashima, S., Okuda, S., Tokimatsu, T., et al. (2007). KEGG for linking genomes to life and the environment. Nucleic Acids Research *36*, D480-D484.

Kanehisa, M., and Goto, S. (2000). KEGG: Kyoto Encyclopedia of Genes and Genomes. Nucleic Acids Research *28*, 27 -30.

Karatsoreos, I. N., Wang, A., Sasanian, J., and Silver, R. (2007). A Role for Androgens in Regulating Circadian Behavior and the Suprachiasmatic Nucleus. Endocrinology *148*, 5487-5495.

Karatsoreos, I. N., Yan, L., LeSauter, J., and Silver, R. (2004). Phenotype Matters: Identification of Light-Responsive Cells in the Mouse Suprachiasmatic Nucleus. J. Neurosci. *24*, 68-75.

Kendziorski, C., Irizarry, R. A., Chen, K.-S., Haag, J. D., and Gould, M. N. (2005). On the utility of pooling biological samples in microarray experiments. Proceedings of the National Academy of Sciences of the United States of America *102*, 4252-4257.

Kraves, S., and Weitz, C. J. (2006). A role for cardiotrophin-like cytokine in the circadian control of mammalian locomotor activity. Nat Neurosci *9*, 212-219.

Kuhlman, S. J., Silver, R., Le Sauter, J., Bult-Ito, A., and McMahon, D. G. (2003). Phase Resetting Light Pulses Induce Per1 and Persistent Spike Activity in a Subpopulation of Biological Clock Neurons. J. Neurosci. *23*, 1441-1450.

Maywood, E. S., Reddy, A. B., Wong, G. K. Y., O'Neill, J. S., O'Brien, J. A., McMahon, D. G., Harmar, A. J., Okamura, H., and Hastings, M. H. (2006). Synchronization and Maintenance of Timekeeping in Suprachiasmatic Circadian Clock Cells by Neuropeptidergic Signaling. Current Biology *16*, 599-605.

Morin, L. P., Shivers, K.-Y., Blanchard, J. H., and Muscat, L. (2006). Complex organization of mouse and rat suprachiasmatic nucleus. Neuroscience *137*, 1285-1297.

Morin, L. P. (2007). SCN organization reconsidered. J Biol Rhythms *22*, 3-13.

Morris, M. E., Viswanathan, N., Kuhlman, S., Davis, F. C., and Weitz, C. J. (1998). A Screen for Genes Induced in the Suprachiasmatic Nucleus by Light. Science *279*, 1544-1547.

Noguchi, T., and Watanabe, K. (2008). Regional differences in circadian period within the suprachiasmatic nucleus. Brain Research *1239*, 119-126.

Okamura, H. (2007). Suprachiasmatic nucleus clock time in the mammalian circadian system. Cold Spring Harb Symp Quant Biol *72*, 551-6.

Panda, S., Antoch, M. P., Miller, B. H., Su, A. I., Schook, A. B., Straume, M., Schultz, P. G., Kay, S. A., Takahashi, J. S., and Hogenesch, J. B. (2002). Coordinated Transcription of Key Pathways in the Mouse by the Circadian Clock. Cell *109*, 307-320.

Piggins, H., Antle, M., and Rusak, B. (1995). Neuropeptides phase shift the mammalian circadian pacemaker. The Journal of Neuroscience *15*, 5612 -5622.

Porterfield, V., Piontkivska, H., and Mintz, E. (2007). Identification of novel light-induced genes in the suprachiasmatic nucleus. BMC Neuroscience *8*, 98.

Reddy, A. B., Field, M. D., Maywood, E. S., and Hastings, M. H. (2002). Differential Resynchronisation of Circadian Clock Gene Expression within the Suprachiasmatic Nuclei of Mice Subjected to Experimental Jet Lag. J. Neurosci. *22*, 7326-7330.

Reppert, S. M., and Weaver, D. R. (2002). Coordination of circadian timing in mammals. Nature *418*, 935-941.

II

Samson, W. K., Said, S. I., and McCann, S. M. (1979). Radioimmunologic localization of vasoactive intestinal polypeptide in hypothalamic and extrahypothalamic sites in the rat brain. Neuroscience Letters *12*, 265-269.

Schwenk, F., Baron, U., and Rajewsky, K. (1995). A cre-transgenic mouse strain for the ubiquitous deletion of loxP-flanked gene segments including deletion in germ cells. Nucleic Acids Res *23*, 5080-5081.

Shigeyoshi, Y., Taguchi, K., Yamamoto, S., Takekida, S., Yan, L., Tei, H., Moriya, T., Shibata, S., Loros, J. J., Dunlap, J. C., et al. (1997). Light-Induced Resetting of a Mammalian Circadian Clock Is Associated with Rapid Induction of the mPer1 Transcript. Cell *91*, 1043-1053.

Shih, J. H., Michalowska, A. M., Dobbin, K., Ye, Y., Qiu, T. H., and Green, J. E. (2004). Effects of pooling mRNA in microarray class comparisons. Bioinformatics *20*, 3318-3325.

Siepka, S. M., Yoo, S.-H., Park, J., Lee, C., and Takahashi, J. S. (2007). Genetics and neurobiology of circadian clocks in mammals. Cold Spring Harb Symp Quant Biol *72*, 251-9.

Silver, R., Sookhoo, A. I., LeSauter, J., Stevens, P., Jansen, H. T., and Lehman, M. N. (1999). Multiple regulatory elements result in regional specificity in circadian rhythms of neuropeptide expression in mouse SCN. Neuroreport *10*, 3165-74.

Smith, M., and Carter, D. A. (1996). In situ hybridization analysis of vasopressin mRNA expression in the mouse hypothalamus: Diurnal variation in the suprachiasmatic nucleus. Journal of Chemical Neuroanatomy *12*, 105-112.

Stephan, F. K., and Zucker, I. (1972). Circadian Rhythms in Drinking Behavior and Locomotor Activity of Rats Are Eliminated by Hypothalamic Lesions. Proc Natl Acad Sci U S A. *69*, 1583–1586.

Stetson, M. H., and Watson-Whitmyre, M. (1976). Nucleus suprachiasmaticus: the biological clock in the hamster? Science *191*, 197-9.

Storch, K.-F., Lipan, O., Leykin, I., Viswanathan, N., Davis, F. C., Wong, W. H., and Weitz, C. J. (2002). Extensive and divergent circadian gene expression in liver and heart. Nature *417*, 78-83.

Stratmann, M., and Schibler, U. (2006). Properties, entrainment, and physiological functions of mammalian peripheral oscillators. J Biol Rhythms *21*, 494-506.

Takahashi, Y., Okamura, H., Yanaihara, N., Hamada, S., Fujita, S., and Ibata, Y. (1989). Vasoactive intestinal peptide immunoreactive neurons in the rat suprachiasmatic nucleus demonstrate diurnal variation. Brain Res *497*, 374-377.

Tominaga, K., Shinohara, K., Otori, Y., Fukuhara, C., and Inouye, S. T. (1992). Circadian rhythms of vasopressin content in the suprachiasmatic nucleus of the rat. Neuroreport *3*, 809-812.

Ueda, H. R., Chen, W., Adachi, A., Wakamatsu, H., Hayashi, S., Takasugi, T., Nagano, M., Nakahama, K.-ichi, Suzuki, Y., Sugano, S., et al. (2002). A transcription factor response element for gene expression during circadian night. Nature *418*, 534-539.

Vandesande, F., Dierickx, K., and Mey, J. (1975). Identification of the vasopressin-neurophysin producing neurons of the rat suprachiasmatic nuclei. Cell Tissue Res. *156*. Available at: http://www.springerlink.com/content/t4833g74v0u77613/ [Accessed April 25, 2011].

Welsh, D. K., Takahashi, J. S., and Kay, S. A. (2010). Suprachiasmatic Nucleus: Cell Autonomy and Network Properties. Annu. Rev. Physiol. *72*, 551-577.

Winslow, S. G., and Henkart, P. A. (1991). Polyinosinlc acid as a carrier in the microscale purification of total RNA. Nucleic Acids Research *19*, 3251 -3253.

Yamaguchi, S., Isejima, H., Matsuo, T., Okura, R., Yagita, K., Kobayashi, M., and Okamura, H. (2003). Synchronization of Cellular Clocks in the Suprachiasmatic Nucleus. Science *302*, 1408-1412.

Yan, L., Karatsoreos, I., LeSauter, J., Welsh, D. K., Kay, S., Foley, D., and Silver, R. (2007). Exploring Spatiotemporal Organization of SCN Circuits. Cold Spring Harbor Symposia on Quantitative Biology *72*, 527 -541.

Yan, L., and Silver, R. (2002). Differential induction and localization of mPer1 and mPer2 during advancing and delaying phase shifts. European Journal of Neuroscience *16*, 1531-1540.

Yan, L., and Silver, R. (2004). Resetting the brain clock: time course and localization of mPER1 and mPER2 protein expression in suprachiasmatic nuclei during phase shifts. European Journal of Neuroscience *19*, 1105-1109.
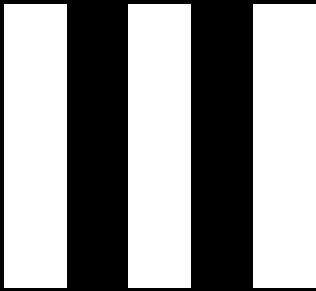
TRANSCRIPTOME OF ROSTRAL AND CAUDAL SCN UNDER DIFFERENT PHOTOPERIODS

Karl Brand[1], Marian Comas[2], Dimitris Rizopoulos[3] Serge Daan[2], Roelof A. Hut[2], Ed Jacobs[1], and Gijsbertus T.J. van der Horst[1],*

[1] Department of Genetics, Erasmus University Medical Center, PO Box 2040, 3000 CA Rotterdam, The Netherlands.
[2] Unit of Chronobiology, Centre for Behaviour and Neurosciences, University of Groningen, PO Box 14, 9750 AA, The Netherlands.
[3] Department of Biostatistics, Erasmus University Medical Center, PO Box 2040, 3000 CA Rotterdam, The Netherlands.
* Corresponding author

ABSTRACT

Photoperiod is used by mammals to synchronize seasonal adaptive responses to the optimum time of year to maximize reproductive success. This process depends on the suprachiasmatic nuclei (SCN) which is responsible for entraining and coordinating daily rhythms and in so doing, encodes a photoperiodic signal in electrical discharge and melatonin rhythm. Separate 'morning' and 'evening' oscillators, entraining independently by dawn and dusk, are believed to reside in rostral and caudal SCN subregions and provide the mechanism for encoding the SCN's photoperiodic output. We sought to clarify the contribution of the rostral and caudal SCN in encoding photoperiod, and expand understanding how this might be accomplished by analyzing the transcriptome of these subregions under short (6 hours light/day), equinoxal (12 hours light/day) and long (18 hours light/day) photoperiods. Rhythmically expressed transcripts were identified from transcription profiles obtained from precisely isolated rostral and caudal subregions collected over a complete circadian cycle. Our results recapitulate those obtained in other photoperiodic and global transcription profiling studies on mouse SCN and demonstrate photoperiodic regulation of the genome. We show that the peak expression of the majority of rhythmic transcripts clusters around dawn and dusk. Within these clusters we find examples of transcripts whose peak expression specifically track dawn or dusk over all photoperiods. Furthermore, we present both photoperiod dependent expression and show photoperiod independent expression for transcripts in both rostral and caudal SCN. Finally, we find evidence that rhythmic transcripts associated with seasonal affective disorder are photoperiodically regulated.

INTRODUCTION

Most organisms have evolved mechanisms to anticipate and respond to the environmental changes imposed by Earth's seasonal variation. The utilization of photoperiod as seasonal cue has been hypothesized as a means for organisms to determine season (Bünning, 1936; Pittendrigh and Minis, 1964) and highlights the role daily timing and light sensing mechanisms play in seasonal adaptation. Studies of photoperiod and seasonal adaptation using animals which demonstrate overt seasonal phenotypes, including birds, sheep and hamsters (Yasuo et al., 2006; Lincoln, 2006; Nakao et al., 2008) reveal mechanisms that detect and drive adaptive responses to annual changes in temperature, light and food availability present at Earth's higher latitudes. A pivotal role has been identified for melatonin and the pars tuberalis (PT) in birds and mammals (Dardente et al., 2004; Nakao et al., 2008; Dupré et al., 2010) which demonstrate the use of day length (photoperiod) to infer time-of-year and induce the observed phenotypic responses. These findings underscore the dependence on photoperiod as a seasonal cue as originally proposed (Bünning, 1936; Pittendrigh and Minis, 1964) and demonstrate transcriptional and hormonal mechanisms utilized for seasonal adaptation (Dardente et al., 2010; Dupré et al., 2010; Masumoto et al., 2010).

The suprachiasmatic nucleus (SCN) also encodes daylength via duration of electrical output (Mrugala et al., 2000; Schaap et al., 2003; VanderLeest et al., 2007) which in principle allow it to directly drive seasonal adaptation without the need for an intermediate readout, ie., duration of melatonin secretion. Embedded dorsally in the optic chiasm, the SCN was identified for its role in synchronizing internal physiology to the local daily light/dark cycle (Stephan and Zucker, 1972; Stetson and Watson-Whitmyre, 1976). This depends on the generation of endogenous approximate 24 hour rhythms by an intracellular molecular clock present in SCN neurons and virtually all peripheral tissues (Balsalobre et al., 1998; Jin et al., 1999; Yagita et al., 2001). This molecular clock depends on a transcription-translation feedback loop to generate cell autonomous, approximate 24 hour rhythms (Dunlap, 1999; Bell-Pedersen et al., 2005). The transcription factors CLOCK and BMAL1 (synonyms, ARNTL, MOP3) heterodimerize and activate expression of the *Period* (*Per1, Per2,* and *Per3*) and *Cryptochrome (Cry1* and *Cry2)* and *Rev-Erbα* genes. Together, PER1/2 and CRY1/2 proteins repress the transcriptional activation by CLOCK-BMAL1, and thus expression of *Per* and *Cry* genes, relaxing repression of their target genes (Reppert and Weaver, 2002). REV-ERBα acts via another circadian promoter element (RORA) and mediates rhythmic expression of the *Bmal1* gene, forming an additional, stabilizing feedback loop (Preitner et al., 2002).

A model which explains both the circadian and photoperiodic phenomena observed in nocturnal rodents under constant conditions was proposed around the time the SCN was implicated in circadian rhythm maintenance (Pittendrigh and Daan, 1976). This posits the existence of two discrete circadian oscillators, mutually interacting but entrained independently by dawn and dusk, defined as 'morning' (*M*) and 'evening' (*E*) oscillators respectively. Support for the *M-E* model first came from the demonstration of two distinct oscillations in electrical output coinciding with dawn and dusk. This was made in

horizontally sectioned hamster SCN and hypothesized that the dawn and dusk peaks arose from rostral and caudal subregions (Jagota et al., 2000). The elucidation of the molecular composition of the circadian clock from which daily rhythms are generated and maintained in organisms allowed an intracellular perspective to review and assess the relevance of the *M-E* model (Daan et al., 2001). Consistent with peaks in electrical output from these subregions at dawn/dusk, analysis of *Per2 Rev-erbα , Dbp* and *Avp* expression in the rostral and caudal subregions of the overtly photoperiodic Syrian hamster (*Mesocricetus auratus*) revealed differential phasing of peak *Per2* expression under long photoperiod. While the peak of *Per2* expression in the caudal SCN (C-SCN) coincided with dawn, in the rostral SCN (R-SCN) *Per2* mRNA levels peak around dusk (Hazlerigg et al., 2005). These results support the possibility of photoperiod encoding by the SCN to the core clock mechanism. Similar observations made in animals lacking melatonin, i.e., C57BL/6J mice, revealed at least three subpopulations of differentially phased SCN neurons under long photoperiod, two in the rostral SCN hemisphere and a third in the caudal hemisphere (Inagaki et al., 2007; Naito et al., 2008). These studies, utilizing a *Per1-luciferase* reporter system to monitor clock function in individual neurons over time, recapitulate studies in hamsters, i.e. localization of *M* and *E* oscillators within caudal and rostral SCN subregions respectively. Whilst these findings strengthen the *M-E* model for entrainment in mammals, they also support the emerging 'network model' of SCN physiology (Butler and Silver, 2009; Foley et al., 2011) given the presence of a smaller population of dawn tracking *M* oscillators observed amongst *E* oscillators within the rostral hemisphere of the SCN. Electrophysiological studies which support the network model of SCN physiology (VanderLeest et al., 2007) do not exclude the possibility of sub-populations of *M* and *E* oscillators enriched in caudal and rostral SCN subregions. Ultimately the interpretation of these and new results, in the context of the aforementioned models, will depend on what constitutes a 'subregion' or defines a 'population' of similarly phased neurons (Helfrich-Förster, 2009).

We sought to clarify and expand understanding of the role of SCN subregions in photoperiod entrainment/encoding. Using laser catapult microdissection (LCM) combined with global transcriptional profiling approach, we determined gene expression levels in the rostral and caudal SCN from mice stably entrained to long, short or equinoxal photoperiod to identify rhythmic, photoperiod responsive transcripts in R-SCN and C-SCN. In a separate analysis we will investigate non-rhythmic transcripts which may be photoperiodically regulated in these subregions. Here, we achieved a comprehensive view of the adaptation of oscillating genes in the rostral and caudal SCN and reveal candidate genes which may contribute to photoperiod encoding and be required for the photoperiodic response observed in mammals.

RESULTS AND DISCUSSION

Identification of rhythmic transcripts in rostral and caudal SCN

To determine the roles of the rostral and caudal SCN in photoperiod responsiveness mice were entrained to either a short (LD 6:18), equinoxal (LD 12:12) or long (LD 18:6) photoperiod for 30 days using a twilight transition protocol (Sosniyenko et al., 2009) to mimic terrestrial light transitions. To diminish light-driven mRNA rhythms, mice were transferred to constant darkness (DD) and brain collection performed at 1.5 hour intervals over the second circadian cycle in constant darkness, similar to (Panda et al., 2002); Figure 1A). Coronal cryosections were made from each brain sample and laser catapult micro-dissection (LCM) used to isolate equal portions of rostral and caudal SCN subregions (Figure 1B). Total RNA was purified, amplified and hybridized, one subregion from each animal per array, to Affymetrix GeneChip 430 2.0 microarrays containing 45,101 unique probe sets representing 36,431 putative target gene transcripts (Cui and Loraine, 2009).

To identify rhythmically expressed transcripts we developed a dual filter approach capable of identifying rhythmic expression with reasonable confidence from data collected over a single circadian cycle and which tolerates asymmetric rhythmic profiles arising from long and short photoperiods (Figure 2; see Materials and Methods and Supporting Information). Filter I utilizes a linear model to identify transcripts which vary significantly over time, irrespective of photoperiod or SCN subregion. Filter II evaluates transcripts identified by Filter I for goodness of fit to a sine based function using F-tested harmonic regression (Oster et al., 2006; Keller et al., 2009). Proven statistical methods were used to control false positive discoveries arising from transcript-wise and condition-wise multiple testing in both Filters I and II (Holm, 1979; Benjamini and Hochberg, 1995). We fine tuned the significance thresholds (α) used for Filters I and II using transcripts known to be rhythmically expressed ('positive trainers') or constitutively expressed ('negative trainers') in the SCN as a 'training set' (see Supporting Information). This allowed us to balance false positive and false negative classification of rhythmic transcripts, i.e. Type I and Type II errors. Using these methods approximately 40% of transcripts with known rhythmic expression in the SCN were found in our data to vary significantly over time (Filter I $p < 0.05$), of which virtually all demonstrate a circadian profile (Filter II $p < 0.10$; see Supplementary Figure S1). We used Q-PCR to independently verify *Per2,* a transcript known to be rhythmic in the SCN. The temporal profiles for *Per2* Q-PCR match well those of our microarray data (Supplementary Figures 2 and 3) and also those reported previously (Inagaki et al., 2007; Naito et al., 2008; Sosniyenko et al., 2009, 2010; Ciarleglio et al., 2011).

Photoperiod dependent and independent expression

To visualize the temporal expression patterns of rhythmic transcripts we constructed heat map matrices with transcripts ordered by phase of peak expression. For both rostral and caudal SCN, under SP and EP peak phases generally clustered within subjective light or subjective dark phase and are demarked by the subjective dawn and dusk (Figure 3A - D). Under LP, whilst dusk demarks peak expression between light and dark phases (as in SP and EP), dawn

A

B
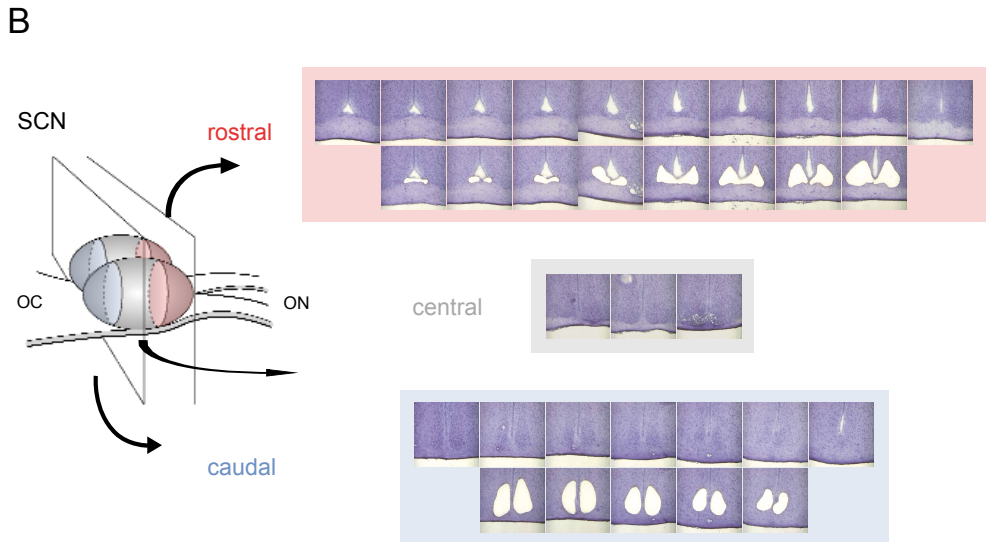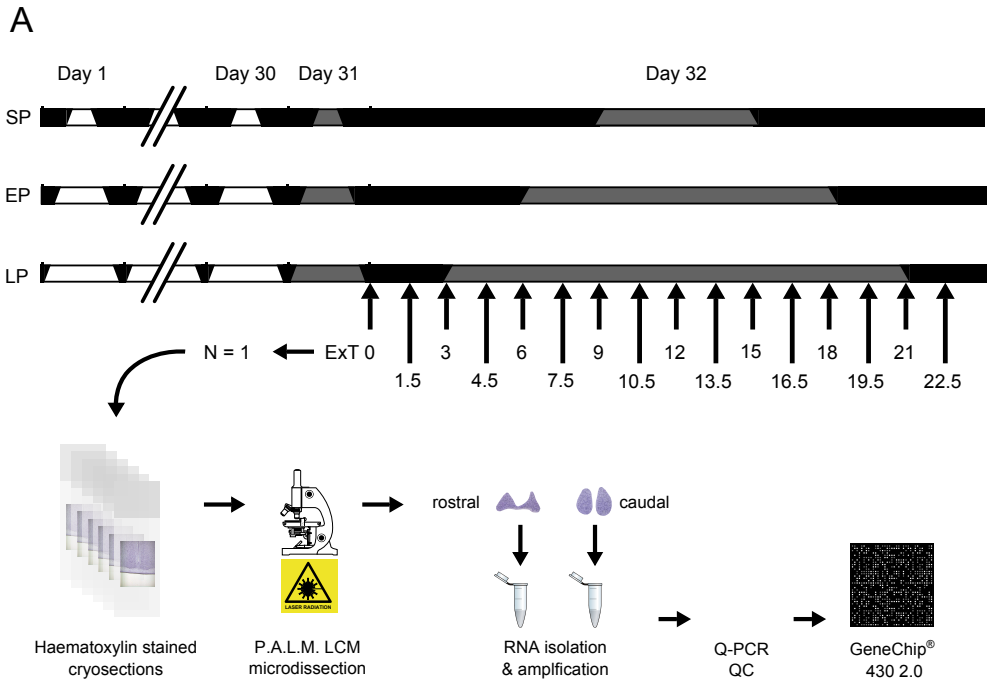
Figure 1. Experimental design and SCN subregion isolation. (A) Mice were entrained to short (LD6:18), equinoxal (LD12:12) and long (LD18:6) photoperiods with twilight transitions between light and dark for at least 30 days. Tissue collection was performed under dim red light illumination on the second consecutive day in constant conditions at external time points (ExT) as indicated. (B) Schematic illustration of the SCN subregions, targeted for analysis and representative example of heamatoxylin stained cryosections before (top panels), and after (bottom panels) laser catapult microdissection and sample capture.

does not (Figure 3E and F). Apparently, there is no obvious separation of peak expression into light and dark phases for both SCN subregions. Interestingly, the dawn demarcation visible in SP and EP (around ExT9 and 8, respectively) remains under LP, despite subjective dawn occurring at least 5 hours earlier than the demarcation. This may reflect photoperiodic imprinting of the central pacemaker, which shows entrainment or phase coupling limitations to longer photoperiods (12:12 - 18:6) by animals raised under shorter photoperiods (6:18 – 12:12, Ciarleglio et al., 2011). As the mice used in this study were raised until adulthood under 12:12, this apparent limit of entrainment/coupling is exceeded under LP as would be expected from Ciarleglio et al., findings.

We next quantified these clusters by plotting the density of transcripts by their peak expression phase (Figure 3G, H and I). Under SP conditions, two major clusters are evident in both SCN subregions: a bimodal 'mid-late night' cluster (ExT2-6) bounded by mid-night and the dawn transition, and a large 'dusk' cluster (ExT14-16) bounded by mid-day and early evening (Figure 3G). The mid-late night cluster consists of two sub-clusters: a 'midnight' cluster with a peak in transcript density around ExT3, and a 'dawn anticipatory' cluster around ExT6 (R-SCN) or ExT8 (C-SCN).

Similarly, under EP conditions two large clusters are evident in both SCN subregions, occurring late in the light and dark phases. The earlier cluster is again composed of 'mid-night' and 'dawn anticipatory' sub-clusters around ExT2, and ExT7-8 respectively (Figure 3H). In contrast to SP demonstrating a single large 'dusk' cluster, under EP late day is characterized by 2 sub-clusters in C-SCN (around ExT14 or 'mid-day' and ExT18 or 'dusk') and a broad cluster in R-SCN, spanning ExT13-18 and

Microarray pre-processing

Raw GeneChip® data

↓

GCRMA normalized data

↓

Invariant probe set

Remove lowly expressed and non-differentially expressed probe sets

↓

Rhythmic gene identification

Filter I: Linear Model (Time)

Identify variance in time
(p < 0.05 with B-H control)

↓

Filter II: Harmonic Regression

CircWaveBatch, sine based F-test
(p < 0.05 with Holm control)

↓

Rythmic gene analysis

Expression peak phase, nadir phase
& peak braodnss

Figure 2. Analysis flowchart of rhythmic transcript identification. Un-normalized expression measures were exported with MAS5.0, normalized across arrays using the GCRMA algorithm and invariantly expressed probe sets subtracted. Rhythmic probe sets were identified using a dual filter approach. Filter I identifies variance within time for any photoperiod or tissue combination, whilst Filter II identifies circadian variance in probe sets passing Filter I.
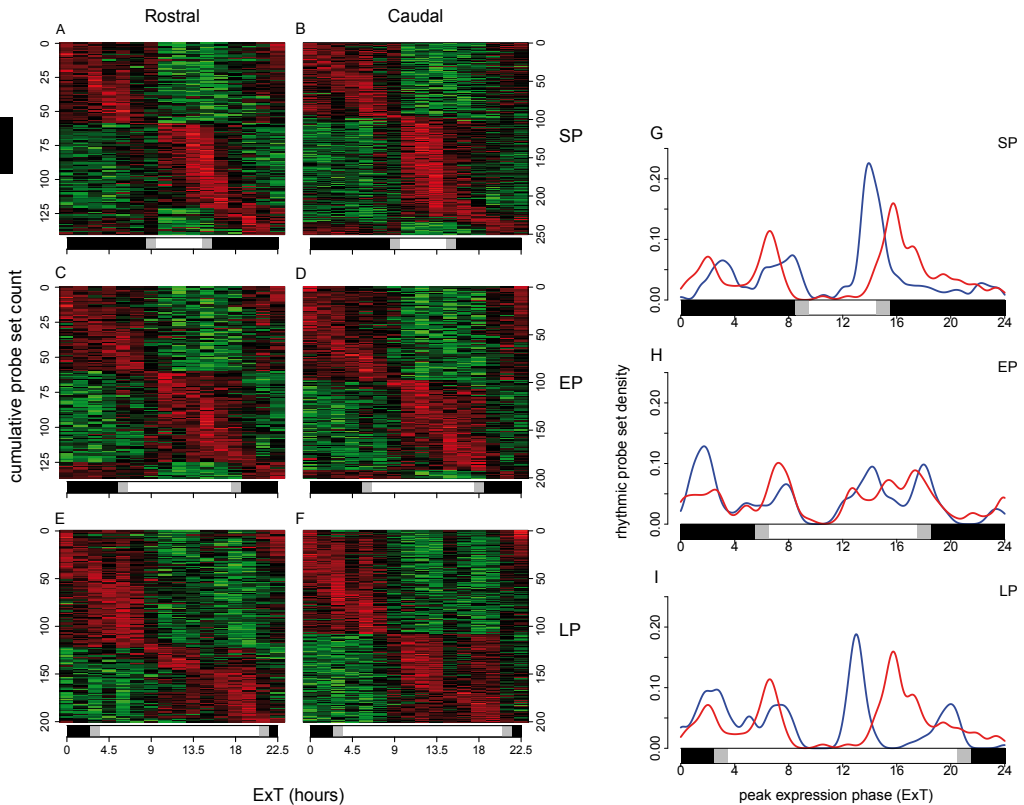
Figure 3. Phase map visualization of rhythmic transcript expression. Probe sets defined as circadian (Filter I and II, $p < 0.05$; see Supporting Information) are ordered by the phase of peak expression estimated by the wave form of best fit obtained from CircWaveBatch. Probe set rows are sorted by phase from earliest (ExT0) to latest (ExT22.5) and expression levels mean centered and scaled to normalize for direct comparison between probe sets. Left panels show expression in rostral SCN under short (A), equinoxal (C) and long (E) photoperiods; middle panels show expression in caudal SCN under short (B), equinoxal (D) and long (F) photoperiods. Right panels show density plots of the proportion of rhythmic probe sets with peak phase expression at a given ExT (% of the total number of rhythmic probe sets identified) for short (G), equinoxal (H) and long (I), photoperiods in rostral (red) and caudal (blue) SCN subregions. Shaded lines underneath panels indicate previous light regime, where black represents night; white, day; and grey, twilight.

possibly containing 3 sub-clusters around ExT 13, ~15 and ~18, representing 'mid-day', 'late-day' and 'dusk', respectively.

In LP the 'midnight' and 'dawn-anticipatory' clusters evident under SP and EP remain in both SCN sub regions around ExT2 and 6, respectively. Given that subjective dawn occurs around ExT3, under LP this cluster can not be referred to as 'dawn-anticipatory' (Figure 3I). Furthermore, as several of the same transcripts (see Figure 4C, D, G, and H; discussed later) compose the cluster around Ext6 (but not around Ext3) in all three photoperiods, a common term, eg. 'ExT6 cluster' is appropriate. Given the common identity of several transcripts in 'ExT6 cluster' under all photoperiods, these, and probably others in this cluster (e.g. those absent in at least one photoperiod due to Type II errors, ie. false negative
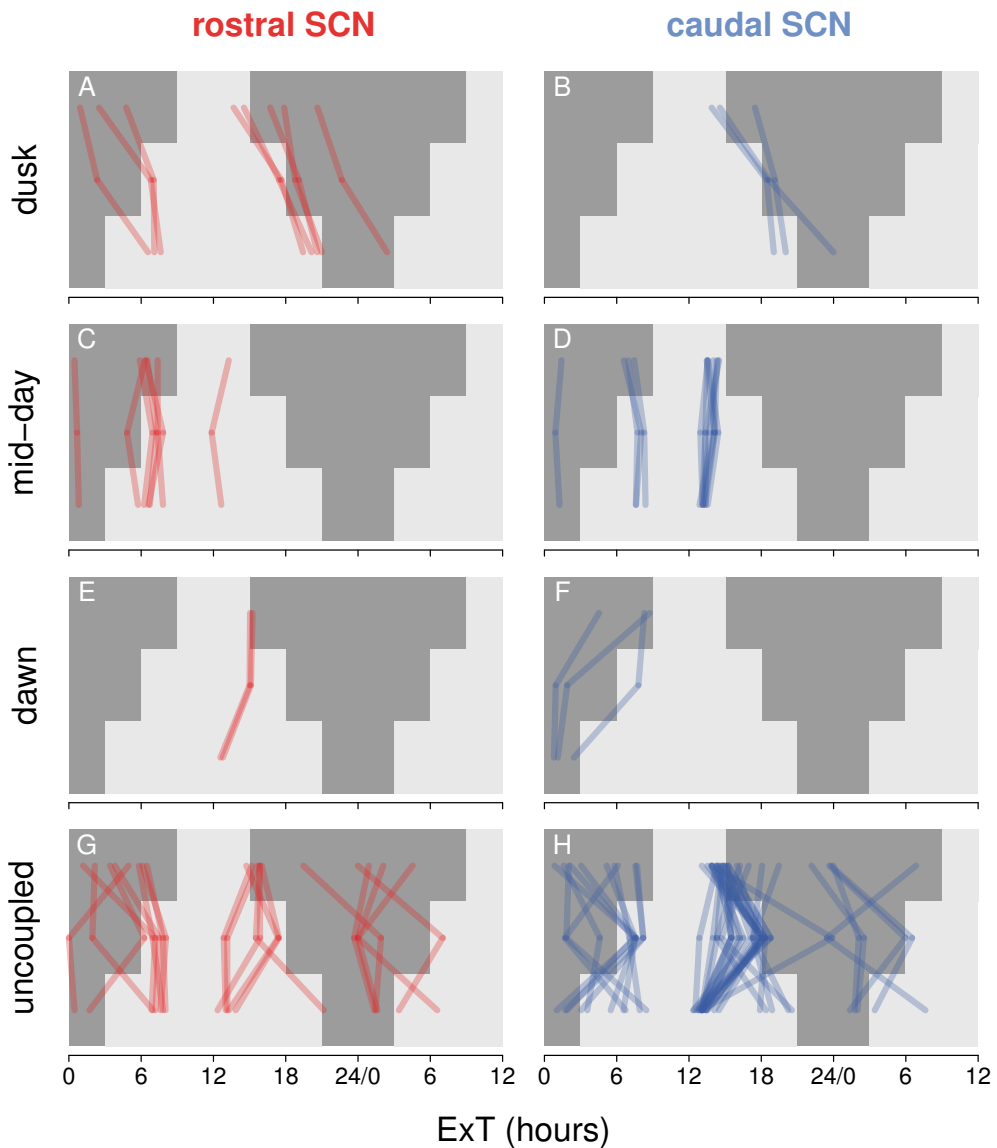
Figure 4. Peak expression phase trajectories. The peak phase of expression for all transcripts which are rhythmic (Filter I and II, $p < 0.05$) in one or more photoperiods and nearly rhythmic (Filter I and II, $p < 0.10$) under the remaining one or two photoperiods were plotted according to photoperiod trajectory. Transcripts with peak phase of expression delaying over the subjective day with increasing day length, defined as a 'dusk trajectory'; are shown in panels A and B. Transcripts with peak phase remaining constant (± 1 hr) over the subjective day with increasing day length, defined as a 'mid-day trajectory', are shown in panels C and D. Transcripts with peak phase advancing over the subjective day with increasing day length, defined as a 'dawn trajectory', are shown in panels E and F. And transcripts with peak phases showing no consistent trajectory between SP, EP and LP, defined as a 'uncoupled', are shown in panels G and H. Dark grey shading represents subject evening and light grey, subjective day.

errors) are candidate photoperiod-independent transcripts. The 'mid-day' cluster evident under EP in C-SCN is the largest cluster visible under LP. As for the 'ExT6' cluster, several transcripts are evident that commonly populate the 'mid-day' cluster under two if not all three photoperiods (see Figure 3C, D, G, and H; discussed later) and thus also represent candidate photoperiod-independent transcripts. In contrast, the most prominent cluster in R-SCN occurring at Ext16, the same time as the 'dusk-cluster' described under SP and EP above, contains no common transcripts between photoperiods (Figure 3C, D, G and H).

Intriguingly, under LP the ExT20 cluster in C-SCN coincides with the beginning of the dusk transition and contains transcripts also present in the 'dusk-clusters' present under SP and EP (Figure 3G and H). These transcripts, with peak expression coinciding with dusk under all photoperiods, represent candidate photoperiodically regulated transcripts and are discussed further below.

Rhythmic transcript trajectories

To examine more closely the extent to which transcripts rhythmic, or nearly so under all photoperiods (transcripts with $p < 0.05$ for Filters I and II under at least one photoperiod and $p < 0.10$ for the remaining one or two photoperiods) coordinate peak expression under different photoperiods we plotted the peak expression time for these transcripts. Transcripts showing photoperiod dependant or independent regulation were plotted separately according their trajectory, i.e. dusk or dawn.

As shown in Figure 4A and B, eleven transcripts show dusk trajectories (8 in R-SCN, 3 in C-SCN), eight of which specifically peak around dusk in all photoperiods. In R-SCN, three transcripts (*Unc5b*, *Tanc1* and *Hunk*) show dusk trajectories, yet with a different phase angle. Sixteen transcripts divided over both SCN subregions appear to be photoperiod independent (Figure 4C and D), with peak expression occurring at fixed times of the day irrespective of photoperiod around ExT1, ExT7 and ExT13. Three C-SCN transcripts demonstrate dawn trajectories (*Nefh*, *Samd1* and *Cyp4x1*) specifically peaking at dawn in all photoperiods (Figure 4F) whereas in R-SCN, only probe sets for *Pgm2l1* and Mm.263265 which show a dawn trajectory across the late light phase (Figure 4E).

Many transcripts in both subregions, although rhythmic under all photoperiods, show no consistent photoperiod dependent trajectory across all photoperiods (Figure 4G - H). Especially for the many transcripts in C-SCN which track dusk under SP and EP but not LP (Figure 4H), this may reflect the limits of phase coupling by the circadian system such that a transcript may couple to a given phase under the SP and EP, but is unable to couple under LP, thus 'uncoupling' from their SP and EP phases, i.e., dusk in this case. As previously mentioned, these observations may be explained by the photoperiodic imprinting of the central pacemaker during perinatal development under EP (Ciarleglio et al., 2011). The lack of precision estimating the phase of peak expression is also likely to contribute to some degree to the apparent lack of consistent trajectories for these transcripts.

Unique and common rhythmic transcripts between photoperiod and SCN subregions

We next investigated to what extent rhythmically expressed transcripts (as listed in Online Supplemental Tables S1 to 6) are unique or common between photoperiods and/or SCN subregions. A Venn diagram of the probe sets under SP, EP and LP in R-SCN (Figure 5A) demonstrate near equality in both the total number of rhythmic probe sets identified for each photoperiod and in the proportions of unique versus shared rhythmic expression in and between photoperiods. A comparable number of overlapping rhythmic probe sets was identified in C-SCN (Figure 5B), although SP stands out with a larger number of rhythmic probe sets (245) compared with EP (151) and LP (186). We also compared for each photoperiod the number of unique and common rhythmic transcripts between R-SCN and C-SCN. Independent of photoperiod, a larger number of transcripts was identified in C-SCN compared to R-SCN (140 vs. 245 under SP, 151 vs 136 under EP and 186 vs. 154 under LP; (Figure 5C-E). The proportion of common to unique rhythmic transcripts between subregions is similar for all photoperiods, where 51 of total 334 (15%) under SP, 48 of 239 (20%) under EP and 57 of 263 (22%) under LP are common between subregions.
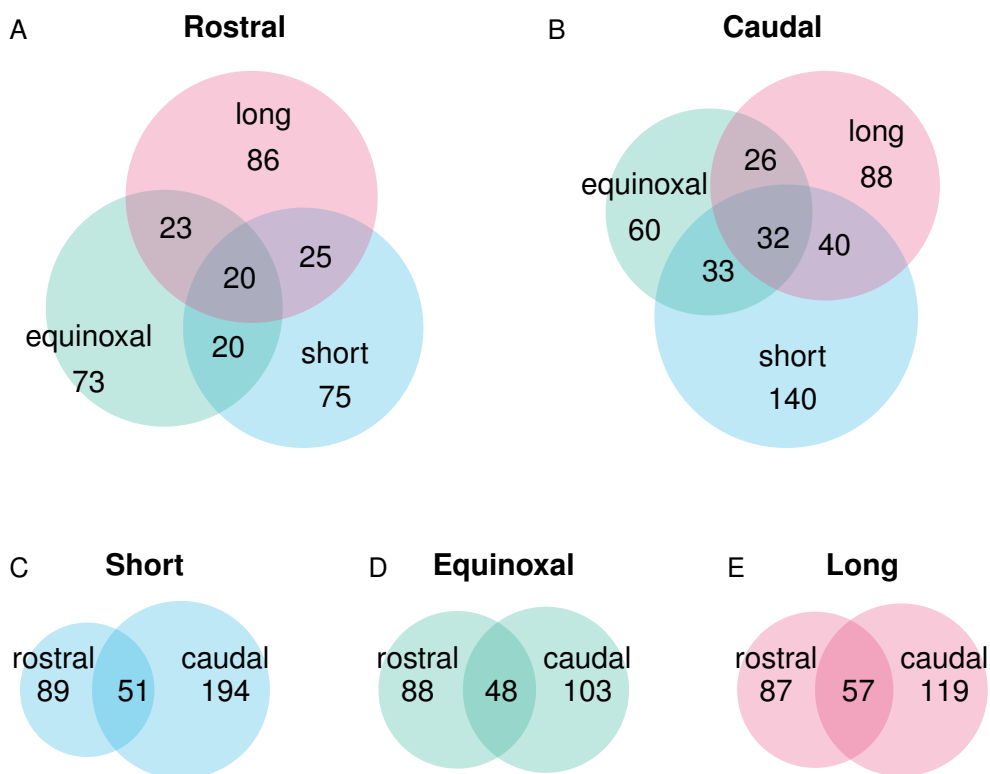
Figure 5. Venn diagram summary of rhythmic transcripts unique and common in R-SCN and C-SCN under different photoperiods. The number of probe sets uniquely and commonly rhythmic (Filter I and II, p < 0.05) between photoperiods in R-SCN (A) and C-SCN (B); and between SCN subregions under short (C), equinoxal (D) and long photoperiod (E).

Taken together, comparisons of rhythmic transcript number, unique and common between all combinations of photoperiod and subregion, demonstrate a near 1:1 ratio of unique to common rhythmic transcripts. Given the confidence levels underpinning the rhythmic genes identified for each condition ($p < 0.05$ that a transcript was falsely identified as rhythmic), the observed 50% overlap is not due to chance alone. Given greater temporal and biological replication allowing a higher rhythmic transcript detection sensitivity, it's likely overlap would increase beyond 50%. Irrespective, from our results we expect some transcripts are truly subregion and/or photoperiod unique, i.e. non-overlapping in their rhythmic expression. These candidate photoperiod/subregion specific transcripts deserve further attention for their potential role in photoperiodic encoding and seasonal adaptation.

Phase comparisons

To compare the peak phase of oscillating transcripts (rhythmic under two or more photoperiods) we plotted for R-SCN as well as for C-SCN the time of peak expression for all combinations of photoperiod (Figure 6, left and middle panels). Similarly, we plotted for each photoperiod the time of peak expression in S-SCN vs R-SCN subregions (Figure 6, right panels). In R-SCN, several clusters of rhythmic transcript peak expression phases are evident in all three pairwise photoperiod comparisons, indicating the existence of transcripts whose expression is regulated by photoperiod (Figures 6A, B and C). A 'dusk' cluster is evident across all pairwise comparisons demonstrating the coordination of several rhythmic transcripts to coincide peak expression with dusk, irrespective of photoperiod. A loose cluster of 'dawn-centric' transcripts with peak expression occurring between late-evening spanning dawn into early-day is also evident in all comparisons. Broadly interpreted, these two clusters appear 'dusk-locked' and 'dawn-locked' respectively, which may reflect a peak in physiological preparedness for subsequent locomotor activity during the dark phase and sleep activity during the light phase. In R-SCN, in contrast to the dusk and dawn-centric clusters, several clusters show a differential peak expression phase between photoperiods.

Comparison of common rhythmic transcripts between photoperiods in C-SCN reveal cluster patterns similar to those observed in R-SCN, including 'dusk' and 'dawn-centric' clusters, indicating that photoperiod regulated transcripts are also present in C-SCN (Figure 6D, E and F). Compared to R-SCN, a greater proportion of rhythmic transcripts in C-SCN show peak expression at mid-day. Intriguingly, some of these transcripts remain true 'mid-clusters' regardless of photoperiod, and others show a differential peak expression phase in peaking at mid-day in one photoperiod and at dusk in another.

Besides photoperiodic comparisons within SCN subregions, we made pairwise comparisons between R-SCN and C-SCN for each photoperiod (Figure 6G, H and I). Given the similarity observed in cluster patterns between SCN subregions for the pairwise photoperiodic comparisons, not surprisingly peak expression phases are positively correlated where Spearman's rank correlation coefficient (ρ) for R-SCN versus C-SCN under SP is 0.45 ($p < 0.001$), under EP is 0.35 ($p < 0.02$) and under LP is 0.89 ($p < 0.001$). Besides the high positive correlation between subregions the clusters observed for the photoperiodic comparison are also reflected in the subregion comparisons. Specifically,
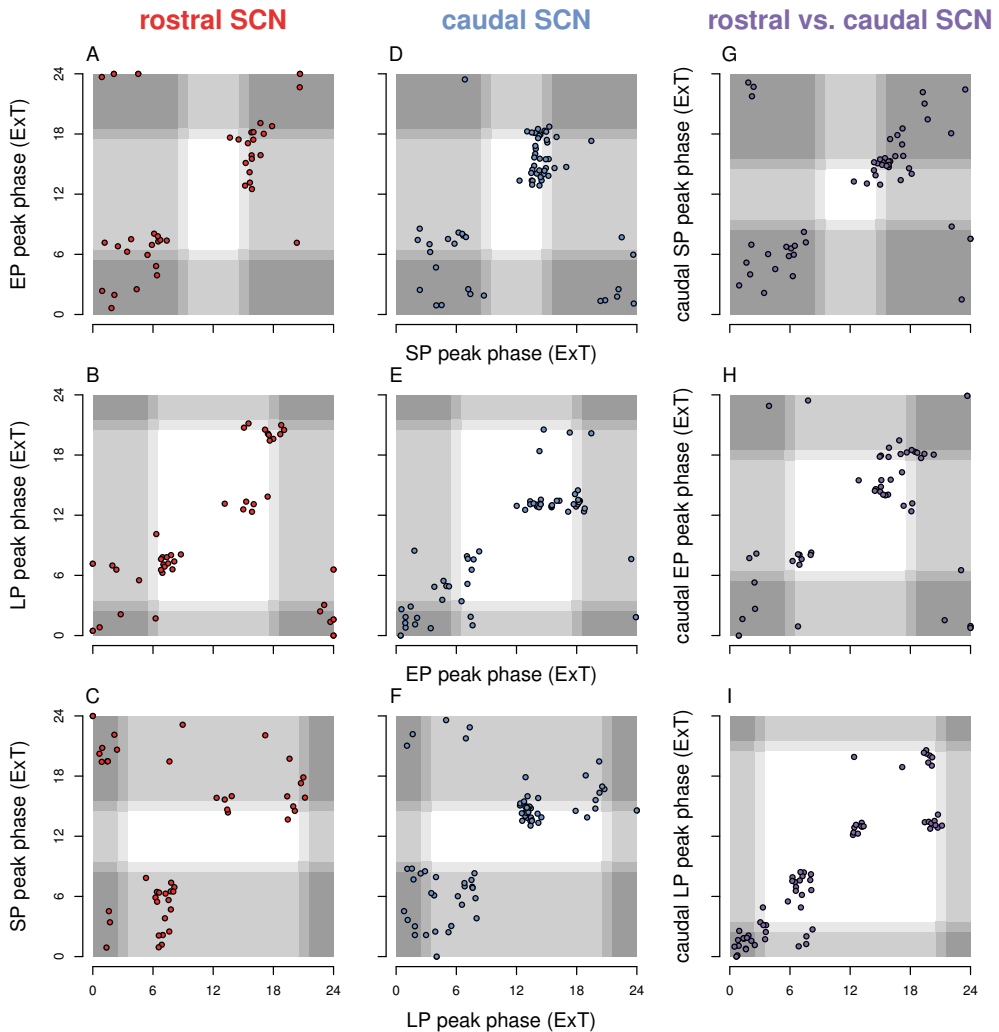
Figure 6. Rhythmic probe sets common between tissue or photo-period cluster by phase of peak expression. Circadianly expressed probe sets common to two or more photoperiods and/or SCN subregions are compared pairwise for rostal vs caudal under short, (A), equinoxal (B) and long (C) photoperiods, and for equinoxal vs short (D and E), equinoxal vs long (F and G), and long versus short (H and I) photoperiod in rostral and caudal SCN respectively.

a group of transcripts tightly cluster peak expression phase at the dusk transition for all three photoperiods reflecting the 'dusk' cluster observed earlier; and under SP and LP a late evening cluster is evident reflecting, in part, the 'dawn-centric' cluster described above.

Expression profile shape

We compared rhythmic transcripts for differences in the shape of their expression profiles over the 24 hour period examined. We calculated the <u>s</u>um <u>m</u>idrange-scaled <u>e</u>xpression <u>v</u>alues (SMEV) to quantify the broadness of the 'peaks' and 'valleys' for all rhythmic transcripts

and identified differences in expression profile shapes between rhythmic transcripts under all photoperiods and for both SCN subregions. To visualize expression profile shape differences, we replotted the rhythmically expressed transcripts (as shown in Figure 3A - F) by first centering each transcript on the phase of peak expression (estimated by CircWaveBatch and set as 0 hr) and subsequently ordering them from highest to lowest SMEV (i.e broadest to narrowest peak shapes) . We refer to these heat map matrices as 'wave-maps' (Figure 7A - F). Under all photoperiods and for both SCN subregions we observe transcripts with SEPs ranging from extremely broad-peaked/narrow valleyed (SMEV ~ +8) to extremely narrow-peaked/ broad valleyed (SMEV ~ -8) with approximately Gaussian distributed SEP intermediates lying between. Having identified large differences in transcript SEPs *within* each photoperiod/ SCN subregion, we examined if overall differences in SEP exist *between* photoperiods and/ or SCN subregions. We plotted SMEV cumulative fractions for comparison of photoperiod distributions within R-SCN and C-SCN (Figure 8A and B respectively) and for comparison of SCN subregions under SP, EP and LP (Figure 8C, D and E respectively). SMEV distribution differences clearly visible between photoperiods in R-SCN and to a lesser degree C-SCN were tested for significance using the Kolmogorov-Smirnov test. We found significant differences between SP and EP ($p < 0.01$) and, SP and LP ($p < 0.02$) in R-SCN and between SP and EP ($p < 0.05$), LP and EP ($p < 0.05$) and, SP and LP ($p < 0.02$) in C-SCN. However no significant differences were identified between R-SCN and C-SCN under any photoperiod. Finally, we used Student's *t*-test to examine differences in SMEV means and determined a significant difference exists between SP (mean SMEV = -0.36) and EP (mean = 0.59, $p < 0.02$) in R-SCN and also in C-SCN (SP mean = -0.38, EP mean = 0.45, $p < 0.01$). The clear differences in expression profile shapes collectively for all rhythmic genes between photoperiods support a role for these subregions in encoding daylength, particularly in R-SCN where this difference is more pronounced than C-SCN.

Global transcription profiles in SCN

We have refined previous global transcription circadian profiling methods applied to the SCN (Panda et al., 2002; Ueda et al., 2002) by combining LCM to isolate SCN sub-regions with efficient, single cycle amplification sufficiently sensitive to discover novel differentially regulated transcripts within sub-regions of the SCN. Qualitatively, we confirmed the identification of rhythmic transcripts identified exclusively by microarray in previous SCN genomic profiling studies (Panda et al., 2002; Ueda et al., 2002) including *Avpr1a, Calcr, Caprin1, Dnajb1, Dusp1, Hmgb3, Rgs16,* and *Sfrs17b,* which together with independently verified SRGs we confirmed, represents approximately 40% of all SRGs in our data for all photoperiods and sub-regions. Quantitatively, Panda et al. (2002), and Ueda et al. (2002), identified 337 and 101 rhythmic transcripts respectively in whole SCN using microarrays containing ~12,000 probe sets. Using the GeneChip 430 2.0 microarray employed in this study, containing ~45,000 probe sets targeting ~36,000 unique transcripts (Cui and Loraine, 2009), by extension would have identified 2 – 3 times this number, i.e. ~1000 and ~300 transcripts. Given similar levels of statistical confidence ($p \leq 0.05$), the total number of unique transcripts we identified, 573 for all photoperiods and sub-regions and ~170 on

rostral   caudal
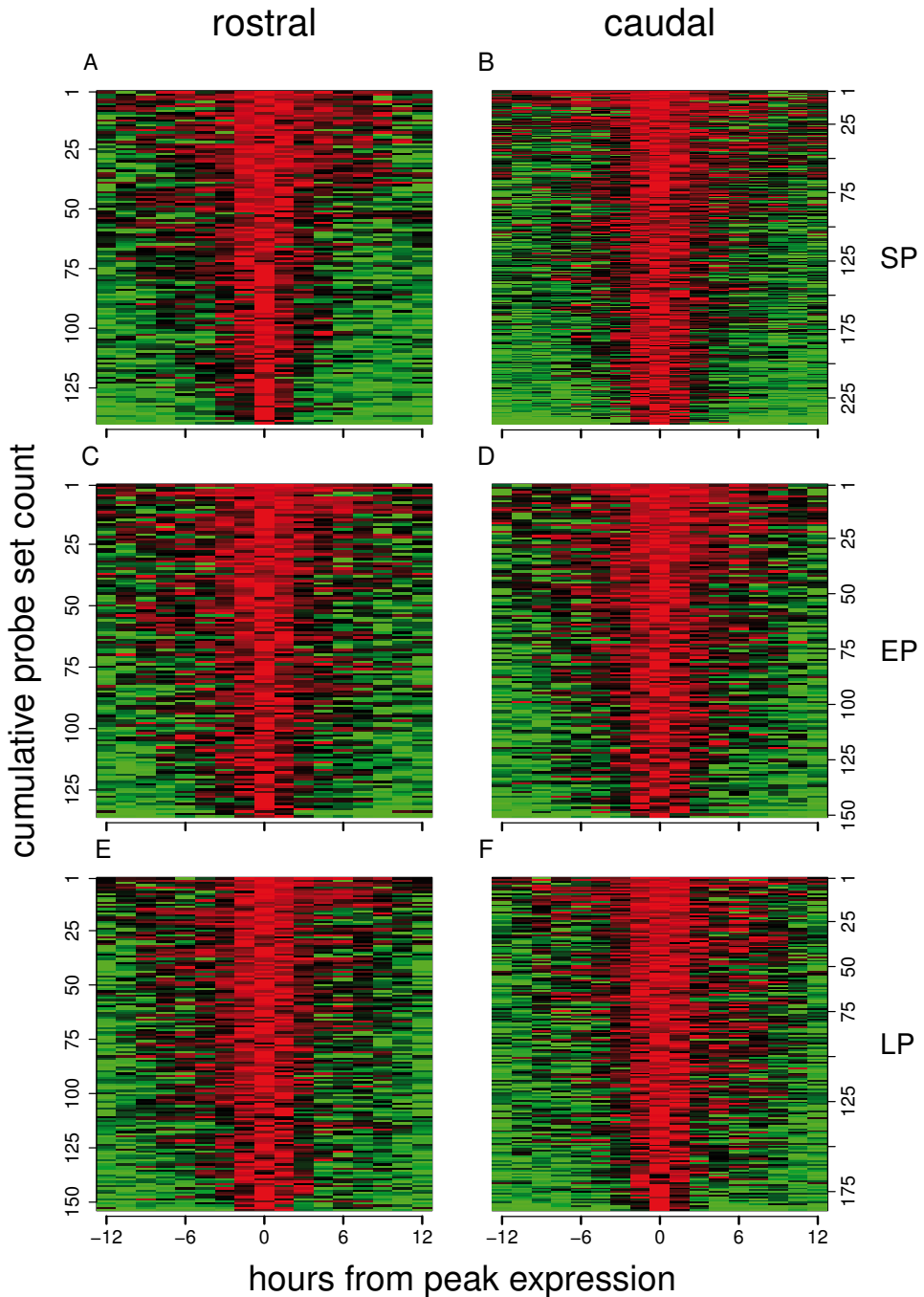
Figure 7. Wave-form maps highlight broader and narrower circadian expression time profile differences. Probe sets defined as circadian are ordered by their sum median-normalized expression values (SMEVs), highest (top) to lowest (bottom). Expression levels are median centered and scaled for SMEV calculation and direct comparison between probe sets. Top panels show wave-form expression in rostral SCN under short (A), equinoxal (B) and long (C) photoperiods; bottom panels show wave-form expression in caudal SCN under short (D), equinoxal (E) and long (F) photoperiods.
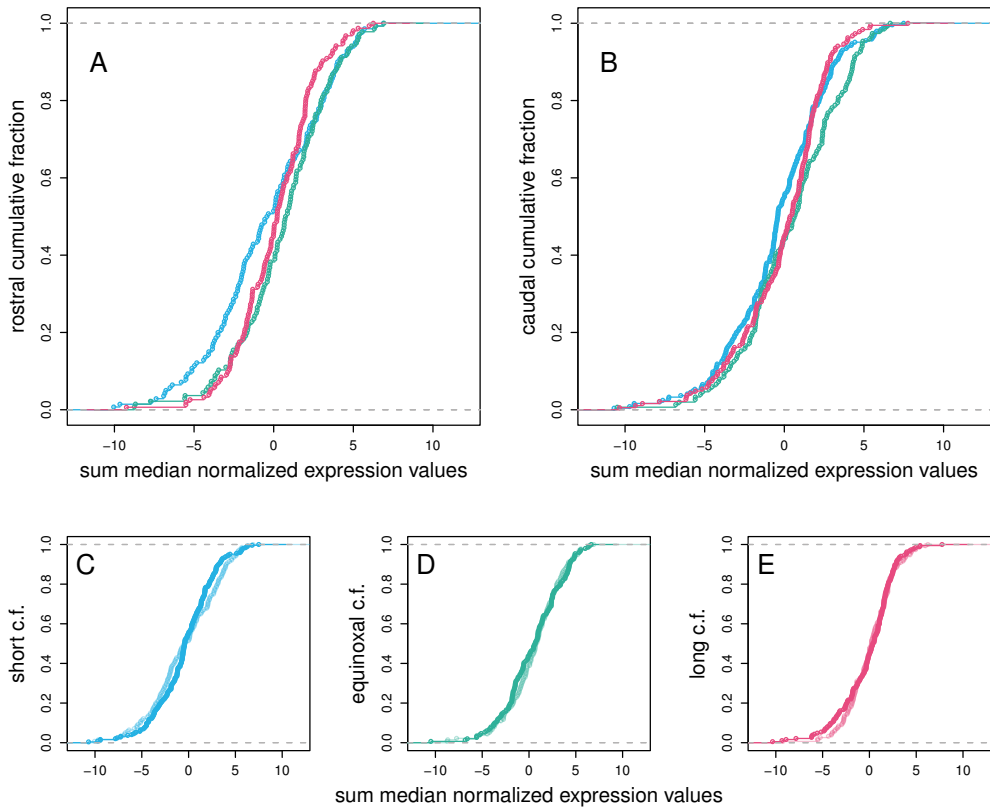
Figure 8. Cumulative distribution plots show overall distribution differences in expression wave forms between photoperiod. Cumulative fractions of the sum median-normalized expression values (SMEVs) obtained from rostral (A) and caudal (B) SCN are shown for short (red), equinoxal (blue) and long (green) photoperiods. Comparison of cumulative fractions between rostral and caudal SCN are shown under short (C), equinoxal (D) and long (E) photoperiods. Significant differences in distributions were identified by the Two-sample Kolmogorov-Smirnov test in rostral SCN between equinoxal and short (p < 0.02) photoperiods; and, in caudal between all photoperiods tested, that is: equinoxal and short (p < 0.05), equinoxal and long (p < 0.05), and, short and long (p < 0.05) photoperiods.

average per subregion and photoperiod is comparable in quantity to Panda et al., (2002) and Ueda et al., (2002). This suggests both our experimental and analytic methods were at least equally sensitive in identifying rhythmic transcripts, despite our reduced biological (n=1) and temporal (circadian cycle=1) sample density. Overall, expression profiles we observe for known SRGs reflect well both within our study for *Per2* assayed by Q-PCR and microarray, and without this study compared with other examples of *Per2* expression in mouse SCN, as well as global transcriptome analyses in the SCN (Panda et al., 2002; Ueda et al., 2002; Sosniyenko et al., 2009, 2010). That we found most rhythmic transcripts with peak phases tracking dawn and dusk in both R-SCN and C-SCN, as well as expression profile shape differences between photoperiods supports a role for photoperiodic encoding within these SCN subregions.

Seasonal affective disorder

Seasonal Affective Disorder (SAD) is characterized by depression typically arising during winter and affects 1 to 3% of the population in temperate climates (Magnusson and Boivin, 2003). The circadian clock may be implicated in this syndrome based on its requirement to transduce photoperiod if not encode it (Levitan, 2007; Barnard and Nolan, 2008). To investigate this we searched the OMIM database for particular genes associated with the terms "Seasonal Affective Disorder" or "SAD". From our list of 573 transcripts rhythmic in any photoperiod or sub-region, we found the following genes associated with these terms: *Bdnf, Serpine1* (synonyms *PAI1, Planh1), Per2, Per3, Npas2, Fos, Prkca, Prkg1*. Of these *Bdnf, Per2, Per3, Fos,* and *Prkca,* are known to be expressed rhythmically in the rodent SCN under constant darkness (Shearman et al., 1997; Liang et al., 1998; Takumi et al., 1998; Grassi-Zucconi et al., 1993; Jakubcakova et al., 2007) and *Serpine1* and *Prkg1* have been shown to be expressed in the SCN (El-Husseini et al., 1999; Revermann et al., 2002; Feil et al., 2005; Mou et al., 2009) where *Serpine1* appears to be rhythmically expressed by microarray assay (Panda et al., 2002). Surprisingly, given the role *Npas2* plays within the forebrain molecular oscillator (McNamara et al., 2001; Reick et al., 2001; Rutter et al., 2001), others failed to detect it in the SCN (Garcia, 2000) let alone finding it rhythmically expressed (Panda et al., 2002; Ueda et al., 2002).

From a circadian perspective, *Per2, Per3, Fos* and *Prkca* might be expected to be associated with SAD. It's been shown that SCN ablation results in compete loss of circannual rhythms (Stetson and Watson-Whitmyre, 1976; Rusak and Morin, 1976). As the central pacemaker relies on the transcription and translation of these genes for normal ~24 hour rhythm generation and synchronization (Albrecht et al., 2001; Silver et al., 1999; Shearman et al., 2000a, 2000b) it's reasonable to expect to that aberrant expression of these core-clock genes will lead to seasonal maladjustment, e.g., SAD. However, amongst our list of rhythmic genes, *Dec1, Dec2, Cry1, Cry2, Dbp, Rev-erbα, Per1 and Rora*, all of which are required for proper SCN function (Lopez-Molina et al., 1997; Shearman et al., 1997; Horst et al., 1999; Honma et al., 2002a; Preitner et al., 2002; Sato et al., 2004), are yet to reveal an association with SAD suggesting that mere disruption of central pacemaker function may alone be insufficient for SAD development.

Per1, Per2, Dec1, Fos and *Prkca* (and others not found in our data to be rhythmic) have been characterized for their roles in photic input of the molecular clock, selective induction by light stimulus throughout the evening phase, and re-entrainment to altered light regimes (Earnest et al., 1990; Colwell and Foster, 1992; Albrecht et al., 1997; Shearman et al., 1997; Honma et al., 2002a; Jakubcakova et al., 2007). The association of *Per2, Fos* and *Prkca*, wth SAD suggests that the entrainment function of the central pacemaker, dependent on these genes for photic input, more than the rhythm maintenance function may underlie the association of the circadian clock with SAD. In support of this, *Dec1, Per1,* and *Per2* expression shows broadening of the wave shape as photoperiod lengthens ie. positive SMEV gradient in at least one (*Per1*, R-SCN; Figure 9B) or both (*Dec1, Per2*) SCN subregions (Figure 9A, B, E and F). Strikingly, *Per3* expression shows the strongest and most consistent broadening of wave shape with increased day length in both subregions,

Rostral circadian gene SMEVs   Caudal circadian gene SMEVs
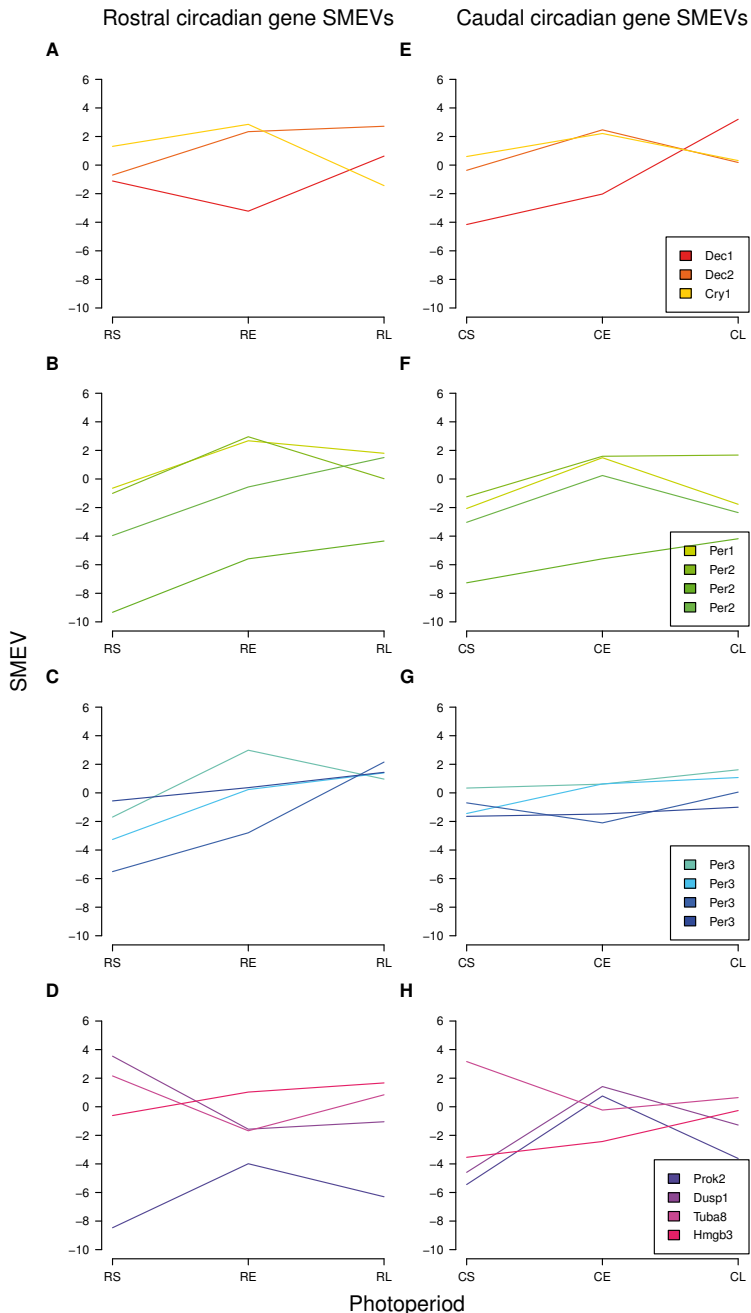
Figure 9. Core clock rhythmic transcripts expression profiles broaden with day length. SMEV values for core-clock gene probe sets which are rhythmic or nearly so (p<0.10) in at least three of the total six combinations of photoperiod and SCN subregions are plotted for Dec1, Dec2, and Cry1 in rostral (A) and caudal (E) SCN; Per1 and Per2 in rostral (B) and caudal (F) SCN; Per3 in in rostral (C) and caudal (G) SCN; and, Prok2, Dusp1, Tuba8 and Hmgb3 in rostral (D) and caudal (H) SCN. RS = rostral SCN, short photoperiod; RE = rostral SCN, equinoxal photoperiod; RL = rostral SCN, long photoperiod; CS = caudal SCN, short photoperiod; CE = caudal SCN, equinoxal photoperiod; CL = caudal SCN, long photoperiod.

especially in rostral. However, unlike *Per2, Fos* and *Prkca*, *Per3* appears not required for resetting in response to phase shifting photic stimuli suggesting a role beyond entrainment (Pendergast et al., 2010).

The expression of *Bdnf, Serpine1* and *Prkg1* in the SCN suggests a role for these genes in rhythm coordination and/or entrainment. BDNF shows diurnal expression levels in both LD and DD in the SCN and plays an important role mediating photic phase shifts (Liang et al., 1998). *Bdnf,* a widely expressed neurotrophin required for neurogenesis in the hippocampus, plays a key role in learning and memory consolidation (reviewed by (Yoshimura et al., 2010). Decrease in BDNF by chronic stress or other factors has been implicated in depression and other mood disorders (reviewed by (Brunoni et al., 2008), although there is limited evidence linking it with SAD presently. *Serpine1,* activated via promoter E/E' box elements by CLOCK-BMAL1 heterodimers (Schoenhard et al., 2003; Chong et al., 2006), repressed by *PER2* (Oishi et al., 2009) and rhythmic in blood plasma (Ohkura et al., 2006), has also been implicated in depression (Tsai et al., 2008; Hou et al., 2009). More recently, an inhibitory role of the phase shifting action of BDNF in the SCN has been shown for *Serpine1* (Mou et al., 2009). *Prkg1,* also implicated in learning and memory (Zhuo et al., 1994; Arancio et al., 1995; Kleppisch et al., 2003), recently has been demonstrated to play a role in photic re-setting and regulation of sleep and wakefulness (Feil et al., 2009; Langmesser et al., 2009). In our study, *Bdnf* and *Sperine1* show clear photoperiod dependent expression, and expression profiles broaden, ie SMEV values increase in R-SCN and especially C-SCN with photoperiod (Figure 10A and C). In view of the known roles for *BDNF, Serpine1* and *Prkg1*, and the consequences of *BDNF* and *Serpine1* dysregulation*,* these genes and their proteins represent candidates for further study of the underlying causes of SAD and potential routes for therapeutic intervention.

Photoperiod influences rhythmic gene expression

Several aforementioned rhythmic SAD associated, core clock genes and other SRGs (*Bdnf*, *Prkg1*, *Dec1*, *Per1*, and *Per2, Per3, Hmgb3*) show a consistent photoperiodic response, i.e., broadening of circadian expression profile as day length increases. For the most part, core clock genes identified as rhythmic, *Cry1, Per1, Per2, Per3, Dec1,*and *Dec2,* show positive SMEV gradients as day length increases except *Cry1* which shows a negative SMEV gradient between SP and EP/LP in both R-SCN and C-SCN (Figure 9A, B, C, D, E and F). These known core clock genes contain E/E' box (*Dec1,* and *Dec2*) and D/D' box regulatory elements (*Cry1, Per1, Per2 and Per3*) which are required for their rhythmic transcription (Ueda et al., 2005; Ukai-Tadenuma et al., 2011). However, *Cry1* is the only gene of this group containing a REV-ERBα/ROR-binding element, which may thus be responsible for its negative SMEV gradient. Additionally, known clock output genes *Prok2* and *Dusp1,* which contain E/E' box elements (Cheng et al., 2002; Doi et al., 2007), show positive SMEV gradients between SP and EP/LP in C-SCN (Figure 9H). Although rhythmic in the SCN (Panda et al., 2002; Ueda et al., 2002), no circadian regulatory elements have been identified for *Tuba8* and *Hmgb3*, the only other consistently rhythmic circadian transcripts we identified. An attempt to attribute the postulated duality to specific genes in the clock

Rostral SAD gene SMEVs   **Caudal SAD gene SMEVs**
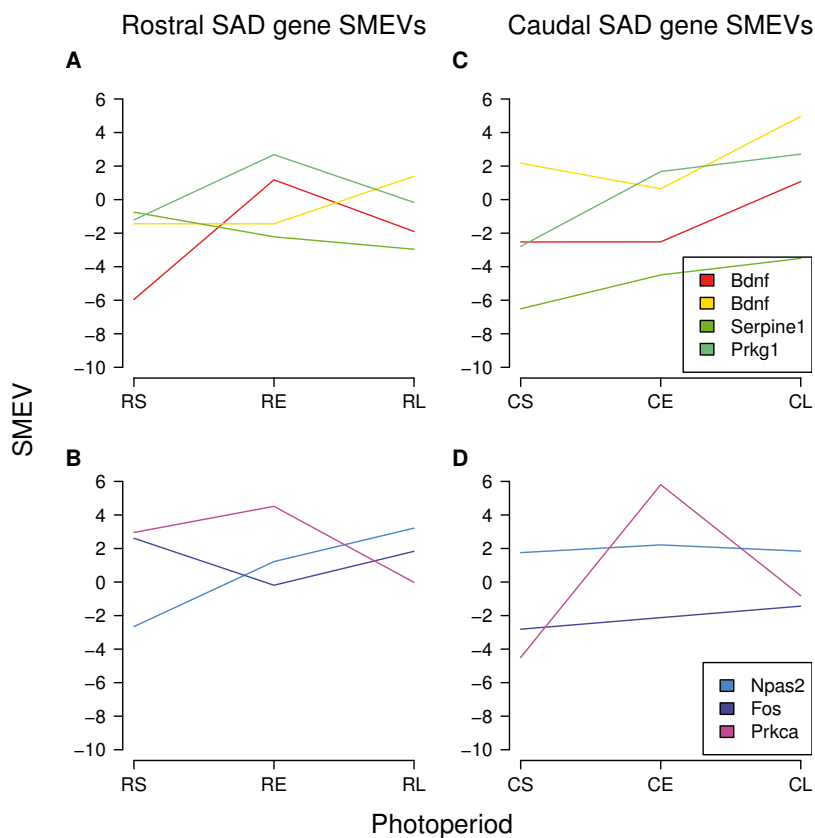
Figure 10. Transcripts associated with seasonal affective disorder expression profiles broaden with day length. SMEV values of probe sets rhythmic (p<0.05) in at least one of the six combinations of photoperiod and SCN subregions are plotted for candidate genes associated with seasonal affective disorder. Bdnf, Serpine1, Prkg1 in rostral (A) and caudal (E); Npas2, Fos, Prkca in rostral (B) and caudal (D). RS = rostral SCN, short photoperiod; RE = rostral SCN, equinoxal photoperiod; RL = rostral SCN, long photoperiod; CS = caudal SCN, short photoperiod; CE = caudal SCN, equinoxal photoperiod; CL = caudal SCN, long photoperiod.

mechanism was launched by (Daan et al., 2001). Their model was refuted when predictions on circadian light responses, though confirmed for the *Per1* and *Per2* genes, did not hold up for the *Cry1* and *Cry2* genes when tested in knock-out mouse strains for these genes (Spoelstra et al., 2004; Spoelstra and Daan, 2008).

The distribution of SMEVs for all rhythmic genes show significant differences between photoperiods and reflect the qualitative observations of SMEV gradients for rhythmic SRGs discussed above (Figure 8A). Specifically, SP has a lower sample mean SMEV, compared to EP (0.36 vs 0.59) confirming that rhythmic transcript expression profiles overall are significantly narrower peaked/broader valleyed in R-SCN under SP compared to EP and LP. This suggests that the majority of rhythmic transcripts are 'light-controlled', such that the shorter period of light under SP concomitantly compress' expression peaks, at least for transcripts with negative SMEV values, ie. those whose peaks are narrower than their

Rostral broadening circadian gene SMEVs

Caudal broadening circadian gene SMEVs

Figure 11. Rhythmic transcripts expression profiles that broaden with day length. SMEV values for rhythmic probe sets which are neither core-clock genes nor SAD associated genes and that are, per SCN subregion, rhythmic (Filter I and II, $p < 0.05$) in one or more photoperiods and nearly rhythmic (Filter I and I, $p < 0.10$) under the remaining one or two photoperiods., ie., the same criteria used to select probe sets for plotting in **Figure 4.** Peak expression phase trajectories. Of these, probe sets whose SMEV increases with lengthening of photoperiod, ie., a broadening temporal expression profile are plotted ofr rostral (A – B) and caudal (C - D). Genes are indicated in the legend. RS = rostral SCN, short photoperiod; RE = rostral SCN, equinoxal photoperiod; RL = rostral SCN, long photoperiod; CS = caudal SCN, short photoperiod; CE = caudal SCN, equinoxal photoperiod; CL = caudal SCN, long photoperiod.

valleys. However for the minority of transcripts whose SEMV values are positive, i.e. have peaks broader than their valleys, the distribution of SMEVs is more positive for transcripts under SP and EP compared to LP, i.e. the opposite of the distributions for transcripts with negative SMEV values. This suggests that transcripts with positive SMEV values, constituting the minority in R-SCN, may be 'dark-driven' given the extended period of darkness under LP. SMEV sample means and distributions for each photoperiod do not differ significantly between SCN sub-regions (Figure 8C, D and E), although the differences observed in R-SCN are reflected to a more modest degree in C-SCN. Differences in sample means between SP and EP (-0.38, 0.45, $p < 0.01$), and distributions between SP and EP ($p < 0.05$) and LP and LP ($p < 0.05$) are evident, but this difference probably arises solely between transcripts with positive SMEV values as the cumulative fractions of transcripts with negative SMEV values virtually overlap (Figure 8B). The stronger photoperiodic
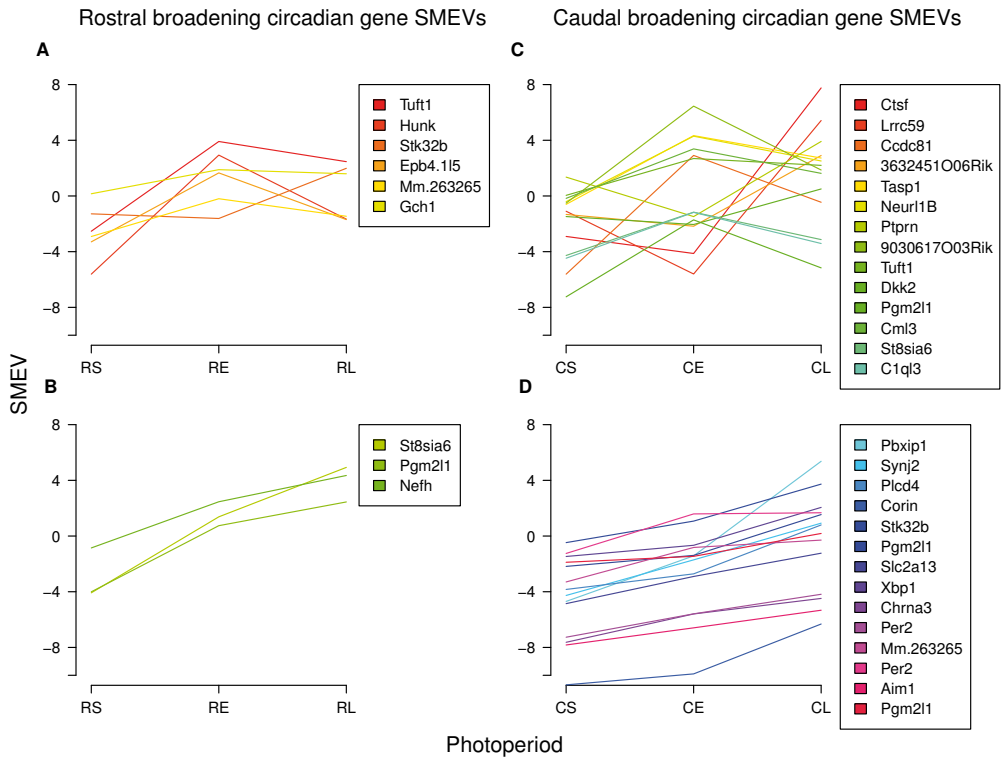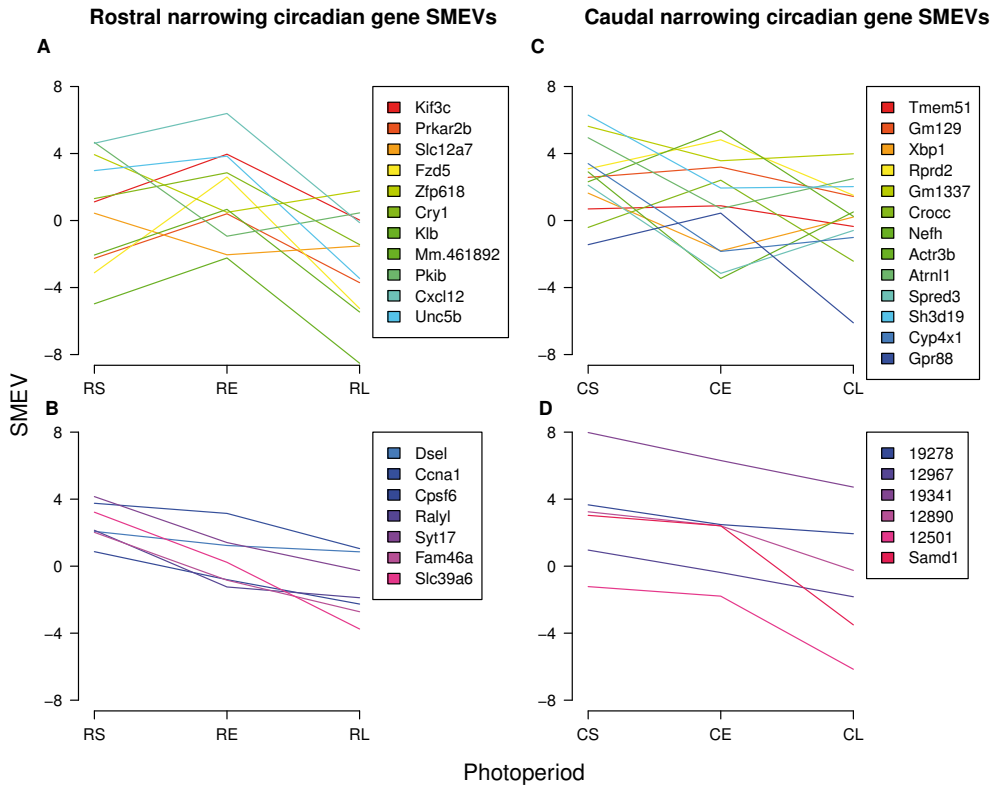
Figure 12. Rhythmic transcripts expression profiles that narrow with day length. SMEV values for rhythmic probe sets which are neither core-clock genes nor SAD associated genes and that are, per SCN subregion, rhythmic (Filter I and II, p < 0.05) in one or more photoperiods and nearly rhythmic (Filter I and I, p < 0.10) under the remaining one or two photoperiods., ie., the same criteria used to select probe sets for plotting in **Figure 4.** Peak expression phase trajectories. Of these, probe sets whose SMEV decreases with lengthening of photoperiod, ie., a narrowing temporal expression profile are plotted ofr rostral (A – B) and caudal (C - D). Genes are indicated in the legend. RS = rostral SCN, short photoperiod; RE = rostral SCN, equinoxal photoperiod; RL = rostral SCN, long photoperiod; CS = caudal SCN, short photoperiod; CE = caudal SCN, equinoxal photoperiod; CL = caudal SCN, long photoperiod.

response observed here in R-SCN versus C-SCN support the photoperiodic regulation of *Per1* peak phase demonstrated in R-SCN but not C-SCN in pervious studies (Inagaki et al., 2007; Naito et al., 2008).

Concluding remarks

Our study is the first attempt to identify novel, photoperiodically regulated transcripts in the mammalian central pacemaker. "Bottom-up" studies on the SCN response to different photoperiod have thus far focused on the behavior of clock genes *Per1, Per2, Rev-erbα, Dbp* and *Avp* in different sub-regions of the SCN, namely the rostral and caudal and electrophysiological output from whole SCN (Hazlerigg et al., 2005; Inagaki et al., 2007; VanderLeest et al., 2007; Naito et al., 2008; Sosniyenko et al., 2009, 2010).

Meanwhile, high throughput "top-down" genomics experiments have until now provided transcription profiles only from whole SCN entrained under standard 12:12 light dark conditions (Panda et al., 2002; Ueda et al., 2002). Here we recapitulate previous findings of photoperiod regulated clock gene expression in mouse SCN sub-regions and reveal novel, candidate photoperiodically regulated transcripts, including those whose peak phases cluster specifically around dawn, mid-day or dusk; those which specifically follow dawn, mid-day or dusk peak phase trajectories; and, those whose circadian peak expression profiles broaden or narrow in response to photoperiod. The potential involvement of these candidate photoperiodically regulated transcripts in human disease, particularly Seasonal Affective Disorder and other syndromes associated with seasonal changes in day length, remains to be elucidated.

MATERIALS AND METHODS

Animal studies

One-month-old male C57BL/6J-OlaHsd mice (Harlan, Horst, The Netherlands) were individually housed in lucite cages (25 x 25 x 40 cm), equipped with a running wheel (14 cm diameter), in a sound attenuated, climate controlled room (temperature 23 ± 1ºC; relative humidity 60%) with food (Hope Farms standard rodent pellets) and water available *ad libitum*. Voluntary wheel running activity (binned to 2 minute intervals) was continuously recorded by an online computer using the ERS program. The room was equipped with 24 separate light-tight compartments, each with a computer controlled variable light intensity provision and all cages (4 cages/compartment) had roughly equal distance (70 cm) to the light source (Osram L58W/31 tubes, Philips; (Comas et al., 2006).

Mice (n=32 animals/group) were entrained for 30 days to either long photoperiod (LP; LD6:18 h), equinox photoperiod (EP; LD12:12 h), or short photoperiod (SP; LD18:6 h). Twilight transitions of 1 h between light and darkness were applied. Starting 30 minutes before the scheduled onset of light, light intensity was increased linearly on a log scale from 0.1 to 100 lux, with 1 log unit / 20 min. The maximum light intensity was 100 lux, equivalent to circa 145mW/m^2 at the cage floor level (light source: white light tubes TDL 36W/85 Philips, The Netherlands). After 30 days entrainment, all animals were placed in constant darkness (DD). On the second cycle in DD one mouse per time point was sacrificed every 1.5 hours. Mice were anaesthetized by inhalation of Forane (Abbott Laboratories, UK). Brains were rapidly dissected under dim red light conditions and frozen in ice-cold Tissue-Tek Oct Compound 4583 embedding medium (Sakura) and stored at -80 °C.

Experiments were conducted in accordance with Dutch and European legal requirements and were approved by the animal ethical committee of the University of Groningen.

SCN subregion isolation, RNA purification and quality assessment

Coronal cryosections (25µm) mounted on 1 mm PALM PEN-membrane slides (P.A.L.M. Microlaser Technologies) were rapidly thawed, fixed for 30 seconds in 70% EtOH and immediately stained with haematoxylin for 3 minutes. Following staining sections were

rinsed in diethylpyrocarbonate (DEPC) treated dH_2O and dehydrated by several rinses in 100% EtOH. Laser catapult microdissection (LCM) of rostral and caudal SCN subregions was accomplished using the PALM Microlaser system (P.A.L.M. Microlaser Technologies) on freshly prepared sections. The quantity of rostral and caudal subregions, as determined by the surface area estimated by the PALM Microlaser software, was not significantly different (Student's t-test, $p<0.01$, data not shown). Isolated SCN subregions were dissolved immediately in Lysis Buffer (Qiagen) and stored at -80°C for subsequent batchwise RNA purification. RNA was purified with the inclusion of 'on-column' DNase treatment using the RNeasy 'Micro' kit (Qiagen) according the manufacturers protocol, except 16S/23S bacterial ribosomal RNA (Roche) was used as a carrier species and an additional elution was performed in the final step to maximize RNA yield. RNA was eluted with RNase free dH_2O and vacuum evaporated for immediate amplification and cDNA generation. Quality of the freshly purified RNA was assayed using the BioAnalyzer 2100 (Agilent) in combination with the RNA 6000 Pico chip (Agilent). Where intact 18S/28S ribosomal RNA peaks were evident, the sample was considered worthy of processing for Q-PCR and/or microarray analysis.

Quantitative RT-PCR

Amplification and complementary DNA strand synthesis of purified sample RNA was accomplished using the Ovation RNA Amplification System V2 (Nugen Technologies) according to the manufacturers protocol. Efficiency of the amplification was assayed quantitatively by 260/280 nm estimation of cDNA concentration, where a yield of at least 4.8 µg cDNA was deemed sufficient for specific amplification of the RNA template. Quality of the cDNA was assessed using the BioAnalyzer 2100 with the RNA 'Nano' chip to confirm a Gaussian distribution of the cDNA product indicative of specific amplification of mRNA transcripts according to the manufactures recommendations (Nugen Technologies). Q-PCR was performed using 2x SYBR green reaction mix according to the manufacturer's protocol (Stratagene). Intron-spanning primers for *Per2* were designed primers using 'Primer3' (Rozen and Skaletsky, 2000): forward (5'-CTC AGG GAG AGG AAC AGA GAG-3') and reverse (5'-ATT GGG AGG CAC AAA GTC AG-3') oligonucleotides used in the reaction mix (10 nM)e.

Labeling and hybridization of purified RNA samples

Samples were amplified similarly as for qRT-PCR and cDNA was labeled with biotin using the Ovation™ RNA Amplification System V2 and FL-Ovation™ cDNA Biotin Module V2, respectively, according to the manufacturer's protocol (Nugen Technologies). Efficiency and quality of amplified cDNA were assayed identically as performed for Q-PCR. Biotin labeled, fragmented cDNA samples were combined with hybridization cocktail including dimethyl sulfoxide (DMSO) according to the manufacturers protocol (Nugen Technologies) and hybridized to GeneChip Mouse Genome 430 2.0 Arrays (Affymetrix) for 18 hrs. Post-hybridization washing, scanning and image analysis were performed using the Fluidics Station 450 (Affymetrix) utilizing the fluidics protocol FS450-0004 and GeneChip Scanner 3000 7G according to the Affymetrix GeneChip Manual.

Expression measure export, normalization and invariant probe set subtraction

Expression measures were exported using the MAS5.0 software suite (Affymetrix), and normalized using the GeneChip Robust Multichip Average method (GCRMA; package version 2.20.0) (Wu and Irizarry, 2004), running in the R environment (version 2.11.1). All subsequent parametric statistical analyses were performed on $\log_2$-transformed expression data, ie., approximately normally distributed data within each micro array. Lowly expressed transcripts and/or transcripts which vary minimally across all microarrays were removed as per (Moshkin et al., 2007) which is based on the clustering methods developed by (Rousseeuw and Driessen, 1999).

Rhythmic transcript identification

Microarray and qRT-PCR probe sets were assessed for rhythmic expression using a two filter approach to estimate the likelihood that a probe is oscillating according to a given sine based function.

Filter I utilizes a linear model to identify probes which vary significantly over time under any combination of photoperiod or SCN subregion. To take into account the fact that the two measurements for each animal (i.e. rostral and caudal) are correlated, a multivariate regression model was used. Moreover, to allow for full flexibility in the specification of the average time effect in each of the six conditions, we considered natural cubic splines of time with four internal knots placed at the corresponding observed percentiles. The hypotheses of 'no time effect' and equality in the expression levels in each gene were tested using appropriately constructed contrasts and an F-test. The resulting p-values were corrected for multiple testing using the Benjamini & Hochberg method ($\alpha = 0.05$). Analysis performed in Filter I used R packages 'nlme' (version 3.1-96), 'splines' (version 2.11.1), 'multcomp' (version 1.1-7), and 'lattice' (version 0.18-8) available from http://cran.r-project.org/ .

Filter II evaluates probe sets identified as significant from Filter I for goodness of fit to a sine based function using F-tested harmonic regression implemented in CircWave as previously described (Oster et al., 2006; Keller et al., 2009). Fundamental sine waves with periods between 18 and 29 hrs, spanning the range of circadian periods observed *in vivo* in mouse tissues 20 through 28 (Hughes et al., 2009), with two harmonics were tested in 0.1 hour intervals for goodness of fit. Probe sets binned by CircWaveBatch into the first (18.0 - 18.1 hrs) and last (29.9 - 30.0 hrs) period bins have an increased likelihood of a Type I error (false positivity) occurring, as compared to any other bins (18.1 though 29.9 hrs), which is characteristic of some 'goodness of fit' methods including CircWaveBatch (Oster et al., 2006). Thus, probe sets with periods less than 18.1 or greater than 29.9 hrs were excluded from further analysis to minimize the Type I error rate. The harmonic regression procedure calculates complex wave shapes without parameter estimations. After correction for multiple testing using the Holm method (Holm, 1979), probe sets were defined as *rhythmically* expressed when the harmonic regression model for any of the fundamental sine waves ('p1') or the first ('p2') or second ('p3') of the harmonics significantly explained the variation in expression levels ($\alpha = 0.05$). Only those probe sets

for which the fundamental sine waves was significant ('p1' < 0.05 after correction) were defined as circadianly expressed. This analysis was performed using CircWaveBatch v3.4.

Compilation of a list of known rhythmic and non-rhythmic SCN transcripts

To help develop our method for identifying rhythmic transcripts and fine tune significance thresholds (α) to discriminate between rhythmic and non-rhythmic transcripts, we generated a compiled list of known SCN rhythmic and non-rhythmic trancripts and their respective probe sets (referred to by the acronym CLOKSRAN) containing SCN rhythmic genes (SRGs) and SCN non-rhythmic genes (SNGs; Lopez-Molina et al., 1997; Sun et al., 1997; Shearman et al., 2000a, 2000b; Yan et al., 2000; Mitsui et al., 2001; Cheng et al., 2002; Harmar et al., 2002; Honma et al., 2002b; Panda et al., 2002; Preitner et al., 2002; Sumi et al., 2002; Ueda et al., 2002; Oster et al., 2003; Sato et al., 2004; Duffield et al., 2009). For SRGs and SNGs for which rhythmic or non-rhythmic expression was demonstrated by *in situ* hybridization or qRT-PCR, probe sets were mapped by Ensembl and Affymetrix. SRGs and SNGs identified through at least two independent microarray studies (thus minimizing Type I errors, ie. false positivity, associated with microarray studies), and for which *equivalent* probe sets detected the same rhythmic transcript in the SCN across these studies, were also included in the list. Specifically, the equivalent probe set on the Affymetrix 430_2.0 array determined using NetAffx database, if available, was included here.

Rhythmic transcript analysis

From the goodness-of-fit to sine based curve approach employed in Filter II to asses probe sets for rhythmicity, several estimates of rhythmic behavior are available including: (i) goodness of fit of the curve (expressed as a p-value describing the significance of the regression), (ii) average expression over 24 hrs, (iii) period, (iv) peak and nadir expression times and levels, and (v) amplitude (difference between peak and nadir levels). Peak and nadir phases were expressed as Internal Time (InT; (Daan et al., 2002) and plotted relative to the preceding light-dark cycle (expressed as External Time, ExT, defined by midnight = ExT0) by multiplying with 24/period. These estimates were used for further analyses as described in the text. Time-course expression profiles were examined for characteristic 'broadness' or 'narrowness' of the wave-form by using the sum of the midrange-scaled expression values (SMEVs), which we developed. Using this method broad peaked/narrow vallyed wave-forms have positive SMEVs are and narrow peaked/broad valleyed wave-form have negative SMEVs.

Analysis of non-rhythmic differentially expressed transcripts

To test for differences in overall expression levels between probe sets exhibiting a *constant average time effect*, a three-step approach was employed. First, probe sets with an unadjusted p-value greater than 0.4 in the F-test, used in Filter I of 'Rhythmic transcript identification', were defined as having 'no time effect'. Second,'no time effect' probe sets were subjected to a multivariate regression model with correlated error terms to allow for detection of different overall expression levels in each condition. The hypothesis of no difference in the expression levels between the six conditions was tested using appropriately constructed

contrasts and an F-test, and the resulting p-values corrected using the Benjamini & Hochberg method (Benjamini and Hochberg, 1995). Finally, the significant probe sets from step two (after correction) were tested again with F-tests and the p-values corrected using Holm's method (Holm, 1979). Probe sets with p-values <0.05 (after correction) were defined as non-rhythmic, differentially expressed transcripts. Such probe sets, differentially expressed between any two or more combinations of photoperiod and/or SCN subregion, were visualized with the methods described below.

Hierarchical clustering

Unsupervised hierarchical clustering was performed using Pearson's correlation co-efficient distance metric with complete linkage and mean scaling of expression values by probe set (row), as previously described by (Eisen et al., 1998).

Correlation matrix

A correlation matrix was produced using Pearson's correlation co-efficient to quantify similarity for all pairwise comparisons between all samples. Principle component analysis was performed sample-wise by calculating Eigenvalues according to (Raychaudhuri et al., 2000).

Online Supplementary Material

Supplementary tables are available at http://bioinf-quad07.erasmusmc.nl/scn/

SUPPORTING INFORMATION

Rhythmic transcript identification

Amplified cDNA was labeled and hybridized to Affymetrix GeneChip® Mouse Genome 430 2.0 Arrays, containing 45,101 unique probe sets representing 36,431 putative target transcripts. An overview of the bioinformatics work flow is shown in Figure 2. Inter-array variation was normalized using the GeneChip robust multi-array analysis method (GCRMA; (Wu and Irizarry, 2004) and lowly expressed and/or invariant transcripts in all arrays were removed as described by (Moshkin et al., 2007). Transcripts were assessed for rhythmic expression using a sequential dual filter approach. Filter I utilizes a linear model to identify transcripts which vary significantly over time, irrespective of photoperiod or SCN subregion; Filter II evaluates transcripts identified by Filter I for goodness of fit to a sine based function using F-tested harmonic regression (Oster et al., 2006; Keller et al., 2009). We chose this approach for several reasons. First, Filters I and II can accommodate a broad range of periods, which may be important given evidence of period changes in animals entrained to different photoperiods (Ciarleglio et al., 2011). Although ultradian periods of ~12 and ~8 hours have been shown in tissues (Hughes et al., 2009), we focused on circadian rhythmicity and limited our search to transcripts whose temporal profiles fit sine based curves (evaluated using filter II, see below) with periods between 18 and 30 hours. Second, Filter I makes no assumptions about temporal

profile whilst Filter II can accommodate two harmonics in addition to the single sine curve. Thus, a large range of asymmetric circadian profiles may be identified as rhythmic. This is important given examples of photoperiodically regulated *Per1* and *Per2* rhythms deviating to a large degree from the classical circadian single sine wave, ie., demonstrating broad peaks after entraining to a long photoperiod, and vice versa- narrow peaks after short photoperiod entrainment (Inagaki et al., 2007; Naito et al., 2008; Sosniyenko et al., 2009). Third, we reduced the likelihood of 'modal failure' by utilizing filters based on different underlying principles (Hughes et al., 2009).

In order to minimize false positive classification of transcripts as rhythmic ('Type I errors') and to minimize a failure in classifying bona fide rhythmic transcripts as non-rhythmic ('Type II errors'), we first empirically determined significance thresholds (α) for both Filters I and II using a 'training set' of known circadianly expressed transcripts. To this end, we compiled a list of known SCN rhythmic and non-rhythmic (CLOKSRAN) probe sets comprising (i) SCN rhythmic genes (SRGs) previously demonstrated to be rhythmically by *in situ* hybridization, immunohistochemistry or qRT-PCR approach, or two independent transcriptome studies, and (ii) SCN non-rhythmic genes (SNGs) commonly used as non-rhythmic controls in circadian gene expression studies, including, but not limited to the reports from which CLOKSRAN SRGs were obtained (see Materials and Methods for references). Supplementary Figure S1 shows a heatmap matrix of CLOKSRAN probe sets for the array data of the two SCN subregions under different photoperiods. For the SRGs, 41% display significant variance over time ($p < 0.05$) in at least one SCN subregion and photoperiod and pass the Filter I selection criteria, whilst no SNG transcripts are significant. Under SP, EP and LP conditions respectively, 9, 10 and 6% of R-SCN SRGs and 20, 23 and 11% of C-SCN SRGs were defined as rhythmic, and as such pass Filter II. Thus, a higher proportion of known circadian transcripts were determined to be rhythmic in the C-SCN compared to R-SCN. In addition, although distinctions between photoperiods are less clear, under long photoperiod a reduced proportion of SRGs appeared rhythmic as compared to short and equinoxal photoperiods. Importantly, none of the SNGs probe sets passed Filters I and II, indicating our approach successfully minimized the false classification of circadian transcripts. The low proportion of SRGs identified as rhythmic (10 - 20%) likely results from the low false positive rate (0.05) we enforced and the fact that we used a high density sampling approach (1.5 hr intervals) with only 1 animal per time point over a single circadian cycle, rather than 4 hour interval sampling with biological replicate, over several circadian cycles as used in other genomic studies of the SCN (Panda et al., 2002; Storch et al., 2002; Ueda et al., 2002; Oster et al., 2006; Hughes et al., 2007; Hughes et al., 2009; Keller et al., 2009). The peak phase of expression of all SRGs composing CLOKSRAN in R-SCN and C-SCN under different photoperiods expands insight into central pacemaker functioning. To this end we show (Supplementary Figure S4) the peak phase expression for all CLOKSRAN SRG probe sets which are significant ($p < 0.05$) in at least one photoperiod for each subregion and nearly so ($p < 0.10$) in the other one or two photoperiods. A non-redundant list of all transcripts determined to be significantly rhythmic ($p < 0.05$) is shown in Online Supplementary Table S7.

We also used over-representation of gene functional annotations including, the Gene Ontology (GO), KEGG and BIOCARTA annotation databases implemented by DAVID (Huang et al., 2009a, 2009b), to assess our success identifying known SRGs. Each list of rhythmic transcripts identified for the six combinations of SCN subregions and photoperiods was assessed for over-representation. For all six lists, the terms "GO:rhythmic process", "GO:circadian rhythms", and "GO:biological rhythms" were significantly over-represented (p<0.01) demonstrating the enrichment of known SRGs in these lists and validating our approach for identifying rhythmic transcripts expressed in rostral and caudal SCN.

Per2 expression in rostral and caudal SCN under different photoperiods

As the differential phasing of *Per1/2* expression between R-SCN and C-SCN in response to different photoperiods guided the design of our study (Hazlerigg et al., 2005; Inagaki et al., 2007; Naito et al., 2008), we first analyzed in more detail *Per2* expression under different photoperiods. As shown in Supplementary Figure S3, expression profiles for *Per2* obtained by Q-PCR assay closely mirror those obtained by microarray (see Supplementary Figure S2). However our microarray and Q-PCR *Per2* profiles do not show the clear peak phase differences between R-SCN and C-SCN under LP as demonstrated in hamsters, where *Per2* peaks around dawn in C-SCN and dusk in R-SCN (Hazlerigg et al., 2005). Although we see a modest advance of *Per2* peak phase under LP in C-SCN (ExT11.3) compared to R-SCN (ExT11.8) by Q-PCR, *Per2* in C-SCN shows a broad peak profile centered around midday, not dusk. On the other hand, our *Per2* expression profiles closely match those assayed by ISH from mice entrained to SP and LP, also using twilight transitions similar to this study; and find a reduction in phase differences between R-SCN and C-SCN with peak phases occurring around dusk and mid-day respectively (Sosniyenko et al., 2009). *Per1* expression in mice assayed by ISH, *Per1::luc* (Inagaki et al., 2007; Naito et al., 2008) and *Per1::GFP* bioluminescence (Ciarleglio et al., 2011) although consistently phase advanced ~2 hours across all photoperiods and SCN sub-regions, match our daily *Per2* profile well. Notably we observe bimodal *Per2* expression in R-SCN under LP with a primary peak around dusk and secondary peak advancing to mid-day or earlier (Supplementary Figure S3E and Figure S2E). These peaks likely represent the neuronal populations referred to as 'anterior evening' and 'anterior morning' phased neurons respectively within R-SCN by Inagaki et al., (2007) and Naito et al., (2008). Comparison of our results with the aforementioned real-time bioluminescence data highlight an important aspect of our study: we assayed arbitrary neuronal populations representing 'rostral' and 'caudal' SCN subregions. Our profiles thus represent the 'average expression' of 100's of neurons, without the ability to resolve individual contributions to this 'average'. Overall, our *Per2* results match well published observations of *Per* expression in mouse SCN sub-divisions entrained to different photoperiods.

ACKNOWLEDGMENTS

III

REFERENCES

1. Albrecht, U., Sun, Z. S., Eichele, G., and Lee, C. C. (1997). A Differential Response of Two Putative Mammalian Circadian Regulators, mper1and mper2, to Light. Cell *91*, 1055-1064.

2. Albrecht, U., Zheng, B., Larkin, D., Sun, Z. S., and Lee, C. C. (2001). mPer1 and mPer2 Are Essential for Normal Resetting of the Circadian Clock. J Biol Rhythms *16*, 100-104.

3. Arancio, O., Kandel, E. R., and Hawkins, R. D. (1995). Activity-dependent long-term enhancement of transmitter release by presynaptic 3[prime],5[prime]-cyclic GMP in cultured hippocampal neurons. Nature *376*, 74-80.

4. Balsalobre, A., Damiola, F., and Schibler, U. (1998). A Serum Shock Induces Circadian Gene Expression in Mammalian Tissue Culture Cells. Cell *93*, 929-937.

5. Barnard, A. R., and Nolan, P. M. (2008). When Clocks Go Bad: Neurobehavioural Consequences of Disrupted Circadian Timing. PLoS Genet *4*, e1000040.

6. Bell-Pedersen, D., Cassone, V. M., Earnest, D. J., Golden, S. S., Hardin, P. E., Thomas, T. L., and Zoran, M. J. (2005). Circadian rhythms from multiple oscillators: lessons from diverse organisms. Nat Rev Genet *6*, 544-556.

7. Benjamini, Y., and Hochberg, Y. (1995). Controlling the False Discovery Rate: A Practical and Powerful Approach to Multiple Testing. Journal of the Royal Statistical Society. Series B (Methodological) *57*, 289-300.

8. Brunoni, A. R., Lopes, M., and Fregni, F. (2008). A systematic review and meta-analysis of clinical studies on major depression and BDNF levels: implications for the role of neuroplasticity in depression. Int. J. Neuropsychopharmacol *11*, 1169-1180.

9. Bünning, E. (1936). Die endogene Tagesrhythmik als Grundlage der photoperiodischen Reaktion. Ber. dtsch. bot. Ges *54*, 35.

10. Butler, M. P., and Silver, R. (2009). Basis of Robustness and Resilience in the Suprachiasmatic Nucleus: Individual Neurons Form Nodes in Circuits that Cycle Daily. J Biol Rhythms *24*, 340-352.

11. Cheng, M. Y., Bullock, C. M., Li, C., Lee, A. G., Bermak, J. C., Belluzzi, J., Weaver, D. R., Leslie, F. M., and Zhou, Q.-Y. (2002). Prokineticin 2 transmits the behavioural circadian rhythm of the suprachiasmatic nucleus. Nature *417*, 405-410.

12. Chong, N. W., Codd, V., Chan, D., and Samani, N. J. (2006). Circadian clock genes cause activation of the human PAI-1 gene promoter with 4G/5G allelic preference. FEBS Letters *580*, 4469-4472.

13. Ciarleglio, C. M., Axley, J. C., Strauss, B. R., Gamble, K. L., and McMahon, D. G. (2011). Perinatal photoperiod imprints the circadian clock. Nat Neurosci *14*, 25-27.

14. Colwell, C. S., and Foster, R. G. (1992). Photic regulation of Fos-like immunoreactivity in the suprachiasmatic nucleus of the mouse. J. Comp. Neurol. *324*, 135-142.

15. Comas, M., Beersma, D. G. M., Spoelstra, K., and Daan, S. (2006). Phase and Period Responses of the Circadian System of Mice (Mus musculus) to Light Stimuli of Different Duration. Journal of Biological Rhythms *21*, 362 -372.

16. Cui, X., and Loraine, A. E. (2009). Consistency Analysis of Redundant Probe Sets on Affymetrix Three-Prime Expression Arrays and Applications to Differential mRNA Processing. PLoS ONE *4*, e4229.

17. Daan, S., Albrecht, U., Van der Horst, G. T. J., Illnerová, H., Roenneberg, T., Wehr, T. A., and Schwartz, W. J. (2001). Assembling a Clock for All Seasons: Are There M and E Oscillators in the Genes? Journal of Biological Rhythms *16*, 105 -116.

18. Daan, S., Merrow, M., and Roenneberg, T. (2002). External time--internal time. J. Biol. Rhythms *17*, 107-109.

19. Dardente, H., Menet, J. S., Challet, E., Tournier, B. B., Pévet, P., and Masson-Pévet, M. (2004). Daily and circadian expression of neuropeptides in the suprachiasmatic nuclei of nocturnal and diurnal rodents. Molecular Brain Research *124*, 143-151.

20. Dardente, H., Wyse, C. A., Birnie, M. J., Dupré, S. M., Loudon, A. S. I., Lincoln, G. A., and Hazlerigg, D. G. (2010). A molecular switch for photoperiod responsiveness in mammals. Curr. Biol *20*, 2193-2198.

21. Doi, M., Cho, S., Yujnovsky, I., Hirayama, J., Cermakian, N., Cato, A. C. B., and Sassone-Corsi, P. (2007). Light-Inducible and Clock-Controlled Expression of MAP Kinase Phosphatase 1 in Mouse Central Pacemaker Neurons. Journal of Biological Rhythms *22*, 127-139.

22. Duffield, G. E., Watson, N. P., Mantani, A., Peirson, S. N., Robles-Murguia, M., Loros, J. J., Israel, M. A., and Dunlap, J. C. (2009). A Role for Id2 in Regulating Photic Entrainment of the Mammalian Circadian System. Current Biology *19*, 297-304.

23. Dunlap, J. C. (1999). Molecular Bases for Circadian Clocks. Cell *96*, 271-290.

24. Dupré, S. M., Miedzinska, K., Duval, C. V., Yu, L., Goodman, R. L., Lincoln, G. A., Davis, J. R. E., McNeilly, A. S., Burt, D. D., and Loudon, A. S. I. (2010). Identification of Eya3 and TAC1 as Long-Day Signals in the Sheep Pituitary. Current Biology *20*, 829-835.

25. Earnest, D. J., Iadarola, M., Yeh, H. H., and Olschowka, J. A. (1990). Photic regulation of c-fos expression in neural components governing the entrainment of circadian rhythms. Exp. Neurol *109*, 353-361.

26. Eisen, M. B., Spellman, P. T., Brown, P. O., and Botstein, D. (1998). Cluster analysis and display of genome-wide expression patterns. Proceedings of the National Academy of Sciences of the United States of America *95*, 14863-14868.

27. El-Husseini, A. E.-D., Williams, J., Reiner, P. B., Pelech, S., and Vincent, S. R. (1999). Localization of the cGMP-dependent protein kinases in relation to nitric oxide synthase in the brain. Journal of Chemical Neuroanatomy *17*, 45-55.

28. Feil, R., Hölter, S. M., Weindl, K., Wurst, W., Langmesser, S., Gerling, A., Feil, S., and Albrecht, U. (2009). cGMP-dependent protein kinase I, the circadian clock, sleep and learning. cib *2*, 298-301.

29. Feil, S., Zimmermann, P., Knorn, A., Brummer, S., Schlossmann, J., Hofmann, F., and Feil, R. (2005). Distribution of cGMP-dependent protein kinase type I and its isoforms in the mouse brain and retina. Neuroscience *135*, 863-868.

30. Foley, N. C., Tong, T. Y., Foley, D., Lesauter, J., Welsh, D. K., and Silver, R. (2011). Characterization of orderly spatiotemporal patterns of clock gene activation in mammalian suprachiasmatic nucleus. Eur J Neurosci *33*, 1851-1865.

31. Garcia, J. A. (2000). Impaired Cued and Contextual Memory in NPAS2-Deficient Mice. Science *288*, 2226-2230.

32. Grassi-Zucconi, G., Menegazzi, M., De Prati, A. C., Bassetti, A., Montagnese, P., Mandile, P., Cosi, C., and Bentivoglio, M. (1993). c-fos mRNA is spontaneously induced in the rat brain during the activity period of the circadian cycle. Eur. J. Neurosci *5*, 1071-1078.

33. Harmar, A. J., Marston, H. M., Shen, S., Spratt, C., West, K. M., Sheward, W. J., Morrison, C. F., Dorin, J. R., Piggins, H. D., Reubi, J.-C., et al. (2002). The VPAC2 Receptor Is Essential for Circadian Function in the Mouse Suprachiasmatic Nuclei. Cell *109*, 497-508.

34. Hazlerigg, D. G., Ebling, F. J. P., and Johnston, J. D. (2005). Photoperiod differentially regulates gene expression rhythms in the rostral and caudal SCN. Current Biology *15*, R449-R450.

35. Helfrich-Förster, C. (2009). Does the Morning and Evening Oscillator Model Fit Better for Flies or Mice? Journal of Biological Rhythms *24*, 259 -270.

36. Holm, S. (1979). A simple sequentially rejective multiple test procedure. Scandinavian Journal of Statistics *6*, 65–70.

37. Honma, S., Kawamoto, T., Takagi, Y., Fujimoto, K., Sato, F., Noshiro, M., Kato, Y., and Honma, K.-ichi (2002a). Dec1 and Dec2 are regulators of the mammalian molecular clock. Nature *419*, 841-844.

38. Honma, S., Kawamoto, T., Takagi, Y., Fujimoto, K., Sato, F., Noshiro, M., Kato, Y., and Honma, K.-ichi (2002b). Dec1 and Dec2 are regulators of the mammalian molecular clock. Nature *419*, 841-844.

39. Horst, G. T. J. van der, Muijtjens, M., Kobayashi, K., Takano, R., Kanno, S.-ichiro, Takao, M., Wit, J. de, Verkerk, A., Eker, A. P. M., Leenen, D. van, et al. (1999). Mammalian Cry1 and Cry2 are essential for maintenance of circadian rhythms. Nature *398*, 627-630.

40. Hou, S.-J., Yen, F.-C., and Tsai, S.-J. (2009). Is dysfunction of the tissue plasminogen activator (tPA)-plasmin pathway a link between major depression and cardiovascular disease? Med. Hypotheses *72*, 166-168.

41. Huang, D. W., Sherman, B. T., and Lempicki, R. A. (2009a). Systematic and integrative analysis of large gene lists using DAVID bioinformatics resources. Nat Protoc *4*, 44-57.

42. Huang, D. W., Sherman, B. T., and Lempicki, R. A. (2009b). Bioinformatics enrichment tools: paths toward the comprehensive functional analysis of large gene lists. Nucl. Acids Res. *37*, 1-13.

43. Hughes, M., DeHaro, L., Pulivarthy, S. R., Gu, J., Hayes, K., Panda, S., and Hogenesch, J. B. (2007). High-resolution Time Course Analysis of Gene Expression from Pituitary. Cold Spring Harbor Symposia on Quantitative Biology *72*, 381-386.

44. Hughes, M. E., DiTacchio, L., Hayes, K. R., Vollmers, C., Pulivarthy, S., Baggs, J. E., Panda, S., and Hogenesch, J. B. (2009). Harmonics of Circadian Gene Transcription in Mammals. PLoS Genet *5*, e1000442.

45. Inagaki, N., Honma, S., Ono, D., Tanahashi, Y., and Honma, K.-ichi (2007). Separate oscillating cell groups in mouse suprachiasmatic nucleus couple photoperiodically to the onset and end of daily activity. Proc Natl Acad Sci U S A. *104*, 7664–7669.

46. Jagota, A., de la Iglesia, H. O., and Schwartz, W. J. (2000). Morning and evening circadian oscillations in the suprachiasmatic nucleus in vitro. Nat Neurosci *3*, 372-376.

47. Jakubcakova, V., Oster, H., Tamanini, F., Cadenas, C., Leitges, M., van der Horst, G. T. J., and Eichele, G. (2007). Light Entrainment of the Mammalian Circadian Clock by a PRKCA-Dependent Posttranslational Mechanism. Neuron *54*, 831-843.

48. Jin, X., Shearman, L. P., Weaver, D. R., Zylka, M. J., de Vries, G. J., and Reppert, S. M. (1999). A molecular mechanism regulating rhythmic output from the suprachiasmatic circadian clock. Cell *96*, 57-68.

49. Keller, M., Mazuch, J., Abraham, U., Eom, G. D., Herzog, E. D., Volk, H.-D., Kramer, A., and Maier, B. (2009). A circadian clock in macrophages controls inflammatory immune responses. Proceedings of the National Academy of Sciences *106*, 21407-21412.

50. Kleppisch, T., Wolfsgruber, W., Feil, S., Allmann, R., Wotjak, C. T., Goebbels, S., Nave, K.-A., Hofmann, F., and Feil, R. (2003). Hippocampal cGMP-Dependent Protein Kinase I Supports an Age- and Protein Synthesis-Dependent Component of Long-Term Potentiation But Is Not Essential for Spatial Reference and Contextual Memory. The Journal of Neuroscience *23*, 6005 -6012.

51. Langmesser, S., Franken, P., Feil, S., Emmenegger, Y., Albrecht, U., and Feil, R. (2009). cGMP-Dependent Protein Kinase Type I Is Implicated in the Regulation of the Timing and Quality of Sleep and Wakefulness. PLoS ONE *4*, e4238.

52. Levitan, R. D. (2007). The chronobiology and neurobiology of winter seasonal affective disorder. Dialogues Clin Neurosci *9*, 315-324.

53. Liang, F.-Q., Walline, R., and Earnest, D. J. (1998). Circadian rhythm of brain-derived neurotrophic factor in the rat suprachiasmatic nucleus. Neuroscience Letters *242*, 89-92.

54. Lincoln, G. A. (2006). Melatonin Entrainment of Circannual Rhythms. Chronobiol Int *23*, 301-306.

55. Lopez-Molina, L., Conquet, F., Dubois-Dauphin, M., and Schibler, U. (1997). The DBP gene is expressed according to a circadian rhythm in the suprachiasmatic nucleus and influences circadian behavior. EMBO J *16*, 6762-6771.

56. Magnusson, A., and Boivin, D. (2003). Seasonal affective disorder: an overview. Chronobiol. Int *20*, 189-207.

57. Masumoto, K.-H., Ukai-Tadenuma, M., Kasukawa, T., Nagano, M., Uno, K. D., Tsujino, K., Horikawa, K., Shigeyoshi, Y., and Ueda, H. R. (2010). Acute induction of Eya3 by late-night light stimulation triggers TSHβ expression in photoperiodism. Curr. Biol *20*, 2199-2206.

58. McNamara, P., Seo, S.-beom, Rudic, R. D., Sehgal, A., Chakravarti, D., and FitzGerald, G. A. (2001). Regulation of CLOCK and MOP4 by Nuclear Hormone Receptors in the Vasculature: A Humoral Mechanism to Reset a Peripheral Clock. Cell *105*, 877-889.

59. Mitsui, S., Yamaguchi, S., Matsuo, T., Ishida, Y., and Okamura, H. (2001). Antagonistic role of E4BP4 and PAR proteins in the circadian oscillatory mechanism. Genes & Development *15*, 995 -1006.

60. Moshkin, Y. M., Mohrmann, L., van Ijcken, W. F. J., and Verrijzer, C. P. (2007). Functional Differentiation of SWI/SNF Remodelers in Transcription and Cell Cycle Control. Mol. Cell. Biol. *27*, 651-661.

61. Mou, X., Peterson, C. B., and Prosser, R. A. (2009). Tissue-type plasminogen activator-plasmin-BDNF modulate glutamate-induced phase-shifts of the mouse suprachiasmatic circadian clock *in vitro*. European Journal of Neuroscience *30*, 1451-1460.

62. Mrugala, M., Zlomanczuk, P., Jagota, A., and Schwartz, W. J. (2000). Rhythmic multiunit neural activity in slices of hamster suprachiasmatic nucleus reflect prior photoperiod. Am J Physiol Regul Integr Comp Physiol *278*, R987-994.

63. Naito, E., Watanabe, T., Tei, H., Yoshimura, T., and Ebihara, S. (2008). Reorganization of the Suprachiasmatic Nucleus Coding for Day Length. Journal of Biological Rhythms *23*, 140 -149.

III

64. Nakao, N., Ono, H., Yamamura, T., Anraku, T., Takagi, T., Higashi, K., Yasuo, S., Katou, Y., Kageyama, S., Uno, Y., et al. (2008). Thyrotrophin in the pars tuberalis triggers photoperiodic response. Nature *452*, 317-322.

65. Ohkura, N., OISHI, K., FUKUSHIMA, N., KASAMATSU, M., ATSUMI, G., ISHIDA, N., HORIE, S., and MATSUDA, J. (2006). Circadian clock molecules CLOCK and CRYs modulate fibrinolytic activity by regulating the PAI-1 gene expression. Journal of Thrombosis and Haemostasis *4*, 2478-2485.

66. Oishi, K., Miyazaki, K., Uchida, D., Ohkura, N., Wakabayashi, M., Doi, R., Matsuda, J., and Ishida, N. (2009). PERIOD2 is a circadian negative regulator of PAI-1 gene expression in mice. Journal of Molecular and Cellular Cardiology *46*, 545-552.

67. Oster, H., Baeriswyl, S., van der Horst, G. T. J., and Albrecht, U. (2003). Loss of circadian rhythmicity in aging mPer1-/- mCry2-/- mutant mice. Genes & Development *17*, 1366-1379.

68. Oster, H., Damerow, S., Hut, R. A., and Eichele, G. (2006). Transcriptional Profiling in the Adrenal Gland Reveals Circadian Regulation of Hormone Biosynthesis Genes and Nucleosome Assembly Genes. Journal of Biological Rhythms *21*, 350 -361.

69. Panda, S., Antoch, M. P., Miller, B. H., Su, A. I., Schook, A. B., Straume, M., Schultz, P. G., Kay, S. A., Takahashi, J. S., and Hogenesch, J. B. (2002). Coordinated Transcription of Key Pathways in the Mouse by the Circadian Clock. Cell *109*, 307-320.

70. Pendergast, J. S., Friday, R. C., and Yamazaki, S. (2010). Photic Entrainment of Period Mutant Mice is Predicted from Their Phase Response Curves. The Journal of Neuroscience *30*, 12179 -12184.

71. Pittendrigh, C. S., and Daan, S. (1976). A functional analysis of circadian pacemakers in nocturnal rodents V. Pacemaker structure: A clock for all seasons. J. Comp. Physiol. *106*, 333-355.

72. Pittendrigh, C. S., and Minis, D. H. (1964). The Entrainment of Circadian Oscillations by Light and Their Role as Photoperiodic Clocks. The American Naturalist *98*, 261-294.

73. Preitner, N., Damiola, F., Luis-Lopez-Molina, Zakany, J., Duboule, D., Albrecht, U., and Schibler, U. (2002). The Orphan Nuclear Receptor REV-ERB[alpha] Controls Circadian Transcription within the Positive Limb of the Mammalian Circadian Oscillator. Cell *110*, 251-260.

74. Raychaudhuri, S., Stuart, J. M., and Altman, R. B. (2000). Principal components analysis to summarize microarray experiments: application to sporulation time series. Pac Symp Biocomput, 455-466.

75. Reick, M., Garcia, J. A., Dudley, C., and McKnight, S. L. (2001). NPAS2: An Analog of Clock Operative in the Mammalian Forebrain. Science *293*, 506 -509.

76. Reppert, S. M., and Weaver, D. R. (2002). Coordination of circadian timing in mammals. Nature *418*, 935-941.

77. Revermann, M., Maronde, E., Ruth, P., and Korf, H.-W. (2002). Protein kinase G I immunoreaction is colocalized with arginine-vasopressin immunoreaction in the rat suprachiasmatic nucleus. Neuroscience Letters *334*, 119-122.

78. Rousseeuw, P. J., and Driessen, K. van (1999). A Fast Algorithm for the Minimum Covariance Determinant Estimator. Technometrics *41*, 212-223.

79. Rusak, B., and Morin, L. P. (1976). Testicular Responses to Photoperiod Are Blocked by Lesions of the Suprachiasmatic Nuclei in Golden Hamsters. Biology of Reproduction *15*, 366 -374.

80. Rutter, J., Reick, M., Wu, L. C., and McKnight, S. L. (2001). Regulation of Clock and NPAS2 DNA Binding by the Redox State of NAD Cofactors. Science *293*, 510 -514.

81. Sato, T. K., Panda, S., Miraglia, L. J., Reyes, T. M., Rudic, R. D., McNamara, P., Naik, K. A., FitzGerald, G. A., Kay, S. A., and Hogenesch, J. B. (2004). A Functional Genomics Strategy Reveals Rora as a Component of the Mammalian Circadian Clock. Neuron *43*, 527-537.

82. Schaap, J., Pennartz, C. M. A., and Meijer, J. H. (2003). Electrophysiology of the circadian pacemaker in mammals. Chronobiol. Int *20*, 171-188.

83. Schoenhard, J. A., Smith, L. H., Painter, C. A., Eren, M., Johnson, C. H., and Vaughan, D. E. (2003). Regulation of the PAI-1 promoter by circadian clock components: differential activation by BMAL1 and BMAL2. Journal of Molecular and Cellular Cardiology *35*, 473-481.

84. Shearman, L. P., Jin, X., Lee, C., Reppert, S. M., and Weaver, D. R. (2000a). Targeted Disruption of the mPer3 Gene: Subtle Effects on Circadian Clock Function. Mol. Cell. Biol. *20*, 6269-6275.

85. Shearman, L. P., Sriram, S., Weaver, D. R., Maywood, E. S., Chaves, I., Zheng, B., Kume, K., Lee, C. C., van der Horst, G. T. J., Hastings, M. H., et al. (2000b). Interacting Molecular Loops in the Mammalian Circadian Clock. Science *288*, 1013-1019.

86. Shearman, L. P., Zylka, M. J., Weaver, D. R., Kolakowski Jr., L. F., and Reppert, S. M. (1997). Two period Homologs: Circadian Expression and Photic Regulation in the Suprachiasmatic Nuclei. Neuron *19*, 1261-1269.

87. Silver, R., Sookhoo, A. I., LeSauter, J., Stevens, P., Jansen, H. T., and Lehman, M. N. (1999). Multiple regulatory elements result in regional specificity in circadian rhythms of neuropeptide expression in mouse SCN. Neuroreport *10*, 3165-74.

88. Sosniyenko, S., Hut, R. A., Daan, S., and Sumová, A. (2009). Influence of photoperiod duration and light-dark transitions on entrainment of Per1 and Per2 gene and protein expression in subdivisions of the mouse suprachiasmatic nucleus. Eur. J. Neurosci *30*, 1802-1814.

89. Sosniyenko, S., Parkanova, D., Illnerova, H., Sladek, M., and Sumova, A. (2010). Different mechanisms of adjustment to a change of the photoperiod in the suprachiasmatic and liver circadian clocks. Am J Physiol Regul Integr Comp Physiol *298*, R959-971.

90. Spoelstra, K., Albrecht, U., van der Horst, G. T. J., Brauer, V., and Daan, S. (2004). Phase Responses to Light Pulses in Mice Lacking Functional per or cry Genes. Journal of Biological Rhythms *19*, 518 -529.

91. Spoelstra, K., and Daan, S. (2008). Effects of constant light on circadian rhythmicity in mice lacking functional cry genes: dissimilar from per mutants. J Comp Physiol A *194*, 235-242.

92. Stephan, F. K., and Zucker, I. (1972). Circadian Rhythms in Drinking Behavior and Locomotor Activity of Rats Are Eliminated by Hypothalamic Lesions. Proc Natl Acad Sci U S A. *69*, 1583–1586.

93. Stetson, M. H., and Watson-Whitmyre, M. (1976). Nucleus suprachiasmaticus: the biological clock in the hamster? Science *191*, 197-9.

94. Storch, K.-F., Lipan, O., Leykin, I., Viswanathan, N., Davis, F. C., Wong, W. H., and Weitz, C. J. (2002). Extensive and divergent circadian gene expression in liver and heart. Nature *417*, 78-83.

95. Sumi, Y., Yagita, K., Yamaguchi, S., Ishida, Y., Kuroda, Y., and Okamura, H. (2002). Rhythmic expression of ROR[beta] mRNA in the mice suprachiasmatic nucleus. Neuroscience Letters *320*, 13-16.

96. Sun, Z. S., Albrecht, U., Zhuchenko, O., Bailey, J., Eichele, G., and Lee, C. C. (1997). RIGUI, a Putative Mammalian Ortholog of the Drosophila period Gene. Cell *90*, 1003-1011.

97. Takumi, T., Taguchi, K., Miyake, S., Sakakida, Y., Takashima, N., Matsubara, C., Maebayashi, Y., Okamura, K., Takekida, S., Yamamoto, S., et al. (1998). A light-independent oscillatory gene mPer3 in mouse SCN and OVLT. EMBO J *17*, 4753-4759.

98. Tsai, S.-J., Hong, C.-J., Liou, Y.-J., Yu, Y. W.-Y., and Chen, T.-J. (2008). Plasminogen activator inhibitor-1 gene is associated with major depression and antidepressant treatment response. Pharmacogenet. Genomics *18*, 869-875.

99. Ueda, H. R., Hayashi, S., Chen, W., Sano, M., Machida, M., Shigeyoshi, Y., Iino, M., and Hashimoto, S. (2005). System-level identification of transcriptional circuits underlying mammalian circadian clocks. Nat Genet *37*, 187-192.

100. Ueda, H. R., Chen, W., Adachi, A., Wakamatsu, H., Hayashi, S., Takasugi, T., Nagano, M., Nakahama, K.-ichi, Suzuki, Y., Sugano, S., et al. (2002). A transcription factor response element for gene expression during circadian night. Nature *418*, 534-539.

101. Ukai-Tadenuma, M., Yamada, R. G., Xu, H., Ripperger, J. A., Liu, A. C., and Ueda, H. R. (2011). Delay in Feedback Repression by Cryptochrome 1 Is Required for Circadian Clock Function. Cell *144*, 268-281.

102. VanderLeest, H. T., Houben, T., Michel, S., Deboer, T., Albus, H., Vansteensel, M. J., Block, G. D., and Meijer, J. H. (2007). Seasonal Encoding by the Circadian Pacemaker of the SCN. Current Biology *17*, 468-473.

103. Wu, Z., and Irizarry, R. A. (2004). Preprocessing of oligonucleotide array data. Nat Biotech *22*, 656-658.

104. Yagita, K., Tamanini, F., van der Horst, G. T. J., and Okamura, H. (2001). Molecular Mechanisms of the Biological Clock in Cultured Fibroblasts. Science *292*, 278 -281.

105. Yan, L., Miyake, S., and Okamura, H. (2000). Distribution and circadian expression of <I>dbp</I> in SCN and extra-SCN areas in the mouse brain. Journal of Neuroscience Research *59*, 291-295.

106. Yasuo, S., Watanabe, M., Iigo, M., Yamamura, T., Nakao, N., Takagi, T., Ebihara, S., and Yoshimura, T. (2006). Molecular Mechanism of Photoperiodic Time Measurement in the Brain of Japanese Quail. Chronobiol Int *23*, 307-315.

107. Yoshimura, R., Ikenouchi-Sugita, A., Hori, H., Umene-Nakano, W., Katsuki, A., Hayashi, K., Atake, K., Ueda, N., and Nakamura, J. (2010). [Brain-derived neurotrophic factor (BDNF) and mood disorder]. Nihon Shinkei Seishin Yakurigaku Zasshi *30*, 181-184.

108. Zhuo, M., Hu, Y., Schultz, C., Kandel, E. R., and Hawkins, R. D. (1994). Role of guanylyl cyclase and cGMP-dependent protein kinase in long-term potentiation. Nature *368*, 635-639.
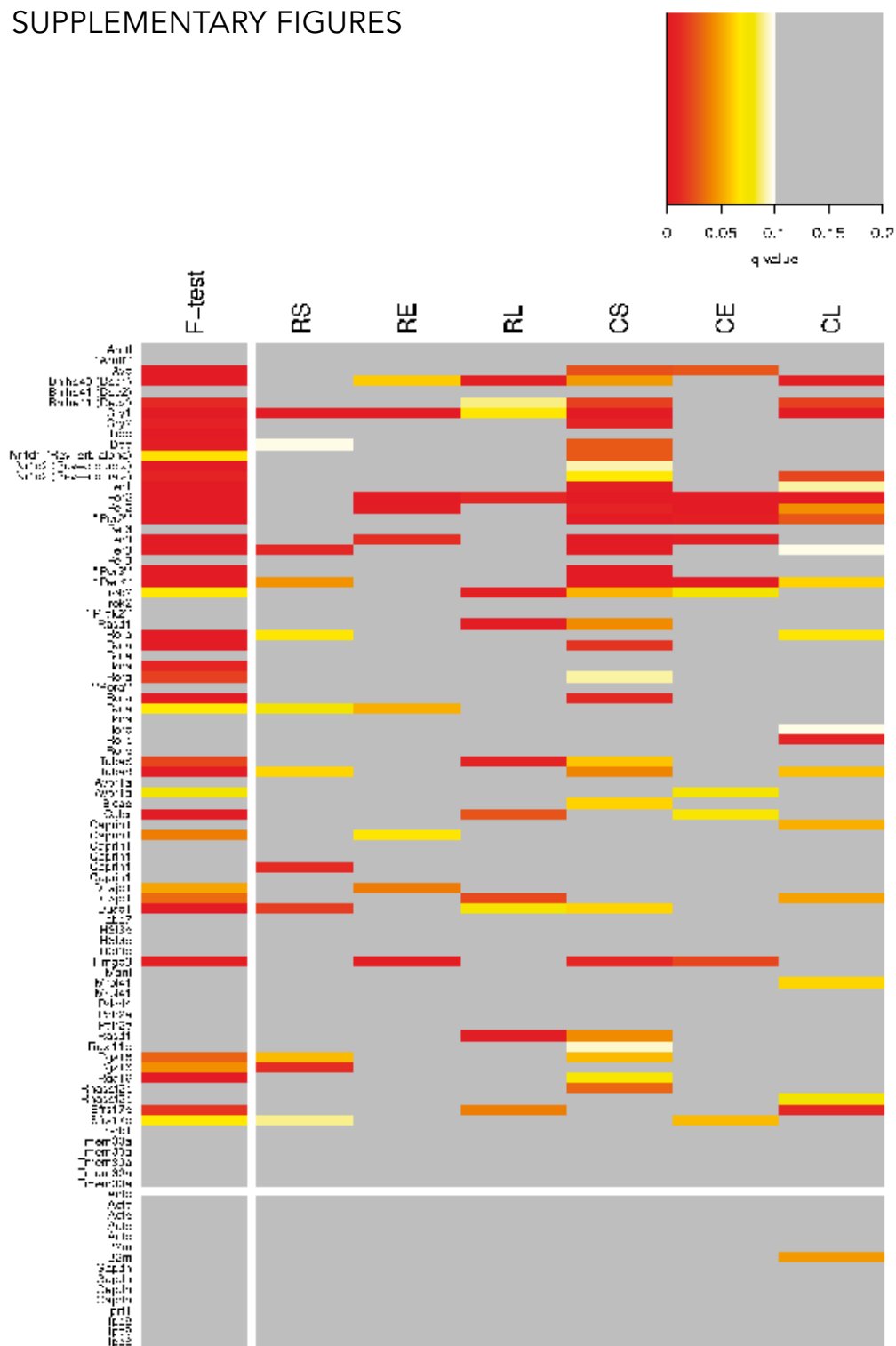
◄ **Figure S1. Validation of significance thrsesholds for discriminating rhythmic from non-rhythmic transcripts.** Heat map representation of adjusted p-values obtained after applying CircWaveBatch (Filter II) to the CLOKSRAN training probe-set identified as significant (adjusted p-value < 0.05) from the overall F-test (Filter I; demarked far left column). Known SCN rhythmic genes (SRGs) are shown in the upper panel and known SCN non-rhythmic genes (SNGs) are shown in the bottom panel. RS = rostral SCN, short photoperiod; RE = rostral SCN, equinoxal photoperiod; RL = rostral SCN, long photoperiod; CS = caudal SCN, short photoperiod; CE = caudal SCN, equinoxal photoperiod; CL = caudal SCN, long photoperiod. The statistical significance of 'rhythmicity' under different photoperiod is indicated quantitatively by the color scale, ranging from deep red (highest significance, p < 0.01) through orange (modest significance, p < 0.05) to white (lowest significance, p < 0.10). Grey indicates absence of significant 'rhythmicity'. The left column displays adjusted p-values for the overall F-test for significant difference in time under any photoperiod in any SCN subregion. The six columns to the right of the overall F-Test show adjusted p-values obtained after applying CircWaveBatch for each of the six photoperiod-subregion conditions. Rows demarked at the bottom list probe sets for gene's known to be non-rhythmic in the SCN.
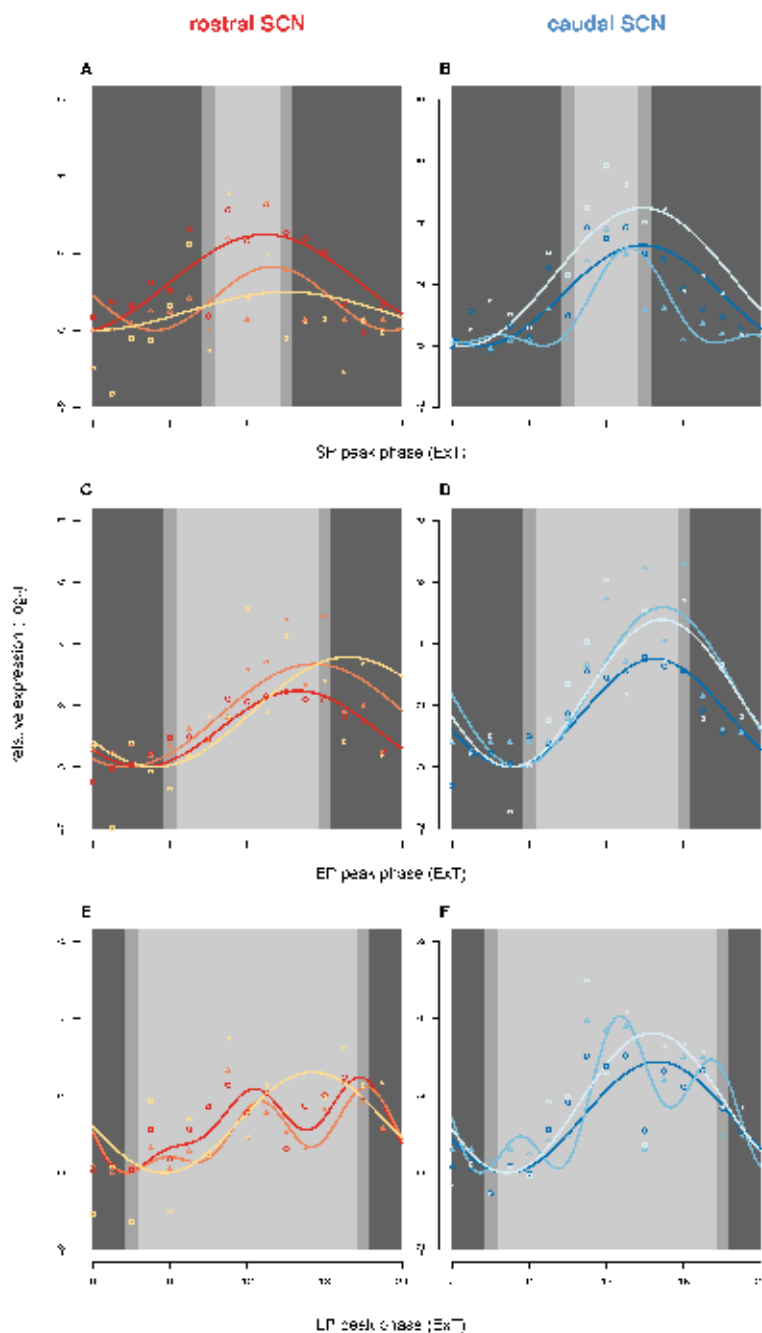
Figure S2. Per2 expression profile as detected by transcriptome analysis. Log_2 transformed expression levels of Affymetrix GeneChip probe sets targeting *Per2* (1417602_at, yellow in R-SCN, light blue in C-SCN; 1417603_at, orange in R-SCN, blue in C-SCN; 1457350_at, red in R-SCN, dark blue in C-SCN) and fitted curves relative to the fitted curve minima are shown for SP in R-SCN (A) and C-SCN (B); EP in R-SCN (C) and C-SCN (D); and, LP in R-SCN (E) and C-SCN (F). Dark grey shading represents subject evening; medium gray, twilight and light grey, subjective day.
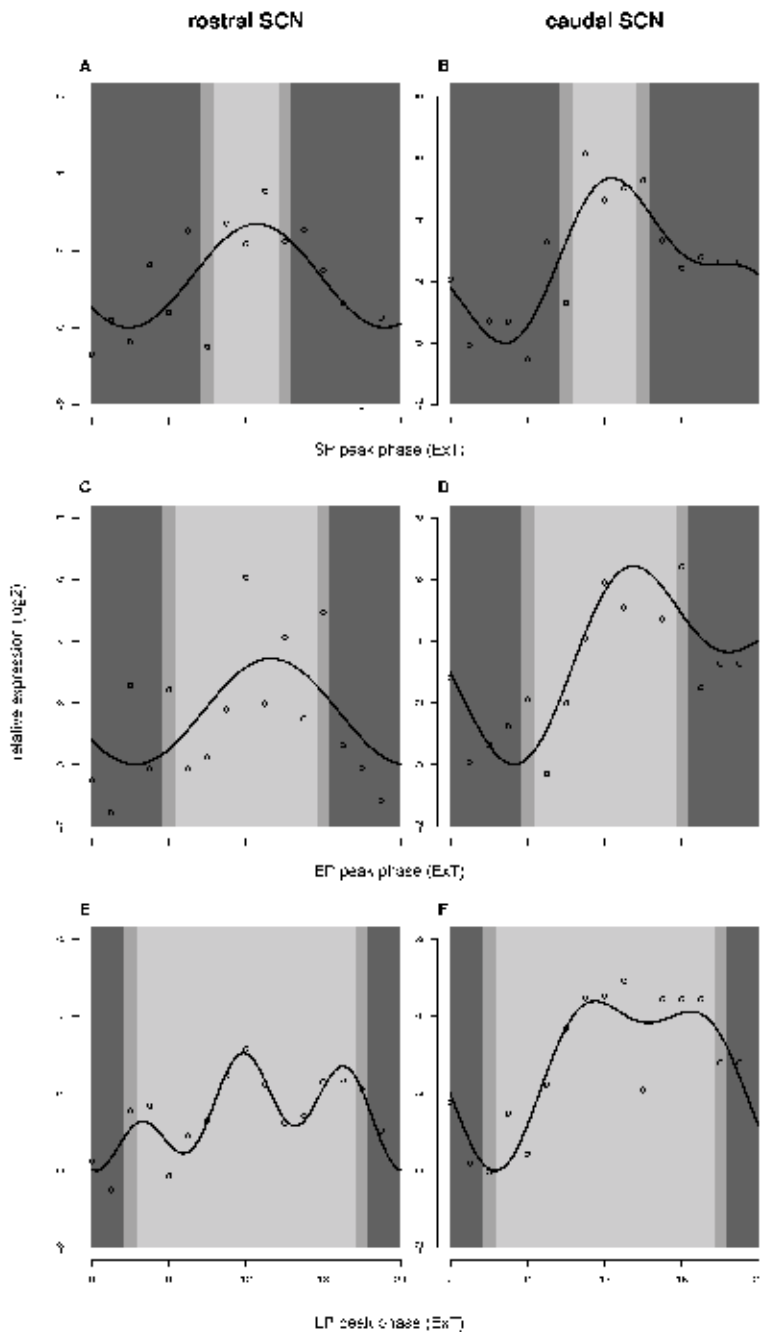
Figure S3. qPCR analysis of Per2 cDNA under different photoperiods. *Per2* transcript levels in rostral and caudal SCN under different photoperiods were assayed by qPCR analysis of the cDNA samples, designated for microarray analysis. Log2 transformed expression levels of Per2 relative to the fitted curve minima is shown for SP in R-SCN (A) and C-SCN (B); EP in R-SCN (C) and C-SCN (D); and, LP in R-SCN (E) and C-SCN (F). All curves are plotted against External Time (ExT0 = midpoint of the dark phase). Curve fitting was performed using CircWaveBatch. Dark grey shading represents subject evening; medium gray, twilight and light grey, subjective day.
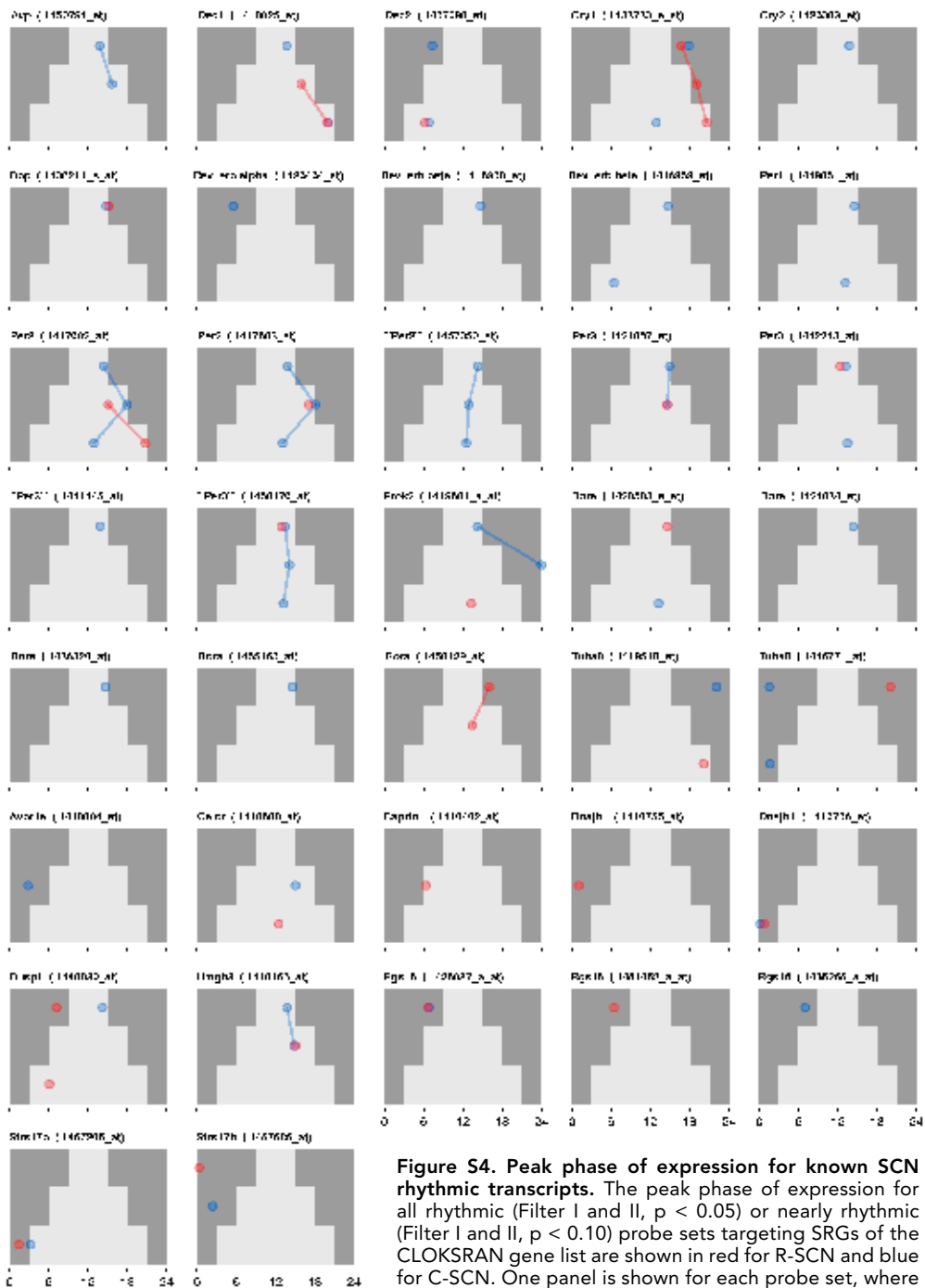
Figure S4. Peak phase of expression for known SCN rhythmic transcripts. The peak phase of expression for all rhythmic (Filter I and II, $p < 0.05$) or nearly rhythmic (Filter I and II, $p < 0.10$) probe sets targeting SRGs of the CLOKSRAN gene list are shown in red for R-SCN and blue for C-SCN. One panel is shown for each probe set, where the top region displays SP, middle region displays EP and bottom region displays LP. Dark grey shading represents subject evening, light grey represents subjective day. External time (ExT) indicated in hours on abscissa of bottom panels. Colored lines highlight phase changes between adjacent photoperiods

IV

DISCUSSION

The modern study of circadian rhythms in mammals has largely focused on characterizing the central pacemaker which resides in the suprachiasmatic nuclei (SCN) and is required for coordinating and synchronizing an animals daily timing with that of the local environment (Stephan and Zucker 1972; Moore & Eichler 1972). It has become increasingly clear that the SCN can not be considered a homogenous collection of neurons. Rather, it is divided into functionally and anatomically distinct subregions.

Round the clock microarray analysis of the SCN transcriptome revealed approximately 10% of the genome was circadianly expressed and identified new genes involved in endogenous rhythm maintenance by the central pacemaker (Panda et al. 2002; Ueda et al. 2002). A shortcoming acknowledged by the authors of these microarray studies was the crude punch-biopsy technique used to acquire the SCN. This imprecise approach resulted in contamination of the sample by unwanted non-SCN tissue and the loss of genuine SCN tissue intended for profiling. Another limitation of these studies is the lack of resolution within the SCN, i.e. the neuronal subpopulations constituting subregions within the SCN. These different subregions were profiled together as one, obscuring their role in central pace maker function.

Our goal was to develop an approach to overcome these shortcomings, allowing us to obtain a global insight into gene expression within various SCN subregions and to better understand their contribution to SCN functioning. Chapter 2 describes our development of a method for acquiring and profiling global transcriptional levels in SCN subregions whilst Chapter 3 presents the application of this method to expanding understanding of the roles played by rostral and caudal SCN (R-SCN; C-SCN) subregions in seasonal adaptation.

As stated above, our motive for developing a method capable of assaying genomic expression levels in mere hundreds of cells arose in response to the striking heterogeneity observed within the SCN (Antle & Silver 2005; Morin et al. 2006; Morin 2007). This diversity in neuronal population has been shown for neuropeptide localization, efferent and afferent projections and core clock behavior (LeSauter & R. Silver 1998; Moore & Rae Silver 1998; Abrahamson & Moore 2001; Yan & Rae Silver 2002; Reddy et al. 2002; Yamaguchi et al. 2003; Quintero et al. 2003). Progress cataloguing SCN content has been made characterizing gene and protein species singly, one by one. The advent of high-throughput microarray technology (Velculescu et al. 1995; Schena et al. 1995; Lockhart et al. 1996) accelerated this progress, beginning with the analysis of the entire SCN (Panda et al. 2002; Ueda et al. 2002). This initial foray into transcriptional profiling of the SCN significantly advanced our holistic view of SCN functioning, but made no attempt to expand SCN subregion understanding. To this end, we set out to assemble a robust approach to assay global transcription levels of any subregion or population of ~100s of neurons in the mouse SCN. Critically, this required optimized methods for brain collection, freezing, cryosectioning, staining and laser catapult microdissection, in combination with a powerful, sensitive amplification protocol, similarly optimized for minimal quantities of sample (i.e. less than 2ng total RNA). **Chapter 2** is a 'proof of principle' demonstration for obtaining transcription profiles from small populations of SCN neurons. Recapitulation of the expression localization of known subregion specific species, *Avp, Vip* and *Grp* provides

confidence in the candidate subregion specific genes and pathways identified from these profiles. Although this study lacks a 'round-the-clock' evaluation of the novel transcripts and pathways identified for each region, its primary purpose was as a pilot demonstration of the power, sensitivity and potential value in assaying SCN subregions by microarray.

Having demonstrated this several applications standout for extending our study of global transcription in ventral, dorsal and central SCN (SCNv, SCNd and SCNce)

First, having gained a single, static snapshot of the transcriptional identities of these three classic SCN subregions at CT22, extending this temporally across a complete circadian cycle will yield several valuable insights- (i) clarification of constitutively expressed makers, (ii) identification of circadianly expressed markers, analogous to *Avp*, *Vip* and *Grp* (Södersten et al. 1985; Zoeller et al. 1992; Shinohara et al. 1993; Karatsoreos et al. 2006) (iii) confirmation of regional specificity at all times, and, (iv) the potential to indentify mRNA species which may *change* localization of expression over time between subregions. This last possibility has not been demonstrated for any gene thus far in the SCN. The wave-like peak expression pattern of core clock genes in SCNd is an example of expression phase changing in both time (daily phase) and space (position in the dorsal SCN; (Yamaguchi et al. 2003; Quintero et al. 2003; Butler & Silver 2009). Given this it is reasonable that other non-core clock species may either regulate this temporally and spatially dynamic expression pattern, or be regulated by it. Characterizing constitutively expressed markers as in (i) will provide the necessary specificity to genetically annul clock function in subregions of interest. Subregion specific genes can be used to generate Cre-recombinase mice that, together with conditional (floxed) Bmal1 mouse can be used for subregion-specific inactivation of the clock. Alternatively or additionally, in combination a subregion specific driven expression of a cytotoxic product, these specific subregions could be precisely ablated without damage to surrounding or efferent SCN neurons. This would be more effective than the crude surgical ablation techniques used thus far (LeSauter et al. 1999a; LeSauter & Silver 1999b). We also demonstrate the value of our approach by confirming the expression of a rat kangaroo photolyase transgene in the SCN of transgenic mice, requisite in attributing a circadian phenotype to the central pace maker (**Appendix I**)

Second, subregion specific transcriptome profiling can be used to investigate global gene expression changes during photic (and non-photic) entrainment. It's known that light regime changes (mimicking jet lag) or brief light pulses which phase advance or phase delay behavioral rhythms, result in a 'dissociation' of the phasing of core clock genes between SCNv and SCNd (Reddy et al. 2002; Yan & Silver 2002; Kuhlman et al. 2003). Specifically, the phases of *Per* and *Cry* mRNAs and proteins of the SCNv advanced rapidly, in phase with the new 'time-zone' or projected light regimen, whist the SCNd lagged behind, advancing slowly from the old eastern 'time-zone' to catch up to the new western one, in phase with locomotor rhythms (Kuhlman et al. 2003). Of particular interest is that this dissociation occurs only during phase advance re-entrainment. In marked contrast, core clock gene expression in SCNv and SCNd remains synchronized during phase delays, i.e. phase-delaying light pulses or light regimes equivalent to east-west jet travel. Assaying these subregions for global transcriptional changes at several time points following aforementioned light

regimes will yield insight into the processes which effect re-entrainment and explain the differential core clock gene response of these subregions between phase advances and delays. In this respect, it is worthwhile mentioning that we have already commenced a pilot study addressing subregion specific transcriptional changes in mice exposed to a phase-advancing light pulse. Preliminary analysis of the data yielded a swathe of genes with known functions in modulating glutamatergic synaptic transmittance, including neuronal pentraxin 1, suggesting a prominent role for synaptic remodeling during re-entrainment (available online at http://bioinf-quad07.erasmusmc.nl/scn/).

Besides using a our approach presented in Chapter 2 to study the role of ventral, dorsal and central SCN in photoentrainment, this technology was used to investigate the role of SCN subregions in seasonal timing. A model positing a role for the circadian clock in seasonal timing distilled by (Pittendrigh & Daan 1976), consists of Morning (*M*) and Evening (*E*) components which independently entrain to dawn and dusk, and by interaction, encode photoperiod. Evidence supporting this model suggest the *M* and *E* components in rodents are localized within the caudal and rostral SCN, respectively (Jagota et al. 2000; Hazlerigg et al. 2005; Inagaki et al. 2007; Naito et al. 2008). **Chapter 3** describes a round the clock analysis of the transcriptome of the rostral and caudal SCN subregions of mice, housed under a short, equinoxal or long photoperiod (representative of winter, spring/autumn and summer, respectively). Using our powerful, sensitive method presented in Chapter 2 we assayed one sample per array at high temporal density and applied robust statistical methods, including linear models and harmonic regression (CircWave, Oster et al. 2006) to distinguish global rhythmic transcript expression. Our results complement previous findings (Hazlerigg et al. 2005; Inagaki et al. 2007; Naito et al. 2008; Sosniyenko et al. 2009) and support a role for the R-SCN and C-SCN as *M* and *E* components. However we find less differential phasing in rhythmic gene expression *between* SCN subregions than other studies and as would be expected from legitimate *M* and *E* oscillators; and, more differential gene expression *within* subregions, particularly R-SCN, in response to different photoperiods. Inagaki et al (2007) and Naito et al., (2008) use *Per1-luc* transgenic mice to examine core clock behavior in different SCN subregions with single cell resolution in mice entrained to different photoperiods. These labs show markedly different phasing of *Per1-luc* by different populations of SCN neurons under long photoperiods which is less evident under EP, and absent under SP. Critically, these studies identified 2-3 subclusters of variously phased neurons within each rostral, mid-rostro/caudal and caudal subregion examined. We examined gene expression in similar rostral and caudal subregions as Naito and coworkers but, not with the resolution needed to resolve these divergently phased subclusters there in. This explicates what we observe in our study: the gene expression data is the *average* expression of divergently phased subclusters. Analysis of these subclusters, probably representing less than ~100 neurons versus the ~500 neurons we assayed for the rostral subregion will provide a clearer picture of photoperiodic encoding by different neuronal subclusters. More generally this example highlights a growing need to analyze smaller and smaller samples, ultimately converging on single cell assay. Further regarding Chapter 3 its worth noting the value in assaying the mid-rostro/caudal which we omitted

during this study due to limitations in resources. Naito et al., show *M* and *E* components present not only within rostral and caudal subregions but also within different *sub-subregions* of the mid-rostro/caudal plane. Intriguingly, these *M* and *E* components are localized within subregions approximately resembling the ventral, dorsal and central SCN subregions assessed in Chapter 1. The extension of our study to other subregions and sub-subregions described above is needed forthwith to gain clearer insight into the contribution made by small neuronal populations to the SCN's role in photoperiodic encoding and entrainment.

The findings of our photoperiodic study warrant follow up especially given the possibility for increasing understanding of disease in humans. We found several rhythmic genes involved in modulating synaptic strength to be associated in literature with seasonal affective disorder (SAD) and critically, which appear to be regulated by photoperiod. An electrophysiological characterization of mice in which the expression in SCN for these genes is disrupted is needed to clarify the role of these genes, and more generally synaptic re-modeling in photoperiodic encoding. Characterization of the photoperiodic response in the SCN of mouse models for depression, aging, addiction etc. is also likely to yield insight into the seasonal contribution of disease in genetically susceptible models of disease. An intriguing possibility for this technology is the development of a 'time of the year' expression assay for forensic applications. Assuming that the subjects mRNA remains sufficiently intact, it's conceivable that a specific gene or combination of genes, core clock or otherwise, may provide insight into the time of year when the 'ticking' of the SCN permanently stopped.

REFERENCES

Abrahamson, E.E. & Moore, R.Y., 2001. Suprachiasmatic nucleus in the mouse: retinal innervation, intrinsic organization and efferent projections. *Brain Research*, 916(1-2), pp.172-191.

Antle, M.C. & Silver, Rae, 2005. Orchestrating time: arrangements of the brain circadian clock. *Trends in Neurosciences*, 28(3), pp.145-151.

Butler, M.P. & Silver, Rae, 2009. Basis of Robustness and Resilience in the Suprachiasmatic Nucleus: Individual Neurons Form Nodes in Circuits that Cycle Daily. *J Biol Rhythms*, 24(5), pp.340-352.

Hazlerigg, D.G., Ebling, F.J.P. & Johnston, J.D., 2005. Photoperiod differentially regulates gene expression rhythms in the rostral and caudal SCN. *Current Biology*, 15(12), p.R449-R450.

Inagaki, N. et al., 2007. Separate oscillating cell groups in mouse suprachiasmatic nucleus couple photoperiodically to the onset and end of daily activity. *Proceedings of the National Academy of Sciences of the United States of America*, 104(18), pp.7664–7669.

Jagota, A., de la Iglesia, H.O. & Schwartz, W.J., 2000. Morning and evening circadian oscillations in the suprachiasmatic nucleus in vitro. *Nat Neurosci*, 3(4), pp.372-376.

Karatsoreos, I.N. et al., 2006. Diurnal regulation of the gastrin-releasing peptide receptor in the mouse circadian clock. *European Journal of Neuroscience*, 23(4), pp.1047-1053.

Kuhlman, S.J. et al., 2003. Phase Resetting Light Pulses Induce Per1 and Persistent Spike Activity in a Subpopulation of Biological Clock Neurons. *J. Neurosci.*, 23(4), pp.1441-1450.

LeSauter, J. et al., 1999. Calbindin expression in the hamster SCN is influenced by circadian genotype and by photic conditions. *Neuroreport*, 10(15), pp.3159-3163.

LeSauter, J. & Silver, R., 1998. Output signals of the SCN. *Chronobiology international*, 15(5), pp.535–550.

LeSauter, J. & Silver, Rae, 1999. Localization of a Suprachiasmatic Nucleus Subregion Regulating Locomotor Rhythmicity. *J. Neurosci.*, 19(13), pp.5574-5585.

IV

Lockhart, D.J. et al., 1996. Expression monitoring by hybridization to high-density oligonucleotide arrays. *Nat Biotech*, 14(13), pp.1675-1680.

Moore, R.Y. & Eichler, V.B., 1972. Loss of a circadian adrenal corticosterone rhythm following suprachiasmatic lesions in the rat. *Brain Research*, 42(1), pp.201-206.

Moore, R.Y. & Silver, Rae, 1998. Suprachiasmatic Nucleus Organization. *Chronobiology International*, 15(5), p.475.

Morin, L.P. et al., 2006. Complex organization of mouse and rat suprachiasmatic nucleus. *Neuroscience*, 137(4), pp.1285-1297.

Morin, Lawrence P, 2007. SCN organization reconsidered. *Journal of Biological Rhythms*, 22(1), pp.3-13.

Naito, E. et al., 2008. Reorganization of the Suprachiasmatic Nucleus Coding for Day Length. *Journal of Biological Rhythms*, 23(2), pp.140 -149.

Oster, H., Damerow, S., et al., 2006. Transcriptional Profiling in the Adrenal Gland Reveals Circadian Regulation of Hormone Biosynthesis Genes and Nucleosome Assembly Genes. *Journal of Biological Rhythms*, 21(5), pp.350 -361.

Panda, S. et al., 2002. Coordinated Transcription of Key Pathways in the Mouse by the Circadian Clock. *Cell*, 109(3), pp.307-320.

Pittendrigh, C.S. & Daan, S., 1976. A functional analysis of circadian pacemakers in nocturnal rodents V. Pacemaker structure: A clock for all seasons. *Journal of Comparative Physiology ? A*, 106(3), pp.333-355.

Quintero, J.E., Kuhlman, S.J. & McMahon, D.G., 2003. The Biological Clock Nucleus: A Multiphasic Oscillator Network Regulated by Light. *J. Neurosci.*, 23(22), pp.8070-8076.

Reddy, A.B. et al., 2002. Differential Resynchronisation of Circadian Clock Gene Expression within the Suprachiasmatic Nuclei of Mice Subjected to Experimental Jet Lag. *J. Neurosci.*, 22(17), pp.7326-7330.

Schena, M. et al., 1995. Quantitative Monitoring of Gene Expression Patterns with a Complementary DNA Microarray. *Science*, 270(5235), pp.467 -470.

Shinohara, K. et al., 1993. Photic regulation of peptides located in the ventrolateral subdivision of the suprachiasmatic nucleus of the rat: daily variations of vasoactive intestinal polypeptide, gastrin-releasing peptide, and neuropeptide Y. *The Journal of Neuroscience: The Official Journal of the Society for Neuroscience*, 13(2), pp.793-800.

Södersten, P. et al., 1985. A daily rhythm in behavioral vasopressin sensitivity and brain vasopressin concentrations. *Neuroscience Letters*, 58(1), pp.37-41.

Sosniyenko, S. et al., 2009. Influence of photoperiod duration and light–dark transitions on entrainment of Per1 and Per2 gene and protein expression in subdivisions of the mouse suprachiasmatic nucleus. *European Journal of Neuroscience*, 30(9), pp.1802-1814.

Stephan, F.K. & Zucker, I., 1972. Circadian Rhythms in Drinking Behavior and Locomotor Activity of Rats Are Eliminated by Hypothalamic Lesions. *Proceedings of the National Academy of Sciences of the United States of America*, 69(6), pp.1583–1586.

Ueda, H.R. et al., 2002. A transcription factor response element for gene expression during circadian night. *Nature*, 418(6897), pp.534-539.

Velculescu, V.E. et al., 1995. Serial Analysis of Gene Expression. *Science*, 270(5235), pp.484 -487.

Yamaguchi, S. et al., 2003. Synchronization of Cellular Clocks in the Suprachiasmatic Nucleus. *Science*, 302(5649), pp.1408-1412.

Yan, L. & Silver, Rae, 2002. Differential induction and localization of mPer1 and mPer2 during advancing and delaying phase shifts. *European Journal of Neuroscience*, 16(8), pp.1531-1540.

Zoeller, R.T. et al., 1992. Cellular levels of messenger ribonucleic acids encoding vasoactive intestinal Peptide and gastrin-releasing Peptide in neurons of the suprachiasmatic nucleus exhibit distinct 24-hour rhythms. *Journal of Neuroendocrinology*, 4(1), pp.119-124.

IV

APPENDIX

THE *POTOROUS* CPD PHOTOLYASE RESCUES A CRYPTOCHROME-DEFICIENT MAMMALIAN CIRCADIAN CLOCK

Inês Chaves[1]*, Romana M. Nijman[1], Magdalena A. Biernat[2], Monika I. Bajek[1], Karl Brand[1], António Carvalho da Silva[1], Shoko Saito[1], Kazuhiro Yagita[3], André P.M. Eker[1] and Gijsbertus T.J. van der Horst[1]*

[1] Department of Genetics, Center for Biomedical Genetics, Erasmus University Medical Center, P.O. Box 2040, 3000 CA Rotterdam, The Netherlands
[2] Laboratory of Virology, Wageningen University, P.O. Box 629, 6700 AP Wageningen
[3] Department of Neuroscience and Cell Biology, Kyoto Prefectural University of Medicine, Kyoto, Japan
* corresponding authors

ABSTRACT

Despite the sequence and structural conservation between cryptochromes and photolyases, members of the cryptochrome/photolyase (flavo)protein family, their functions are divergent. Whereas photolyases are DNA repair enzymes that use visible light to lesion-specifically remove UV-induced DNA damage, cryptochromes act as photoreceptors and circadian clock proteins. To address the functional diversity of cryptochromes and photolyases, we investigated the effect of ectopically expressed *Arabidopsis thaliana* (6-4)PP photolyase and *Potorous tridactylus* CPD-photolyase (close and distant relatives of mammalian cryptochromes, respectively), on the performance of the mammalian cryptochromes in the mammalian circadian clock. Using photolyase transgenic mice, we show that *Potorous* CPD-photolyase, rather than *Arabidopsis* (6-4)PP photolyase, affects the clock by shortening the period of behavioral rhythms. Furthermore, constitutively expressed CPD-photolyase is shown to reduce the amplitude of circadian oscillations in cultured cells and to inhibit CLOCK/BMAL1 driven transcription by interacting with CLOCK. Importantly, we show that *Potorous* CPD-photolyase can restore the molecular oscillator in the liver of (clock-deficient) *Cry1/Cry2* double knockout mice. These data demonstrate that a photolyase can act as a true cryptochrome. These findings shed new light on the importance of the core structure of mammalian cryptochromes in relation to its function in the circadian clock and contribute to our further understanding of the evolution of the cryptochrome/photolyase protein family.

A1

INTRODUCTION

Life is subject to the 24-hour rotation cycle of the earth, which imposes rhythmic changes in light and temperature conditions. In order to anticipate these environmental changes, most organisms have developed a circadian clock with a period of approximately 24 hours that allows them to adjust behavior, physiology and metabolism to the momentum of the day. To keep pace with the day/night cycle, this internal clock needs to be reset every day, using light (the most predictable environmental cue) as the strongest Zeitgeber (German for "time giver" or synchronizer). The mammalian master clock is located in the suprachiasmatic nuclei (SCN) of the hypothalamus, which receives light-induced signals from the retina via the retino-hypothalamic tract (1). In turn, this master clock sends humoral and neuronal signals that synchronize peripheral oscillators, located in virtually every cell or tissue (2-5).

The mammalian cryptochrome proteins (CRY1 and CRY2) belong to the cryptochrome/photolyase family (CPF) of flavoproteins and were initially identified as homologues of photolyase (6, 7). In view of their strong resemblance to plant cryptochrome proteins, which act as blue light photoreceptors, the mammalian CRY proteins were hypothesized to act as photoreceptors for resetting of the circadian clock (6, 8). Unexpectedly however, inactivation of the *Cry1* and *Cry2* genes in the mouse was shown to shorten or lengthen the period length of the circadian clock respectively, whereas in the absence of both genes circadian rhythmicity was completely lost (9-11). This observation, together with the finding that the *Cry* genes encode the most potent inhibitors of the circadian transcription activator CLOCK/BMAL1 (12), positioned the mammalian CRY proteins at the heart of the circadian core oscillator.

The mammalian circadian clock consists of a molecular oscillator, composed of a set of clock genes that act in transcription-translation-based feedback loops. The CLOCK/BMAL1 heterodimer activates transcription of the *Period* (*Per1*, *Per2*) and *Cryptochrome* (*Cry1*, *Cry2*) clock genes through E-box elements in their promoter. Following synthesis, the PER and CRY proteins will gradually accumulate in the nucleus and ultimately repress CLOCK/BMAL1, and thereby transcription of their own gene (13-15). A second loop is formed by REV-ERBα, which cyclically inhibits RORα-driven transcription of the *Bmal1* gene (16-19). Adding to this transcription/translation feedback loop mechanism is a network of post-translational modifications of the clock proteins (phosphorylation, (de)acetylation, sumoylation and ubiquitylation) that fine-tune the period length of the circadian oscillator and confers robustness and persistence to the molecular clock (20-27).

Photolyases, the other members of the CPF, are DNA repair enzymes that use visible light to lesion-specifically remove ultraviolet light-induced cyclobutane pyrimidine dimers (CPDs) or (6-4) pyrimidine-pyrimidone photoproducts ((6-4)PPs) from the DNA in a reaction called photoreactivation (see 28, 29). Placental mammals have lost photolyase genes during evolution and solely rely on nucleotide excision repair for removal of CPDs and (6-4)PPs (30). Nevertheless, when expressed in the mouse, CPD and (6-4)PP photolyases rapidly remove these UV-induced lesions in a light-dependent manner and protect the animal from sunburn, mutation induction, and skin cancer development (31-33).

Phylogenetic analysis has shown that the CPF is divided in two major subgroups. The first subgroup encompasses (i) class I CPD photolyases, (ii) (6-4)PP photolyases and animal

crypochromes, (iii) plant cryptochromes, and (iv) DASH cryptochromes, whereas the second subgroup is solely composed of class II CPD photolyases (29). It is accepted that all members of the photolyase/cryptochrome protein family evolved from a common ancestor CPD photolyase by multiple gene duplications (34). Cryptochromes and photolyases on the one hand share a common backbone, the core domain, which binds two chromophoric cofactors (i.e. FAD and either 5,10-methenyl-tetrahydrofolate or 8-hydroxy-5-deazaflavin), but on the other hand differ in the presence of N- and C-terminal extensions (see Figure 1). Whereas eukaryotic photolyases have an N-terminal extension, containing nuclear and mitochondrial localization signals, cryptochromes contain a unique C-terminal extension of variable length and amino acid composition. It is currently accepted that the functional diversity among cryptochromes (i.e. photoreceptor, circadian photoreceptor, or core clock protein) is achieved by the diversity of their C-terminal extensions.

Detailed structure/function analysis of the C-terminal region of mammalian CRY1 allowed us to identify a putative coiled-coil domain at the beginning of the C-terminal extension as a potential PER and BMAL1 binding site (35). Deletion of the complete C-terminal extension (aa 471-606 of mouse CRY1) abolished the CLOCK/BMAL1 transcription inhibitory potential of CRY1, Similarly, Green and co-workers have demonstrated that the C-terminal extension of *Xenopus laevis* CRY proteins is crucial for transcription repression (36). Interestingly, specific deletion of either the coiled-coil domain (aa 471-493) or the downstream tail region (aa 494-606) of mammalian CRY1 failed to eliminate its ability to inhibit CLOCK/BMAL1-mediated transcription (35), likely because these mutant proteins can still bind to CLOCK via a yet unidentified region of the core domain. This finding lead us to suggest that an interaction between the C-terminal extension and the core domain is mandatory for the clock function of mammalian cryptochromes, possibly by providing structure to the latter (35).

In the present study, we have explored the importance of the core domain of mammalian CRY proteins for core oscillator function by addressing the question to what extent photolyase enzymes affect circadian core oscillator function. Using *in vivo* (photolyase transgenic mice) and *in vitro* (cellular clock reporter and CLOCK/BMAL1 transcription assays) approaches, we show that *Potorous tridactylus* CPD photolyase (hereafter referred to as *Pt*CPD-PL) not only displays cryptochrome-associated functions, but also that it can replace the CRY proteins in the mammalian circadian core oscillator.

RESULTS

Potorous tridactylus CPD photolyase transgenic mice have a short period circadian clock

To investigate whether their strong structural resemblance to cryptochromes (see Figure 1) allows photolyases to interfere with mammalian circadian core oscillator function, we took advantage of the availability of β-actin promoter-driven *Potorous tridactylus* CPD photolyase and *Arabidopsis thaliana* (6-4)PP photolyase transgenic mice (hereafter referred to as *Pt*CPD-PL and *At*(6-4)PP-PL mice), previously generated in our laboratory
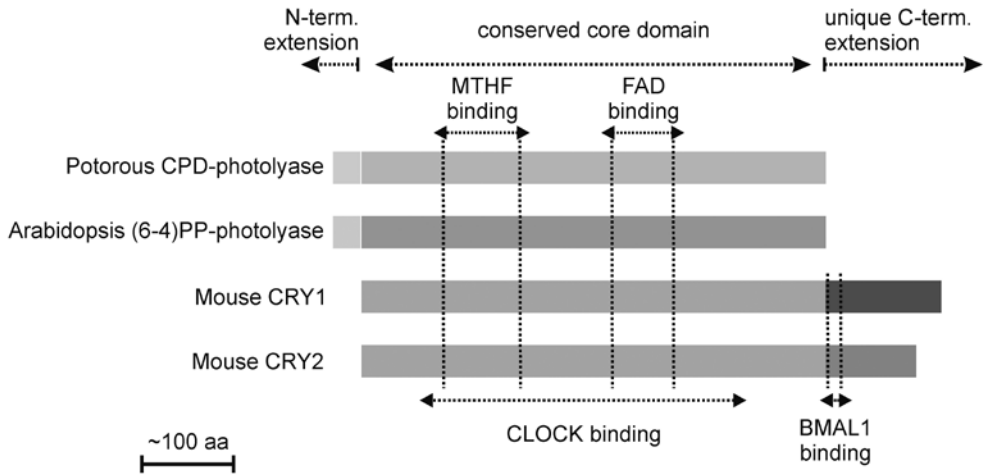
Figure 1. Cryptochromes and photolyases. Schematic representation of *Pt*CPD-PL, *At*(6-4)PP-PL and mouse CRY1 and 2. Conserved and unique domain are indicated above, chromophore binding site are indicated by vertical doted lines. CLOCK and BMAL1 binding regions in mouse CRY and indicated below.

(31, 33). As shown in Figure 2A, and as could be expected on the basis of the ubiquitous expression of the *β-actin* promoter, quantitative RT-PCR analysis of mRNA derived from laser microdissected SCN revealed that *Pt*CPD-PL and *At*(6-4)PP-PL mice express the photolyase transgene in the SCN at comparable levels to the *Hprt* gene.

We next addressed the question whether expression of photolyase in the SCN would affect the circadian behavior of the mouse. To this end, we measured circadian wheel-running behavior of photolyase transgenic mice and sex and age-matched control littermates under normal light/dark (LD) cycles and in constant darkness (dark/dark; DD). As shown in Figure 2B, the period length (tau or τ) of circadian behavior of *At*(6-4)PP-PL transgenic mice is indistinguishable from that of the corresponding wild type littermates. In marked contrast, *Pt*CPD-PL transgenic mice revealed a small but significant shortening of the period length of (15 to 20 min, p<0.05), as compared to wild type littermates (Figure 2C). In addition, the tau of the *Pt*CPD-PL mice has a larger (2-fold) variation than that of control littermates, which indicates individual differences in expression levels.

These findings strongly suggest that expression of *Potorous tridactylus* CPD photolyase in the SCN interferes with circadian clock performance, whereas *Arabidopsis thaliana* (6-4) PP photolyase does not. This observation is in agreement with our finding that *At*(6-4) PP-PL is not able to inhibit CLOCK/BMAL1 (35).

Potorous tridactylus CPD photolyase dampens the circadian core oscillator

As photolyases structurally resemble cryptochromes (29, 34), and given the observation that transient constitutive overexpression of the CRY1 protein suppresses the rhythmic expression of a cotransfected Bmal1::Luc reporter gene (Figure 3A), we next investigated
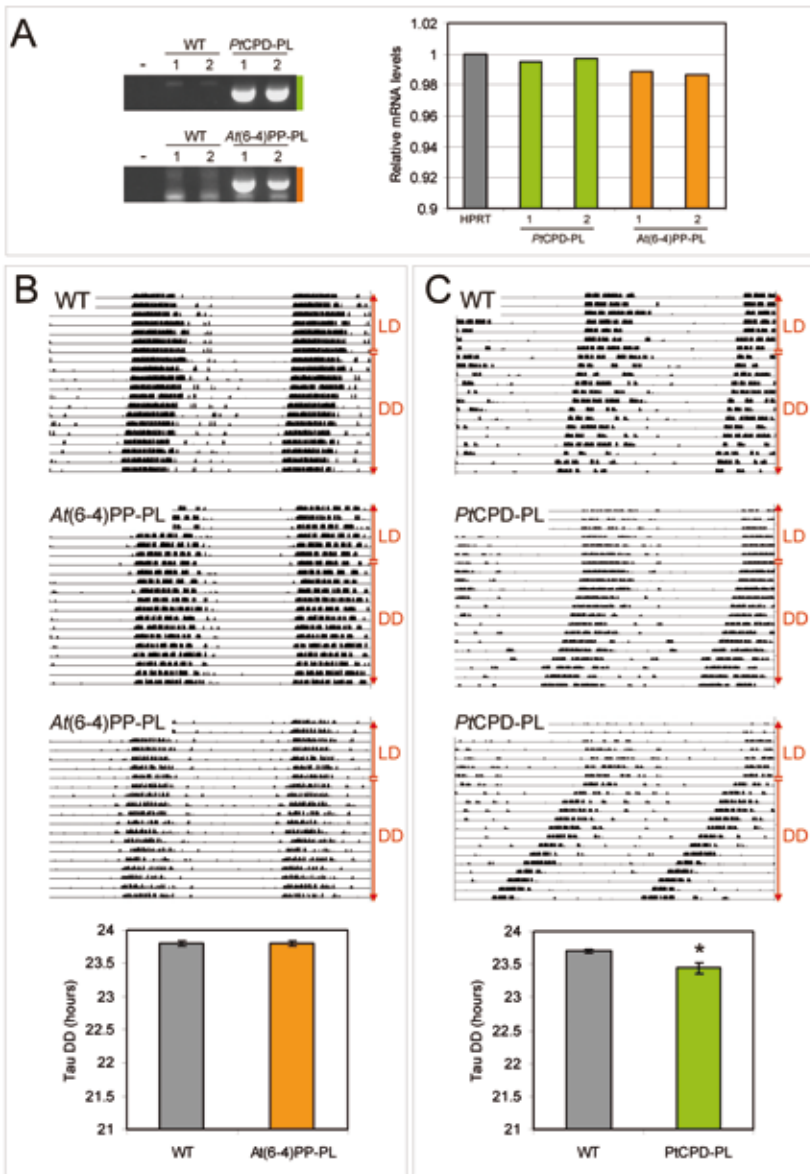
Figure 2. Circadian behavior of photolyase transgenic mice. (A) Quantitative RT-PCR analysis of photolyase mRNA levels in the laser-microdissected SCN of *Pt*CPD-PL and *At*(6-4)PP-PL transgenic mice. Left panel: Ethidium bromide stained gel of PCR amplified cDNA, obtained from two independent transgenic mice and corresponding wild type littermates. Right panel: graphic representation of quantitative RT-PCR amplification data from two independent animals per genotype (see Experimental procedures for details). The Y-axis represents the *Pt*CPD-PL and *At*(6-4)PP-PL mRNA levels relative to that of *Hprt*. **(B,C)** Circadian behavior of *At*(6-4)PP-PL (B) and *Pt*CPD-PL (C) transgenic mice and corresponding littermates (n = 10 per genotype). Animals were kept under normal light conditions (LD 12:12 h) and subsequently exposed to constant darkness (DD) (indicated on the right side of the panels). Shown are representative examples of double-plotted actograms and graphic representations of the free-running period (τ) in constant darkness (bottom panels). Error bars represent the standard error of the mean (SEM); the asterisk indicates significance (p=0.03).

the effect of transient overexpression of *Pt*CPD-PL on the circadian clock of cultured fibroblasts. After synchronization of the individual intracellular circadian clocks with forskolin (37), cells cotransfected with the Bmal1::Luc reporter construct and empty pcDNA3 vector (used as a negative control) were shown to oscillate with a period of 25.6 ± 0.2 hr (n=11). Interestingly, overexpression of *Pt*CPD-PL reduces the amplitude of the oscillations in a dose-dependent manner (Fig. 3B). Similar results were obtained when the Bmal1::Luc reporter was replaced by the Per2:Luc reporter (data not shown).

To study the influence of CPD photolyase on core oscillator performance under physiological conditions, *Pt*CPD-PL mice were interbred with *Per2::Luc* mice to obtain primary CPD-photolyases mouse dermal fibroblast (MDF) lines containing a clock reporter. Bioluminescence rhythms in *Pt*CPD-PL/Per2::Luc MDFs show a reduction in amplitude (38 ± 5 %) when compared to those in Per2::luc (control) fibroblasts (Figure 3C), thus confirming the data obtained in the transient expression studies. Interestingly, and in line with the animal studies, the period of oscillations in *Pt*CPD-PL/Per2::Luc MDFs (22.7
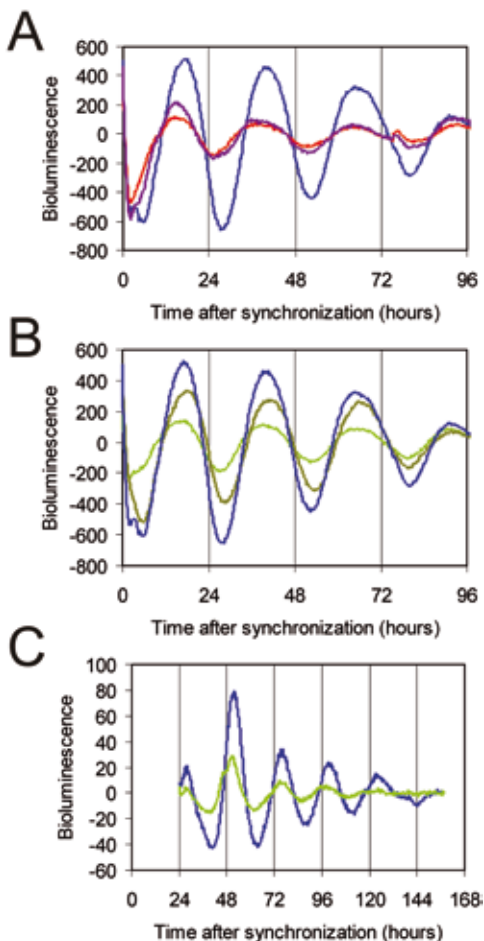
Figure 3. *Pt*CPD photolyase dampens circadian oscillations. (A, B) Representative examples of bioluminescence rhythms in NIH3T3 cells co-transfected with a mBmal1::luciferase reporter construct and either empty pcDNA3 (blue line), pcDNA-Cry1, (100 ng, purple line; 200 ng, red line) or pcDNA-CPD photolyase (200 ng, olive line; 400 ng,,green line). **(C)** Representative example of bioluminescence rhythms in primary MDFs, derived from *Pt*CPD photolyase transgenic mice (green line) and wild type littermates (blue line), transiently expressing the Bmal1::luciferase reporter gene. Bioluminescence recordings were started immediately after forskolin synchronization of the individual cellular clocks. The Y-axis represents base line subtracted bioluminescence values.

± 0.4 hr; n=4) is approximately 50 min shorter (p<0.05) than that of *Per2::luc* fibroblasts that do not carry the CPD photolyase transgene (23.8 ± 0.2 hr; n=4).

Taken together, these data demonstrate that the *Pt*CPD-PL exerts a dominant negative effect on the circadian clock by dampening the oscillations and shortening the period length, likely by interfering with CRY mediated functions.

Potorous tridactylus CPD photolyase inhibits CLOCK/BMAL1-driven transcription

The dominant negative effect of CPD photolyase on cellular clock performance and circadian behavior, as evident from the *in vivo* and *in vitro* studies, prompted us to investigate the underlying mode of action. Since CRY proteins are strong inhibitors of the CLOCK/BMAL1 transcription activator (12), we used a COS7 cell based reporter assay to analyze the ability of *Pt*CPD-PL to inhibit CLOCK/BMAL1-driven transcription of the *mPer1* promoter-driven luciferase reporter gene. Consistent with previous studies (see 12, 35) simultaneous expression of CLOCK and BMAL1 causes a 30-fold induction in transcription of the luciferase gene, which is strongly repressed in the presence of CRY1 (Figure 4A). Interestingly, notwithstanding the fact that the protein should be expressed at high level, the *Pt*CPD-PL is also capable of significantly suppressing CLOCK/BMAL1 activity.

From these data we conclude that *Pt*CPD-PL is able to interfere with mammalian core oscillator performance by exerting a cryptochrome-like function, i.e. inhibition of CLOCK/BMAL1-mediated transcription.

Potorous tridactylus CPD photolyase interacts with CLOCK

We have previously shown that the inhibition of CLOCK/BMAL1 mediated transcription by CRY1 requires a complex network of interactions with CLOCK and BMAL1, involving the CRY1 core domain and C-terminal extension (35) (se also Figure 1). We therefore next asked the question whether *Pt*CPD-PL, like CRY proteins, can physically interact with CLOCK and BMAL1. To this end, we performed a co-immunoprecipitation experiment using HEK293T cells overexpressing the FLAG-CLOCK or FLAG-BMAL1 proteins alone, or in combination with *Pt*CPD-PL (Figure 4B). In the absence of *Pt*CPD-PL neither CLOCK nor BMAL1 were pulled down with anti-*Pt*CPD-PL antibodies, which excludes non-specific binding of the antibodies to these proteins. However, in the presence of *Pt*CPD-PL, the CLOCK protein is shown to co-precipitate with *Pt*CPD-PL, whereas the BMAL1 protein is not. This result indicates that *Pt*CPD photolyase inhibits CLOCK/BMAL1-mediated transcription through direct interaction with CLOCK.

Potorous tridactylus CPD photolyase can replace cryptochromes in the mammalian circadian oscillator

Having shown that *Pt*CPD-PL can interact with CLOCK, leading to inhibition of CLOCK/BMAL1-driven transcription, the intriguing question arises whether this photolyase can actually replace the CRY proteins in the mammalian circadian oscillator and rescue the arrhythmicity of *Cry1*^{-/-}/*Cry2*^{-/-} mice. Generation of a new *Cry1* promoter-driven *Pt*CPD-PL
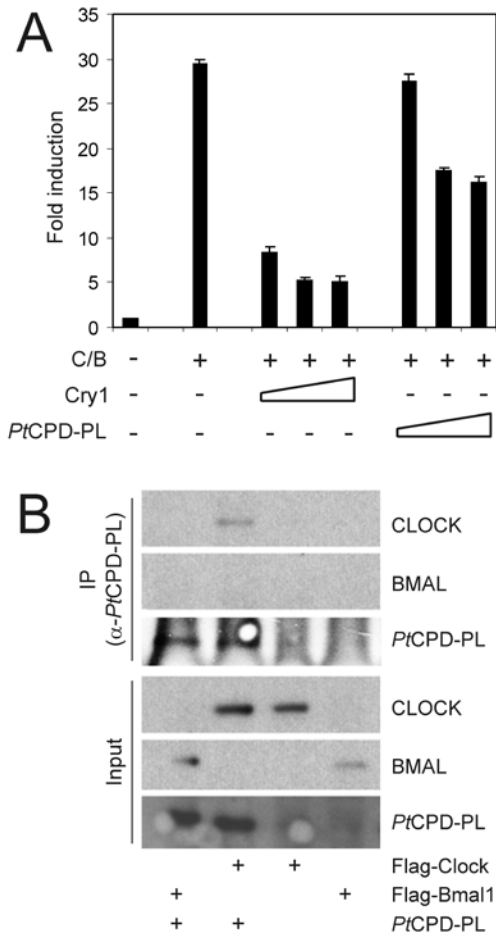
Figure 4. *Pt*CPD photolyase represses CLOCK/BMAL1-driven transcription and interacts with CLOCK. **(A)** COS7 cell-based CLOCK/BMAL1 transcription assay using a *mPer1* E-box promoter-luciferase reporter construct. Luminescence, shown as x-fold induction from the basal expression level (set to 1), is indicated on the Y axis. pcDNA3, pRL-CMV, and the mPer2::luc were added in all reactions. The presence or absence of Cry1 (10-100 ng) and *Pt*CPD-PL (100-300 ng) expression plasmids is indicated below the graph. Mean and standard deviation of triplicate samples are shown. **(B)** Identification of photolyase-binding proteins. *Pt*CPD-PL was precipitated from HEK293T cells, transfected with *Pt*CPD-PL, Flag-Clock or Flag-Bmal1 or double transfected with *Pt*CPD-PL and either Flag-Clock or Flag-Bmal1. Upper panels (IP): Immunoblot analysis of precipitated *Pt*CPD-PL (anti-*Pt*CPD-PL antibodies) and CLOCK and BMAL1 (anti-FLAG antibodies). Lower panels: Immunoblot analysis of total cell lysates, confirming the presence of the various transiently expressed proteins.

transgenic mouse line in a *Cry*-deficient background and subsequent behavioral analysis would be extremely time-consuming. Taking into account that peripheral circadian clocks form a good model for the master clock in the SCN (38, 39), we took an alternative approach by applying the hydroporation technique (40) to introduce clock reporter and CPD photolyase expression constructs in the mouse liver. Twenty-four hours after co-injection of pGL4.11-Bmal1::Luc and either pCry1::*Pt*CPD-PL or the empty vector in the tail vein of the mouse, liver slices were prepared and clock performance was monitored by real-time imaging of bioluminescence. Co-injection of the Bmal1::Luc reporter plasmid and empty vector in *Cry1⁻/⁻/Cry2⁻/⁻* mice and *Cry1⁺/⁻/Cry2⁺/⁻* littermate controls resulted in rhythmic expression of the luciferase reporter gene in *Cry1⁺/⁻/Cry2⁺/⁻* liver slices (Fig. 5A and B), whereas, in line with the absence of a circadian clock, bioluminescence levels remained flat in liver slices from *Cry1⁻/⁻/Cry2⁻/⁻* mice (Figure 5C and D), thus validating the hydroporation approach. Interestingly, upon co-injection of the Bmal1::Luc reporter plasmid and pCry1::*Pt*CPD-PL and *Pt*CPD-PL expression construct in *Cry1⁻/*
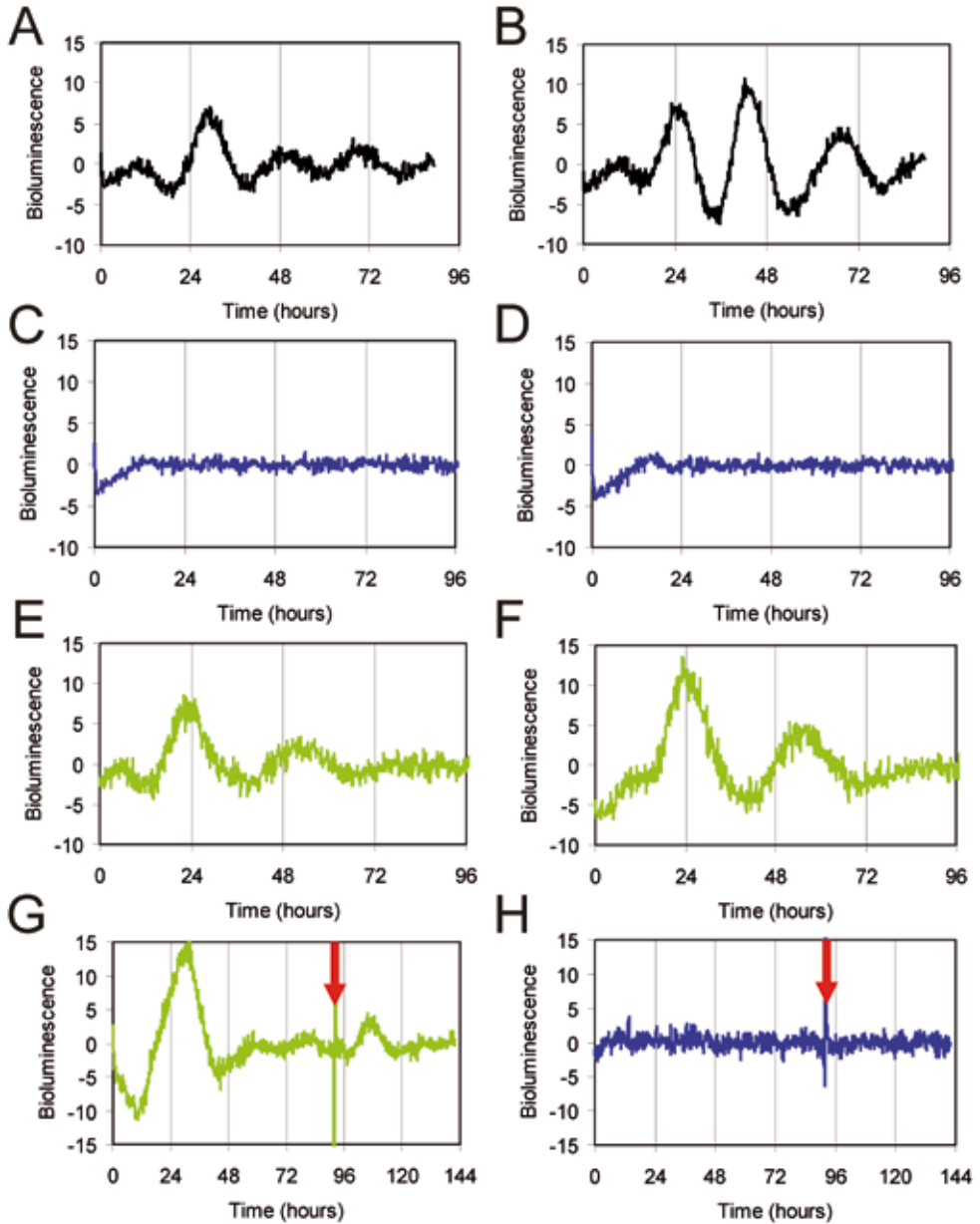
Figure 5. *Pt*CPD photolyase corrects the circadian clock in the liver of CRY-deficient mice. Representative examples of bioluminescence rhythms in liver slices obtained from mice hydroporated with pGL4.11-Bmal1::Luc (black line), together with either empty pcDNA3 (blue line) or pcDNA-CPD photolyase constructs (green line). **(A, B)** Liver slices from control mice, injected with the reporter construct only. **(C-H)** Liver slices from *Cry1⁻/⁻/Cry2⁻/⁻* mice injected with either empty pcDNA3 (C, D, H) or pcCry1::*Pt*CPD-PL (E-G), in addition to the reporter construct. In some experiments (G and H) the slices were treated with Forskolin at 96h to resynchronize the circadian clock. The Y-axis represents base line subtracted bioluminescence values.

Cry2−/− animals, we observed a robust reinitiation of circadian rhythmicity in *Cry*-deficient liver slices for at least two cycles (Figure 5E and F). This oscillation dampened rapidly, but could be revived for at least one cycle by forskolin treatment of the liver slices (Figure 5G). As in the absence of *Pt*CPD-PL forskolin did not exert any effect on bioluminescence levels in *Cry1*−/−/*Cry2*−/− slices (Figure 5H), the forskolin-induced bioluminescence rhythm in *Pt*CPD-PL expressing *Cry1*−/−/*Cry2*−/− slices can only be explained by resynchronization of (running) intracellular clocks.

From these data we conclude that rhythmically expressed *Pt*CPD photolyase can functionally substitute for CRY proteins in the mammalian circadian oscillator and that such a *Pt*CPD-PL-driven molecular oscillator can still respond to non-photic clock-synchronizing stimuli (i.e. forskolin).

DISCUSSION

In the present study, we analyzed the capacity of two different photolyases to interfere with circadian clock performance: the Class II CPD photolyase from *Potorous tridactylus* (*Pt*CPD-PL), which is only distantly related to CRY1, and the (6-4)PP photolyase from *Arabidopsis thaliana* (*At*(6-4)PP-PL), which is closely related to CRY1. In line with our observation that *At*(6-4)PP-PL does not inhibit CLOCK/BMAL1 transcriptional activity (35), analysis of the circadian behavior of *β-actin* promoter-driven *At*(6-4)PP-PL transgenic mice (ubiquitously expressing the transgene, including the in SCN) did not reveal any dominant negative effect of the photolyase on circadian period length. In marked contrast, however, *β-actin* promoter-driven *Pt*CPD-PL transgenic mice showed a small but significant reduction of the period length of circadian behavior. In support of this *in vivo* observation, we also obtained a shortening of the period length of the molecular oscillator in cultured *Pt*CPD-PL dermal fibroblasts. This accelerated clock in *Pt*CPD-PL transgenic mice is unlikely an artifact resulting from unintended inactivation of known (core) clock genes, as analysis of the sequences flanking the integration site of the transgene excluded the presence of such genes (data not shown). Moreover, similar to CRY1, transiently overexpressed *Pt*CPD-PL was able to dampen the circadian oscillator in NIH3T3 cells. The effect of *Pt*CPD-PL on circadian rhythms is mediated by repression of CLOCK/BMAL1-mediated transcription via direct physical interaction with CLOCK, but not with BMAL1.

Previously, we have shown that removal of the complete C-terminal extension of CRY1 abolishes repressor activity towards CLOCK/BMAL1 driven transcription of E-box containing clock genes and clock-controlled genes (35). In the same study, we demonstrated that whereas *At*(6-4)PP-PL by itself has no effect on CLOCK/BMAL1, fusion of the last 100 aa of the CRY1 core domain in conjunction with its C-terminal extension (aa 371-606) to *At*(6-4)PP-PL) resulted in a chimeric protein which is still able to inhibit CLOCK/BMAL1-mediated transcription. Based on these findings, we hypothesized that acquirement of C-terminal extensions (to the core domain) during evolution functionally separated cryptochromes from photolyase and conferred a clock function to the CRY proteins (35). We now provide evidence that *Pt*CPD-PL harbors core clock features that allow it to repress

CLOCK/BMAL1 transcriptional activity and function as a true cryptochrome. Considering that *At*(6-4)PP-PL is more homologous to CRY1 than *Pt*CPD-PL, our findings suggest that it is not the primary amino acid sequence per sé, but rather the overall structure of the core domain, that makes a photolyase repressing CLOCK/BMAL1-mediated transcription. Our results indicate that the *Pt*CPD-PL by itself has the proper structure, whereas *At*(6-4) PP-PL gains such a structure after fusion with a C-terminal extension of mammalian CRY1 (35). In addition, as *Pt*CPD-PL fails to bind BMAL1, interaction with CLOCK is sufficient to inhibit CLOCK-BMAL1-mediated transcription, which is in complete agreement with our previous observation that the BMAL1-binding coiled-coil domain in the C-terminal extension of CRY1 can be deleted without major consequences (35).

Given the dominant negative effect of constitutive *Pt*CPD-PL expression on circadian behavior of the mouse (*in vivo* data), it is tempting to speculate on the underlying molecular mechanism by which *Pt*CPD-PL can inhibit CLOCK/BMAL1-driven transcription (*in vitro* data) and its impact on circadian core oscillator performance. By interacting with CLOCK, *Pt*CPD-PL may prevent the formation of CLOCK/BMAL1 heterodimers and/or binding of the CLOCK/BMAL1 heterodimer to E-box promoters in the DNA. In this scenario, the photolyase reduces the efficiency at which E-box containing clock (controlled) genes are transcribed by reducing the number of available transcription activators. However, as we have shown that a *Chrysodeixis chalcites* nucleopolyhedroviral photolyase can bind to mammalian CLOCK without affecting CLOCK/BMAL1 transcription potential, binding of a CPF protein per se does not prevent CLOCK/BMAL1 heterodimerization and DNA binding (Biernat and Chaves, unpublished data). Therefore, a more plausible explanation would be that binding of *Pt*CPD-PL to CLOCK inhibits transcription activation of E-box promoter-bound CLOCK/BMAL1 heterodimers in a cryptochrome like manner. Strikingly, using an *in vivo* hydroporation approach, we show that *Pt*CPD-PL can rescue the lost circadian oscillator in CRY-deficient cells. When expressed from the *Cry1* promoter, *Pt*CPD-PL revived rhythmic expression of the *Bmal1::luciferase* reporter gene in the *Cry1$^{-/-}$/Cry2$^{-/-}$* mouse liver explants. Moreover, the period of oscillations was in the same range as that of a CRY-driven oscillator and responds to non-photic phase synchronizing stimuli (i.e. forskolin). We therefore conclude that the *Pt*CPD-PL protein has the potential to act as a true mammalian CRY protein.

While this work was in progress, two other members of the CPF have been shown to maintain dual functions: the *Pt*CPF1 protein from the marine diatom *Phaeodactylum tricornutum* and the *Ot*CPF1 protein from the green algae *Ostreococcus tauri*. These proteins hold (6-4)PP photolyase activity and (like *Potorous* CPD-PL) can inhibit CLOCK/BMAL1 driven transcription in a heterologous mammalian system (41, 42) and are therefore considered a missing link in evolution. Interestingly, we found that *Arabidopsis thaliana* (6-4)PP photolyase does not inhibit CLOCK/BMAL1 (35) or affect circadian behavior, whereas the distantly related *Potorous* CPD photolyase does. Moreover, we show that this marsupial class II CPD-photolyase can actually substitute for CRY proteins in the mammalian circadian oscillator. In a parallel study, we have shown that the *Chrysodeixis chalcites* nucleopolyhedrovirus PHR2 protein, another class II CPD photolyase, is able

to interact with CLOCK and affect circadian rhythms *in vitro* (Biernat and Chaves, unpublished data).

These findings contribute to understanding the functional evolution of cryptochromes and photolyases. So far, the identified CPF members with a dual function are either (6-4)PP photolyases from lower eukaryotes (41, 42) or class II CPD photolyases (this manuscript; Biernat and Chaves, unpublished data). Ancestral CPF members were likely proteins with both DNA repair and circadian clock function. We propose that after the divergence of classes I and II, class II CPD photolyases have kept this dual function throughout evolution. Class I CPD photolyases and (6-4)PP photolyases, however, have lost the circadian function in time, which was taken by cryptochromes. In view of this hypothesis, it will be challenging to study molecular clocks in organisms that have both a photolyase with a dual function and cryptochromes, as is the case of marsupials, such as *Potorous* and *Monodelphis*. The genome of *Monodelphis domesticus* has been sequenced and reveals the presence of cryptochrome genes, as well as photolyase. It will be of interest to determine how the clock of non-placental mammals will respond to the loss of photolyase. On the basis of our data, one would predict a change in tau, suggesting that the circadian clock of placental mammals has adapted to the loss of photolyase by adjusting period. Studying the marsupial circadian system at the cellular and molecular level will answer these questions and shed light on the functional evolution of the CPF.

The present study has identified the *Potorous tridactylus* CPD photolyase as an attractive candidate for further structure-function studies, aiming at understanding the functional diversity between cryptochromes and photolyases. Analogous to our previous study with mammalian CRY1 - *Arabidopsis* (6-4)PP photolyase chimeric proteins, it will be informative to swap domains between *Potorous* CPD photolyase and CRY proteins for functional mapping. Such studies will ultimately reveal how nature uses the same core sequence for completely different functions (e.g photoreactivation by photolyases vs clock function of cryptochromes).

MATERIALS AND METHODS

Mouse lines and monitoring of circadian behavior

β-actin::*At*(6-4)PP-PL (33), β-actin::*Pt*CPD-PL (31), and *Per2::Luc* transgenic mice (generation described below), as well as $Cry1^{-/-}/Cry2^{-/-}$ knockout mice (9), all in a C57BL/6J background, were housed under standard conditions and fed *ad libitum*. For the monitoring of locomotor activity rhythms, male mice (12-16 weeks) were individually housed in a light-proof chamber in cages (30 x 45 cm) equipped with a running wheel (14 cm in diameter) and a sensor system to detect wheel revolutions. Animals were maintained in a cycle of 12 h light (150 lux) and 12 h darkness (LD) or in continuous darkness (DD) in constant ambient temperature with water and food available *ad libitum*. Voluntary wheel running (wheel revolutions per unit of time) was continuously recorded by an online computer using the ERS program. Activity records were plotted as actograms and the period of locomotor activity was determined by the chi-square method. Unpaired Student's t-tests were used

to make statistical comparisons between the different genotypes. This animal study was approved by an independent Animal Ethical Committee, the DEC-Consult, review board of the Erasmus University Medical Center (Dutch equivalent of the IACUC), permit number DEC 139-09-12 (EUR 1761).

Generation of Per2::Luc transgenic mice

The construct used to generate the *Per2::Luc* transgenic mice consists of the luciferase gene under control of the *mPer2 promoter,* cloned in pBS (Supplementary Figure S1). The primers used to amplify the 4.2 Kb mPer2 promoter fragment are indicated in Supplementary Figure S1. Intronic sequences from the rabbit β-globin locus were included in the expression construct for messenger stability. The expression construct fragment was excised from the plasmid using appropriate restriction enzymes, separated from the vector DNA by agarose gel electrophoresis, isolated from the gel with the GeneClean II kit (Bio101), and further purified using elutip-D-mini columns (Schleicher and Schuell, Dassel, Germany). The fragment was dissolved in injection buffer (10 mM Tris–HCl pH 7.5, 0.08 mM EDTA) and injected in the pronucleus of fertilized eggs derived from FVB/N intercrosses as described previously (43). Animals were backcrossed in a C57BL/6J background. Genotyping was performed by PCR using primers located in the luciferase gene (Supplementary Figure S1). Annealing was performed at 55ºC. DNA derived from transgenic mice rendered a PCR product of 475 bp, whereas no product was detected using DNA from wild type litter mates.

RNA isolation and quantitative PCR

Coronal cryrosections (25μm) mounted on 1 mm PALM pen-membraneTM slides were rapidly thawed, fixed for 30 seconds in 70% EtOH and immediately stained with haematoxylin for 3 minutes. Following staining sections were rinsed in DEPC treated dH2O and dehydrated by several rinses in 100% EtOH. Laser catapult microdissection (LCM) of the SCN was accomplished using the PALM Microlaser system on freshly prepared sections. Isolated SCN was dissolved immediately in Lysis Buffer (Qiagen) and stored at –80°C for subsequent batch wise RNA purification. RNA was purified with the inclusion of 'on-column' DNase treatment using the Qiagen RNeasy 'Micro' kit according the manufacturers protocol, except that an additional elution was performed in the final step to maximize RNA yield. RNA eluted with RNase-free dH$_2$O was vacuum evaporated for immediate amplification and cDNA generation. Quality of the freshly purified RNA was assayed using the Agilent BioAnalyser in combination with the RNA 'Pico' chip. When intact 18S/28S ribosomal RNA peaks were evident, the sample was considered worthy of assay by Q-PCR.

Amplification was accomplished using the Ovation RNA Amplification System V2 according to the manufactures protocols (Nugen Technologies). Efficiency of the amplification was assayed quantitatively by 260/280nm estimation of cDNA concentration, where a yield of at least 4.8 μg cDNA was deemed sufficient for specific amplification of the RNA template; and qualitatively using the BioAnalyser with the RNA 'Nano' chip to confirm that the majority of unfragmented, amplified cDNA is approximately of 900bp in

length. Quantitative PCR for the determination of At(6-4)PP-PL and PtCPD-PL mRNA levels was performed in triplicate using an iCycler iQ™ Real-Time PCR Detection System (BioRad), SYBR-green and primers (31, 33) generating intron-spanning products of 150-300 bp. Expression levels were normalized to $Hprt$ (hypoxanthine guanine phosphoribosyl transferase) mRNA levels. The generation of specific products was confirmed by melting curve analysis, and primer pairs were tested with a logarithmic dilution of a cDNA mix to generate a linear standard curve, which was used to calculate primer pair efficiencies.

Cell culture and transfection

COS7 (35), NIH3T3 (American Type Culture Collection), and HEK293T (American Type Culture Collection) cells, as well as primary wild type and PtCPD-PL mouse dermal fibroblasts (MDFs) were cultured in Dulbecco's modified Eagle's medium-F10-Pen/Strep-10% fetal calf serum. To generate MDFs, mice were sacrificed by cervical dislocation, and a small piece of back skin of the mouse was removed and cut into pieces with a razor blade (this animal study was approved by an independent Animal Ethical Committee, the DEC-Consult, review board of the Erasmus University Medical Center (Dutch equivalent of the IACUC), permit number DEC 139-09-11 (EUR 1760)). Skin pieces were washed in ethanol, rinsed in phosphate-buffered saline, and incubated overnight in medium supplemented with 1.6 mg/ml collagenase type II. Single cells were obtained by passing through a cell strainer, and collected by centrifugation for 5 min at 500 g, resuspended in culture medium, and seeded onto a 10 cm dish. MDFs were cultured in a low-oxygen incubator (5% CO_2, 3% O_2). Transient expression studies were performed by transfecting cells with plasmids using Fugene reagent (Boehringer) according to the manufacturer's instructions. The following pCDNA3-based plasmids (Invitrogen) were used: pcDNA-HA-mCry1, pcDNA-PtCPD-PL, pcDNA-Bmal1 and pcDNA-Clock. pcDNA-PtCPD-PL is based on the construct used to generate the transgenic mice (31). For luminescence measurements pGl4.11-Bmal1::luciferase (kindly provided by Dr. U. Schibler, Geneva) was used as a reporter.

Real time bioluminescence monitoring

To monitor circadian oscillations in cultured cells in real time, cells were cultured in medium buffered with 25 mM HEPES and containing 0.1 mM luciferin (Sigma). After synchronization of intracellular clocks by treatment of confluent cultures with forskolin (dissolved in 100% ethanol, added to the culture medium at a final concentration of 30 μM), bioluminescence was recorded for 7 days (75 sec measurements at 10 min intervals) with a LumiCycle 32-channel automated luminometer (Actimetrics) placed in a dry, temperature-controlled incubator at 37°C. Data was analyzed with the Actimetrics software and two sample comparisons were done using a Students T-test.

CLOCK/BMAL1 transcription reporter assay

To determine the capacity of PtCPD-PL to inhibit CLOCK/BMAL1 driven transcription, we used a luciferase reporter assay as previously described (12, 35). COS7 cells were transfected

with 200 ng of the *mPer1::luciferase* reporter construct and 15 ng of null-*Renilla luc*, which was used as an internal control. Clock, Bmal1, Cry1 and *Pt*CPD-PL plasmids were added as indicated in the figure legend. The total amount of DNA transfected was kept constant at 2 μg by supplementing with empty pcDNA3.1 vector (Invitrogen). Transcriptional activity was assessed with the Dual-Luciferase 10 Reporter Assay System (Promega) by measuring a ratio of firefly luciferase activity to *Renilla* luciferase activity in each cellular lysate.

Co-immunoprecipitation experiments

Co-immunoprecipitation studies were performed as described previously (21). In short, we transiently expressed a *Pt*CPD-PL and either Flag-Bmal1 and/or Flag-Clock in HEK 293T cells and used anti-FLAG antibodies (Sigma) and anti-*Pt*CPD-PL (31) antibodies for the immunoprecipitation and immunoblot analysis step (1:1000 dilution). As secondary antibody, we used horseradish peroxidase conjugated anti-mouse IgG (DAKO) and anti-rabbit IgG (BioSource) at a 1:1000 dilution. Chemoluminescence was detected using the ECL system (Pharmacia Biotech).

Hydroporation experiments

Hydrodynamic tail vein injection experiments were performed as described (37). In brief, a sterile Ringers Solution (0.9% NaCl, 0.3% KCl, 0.13% $CaCl_2$) containing a total of 10 μg plasmid DNA was rapidly injected (8-10 sec) in the tail vein of the mouse under isoflurane anesthesia. This induces uptake of DNA by the liver, which is initially transient and a small proportion will integrate upon regeneration of the liver. Expression of the hydroporated constructs was non-invasively analyzed using an IVIS® Spectrum imaging device (Caliper/ Xenogen) (Supplementary Figure S2), and positive mice were selected for liver isolation and slicing. Animals were sacrificed 24 h after injection and the livers were rapidly removed and placed in ice cold hank's balanced salt solution supplemented with 50 mM glucose, 4 mM sodium bicarbonate, 10 mM HEPES, 10 ml 10.000 unit/ml penicillin/10.000 μg/ ml streptomycin (5). Liver slices (200 μm) were prepared using an automated Krumdieck tissue slicer (Alabama R&D). Individual slices were placed on a membrane insert (Millipore) in a 35-mm dish in imaging medium (DMEM supplemented with 0.1 mM luciferin, 2% B27 supplement, 4 mM sodium bicarbonate, 10 mM HEPES, 2.5 ml 10.000 units/ml penicillin/10.000 μg/ml streptomycin). Real time imaging and synchronization were performed as described above. The plasmids used were pGl4.11-Bmal1::luciferase and pcCry1::PtCPD-PL. Cloning and characterization of the *Cry1* promoter will be described elsewhere (Saito and van der Horst, unpublished data). This animal study was approved by an independent Animal Ethical Committee (Dutch equivalent of the IACUC).

REFERENCES

Rusak B, Meijer JH, Harrington ME (1989) Hamster circadian rhythms are phase-shifted by electrical stimulation of the geniculo-hypothalamic tract. Brain Res 493: 283-91.

Balsalobre A, Damiola F, Schibler U (1998) A serum shock induces circadian gene expression in mammalian tissue culture cells. Cell 93: 929-37.

McNamara P, Seo SB, Rudic RD, Sehgal A, Chakravarti D, FitzGerald GA (2001) Regulation of CLOCK and MOP4 by nuclear hormone receptors in the vasculature: a humoral mechanism to reset a peripheral clock. Cell 105: 877-89.

Pando MP, Morse D, Cermakian N, Sassone-Corsi P (2002) Phenotypic rescue of a peripheral clock genetic defect via SCN hierarchical dominance. Cell 110: 107-17.

Yoo SH, Yamazaki S, Lowrey PL, Shimomura K, Ko CH et al. (2004) PERIOD2::LUCIFERASE real-time reporting of circadian dynamics reveals persistent circadian oscillations in mouse peripheral tissues. Proc Natl Acad Sci U S A 101: 5339-46.

Todo T, Ryo H, Yamamoto K, Toh H, Inui T, et al. (1996) Similarity among the Drosophila (6-4)photolyase, a human photolyase homolog, and the DNA photolyase-blue-light photoreceptor family. Science 272: 109-12.

van der Spek PJ, Kobayashi K, Bootsma D, Takao M, Eker AP, Yasui A (1996) Cloning, tissue expression, and mapping of a human photolyase homolog with similarity to plant blue-light receptors. Genomics 37: 177-82.

Hsu DS, Zhao X, Zhao S, Kazantsev A, Wang RP et al. (1996) Putative human blue-light photoreceptors hCRY1 and hCRY2 are flavoproteins. Biochemistry 35: 13871-7.

van der Horst GT, Muijtjens M, Kobayashi K, Takano R, Kanno S, et al. (1999) Mammalian Cry1 and Cry2 are essential for maintenance of circadian rhythms. Nature 398: 627-30.

Vitaterna MH, Selby CP, Todo T, Niwa H, Thompson C, et al. (1999) Differential regulation of mammalian period genes and circadian rhythmicity by cryptochromes 1 and 2. Proc Natl Acad Sci U S A 96: 12114-9.

Okamura H, Miyake S, Sumi Y, Yamaguchi S, Yasui A, et al. (1999) Photic induction of mPer1 and mPer2 in Cry-deficient mice lacking a biological clock. Science 286: 2531-4.

Kume K, Zylka MJ, Sriram S, Shearman LP, Weaver DR et al. (1999) mCRY1 and mCRY2 are essential components of the negative limb of the circadian clock feedback loop. Cell 98: 193-205.

Reppert SM, Weaver DR (2001) Molecular analysis of mammalian circadian rhythms. Annu Rev Physiol 63: 647-76.

Young MW, Kay SA (2001) Time zones: a comparative genetics of circadian clocks. Nat Rev Genet 2: 702-15.

Ko CH, Takahashi JS (2006) Molecular components of the mammalian circadian clock. Hum Mol Genet 15:R271-7.

Preitner N, Damiola F, Lopez-Molina L, Zakany J, Duboule D et al. (2002) The orphan nuclear receptor REV-ERBalpha controls circadian transcription within the positive limb of the mammalian circadian oscillator. Cell 110: 251-60.

Etchegaray JP, Lee C, Wade PA, Reppert SM (2003) Rhythmic histone acetylation underlies transcription in the mammalian circadian clock. Nature 421: 177-82.

Sato TK, Panda S, Miraglia LJ, Reyes TM, Rudic RD et al. (2004) A functional genomics strategy reveals Rora as a component of the mammalian circadian clock. Neuron 43: 527-37.

Tsai TY, Choi YS, Ma W, Pomerening JR, Tang C, Ferrell JE Jr. (2008) Robust, tunable biological oscillations from interlinked positive and negative feedback loops. Science 321: 126-9.

Toh KL, Jones CR, He Y, Eide EJ, Hinz WA et al. (2001) An hPer2 phosphorylation site mutation in familial advanced sleep phase syndrome. Science 291: 1040-3.

Yagita K, Tamanini F, Yasuda M, Hoeijmakers JH, van der Horst GT et al. (2002) Nucleocytoplasmic shuttling and mCRY-dependent inhibition of ubiquitylation of the mPER2 clock protein. Embo J 21: 1301-14.

Cardone L, Hirayama J, Giordano F, Tamaru T, Palvimo JJ et al. (2005) Circadian clock control by SUMOylation of BMAL1. Science 309: 1390-4.

Lee J, Lee Y, Lee MJ, Park E, Kang SH et al. (2008) Dual modification of BMAL1 by SUMO2/3 and ubiquitin promotes circadian activation of the CLOCK/BMAL1 complex. Mol Cell Biol 28: 6056-65.

Asher G, Gatfield D, Stratmann M, Reinke H, Dibner C et al. (2008) SIRT1 regulates circadian clock gene expression through PER2 deacetylation. Cell 134: 317-28.

Nakahata Y, Kaluzova M, Grimaldi B, Sahar S, Hirayama J et al. (2008) The NAD+-dependent deacetylase SIRT1 modulates CLOCK-mediated chromatin remodeling and circadian control. Cell 134: 329-40.

Gallego M, Virshup DM (2007) Post-translational modifications regulate the ticking of the circadian clock. Nat Rev Mol Cell Biol. 8: 139-48.

Vanselow K, Kramer A (2007) Role of phosphorylation in the mammalian circadian clock. Cold Spring Harb Symp Quant Biol. 72: 167-76.

Sancar A, (2003) Structure and function of DNA photolyase and cryptochrome blue-light photoreceptors. Chem Rev 103: 2203-37.

Eker APM, Quayle C, Chaves I, van der Horst GTJ (2009) Direct DNA damage reversal: elegant solutions for nasty problems. Cell Mol Life Sci 66: 968-980.

Yasui A, Eker AP, Yasuhira S, Yajima H, Kobayashi T, et al. (1994) A new class of DNA photolyases present in various organisms including aplacental mammals. Embo J 13: 6143-51.

Schul W, Jans J, Rijksen YM, Klemann KH, Eker AP et al. (2002) Enhanced repair of cyclobutane pyrimidine dimers and improved UV resistance in photolyase transgenic mice. Embo J 21: 4719-29.

Jans J, Schul W, Sert YG, Rijksen Y, Rebel H et al. (2005) Powerful skin cancer protection by a CPD-photolyase transgene. Curr Biol 15: 105-15.

Jans J, Garinis GA, Schul W, van Oudenaren A, Moorhouse M et al. (2006) Differential role of basal keratino-cytes in UV-induced immunosuppression and skin cancer. Mol Cell Biol 26: 8515-26.

Kanai S, Kikuno R, Toh H, Ryo H, Todo T (1997) Molecular evolution of the photolyase-blue-light photore-ceptor family. J Mol Evol 45: 535-48.

Chaves I, Yagita K, Barnhoorn S, Okamura H, van der Horst GT, Tamanini F.et al. (2006) Functional evolu-tion of the photolyase/cryptochrome protein family: importance of the C terminus of mammalian CRY1 for circadian core oscillator performance. Mol Cell Biol 26: 1743-53.

van der Schalie EA, Conte FE, Marz KE, Green CB. et al. (2007) Structure/function analysis of Xenopus cryp-tochromes 1 and 2 reveals differential nuclear localization mechanisms and functional domains important for interaction with and repression of CLOCK-BMAL1. Mol Cell Biol 27: 2120-9.

Balsalobre A, Marcacci L, Schibler U (2000) Multiple signaling pathways elicit circadian gene expression in cultured Rat-1 fibroblasts. Curr. Biol. 10: 1291-1294.

Balsalobre A, Damiola F, Schibler U (1998). A serum shock induces circadian gene expression in mamma-lian tissue culture cells. Cell 93: 929–937.

Yagita K, Tamanini F, van der Horst GT, Okamura H (2001) Molecular mechanisms of the biological clock in cultured fibroblasts. Science 292: 278-281.

Liu F, Song YK, Liu D (1999) Hydrodynamics-based transfection in animals by systemic administration of plasmid DNA. Gene Therapy 6: 1258–1266.

Coesel S, Mangogna M, Ishikawa T, Heijde M, Rogato A et al. (2009) Diatom PtCPF1 is a new cryptochrome/photolyase family member with DNA repair and transcription regulation activity. EMBO Rep 10: 655-61.

Heijde M, Zabulon G, Corellou F, Ishikawa T, Brazard J et al. (2010) Characterization of two members of the cryptochrome/photolyase family from Ostreococcus tauri provides insights into the origin and evolution of cryptochromes. Plant Cell Environ 33: 1614-26.

Hogan B, Beddington R, Costantini F, Lacy E (1994) *Manipulating the Mouse Embryo Section E: Production of Transgenic Mice.* Cold Spring Harbor Laboratory Press, Cold Spring Harbor, NY 217–52.

ACKNOWLEDGMENTS

ETHICS STATEMENT:

This animal study and fibroblast cell line generation was approved by an independent Animal Ethical Committee, the DEC-Consult, review board of the Erasmus University Medical Center (Dutch equivalent of the IACUC), permit numbers: DEC 139-09-11/12 (EUR 1760/1761).

SUPPLEMENTARY FIGURES

A mPer2::Luc Tg vector
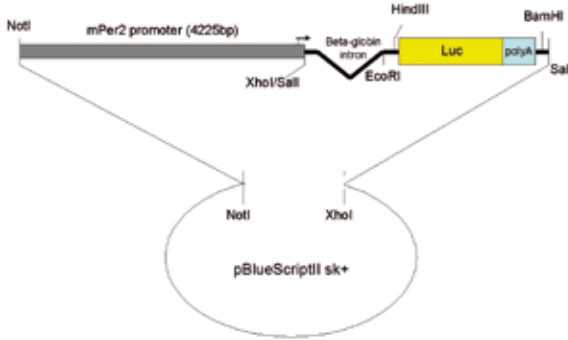
B mPer2 promoter primers

5' primer: 5'- AGCGGCCGC ATTTGGGAATGTCTTGTGCGAAG -3'
　　　　　　　　　NotI

3' primer: 5'- ACTCGAG CCGCTAGTCCCAGTAGCG -3'
　　　　　　　　XhoI

C Luciferase genotyping primers

5' primer: 5'- CGAGTCGTCTTAATGTTAAGATT -3'

3' primer: 5'- TGTAGCCATCCATCCTTGTC -3'

Supplementary Figure S1. Schematic representation of the mPer2::Luc construct used to generate transgenic clock reporter mice. (A) The luciferase gene is cloned in front of the *mPer2 promoter,* using pBS as backbone. Intronic sequences from the rabbit β-globin locus were included in the expression construct for messenger stability. Restriction enzyme sites are indicated. **(B)** Sequence of the primers used to amplify the 4.2 kb *mPer2* promoter fragment. **(C)** Sequence of the luciferase primers used to genotype mPer2::Luc mice.
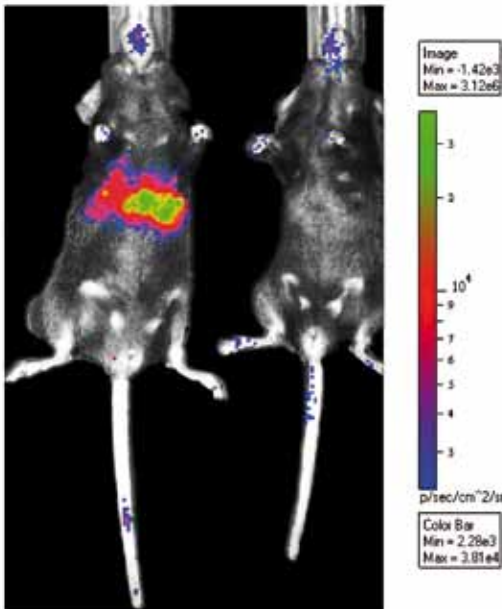
Supplementary Figure S2. Detection of luminescence in the liver of hydroporated mice. Representative examples of dorsal luminescence images, obtained 24 hour after hydroporation of mice with either the Bmal1::Luc reporter construct (left) or the empty vector (right). Expression of the hydroporated constructs was non-invasively monitored in isoflurane anesthetized animals using an IVIS® Spectrum imaging device (Caliper/Xenogen). Colors indicate signal intensity. Note that the reporter is prominently expressed in the liver.

APPENDIX II

SHORT-TERM DIETARY RESTRICTION AND FASTING PRECONDITION AGAINST ISCHEMIA REPERFUSION INJURY IN MICE

IJames R. Mitchell[1,6], Marielle Verweij[2], Karl Brand[1], Marieke van de Ven[1], Natascha Goemaere[4], Sandra van den Engel[2], Timothy Chu[6], Flavio Forrer[3], Cristina Müller[3], Marion de Jong[3], Wilfred van Ijcken[5], Jan N. M. IJzermans[2], Jan H. J. Hoeijmakers[1], Ron W. F. de Bruin[2]

Departments of Genetics[1], Surgery[2], Nuclear Medicine[3] and Pathology[4], Center for Biomics[5], Erasmus Medical Center, Cancer Genomics Center[1], Dr. Molewaterplein 50, 3015 GE, Rotterdam, the Netherlands
[6]Department of Genetics and Complex Diseases, Harvard School of Public Health, 655 Huntington Ave, Boston, MA, 02115 USA

ABSTRACT

Dietary restriction (DR) extends lifespan and increases resistance to multiple forms of stress, including ischemia reperfusion injury to the brain and heart in rodents. While maximal effects on lifespan require long-term restriction, the kinetics of onset of benefits against acute stress are not known. Here we show that 2-4 weeks of 30% dietary restriction improved survival and kidney function following renal ischemia reperfusion injury in mice. Brief periods of water-only fasting were similarly effective at protecting against ischemic damage. Significant protection occurred within one day, persisted for several days beyond the fasting period and extended to another organ, the liver. Protection by both short-term DR and fasting correlated with improved insulin sensitivity, increased expression of markers of antioxidant defense and reduced expression of markers of inflammation and insulin/insulin-like growth factor-1 signaling. Unbiased transcriptional profiling of kidney from mice subject to short-term DR or fasting revealed a significant enrichment of signature genes of long-term DR. These data demonstrate that brief periods of reduced food intake, including short-term daily restriction and fasting, can increase resistance to ischemia reperfusion injury in rodents and suggest a rapid onset of benefits of DR in mammals.

A II

INTRODUCTION

Dietary restriction (DR) encompasses a variety of interventions resulting in reduced nutrient and energy intake without malnutrition. DR is best known for its ability to extend lifespan in a wide variety of organisms (Weindruch et al. 1986; Masoro 2003; Bishop and Guarente 2007). Longevity effects were first reported in rodents in 1935 (McCay et al. 1935) and extended in subsequent decades to fish (Comfort 1963), worms (Klass 1977), flies (Partridge et al. 1987; Chippindale et al. 1993), yeast (Jiang et al. 2000; Lin et al. 2000) and non-human primates (Colman et al. 2009). Effects on human longevity are not known, but prospective studies show a favorable impact on markers of aging and predictors of long-term health, including improved cardiovascular fitness, body-mass index and insulin sensitivity (Heilbronn et al. 2006; Weiss et al. 2006; Fontana and Klein 2007).

The kinetics of onset and loss of longevity benefits of DR are best understood in the fruit fly Drosophila melanogaster. In young adult flies, maximal effects of DR on longevity, measured as a function of daily mortality rate, are achieved within 1-3 days of switching from a normal to a restricted diet and vice versa (Mair et al. 2003). The use of daily mortality rate as an endpoint in young adult rodents would require large numbers of animals due to low daily mortality rates and is thus considered impractical.

In addition to extended lifespan, another common property of organisms on DR is increased resistance to multiple forms of acute stress (Sinclair 2005; Brown-Borg 2006). In rodents, this includes resistance to paraquat toxicity and ischemia reperfusion injury. Paraquat is a free radical generator that primarily targets the lungs, and mice subject to ~5 or 8 months of 40% DR have a significant survival advantage over ad libitum fed animals (Sun et al. 2001; Richardson et al. 2004). Ischemia reperfusion injury is initiated by a lack of blood flow (ischemia) resulting in a state of tissue oxygen and nutrient deprivation characterized chiefly by ATP depletion, loss of ion gradients across membranes and buildup of toxic byproducts. Restoration of blood flow (reperfusion) causes further damage at first by inappropriate activation of cellular oxidases and subsequently by inflammatory mediators in response to tissue damage (Friedewald and Rabb 2004). Rodents on a restricted diet for 3 months to 1 year have reduced damage upon ischemic injury to the heart and brain in models of heart attack and stroke, respectively (Yu and Mattson 1999; Chandrasekar et al. 2001; Ahmet et al. 2005).

The length of time on a restricted diet required for the onset of increased stress resistance is not well characterized in any organism. Here, we examined the kinetics of onset and loss of protection against renal and hepatic ischemia reperfusion injury in mice using brief periods of food restriction, including 2-4 weeks of 30% reduced daily food availability (defined here as short-term DR) or 1-3 days of 100% restriction (water-only fasting).

RESULTS

Bilateral renal ischemia was induced by clamping both renal pedicles for 37 minutes, followed by clamp removal to reinitiate blood flow. Under these conditions, 60% of control mice fed ad libitum prior to surgery died or were sacrificed due to morbidity (including excessive weight loss, drop in body temperature, ruffled fur, decreased activity and hunched body posture) and the associated buildup of toxic waste products (urea, creatinine) in the blood indicative of irreversible kidney failure by the fourth day following surgery (Fig 1A-D). In contrast, mice restricted daily to 70% of their ad libitum food intake (30% DR) for four weeks prior to challenge with renal IRI were protected from mortality, weight loss and kidney dysfunction (Fig 1A-D).

To investigate shorter periods of more severe restriction, we tested the effects of water-only fasting. As with 4 wks of 30% DR, 3 days of fasting resulted in 100% survival, post-operative weight gain and reduced kidney dysfunction (Fig 1A-D). Protection afforded by both DR and fasting was further confirmed on the level of organ damage by longitudinal assessment of lactate dehydrogenase (LDH) in the serum (Fig 1E). Upon cellular damage or death, cytoplasmic LDH is released into the blood and can thus serve as a marker of acute tissue injury. Although LDH levels were significantly elevated in all groups 2 and 6 hours after reperfusion, they returned to preoperative levels 24 hours after reperfusion only in the DR and fasted groups. LDH levels were also significantly lower in the DR group at the 2 hour timepoint. Kidney damage was further assessed on the histological level by scoring acute tubular necrosis (ATN) on a five point scale (Leemans et al. 2005) before and after injury (Fig 1F). Both DR and fasted groups had significantly less ATN than the ad libitum fed group on days 1 and 2 after injury, consistent with better outcome. Following ischemic injury, damaged tubules have a limited capacity to regenerate. We measured cellular proliferation on the histological level using the proliferative markers PCNA and Ki67 (Fig 1G) on the second day following reperfusion coincident with the onset of organ regeneration. Both markers were elevated in animals subject to renal IRI relative to mock treated animals. There were no significant effects of dietary pretreatment on absolute proliferation levels. Taken together, these data are consistent with better outcome in the DR and fasted groups.

We next tested the kinetics of onset and loss of benefits of DR and fasting using a unilateral occlusion mode in which the left kidney was occluded for 37 minutes followed by removal of the right (undamaged) kidney. This model represents a more severe stress than the bilateral model with the same ischemic time because the recovery of renal function and animal survival depends on regeneration of a single damaged kidney. Under these conditions, 90% of ad libitum fed mice died or were sacrificed due to morbidity indicative of irreversible kidney failure by the fourth day following IRI. Mice on 30% DR for 4 weeks or 3 days had significantly elevated survival rates (both 100%; Fig 2A) and improved renal function (Fig 2B) as in the bilateral model. Two weeks of 30% DR was similarly effective as four weeks with respect to survival and kidney function (Fig 2A, B), indicating a rapid onset of benefits of DR. Similarly, 2 or even 1 day of water-only fasting prior to ischemia
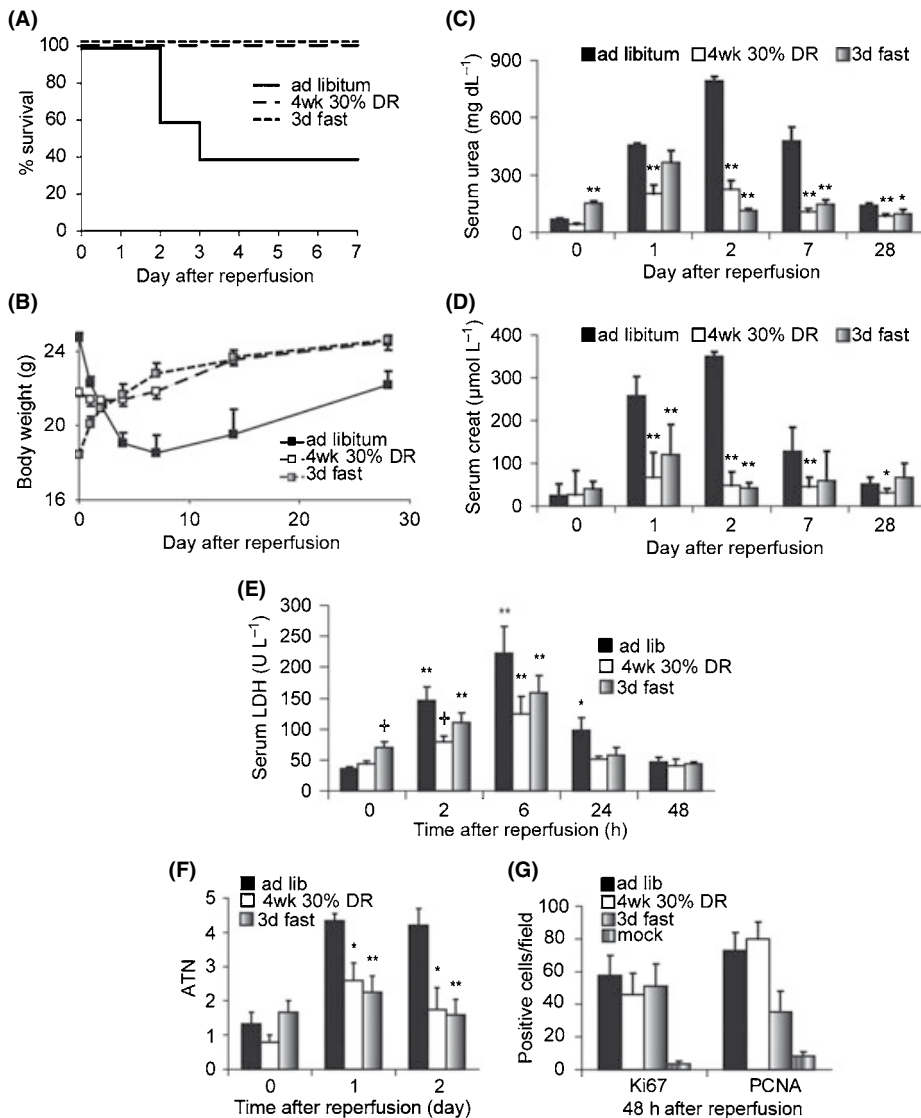
Figure 1. DR protects against the damaging effects of renal IRI. A. Survival curves of male mice fed ad libitum, restricted to 70% of ad libitum food consumption for 4 weeks, or fasted for 3 days prior to induction of 37 minutes of bilateral renal IRI (n=10 per group). No further mortality was observed beyond day 4 after surgery. Both dietary treatments led to a significant survival advantage by Kaplan Meier analysis (log rank test, $p<0.01$). B. Body weight of mice over a 28-day time course following renal IRI. C, D. Kidney function as measured by serum urea (C) and creatinine (D) concentrations on the indicated days following surgery. Asterisks indicate the significance of the difference as compared to the ad libitum group at the same time point (* $p<0.05$; ** $p<0.01$). E. Blood serum LDH of the indicated groups over a time course following reperfusion. Asterisks indicate significant differences relative to time 0 of the same treatment; crosses represent significant differences relative to the ad libitum group at the indicated time point. F. Quantification of acute tubular necrosis on a 5 point scale before and after renal IRI based on blind scoring of hemotoxylin/eosin stained kidney sections as described previously (Leemans et al. 2005). Asterisks represent significant differences relative to the ad libitum group at the indicated time point (* $p<0.05$; ** $p<0.01$). G. Percentage of cells expressing Ki67 or PCNA proliferative markers in a microscopic field of the indicated group on the second day following IRI. All groups were significantly elevated vs. the mock control.
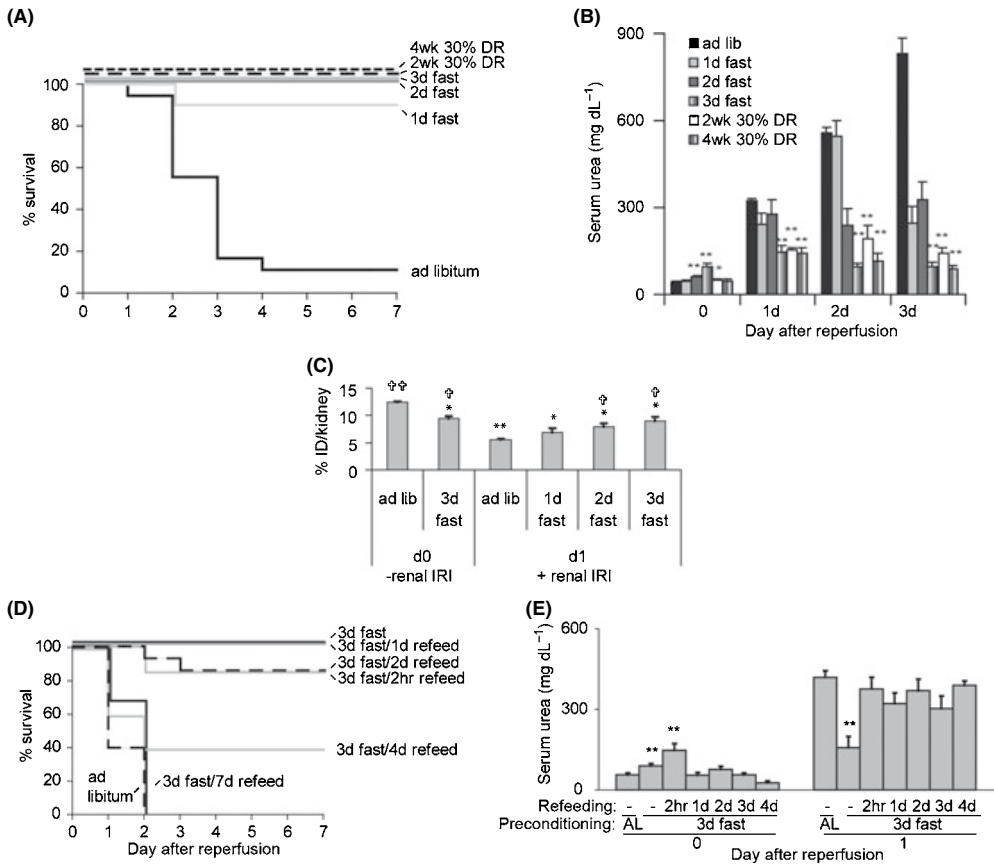
Figure 2. Rapid onset and loss of protective effects of short-term DR and fasting. A-C. Rapid onset: A. Survival curves of male mice fed ad libitum, 30% restricted for 2-4 weeks, or fasted for 1-3 days prior to induction of 37 minutes of unilateral renal IRI with contralateral nephrectomy (n=10-18 per group). B. Kidney function as measured by serum urea following 37 minutes of unilateral renal IRI in the indicated groups (serum from 4-10 individual animals was sampled per data point). Asterisks indicate the significance of the difference as compared to the ad libitum group at the same time point (** $p<0.01$). C. Mice fasted for 0-3 days (4-10 animals per group) were analyzed for kidney function either in the absence of renal ischemia (day 0, -renal IRI) or one day following 37 minutes renal ischemia (day 1, +renal IRI) by measuring radioactivity in the kidney with a gamma-counter 4 h after injection of ^{99m}Tc-DMSA, expressed as a percentage of the injected dose per one kidney (% ID/ kidney). Note the reduced percentage of ^{99m}Tc-DMSA in the kidneys of the ad libitum group 24 hours after renal IRI (12.4% to 5.6%), indicative of renal dysfunction. The significance of the difference as compared to the ad libitum group prior to (asterisks) or one day after (crosses) renal IRI is indicated. D, E. Rapid loss: D. Survival curves of the indicated groups. Survival of animals refed for 2hr, 1 and 2 days was significantly different than ad libitum fed animals (p<0.002); survival of animals refed for 4 and 7 days was not significantly different than ad libitum fed animals. E. Kidney function as measured by serum urea prior to and one day following IRI. Data from three independent experiments with 4-12 animals per group are averaged. In the day 0 group asterisks indicate significant differences vs. the ad libitum fed control group; in the day 1 group, asterisks indicate significant difference between 3 days of fasting without refeeding and ad libitum (AL) fed animals as well as each of the refed groups (**p<0.01). There were no significant differences between the ad libitum group and any of the refed groups on day 1 following renal IRI.

significantly elevated survival rates (100% and 90%, respectively, Fig 2A). Interestingly, despite maximal effects on survival within 2 days, protection against kidney dysfunction increased in a dose-dependent manner for up to 3 days, reaching protection levels similar to 2 or 4 weeks of 30% DR (Fig 2B).

Assessment of kidney function by serum-based measures including creatinine and urea can in some cases be affected by confounding factors such as differences in muscle mass or diet. We thus sought to confirm the rapid onset of protection afforded by fasting with a more direct measure of kidney function. The uptake of technetium-99m-radiolabeled dimercaptosuccinic acid (^{99m}Tc-DMSA) by the kidneys is directly related to kidney tubular reabsorption. 24 hours after IRI significantly less ^{99m}Tc-DMSA accumulated in the ad libitum group relative to the mock-treated animals, indicative of kidney dysfunction. In mice fasted 48 and 72 hours prior to IRI, this reduction was significantly ameliorated (Fig 2C).

In order to determine the kinetics of loss of the protective effect of fasting from renal IRI, we allowed animals ad libitum access to food for variable times following a three day fast and tested their resistance to ischemic injury. Significant benefits on animal survival remained for at least two days after refeeding but were lost after 4 days (Fig 2D). Despite these lingering survival benefits, protection from kidney dysfunction was lost by as little as two hours of refeeding prior to surgery (Fig 2E).

In contrast to ad libitum fed mice, food-restricted mice started eating shortly after awaking from surgery. As a result they gained weight rapidly following surgery, whereas the ad libitum fed mice did not eat in the first days following surgery and as a result lost weight (Fig 1B). We thus asked if benefits of fasting were due to diet-induced changes present at the time of renal IRI (preconditioning) or differences in eating behavior after the injury leading to weight gain in the protected groups. To do this, we prevented access to food for one day following reperfusion in ad libitum fed animals as well as those fasted for two days prior to bilateral renal IRI. Although both groups continued to lose weight the first day after surgery (Fig 3A), animals fasted for two days prior to IRI had a significant survival advantage (Fig 3B) and significantly better renal function on the second day following the injury (Fig 3C). We cannot rule out the possibility that differential feeding after this initial 24 hour post-operative period, or other physiological post-operative differences between fasted and fed mice, contribute to the observed protection in the fasted group. However, our data are consistent with a substantial impact of diet *prior* to the onset of injury. We thus conclude that the impact of diet on the ability to withstand renal IRI is largely due to a preconditioning effect. The best known preconditioning technique is ischemic preconditioning, in which brief periods of ischemia are protective against longer, subsequent bouts of ischemia (Murray et al. 1986). Hereafter we refer to the effects observed here as dietary preconditioning.

To find out if the protection afforded by brief fasting against IRI was specific to the kidney or more broadly applicable, we used a model of liver IRI. 70% hepatic ischemia was induced by clamping the portal vein, hepatic artery and bile duct to the left and median hepatic lobes for 75 minutes. Because no mortality is associated with this model, we monitored ischemic liver damage by measuring the release of the liver-specific enzyme ALAT from dead or damaged cells into the blood for up to 24 hours (Fig 4A). Six hours after reperfusion, serum ALAT levels

(A)

(B)

(C)
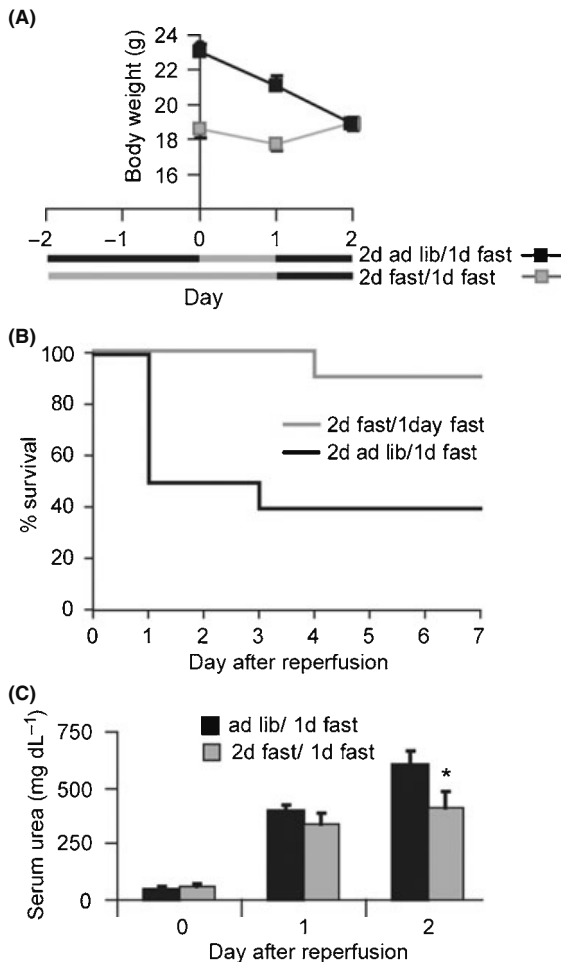
Figure 3. Protection is a preconditioning effect. A. Black bars indicate periods of free access to chow; grey bars indicate periods without access to chow. Body weights of the two groups at the time of surgery (day 0) are indicated. Error bars indicating SEM are contained within the symbols. B. Survival following renal IRI; fasted animals retained their survival advantage (p < 0.02) despite lack of refeeding for one day following renal IRI. C. Kidney function as measured by serum urea levels before and after IRI. Asterisk indicates a significant difference between the fasted and ad libitum fed groups (p<0.05) on the second day following surgery.

were elevated above baseline in all groups. However, they were significantly lower in the 2 and 3 day fasted groups than in the ad libitum fed group. Twenty-four hours after reperfusion, serum ALAT levels were significantly lower in each of the fasted groups. Histological sections prepared 24 hours after reperfusion showed less hemorrhagic necrosis in the 3 day-fasted group than in the ad libitum fed group (Fig 4B). Thus as in the renal ischemia model, 1-3 days of water-only fasting significantly protected against ischemic damage to the liver.

The mechanisms underlying the benefits of long-term DR, including resistance to IRI and extended longevity, remain unclear. Attenuation of oxidative stress, upregulation of stress proteins and reduced inflammation have emerged as potential mechanisms of resistance to heart and brain ischemia by long-term DR (Yu and Mattson 1999; Chandrasekar et al. 2001; Ahmet et al. 2005), while improved insulin sensitivity, reduced insulin/insulin-like growth factor (IGF)-1 signaling, upregulation of stress proteins, reduced mitochondrial free radical production and reduced inflammation are thought to contribute to extended longevity by long-term DR (Gredilla and Barja 2005; Sinclair 2005). We asked if dietary preconditioning

(A)

(B) 24 h after reperfusion

ad lib

3d fast
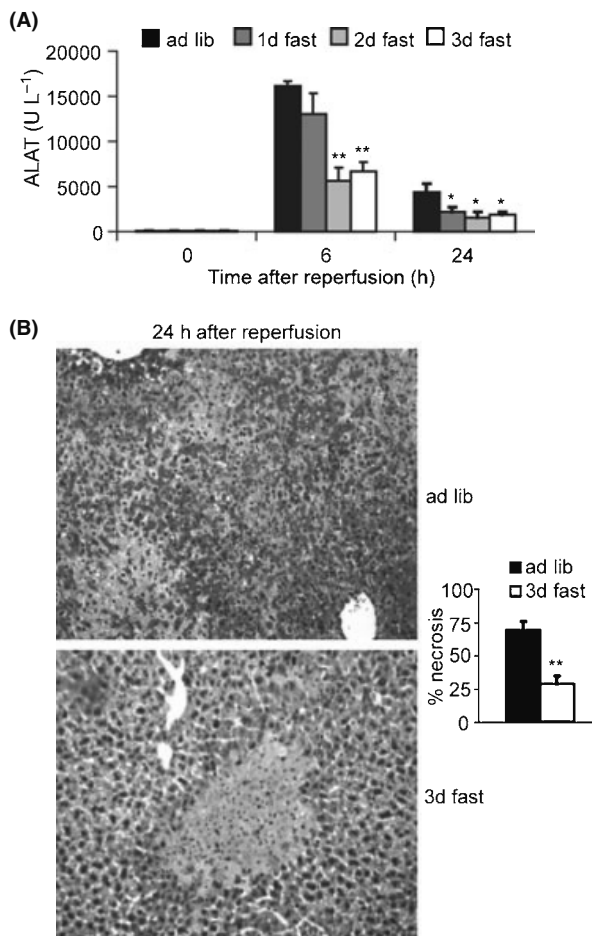
Figure 4. Dietary preconditioning in the liver. A. Reduced injury markers upon liver IRI in fasted mice. Mice (5-8 animals per group) were fasted for the indicated times prior to induction of 75 minutes of warm ischemia to the liver. Serum concentration of the liver-specific enzyme alanine aminotransferase (ALAT) indicative of liver damage was measured at the indicated times following reperfusion. Asterisks indicate the significance of the difference as compared to the ad libitum group at the same time point using a Mann-Whitney U-test (* $p<0.05$; ** $p<0.01$). B. Representative hematoxylin/eosin-stained liver sections from mice 24 hours after reperfusion Note the large areas of hemorrhagic necrosis (in red) in the mouse fed ad libitum prior to IRI and its relative absence in the mouse fasted for 3 days prior. Magnification 100X. Right: Quantification of hemorrhagic necrosis. Liver necrosis was scored blindly on a scale from 0-4, with 4 representing 100% of the area covered by hemorrhagic necrosis. Asterisks indicate the significance of the difference as compared to the ad libitum group (** $p<0.01$).

by short-term DR (defined here as 4 weeks or less) and/or fasting could function via these candidate mechanisms. We first measured insulin sensitivity of animals fasted for 1 or 3 days or 30% restricted for 4 wks relative to ad libitum fed mice by injecting a bolus of insulin into the intraperitoneal cavity and measuring changes in blood glucose over time. The area under each curve is inversely proportional to that group's ability to clear glucose in response to insulin challenge. Fasting and short-term DR resulted in improved insulin sensitivity relative to ad libitum fed mice, correlating with improved outcome following renal IR among our experimental groups (Fig 5A). Fasting improved insulin sensitivity in a dose-dependant manner from 1 to 3 days, with 3 days leading to an equivalent area under the curve as 4 weeks of DR.

We next analyzed components of the insulin/IGF-1 signaling pathway and the inflammatory response on the transcriptional level. At baseline, levels of kidney growth hormone receptor (Ghr) mRNA were significantly reduced in fasted relative to ad libitum fed animals (Fig 5B). Transcription of Igf-1 is dependent on binding of growth hormone
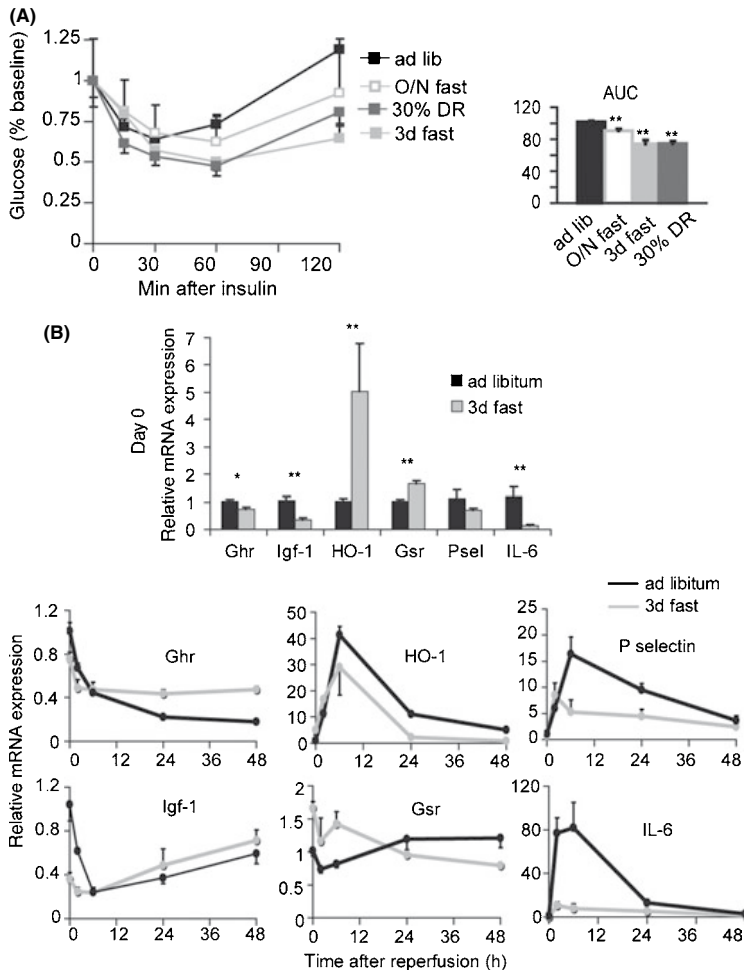
Figure 5. Insulin and IGF-1 signaling in dietary preconditioning. A. Improved insulin sensitivity in preconditioned mice. Whole blood glucose levels at the indicated timepoints following intraperitoneal injection of insulin into animals following the indicated preconditioning regimens. Right: area under the curves (AUC). Statistically significant differences relative to the ad libitum group are indicated by asterisks (** $p<0.01$; * $p<0.05$). B. Differential expression of markers of antioxidant protection, inflammation and GH/IGF-1 axis. Changes in steady state mRNA levels of the indicated genes at baseline (bar graph, top) and over a two day time course following reperfusion (line graphs, bottom) as determined by quantitative real-time PCR. All data points are expressed relative to the ad libitum group at t=0 prior to renal IR. Each data point represents the mean expression value from 5 animals. HO-1, hemeoxygenase-1; Gsr, glutathione reductase; IL-6, interleukin-6; Ghr, growth hormone receptor; Igf-1, insulin-like growth factor-1. Top: asterisks indicate the significance of the difference as compared to the ad libitum group (* $p<0.05$; ** $p<0.01$).

to its cognate receptor, Ghr. Similar to Ghr, Igf-1 mRNA was significantly reduced in the fasted group (Fig 5B). Markers of antioxidant protection, including the inducible form of hemeoxygenase 1 (HO-1) and glutathione reductase (Gsr), were significantly elevated on the transcriptional level in fasted relative to ad libitum fed animals (Fig 5B). Following renal IRI, Ghr and Igf-1 mRNA levels fell below baseline in both groups. Interestingly, their

decline was proportionately less in the fasted group than in the ad libitum group. Also, relative to baseline, the levels 48 hrs after reperfusion were higher in the fasted group than in the ad libitum group. HO-1 was strongly induced in both groups following ischemia, but to significantly lower levels and with a more rapid return to baseline in the fasted group. Gsr mRNA levels fell in the fasted group and increased in the fed group over the 48-hr time course following reperfusion. Markers of inflammation including the proinflammatory cytokine interleukin-6 and the neutrophil-recruiting endothelial adhesion molecule P-selectin were upregulated on the transcriptional level following IRI in both groups with similar kinetics, but to a significantly lower degree in the fasted group (Fig 5B).

We turned to a global approach to quantify the degree to which changes in gene expression due to fasting and short-term DR overlap with each other and with long-term DR. To this end, we compared kidney transcriptomes of animals preconditioned with 4 weeks 30% DR or 3 days fasting to a common group of ad libitum fed animals (n=3 animals per group) using Affymetrix arrays with 45,101 unique probe sets representing 36,431 target genes. 642 (fasted) and 161 (short-term DR) probe sets were significantly differentially regulated vs. the ad libitum control group using the criteria of fold change >1.5 with a p value of <0.001 (Fig 6A). 24 probe sets were common to both (Table 1), representing 14% and 4% of the total significant DR and fasted group probe sets, respectively. 79% of these changes occurred in the same direction, with a Pearson's correlation of 0.529 and a Spearman's rho of 0.464. Notable in this group of genes is a number involved in lipid metabolism (Lpl, Acsm3, Cyp51, Decr2, and Ces1), organelle/membrane trafficking (Ccdc91, Vsp8 and Bnip1) and protein turnover (Cndp2, Wdr40b, Rnf180 and Mmp13).

In light of this modest number of overlapping genes between dietary groups, we next asked which pathways were significantly affected by short-term DR and fasting, and how many were common to both. To this end, we looked for over-representation of pre-defined gene sets within each data set genes using GAzer (Kim et al. 2007) with a false discovery rate of q<0.05. Within the Gene Ontology (GO) category of Biological Processes (GO-BP), 43 and 27 genes sets were significantly over-represented in the DR and fasted groups, respectively. 13 of these were common to both treatments, with Z scores indicating the same directionality in all 13 gene sets. In GENMAPP Pathway, 19 and 9 gene sets were significantly over-represented in the DR and fasted groups, respectively, with 4 of the 6 in common in the same direction. Heat maps of these enriched gene sets in both treatment groups ordered by Z score of the DR group are shown in Fig 6B,C. Similar overlaps were seen within other sets of pre-defined gene sets, including GO Molecular Functions (GO-MF; 40 DR and 25 fasted significant gene sets, 12 common to both, all in the same direction) GO Cellular Component (GO-CC; 18 DR and 7 fasted significant gene sets, 3 common to both, all in the same direction) and Interpro (41 DR and 49 fasted significant gene sets, 19 in common, all in the same direction). Thus, despite only modest overlap on the level of individual genes, 53 out of the 161 and 117 significant gene sets in the short-term DR and fasted groups, respectively, were common to both treatments, with 51 of these in the same direction.

Amongst these pathways were many expected for nutrient/energy deprivation by either fasting or DR, including downregulation of fatty acid, cholesterol and steroid biosynthesis.

Pathways previously reported to be downregulated upon dietary restriction, such as DNA repair (Stuart et al. 2004), were also downregulated (although not significantly) in the fasted group. In addition, shared pathways consistent with increased resistance to IRI were significantly over-represented, including increased GO-BP negative regulation of apoptosis (upregulated anti-apoptotic genes included angiopoietin-like 4 in both groups and Bcl2-like 1 in the fasted group), increased GO-MF glutathione transferase activity (increased Gstm1, Gstm3 in DR; increased Mgst-1, Gsta1, Gsta2, Gsta3, Gsto1, Gstt2, Gstm1 in FA) and decreased GO-BP complement activation. Of the 19 common significant pathways represented in Fig 6B, differences between dietary treatments were observed in only 2, Statin and Electron Transport Chain (ETC). In the ETC Pathway, for example, a number of genes encoding subunits of cytochrome c oxidase, NADH dehydrogenase and ATP synthase were significantly upregulated in DR and downregulated in FA, accounting for the difference in directionality. Although ROS production and/or detoxification is thought to be a key player in the anti-aging effects of DR, the role of mitochondrial respiration itself remains controversial (Kaeberlein et al. 2005). Further experiments will be required to test which if any of these pathways are involved in the beneficial effects of dietary preconditioning against IRI.

Finally, we asked if the effects of short-term DR and fasting on gene expression in the kidney were similar to what has been previously reported for long-term DR in other mouse tissues. For data regarding long-term DR, we turned to a meta-analysis covering ten mouse tissues subject to varying lengths (2d-2yr, average 6 mo) and severity (10-75%, average 36%) of DR (Swindell 2008). 28 genes that change significantly upon DR in at least 5 tissues were identified in this meta-analysis. Within this group of 28 genes/48 probe sets), 2 genes/2 probe sets (PER2, TSPAN4) from our DR data set and 8 genes/9 probe sets (CD74, COL3A1, TSPAN 4, FKBP5, RBM3, PECI, SERPINH1 and CDKN1A) from our fasted data set were significantly differentially regulated in the kidney (fold change >1.5, p<0.001). This degree of enrichment makes it amongst the most significant of any pre-defined gene set tested (p= 0.013 and p =2.353e-8 for DR and fasted, respectively, by Fisher's exact test). A heat map representing expression levels of probe sets corresponding to the 28 DR-associated genes is presented in Fig 6D.

Figure 6. Global transcriptional changes upon short-term dietary restriction and fasting. A. Venn ▶ diagram representing numbers and overlap of probesets significantly differentially regulated in kidney as a result of dietary preconditioning (4 wk 30% DR or 3 days fasting, FA) as compared to ad libitum fed controls. Significance cutoffs were set by fold change of greater than 1.5 and p value of <0.001. B, C. All Gene Ontology - Biological Processes (B) and GENMAPP Pathway (C) gene sets over-represented within either the short-term DR or fasted vs. ad libitum data sets were aligned according to Z score. Red, green and black indicate upregulation, downregulation and or no change, respectively, of that biological process due to the given dietary treatment relative to ad libitum feeding. Gene sets are ordered by Z score of the 30% DR group. Note that all gene sets significantly over-represented in either treatment group (DR or FA) are included in the heat maps, and that those gene sets significantly over-represented in both treatment groups are in bold. D. Similarity to long-term DR. Heat map of gene expression changes in a pre-defined set of 28 genes comprising a common transcriptional signature of DR across multiple mouse tissues (Swindell 2008). Long-term DR probesets are indicated either as up (red) or down (green) without regard to magnitude of expression; probesets corresponding to short-term DR and fasted groups are colored as in B. Significant genes from the short-term DR and fasted data sets as defined by fold change > 1.5 and p value <0.001 are in bold, with crosses and asterisks corresponding to short-term DR and fasting, respectively.

(A)

FA vs AL 642 | 24 | DR vs AL 161

(B)

−3.0 0 3.0

DR FA GO Biological process

Rhythmic process
Circadian rhythm
GPCR protein signaling pathway
Ion transport
Signal transduction
Negative regulation of apoptosis
Development
Synaptic transmission
Cell differentiation
Growth
Transmembrane RTK signaling pathway
Potassium ion transport
Organogenesis
Neuron cell differentiation
Neurogenesis
Response to oxidative stress
Cell-cell signaling
Calcium ion transport
Regulation of transcription, DNA-dependent
Response to heat
Lipid metabolism
Lipid catabolism
ATP synthesis coupled proton transport
Proton transport
Fatty acid metabolism
ATP biosynthesis
Nucleosome assembly
Tricarboxylic acid cycle
Intracellular protein transport
Chromosome organization and biogenesis
Fatty acid biosynthesis
Aromatic compound metabolism
Nucleotide metabolism
Microtubule cytoskeleton organisation/biogenesis
Chromatin modification
Protein catabolism
Cholesterol metabolism
Cytokinesis
DNA replication
Cell cycle
DNA repair
RNA processing
Mitosis
Nuclear mRNA splicing, via spliceosome
phosphate transport
Complement activation
Complement activation, classical pathway
Blood coagulation
mRNA processing
tRNA aminoacylation for protein translation
Protein folding
Protein transport
Ubiquitin cycle
Steroid biosynthesis
Cholesterol biosynthesis
Lipid biosynthesis
Sterol biosynthesis

(C)

DR FA GENMAPP Pathway

Ovarian Infertility genes
Monoamine GPCRs
Circadan exercise
GPCRDB other
GPCRDB class A Rhodopsin-like
Nuclear receptors
Electron transport chain
Wnt signaling
Smooth muscle contraction
Blood clotting cascade
Mitochondrial fatty acid betaoxidation
Translation factors
Fatty acid degradation
Glycogen metabolism
G1 to S cell cycle reactome
Inflammatory response pathway
Statin pathway pharmGKB
mRNA processing binding reactome
Complement activation classical
RNA transcription reactome
DNA replication reactome
Cholesterol biosynthesis

(D)

Long-term DR | Short-term DR | Fasting | **GENE (probe set)**

⇧*TSPAN4 (1448276_at)
SULT1A1 (1427345_a_at)
*RBM3 (1422660_at)
RBM3 (1429169_at)
PPARA (1449051 at)
PNPLA2 (1428591_at)
PNPLA2 (1428143_a_at)
PIM3 (1437100_x_at)
PIM3 (1451069_at)
PER2 (1417609_at)
PER2 (1445892_at)
⇧PER2 (1457350_at)
PER2 (1417602_at)
PER1 (1449851_at)
*PECI (1431012_a_at)
NFKBIA (1420088_at)
NFKBIA (1448306_at)
NFKBIA (1449731_s_at)
NFKBIA (1438157_s_at)
MT2 (1428942_at)
MT1 (1422557_s_at)
MT1 (1451612_at)
MGI : 19 24575 (1436316_at)
FKBP 5 (1416125_at)
FKBP 5 (1448231_at)
FKBP 5 (1458089_at)
FKBP 5 (1441799_at)
DDIT4 (1428306_at)
CDKN1A (1424638)_at)
*CDKN1A (1421679_a_at
TGTP (1449009_at)
*SERPINH1 (1450843_a_at)
*SERPINH1 (1456733_x_at)
IFITM3 (1423754_at)
IFI27 (1426278_at)
HSP110 (1440575_at)
HSP110 (1416146_at)
H2-EA (1422891_at)
H2-EA (1422892_s_at)
GNG11 (1448942_at)
*COL3A1 (1427883_a_at)
COL1A1 (1423669_at)
*CD74 (1425519_a_at)
CCL9 (1417936_at)
CCL9 (1448898_at)
C1QB (1417063_at)
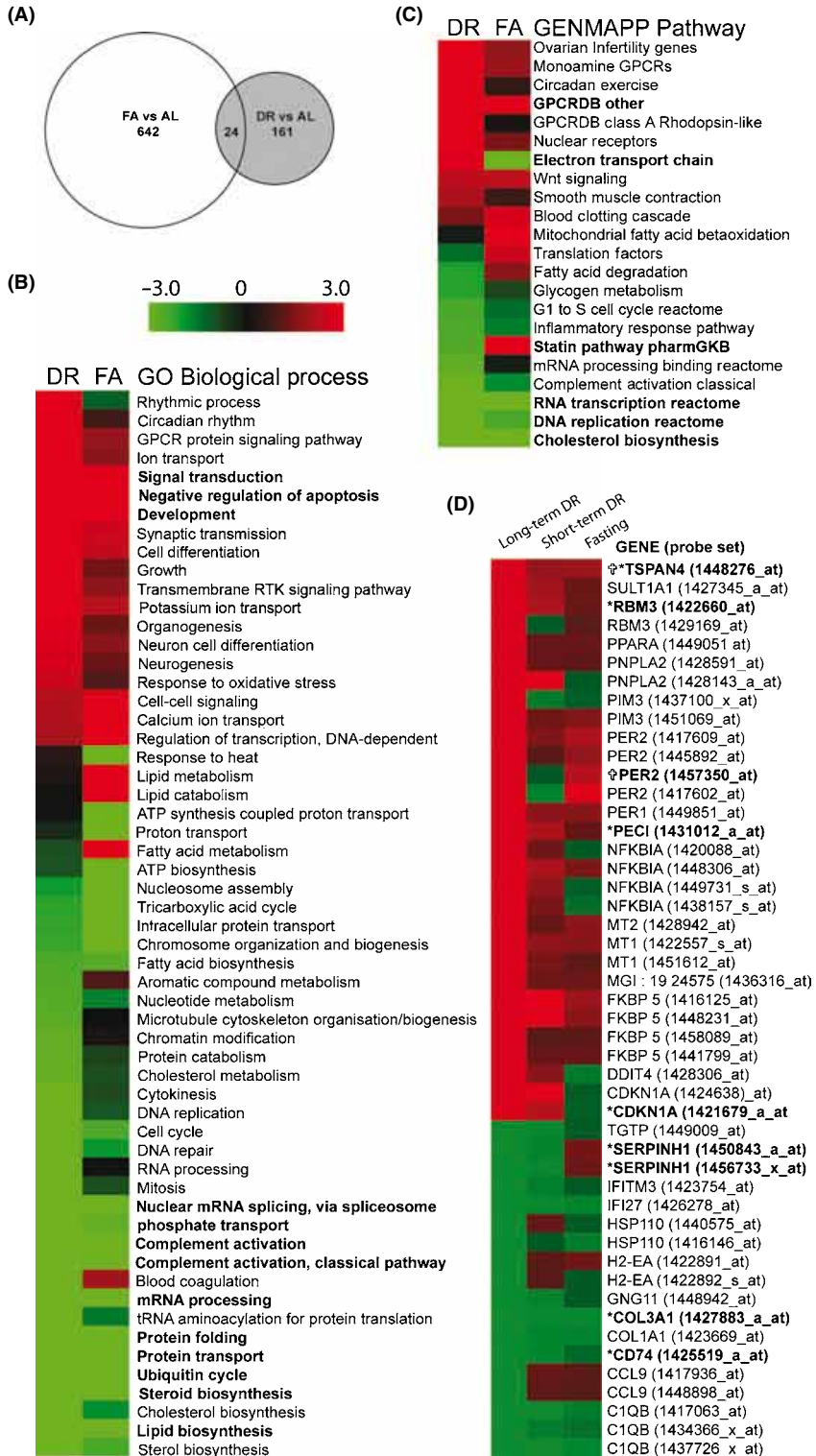C1QB (1434366_x_at)
C1QB (1437726_x_at)

Table 1. 24 genes significantly differentially regulated in both short-term DR and fasted (FA) groups with fold changes >1.5 and p values <0.001. Expression level indicates the group geometric mean of the RMA normalized Affymetrix data, ordered by the ad libitum (AL) group.

Gene	Symbol	Expression level			Fold change vs. AL		Putative Function
		AL	DR	FA	DR	FA	
CNDP dipeptidase 2 (metallopeptidase M20 family)	Cndp2	14684	7766	3922	-1,9	-3,7	proteolysis of nonspecific dipeptides in cytosol
lipoprotein lipase	Lpl	10727	6045	5504	-1,8	-1,9	triacylglycerol hydrolysis, lipoprotein uptake
acyl-CoA synthetase medium-chain family member 3	Acsm3	7964	3417	3306	-2,3	-2,4	activation of fatty acids for anabolism or catabolism
dopa decarboxylase	Ddc	2558	1241	6356	-2,1	2,5	catecholamine biosynthesis
solute carrier family 22 member 7	Slc22a7	2231	859	276	-2,6	-8,1	bidirectional **facilitory** cGMP transporter
flavin containing monooxygenase 2	Fmo2	2100	3792	3450	1,8	1,6	oxidation of xenobiotics
cytochrome P450, family 51	Cyp51	1731	1010	425	-1,7	-4,1	key demethylase enzyme in all sterol biosynthesis
coenzyme Q10 homolog B (S. cerevisiae)	Coq10b	974	2069	453	2,1	-2,2	ubiquinone binding protein in yeast
solute carrier family 6, member 6	Slc6a6	811	2177	2302	2,7	2,8	taurine transporter
vacuolar protein sorting 8 homolog (S. cerevisiae)	Vps8	698	437	170	-1,6	-4,1	endosomal/lysosomal biogenesis
tetraspanin 4	Tspan4	643	1186	1119	1,8	1,7	cell surface transmembrane integrin signaling
2-4-dienoyl-Coenzyme A reductase 2, peroxisomal	Decr2	426	678	876	1,6	2,1	peroxisomal oxidation of unsaturated fatty acids
RIKEN cDNA D630039A03 gene	D630039A03Rik	323	156	618	-2,1	1,9	unknown
RIKEN cDNA 2310028N02 gene	2310028N02Rik	286	177	184	-1,6	-1,6	transmembrane protein
carboxylesterase 1	Ces1	249	87	74	-2,9	-3,4	detoxification of xenobiotics, cholesterol metabolism
coiled-coil domain containing 91	Ccdc91	245	136	130	-1,8	-1,9	sorting of acid hydrolase to endosomes
BCL2/adenovirus E1B interacting protein 1, NIP1	Bnip1	187	119	115	-1,6	-1,6	anti-apoptotic factor/ER membrane fusion
mannan-binding lectin serine peptidase 1	Masp1	185	303	118	1,6	-1,6	complement activation and immune response
aryl hydrocarbon receptor nuclear translocator-like	Arntl (Bmal1)	107	56	219	-1,9	2,0	transcription factor required for circadian rhythmicity
WD repeat domain 40B	Wdr40b	80	45	48	-1,8	-1,7	associated with DDB1/Cullin 4 ubiquitin ligase
matrix metallopeptidase 13	Mmp13	48	25	18	-1,9	-2,7	breakdown of extracellular matrix
RIKEN cDNA 0610007P08 gene	0610007P08Rik	37	23	21	-1,6	-1,7	possible DNA damage response
ring finger protein 180	Rnf180	37	18	15	-2,1	-2,5	membrane bound ubiquitin ligase
similar to MOSC domain-containing protein 1	LOC100045982	30	69	642	2,3	21,1	possible molybdenum cofactor biosythesis

DISCUSSION

Timing of onset of benefits of DR

Voluntary adherence to a restricted diet is difficult for most people. Potential benefits of DR requiring long-term application, such as extended longevity, are thus considered moot in a clinical setting. However, extended longevity is only one of the potential benefits of DR (albeit a widely popularized one). DR also increases acute stress resistance in most organisms tested, including mammals. For example, DR lasting between 3 months and 1 year mitigates injury in rodent models of cardiac and cerebral ischemia (Yu and Mattson 1999; Chandrasekar et al. 2001; Ahmet et al. 2005). What is currently not known is the length of restriction required for the onset of such benefits. Here we show that as little as 2-4 weeks of 30% reduced daily feeding in mice led to significant protection against renal IRI. Interestingly, there was no increase in protection between 2 and 4 weeks of DR, suggesting that the maximal protection afforded by these short-term treatments was already reached by 2 weeks of DR. Whether or not longer periods of restriction will further increase protection remains to be experimentally determined.

In rodents, longevity extension by DR is roughly proportional to the amount of energy restriction (0-65%) up to the point of starvation (Weindruch et al. 1986; Merry 2002). Beyond this point, restriction can lead to irreversible consequences and is eventually fatal. However, 100% restriction (water-only fasting) for shorter periods of time is possible without irreversible side-effects. We found that 3 days of water-only fasting led to protection against renal ischemic injury similar in magnitude to 2-4 weeks of 30% DR. Significant benefits were observed with respect to both survival and kidney function; however, the kinetics of onset and loss differed between these endpoints. Significant survival benefits occurred after a single overnight fast, while protection against renal dysfunction increased each fasting day for up to three days. Similarly, functional protection afforded by a 3 day fast was rapidly lost within hours of refeeding despite lingering survival benefits for up to several days. The reason for these apparent discrepancies in timing of onset and loss of benefits is currently not known. One possibility is that death and kidney dysfunction, although both initiated by renal IRI, have partially different causes. For example, mortality may be caused by reperfusion injury to distant organs such as the heart, lungs and brain (Kelly 2003) in addition to renal failure. Fasting may more rapidly affect the body's ability to withstand remote ischemic injury than acute renal ischemic injury. Another, non-mutually exclusive possibility is that different mechanisms of protection exist and that they are gained and lost at different rates. For example, transcriptional upregulation of stress resistance genes including HO-1 and Gsr may require several days of reduced insulin/IGF-1 signaling, but be rapidly lost upon the return of such signaling. Future experiments will be required to determine molecular mechanisms underlying individual benefits and their timing of onset and loss as a function of different dietary regimens.

This is the first demonstration of the rapid onset of resistance to renal ischemic damage by short-term DR and fasting. However, it is consistent with a larger body of work demonstrating rapid onset of benefits of energy/nutrient deprivation, including both fasting and DR, in different organisms using different endpoints. For example, in fruit flies maximal effects on daily mortality rate are achieved within one to three days of DR (Mair et al. 2003). Resistance

to starvation stress is also increased by four days of DR and scales with the percent restriction (Chippindale et al. 1993). In mice, 40% DR for 12-15 days is effective at preventing growth of tumor xenografts (Kalaany and Sabatini 2009). DR initiated late in life rapidly shifts liver gene expression towards a long-term DR profile, beginning in a little as 2 weeks, and impacts longevity within two months (Dhahbi et al. 2004). Two weeks of DR also leads to feminization of liver gene expression in males (Estep et al. 2009), an intriguing finding in light of the dramatically increased resistance of females to renal IRI relative to males in both humans and mice (Kher et al. 2005). Shorter periods of more severe restriction have also proven efficacious in protecting against acute stress. For example, fasting for 3-4 days improves organ and animal survival in rodent models of orthotopic liver transplantation (Sumimoto et al. 1993) and heterotopic heart transplantation (Nishihara et al. 1997). Finally, two days of water-only fasting protects mice against the toxic effects of chemotherapeutic agents (Raffaghello et al. 2008). Although most of these studies were not designed to interrogate the time on a restricted diet required for the onset of maximal benefit, taken together with our own studies they suggest that benefits of nutrient/energy restriction measured by a variety of outcomes, including acute stress resistance, do not require long-term application.

Potential overlap between mechanisms of protection by fasting, short-term and long-term DR

One of the consequences of nutrient/energy deprivation is reduced insulin/IGF-1 signaling. Reduced signaling through these pathways increases stress resistance and extends longevity in part through activation of transcription factors leading to increased expression of stress resistance genes (Tatar et al. 2003). In rodents, improved insulin sensitivity is indicative of reduced baseline insulin signaling and is observed in both genetic and dietary models of extended longevity and increased stress resistance. Relative to ad libitum fed mice, we observed improved insulin sensitivity upon both fasting and short-term DR. We also observed reduced levels of growth hormone receptor and IGF-1 mRNAs in the kidney itself, as well as upregulation of genes involved in antioxidant defense. These data are consistent with a model of increased stress resistance by both fasting and short-term DR involving reduced insulin/IGF signaling and concomitant upregulation of cellular stress resistance mechanisms. As a consequence, oxidative injury, cell death and inflammation are all reduced subsequent to ischemic injury.

In a variety of experimental models, reduced signaling through insulin/insulin-like peptides results in extended longevity and increased stress resistance (Brown-Borg 2006). This may seem at odds with the well-documented pro-growth and pro-survival effects these factors have in other settings, for example in response to ischemic insult to the brain, heart or kidney (Miller et al. 1992; Guan et al. 2003; Takeda et al. 2006; Suleiman et al. 2007). Here we observed improved insulin sensitivity and reduced Ghr and Igf-1 mRNA in fasted mice consistent with reduced signaling through these pathways at baseline prior to IRI. Interestingly, we also observed a relative increase in mRNA levels of Ghr and Igf-1 after injury in the fasted group. Although further experiments are required to determine actual levels of GH/IGF-1 signaling, the present data are consistent with *increased* signaling through these

pathways after ischemic insult and better survival. Based on these data, we hypothesize that the benefits of reduced and increased insulin/IGF signaling can be separated by time relative to an acute injury, and are thus not mutually exclusive. According to this hypothesis, reduced IGF-1 signaling as a result of DR or fasting prior to ischemic insult may have two beneficial effects: upregulation of stress resistance resulting in less initial damage, and improved IGF-1 sensitivity resulting in increased survival signaling after injury.

In lower organisms, the genetic requirements for lifespan extension and stress resistance are more extensively characterized than in mammals, and appear to vary depending on the type of DR method employed. In worms, for example, the source of bacteria (liquid culture vs. solid agar plates) and the timing of onset of DR can both affect the genetic requirements for longevity extension (Greer et al. 2007). Here we used two distinct dietary interventions, fasting and short-term DR, to modulate resistance to ischemic injury and found similar beneficial effects with both. On the level of global changes in the kidney transcriptome, 31% of the significant short-term DR and 49% of the significant fasting annotated gene sets identified in GO-BP, GO-MF, GO-CC, GENMAPP Pathway and Interpro were common to both treatment groups. Of the 53 significant gene sets in common, 51 were changed in the same direction. Furthermore, gene expression markers identified previously in a meta-analysis of mostly long-term DR studies of multiple mouse organs (Swindell 2008) were significantly enriched in our kidney data set from both short-term DR and fasted animals. Taken together, these data are consistent with an overlapping transcriptional response to fasting, short-term DR and long-term DR in the kidney. However, they are also consistent with different genetic requirements for different DR regimens as in lower organisms. Future experiments will be required to determine which of these changes, if any, underlie the benefits of dietary restriction on acute stress resistance.

Finally, it will be of great future interest to elucidate the relationship between acute stress resistance and other benefits of DR such as extended longevity. Without any detailed understanding of the mechanism (or mechanisms) underlying either of these benefits, the relationship between them remains only correlative in nature. It is easy to envisage how improved stress resistance could extend longevity, for example by increasing the likelihood of surviving a heart attack or stroke on any given day. What remains unclear is if, or how, this relates to the reduction in the rate of aging achieved by DR.

Fasting in DR and acute stress resistance

The role of periods of fasting in the beneficial action of DR remains unclear (Mattson 2005). DR regimens in rodents involve extended periods of fasting between meals, as animals are hungry and consume their food allotment quickly when fed. The length of these periods is not widely reported and likely depends both on the percent restriction as well as the frequency of meals (typically once daily to thrice weekly). Intermittent fasting regimens with ad libitum feeding between periods of fasting (for example, every other day fasting or 4 days fasting every two weeks) have beneficial effects in rodents similar to DR, including extended lifespan (Goodrick et al. 1982; Sogawa and Kubo 2000) and increased stress resistance (Anson et al. 2003). In some strains, intermittent fasting is associated with reduced total food intake and

A II

reduced body weight typical of DR (Varady and Hellerstein 2007), while in others, it produces tangible health benefits in the absence of weight loss (Sogawa and Kubo 2000; Anson et al. 2003). This suggests that periods of fasting rather than reduced overall calorie intake per se may underlie some of the benefits of DR. On the other hand, altering the temporal pattern of feeding of a restricted diet from once to twice daily, while affecting circadian rhythmicity, has no significant impact on lifespan (Masoro et al. 1995). This suggests that overall nutrient/ energy restriction is more important than timing of food intake at least for longevity extension by DR. Nevertheless, these experiments did not rule out the potential role of fasting between meals, as both groups still underwent extended periods of fasting relative to the ad libitum group (Masoro 2004). Experimental separation of reduced nutrient/energy intake from periods of fasting in experimental rodents remains challenging, and further experiments will be required to resolve the contribution of periods of fasting, if any, to the benefits of DR. Our data are consistent with a role of fasting in at least one of these benefits, acute stress resistance, during the initiation phase of DR.

The benefits of fasting have been known at least since the time of Hippocrates, but the practice is largely absent from Western medicine today. Instead, it is often associated with malnutrition, a risk factor for postoperative survival (Studley 1936), wound healing, infection and multiple organ failure (Chung 2002). One of the few modern clinical applications of fasting is to reduce the risk of pulmonary aspiration of regurgitated stomach contents prior to operations involving anesthesia. The origins in the 1960s of the standard "nil by mouth after midnight" preoperative fast are somewhat obscure (Maltby 2006), and today even this relatively short fast is perceived as overcautious and possibly detrimental to patient subjective well-being and postoperative recovery (Diks et al. 2005). Current more liberal guidelines allow consumption of solids up to six hours prior to surgery and recommend consumption of liquids, including carbohydrate-rich beverages, up to two hours prior to surgery (Soreide et al. 2005). Our data suggest that slightly longer periods of fasting, or short periods of DR, prior to surgery may be beneficial for an entirely different purpose – protection against certain types of acute organ stress. Fasting may thus represent a non-invasive, cost-free method of protecting against multiple types of acute stress, including surgical ischemia reperfusion injury unavoidably encountered in elective surgeries including living-donor organ transplantation, cardiac surgery, vascular surgery and liver resection. It remains to be seen if the benefits of fasting and short-term DR and their rapid onset observed in rodents will translate to humans. However, the conservation of rapid onset of DR benefits between flies (Mair et al. 2003) and rodents, combined with the efficacy of DR in improving markers of healthspan in both non-human primates (Colman et al. 2008; Colman et al. 2009) and humans (Fontana and Klein 2007) suggests that it might.

EXPERIMENTAL PROCEDURES

Mice

Male C57BL/6J mice in the age/weight range of 22-25 grams/10-14 weeks were purchased from Charles River Laboratories, Maastricht, the Netherlands. Animals were kept under

standard laboratory conditions (temperature 20-24ºC, relative humidity 50-60%, 12 h light/12 h dark) with 3-4 animals per cage and allowed free access to water and food (Hope Farms, Woerden, The Netherlands) except where noted. All experiments were performed with the approval of the appropriate local ethical board.

Dietary regimens

The amount of food eaten ad libitum was approximately 3.5 gram/day as determined by weighing the remaining food on a daily basis for one week. DR was applied for 2-4 weeks by feeding mice 70% of this amount on a daily basis. Fasting was applied by transferring mice to a fresh cage without food for 1-3 days. Despite significant weight loss as a result of short-term DR and fasting, no morbidity or mortality was observed as a function of the diets alone.

Renal ischemia model

Mice were anaesthetized by isoflurane inhalation (5% isoflurane initially and then 2-2.5% with oxygen for maintenance). Body temperature was maintained by placing the animals on heating pads until recovery from anesthesia. Following a midline abdominal incision, the left renal pedicle was localized and the renal artery and vein were dissected. An atraumatic microvascular clamp was used to occlude the left kidney for 37 minutes. For bilateral occlusion, the procedure was repeated immediately on the right kidney. After inspection for signs of ischemia (purple color), the wound was covered with phosphate-buffered saline (PBS)-soaked cotton and the animal placed under an aluminum foil blanket to maintain body temperature. After release of the clamp, restoration of blood-flow was inspected by return of the kidney to normal color. In the case of unilateral occlusion, a contralateral nephrectomy was performed immediately following clamp release. The abdominal wound was closed in two layers using 5/0 sutures. Animals were given 0.5 mL PBS subcutaneously for maintenance of fluid balance and kept warm under a heat lamp. All animals were observed to have regained consciousness before moving their cages from the operating room to the stable.

Kidney function analysis

Unlabeled DMSA kits were purchased from GE Healthcare (Roosendaal, the Netherlands) and radiolabeled with ^{99m}Tc according to manufacturer's instructions. Mice were injected in a lateral tail vein with 30 MBq ^{99m}Tc-DMSA. Four hours post injection the mice were sacrificed, the kidney was removed, and the absorbed radioactivity was measured in a gamma counter (Perkin Elmer, Groningen, the Netherlands) and expressed as percentage of injected dose per kidney (%ID/kidney).

Liver ischemia model

Liver IRI was performed by visualizing the liver hilus and clamping the portal vein, hepatic artery and bile duct to the left and median hepatic lobes with an atraumatic clamp for

75 minutes. In this model, 70% of the liver tissue becomes ischemic, and blood outflow from the small intestine is preserved through the right anterior and caudate liver lobes. Mortality associated with this amount of ischemic damage to the liver was not observed. Liver samples were fixed in formalin for 24 hr prior to embedding in paraffin. 4 μm sections were cut and stained with hematoxylin and eosin. Liver necrosis was scored blindly on a scale from 0-4, with 4 representing 100% of the area covered by hemorrhagic necrosis.

Serum measurements

Blood samples were collected by retro-orbital puncture. Serum urea and creatinine levels were measured using QuantiChrom assay kits based on the improved Jung and Jaffe methods, respectively (DIUR-500 and DICT-500, Gentaur, Brussels, Belgium). Serum ALAT levels were determined using an ELAN analyzer (Eppendorf Merck, Hamburg, Germany) with Ecoline S+ reagents (Diagnostic Systems GmbH, Holzheim, Germany) according to manufacturer's instructions. Serum LDH levels were determined using Ecoline S+ reagents according to manufacturer's instructions in a 96-well format on a Varioskan microplate reader (Thermo Scientific).

Histology

Organs were harvested, fixed for 24 hr in formalin and embedded in paraffin. 3 μm sections were stained with hematoxylin and eosin. Tubular injury was assessed in a blind fashion on a five point scale as described previously (Leemans et al. 2005).

Insulin sensitivity tests

Following baseline blood glucose determination from tail blood of conscious, restrained mice, animals were injected with a bolus of insulin (Novorapid; 0.75 U/kg body weight) into the intraperitoneal cavity. Blood glucose determinations were performed at the indicated times after injection using a HemoCue glucose 201 RT blood glucose analyzer (HemoCue, Ängelholm, Sweden) according to the manufacturer's instructions.

Quantitative real time PCR

Total RNA was extracted from frozen kidney tissue using Ambion mirVana miRNA Isolation Kit and oligodT or hexamer-primed cDNA synthesized using SuperScript II (Invitrogen) according to the manufacturer's instructions. Quantitative real-time PCR was performed using a MyIQ (BioRad) with SYBR Green incorporation. Relative expression was calculated using the equation $1.8^{-(\Delta Ct\ sample\ -\ \Delta Ct\ control)}$ (Pfaffl 2001). Each sample was tested in duplo at least two times.

Microarrays

Purified total RNA extracted from frozen kidneys (three per group) was used as template to generate biotin labeled cRNA and hybridized to 430-2.0 GeneChips according to the manufacture's protocol (Affymetrix). Raw data was RMA normalized (Irizarry et al. 2003) and assessed for differential gene expression using limma (Smyth 2004). Annotated

pathway over-representation was performed using GAzer (Kim et al. 2007). Fisher's Exact test was performed using the web application available at http://www.langsrud.com/fisher.htm. Spearman's rho and Pearson's correlation coefficients were calculated using SPPS11. Affymetrix 430-2.0 probe sets representative of the 28 common dietary restricted genes (Swindell 2008) were obtained from Ensembl (http://www.ensembl.org/), based on the NCBI m37 mouse assembly; expect for MGI:1924575 which was obtained from the Mouse Genome Informatics data base (http://www.informatics.jax.org/) given the absence of annotations in Ensembl for this transcript at the time of submission.

Statistics

Data are expressed as the mean ± SEM. Statistical analyses of data on urea, creatinine, histomorphology, immunohistochemistry and immunoblot was preformed using a Student's T test unless otherwise indicated. Survival was analyzed by Kaplan-Meier (SPSSv11). Area under the curve was calculated using GraphPad Prism 4.0, and the significance calculated usin g a Student's T test.
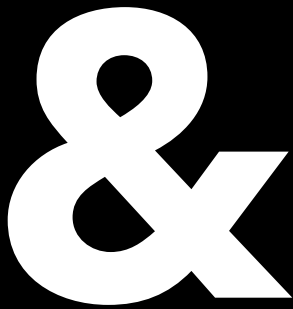
ACKNOWLEDGEMENTS

REFERENCES

Ahmet, I., R. Wan, M.P. Mattson, E.G. Lakatta, and M. Talan. 2005. Cardioprotection by intermittent fasting in rats. *Circulation* **112**: 3115-21.

Anson, R.M., Z. Guo, R. de Cabo, T. Iyun, M. Rios, A. Hagepanos, D.K. Ingram, M.A. Lane, and M.P. Mattson. 2003. Intermittent fasting dissociates beneficial effects of dietary restriction on glucose metabolism and neuronal resistance to injury from calorie intake. *Proc Natl Acad Sci U S A* **100**: 6216-20.

Bishop, N.A. and L. Guarente. 2007. Genetic links between diet and lifespan: shared mechanisms from yeast to humans. *Nat Rev Genet* **8**: 835-44.

Brown-Borg, H.M. 2006. Longevity in mice: is stress resistance a common factor? *AGE* **28**: 145-162.

Chandrasekar, B., J.F. Nelson, J.T. Colston, and G.L. Freeman. 2001. Calorie restriction attenuates inflammatory responses to myocardial ischemia-reperfusion injury. *Am J Physiol Heart Circ Physiol* **280**: H2094-102.

Chippindale, A.K., A.M. Leroi, S.B. Kim, and M.R. Rose. 1993. Phenotypic plasticity and selection in Drosophila life-history evolution. I. Nutrition and the cost of reproduction. *Journal of Evolutionary Biology* **6**: 171-193.

Chung, A. 2002. Perioperative nutrition support. *Nutrition* **18**: 207-8.

Colman, R.J., R.M. Anderson, S.C. Johnson, E.K. Kastman, K.J. Kosmatka, T.M. Beasley, D.B. Allison, C. Cruzen, H.A. Simmons, J.W. Kemnitz, and R. Weindruch. 2009. Caloric restriction delays disease onset and mortality in rhesus monkeys. *Science* **325**: 201-4.

Colman, R.J., T.M. Beasley, D.B. Allison, and R. Weindruch. 2008. Attenuation of sarcopenia by dietary restriction in rhesus monkeys. *J Gerontol A Biol Sci Med Sci* **63**: 556-9.

Comfort, A. 1963. Effect of delayed and resumed growth on the longevity of a fish (Lebistes reticulatus Peters) in captivity. *Gerontologia (Basel)* **8**: 150-155.

Dhahbi, J.M., H.J. Kim, P.L. Mote, R.J. Beaver, and S.R. Spindler. 2004. Temporal linkage between the phenotypic and genomic responses to caloric restriction. *Proc Natl Acad Sci U S A* **101**: 5524-9.

Diks, J., D.E. van Hoorn, R.J. Nijveldt, P.G. Boelens, Z. Hofman, H. Bouritius, K. van Norren, and P.A. van Leeuwen. 2005. Preoperative fasting: an outdated concept? *JPEN J Parenter Enteral Nutr* **29**: 298-304.

Estep, P.W., 3rd, J.B. Warner, and M.L. Bulyk. 2009. Short-term calorie restriction in male mice feminizes gene expression and alters key regulators of conserved aging regulatory pathways. *PLoS One* **4**: e5242.

Fontana, L. and S. Klein. 2007. Aging, adiposity, and calorie restriction. *Jama* **297**: 986-94.

Friedewald, J.J. and H. Rabb. 2004. Inflammatory cells in ischemic acute renal failure. *Kidney Int* **66**: 486-91.

Goodrick, C.L., D.K. Ingram, M.A. Reynolds, J.R. Freeman, and N.L. Cider. 1982. Effects of intermittent feeding upon growth and life span in rats. *Gerontology* **28**: 233-41.

Gredilla, R. and G. Barja. 2005. Minireview: the role of oxidative stress in relation to caloric restriction and longevity. *Endocrinology* **146**: 3713-7.

Greer, E.L., D. Dowlatshahi, M.R. Banko, J. Villen, K. Hoang, D. Blanchard, S.P. Gygi, and A. Brunet. 2007. An AMPK-FOXO pathway mediates longevity induced by a novel method of dietary restriction in C. elegans. *Curr Biol* **17**: 1646-56.

Guan, J., L. Bennet, P.D. Gluckman, and A.J. Gunn. 2003. Insulin-like growth factor-1 and post-ischemic brain injury. *Prog Neurobiol* **70**: 443-62.

Heilbronn, L.K., L. de Jonge, M.I. Frisard, J.P. DeLany, D.E. Larson-Meyer, J. Rood, T. Nguyen, C.K. Martin, J. Volaufova, M.M. Most, F.L. Greenway, S.R. Smith, W.A. Deutsch, D.A. Williamson, and E. Ravussin. 2006. Effect of 6-month calorie restriction on biomarkers of longevity, metabolic adaptation, and oxidative stress in overweight individuals: a randomized controlled trial. *Jama* **295**: 1539-48.

Irizarry, R.A., B.M. Bolstad, F. Collin, L.M. Cope, B. Hobbs, and T.P. Speed. 2003. Summaries of Affymetrix GeneChip probe level data. *Nucleic Acids Res* **31**: e15.

Jiang, J.C., E. Jaruga, M.V. Repnevskaya, and S.M. Jazwinski. 2000. An intervention resembling caloric restriction prolongs life span and retards aging in yeast. *Faseb J* **14**: 2135-7.

Kaeberlein, M., D. Hu, E.O. Kerr, M. Tsuchiya, E.A. Westman, N. Dang, S. Fields, and B.K. Kennedy. 2005. Increased life span due to calorie restriction in respiratory-deficient yeast. *PLoS Genet* **1**: e69.

Kalaany, N.Y. and D.M. Sabatini. 2009. Tumours with PI3K activation are resistant to dietary restriction. *Nature* **458**: 725-31.

Kelly, K.J. 2003. Distant effects of experimental renal ischemia/reperfusion injury. *J Am Soc Nephrol* **14**: 1549-58.

Kher, A., K.K. Meldrum, M. Wang, B.M. Tsai, J.M. Pitcher, and D.R. Meldrum. 2005. Cellular and molecular mechanisms of sex differences in renal ischemia-reperfusion injury. *Cardiovasc Res* **67**: 594-603.

Kim, S.B., S. Yang, S.K. Kim, S.C. Kim, H.G. Woo, D.J. Volsky, S.Y. Kim, and I.S. Chu. 2007. GAzer: gene set analyzer. *Bioinformatics* **23**: 1697-9.

Klass, M.R. 1977. Aging in the nematode Caenorhabditis elegans: major biological and environmental factors influencing life span. *Mech Ageing Dev* **6**: 413-29.

Leemans, J.C., G. Stokman, N. Claessen, K.M. Rouschop, G.J. Teske, C.J. Kirschning, S. Akira, T. van der Poll, J.J. Weening, and S. Florquin. 2005. Renal-associated TLR2 mediates ischemia/reperfusion injury in the kidney. *J Clin Invest* **115**: 2894-903.

Lin, S.J., P.A. Defossez, and L. Guarente. 2000. Requirement of NAD and SIR2 for life-span extension by calorie restriction in Saccharomyces cerevisiae. *Science* **289**: 2126-8.

Mair, W., P. Goymer, S.D. Pletcher, and L. Partridge. 2003. Demography of dietary restriction and death in Drosophila. *Science* **301**: 1731-3.

Maltby, J.R. 2006. Fasting from midnight--the history behind the dogma. *Best Pract Res Clin Anaesthesiol* **20**: 363-78.

Masoro, E.J. 2003. Subfield history: caloric restriction, slowing aging, and extending life. *Sci Aging Knowledge Environ* **2003**: RE2.

-. 2004. **Caloric intake versus temporal pattern of food intake.** *Aging Clin Exp Res* **16: 423-4.**

Masoro, E.J., I. Shimokawa, Y. Higami, C.A. McMahan, and B.P. Yu. 1995. Temporal pattern of food intake not a factor in the retardation of aging processes by dietary restriction. *J Gerontol A Biol Sci Med Sci* **50A**: B48-53.

A II

Mattson, M.P. 2005. The need for controlled studies of the effects of meal frequency on health. *Lancet* **365**: 1978-80.

McCay, C.M., M.F. Crowel, and L.A. Maynard. 1935. The effect of retarded growth upon the length of the life span and upon the ultimate body size. *J Nutr* **10**: 63-79.

Merry, B.J. 2002. Molecular mechanisms linking calorie restriction and longevity. *Int J Biochem Cell Biol* **34**: 1340-54.

Miller, S.B., D.R. Martin, J. Kissane, and M.R. Hammerman. 1992. Insulin-like growth factor I accelerates recovery from ischemic acute tubular necrosis in the rat. *Proc Natl Acad Sci U S A* **89**: 11876-80.

Murray, C.E., R.B. Jennings, and K.A. Reimer. 1986. Preconditioning with ischemia: a delay of lethal cell injury in ischemic myocardium. *Circulation* **74**: 1124-1136.

Nishihara, V., R. Sumimoto, Y. Fukuda, J.H. Southard, T. Asahara, and K. Dohi. 1997. Inhibition of warm ischemic injury to rat liver, pancreas, and heart grafts by controlling the nutritional status of both donor and recipient. *Surg Today* **27**: 645-50.

Partridge, L., A. Green, and K. Fowler. 1987. Effects of egg-production and of exposure to males on female survival in Drosophila melanogaster. *Journal of Insect Physiology* **33**: 745-749.

Pfaffl, M.W. 2001. A new mathematical model for relative quantification in real-time RT-PCR. *Nucleic Acids Res* **29**: e45.

Raffaghello, L., C. Lee, F.M. Safdie, M. Wei, F. Madia, G. Bianchi, and V.D. Longo. 2008. Starvation-dependent differential stress resistance protects normal but not cancer cells against high-dose chemotherapy. *Proc Natl Acad Sci U S A* **105**: 8215-20.

Richardson, A., F. Liu, M.L. Adamo, H. Van Remmen, and J.F. Nelson. 2004. The role of insulin and insulin-like growth factor-I in mammalian ageing. *Best Pract Res Clin Endocrinol Metab* **18**: 393-406.

Sinclair, D.A. 2005. Toward a unified theory of caloric restriction and longevity regulation. *Mech Ageing Dev* **126**: 987-1002.

Smyth, G.K. 2004. Linear models and empirical bayes methods for assessing differential expression in microarray experiments. *Stat Appl Genet Mol Biol* **3**: Article3.

Sogawa, H. and C. Kubo. 2000. Influence of short-term repeated fasting on the longevity of female (NZB x NZW)F1 mice. *Mech Ageing Dev* **115**: 61-71.

Soreide, E., L.I. Eriksson, G. Hirlekar, H. Eriksson, S.W. Henneberg, R. Sandin, and J. Raeder. 2005. Pre-operative fasting guidelines: an update. *Acta Anaesthesiol Scand* **49**: 1041-7.

Stuart, J.A., B. Karahalil, B.A. Hogue, N.C. Souza-Pinto, and V.A. Bohr. 2004. Mitochondrial and nuclear DNA base excision repair are affected differently by caloric restriction. *Faseb J* **18**: 595-7.

Studley, H.O. 1936. Percentage of weight loss: a basic indicator of surgical risk in patients with chronic peptic ulcer. *JAMA* **106**: 458-60.

Suleiman, M.S., R.J. Singh, and C.E. Stewart. 2007. Apoptosis and the cardiac action of insulin-like growth factor I. *Pharmacol Ther* **114**: 278-94.

Sumimoto, R., J.H. Southard, and F.O. Belzer. 1993. Livers from fasted rats acquire resistance to warm and cold ischemia injury. *Transplantation* **55**: 728-32.

Sun, D., A.R. Muthukumar, R.A. Lawrence, and G. Fernandes. 2001. Effects of calorie restriction on polymicrobial peritonitis induced by cecum ligation and puncture in young C57BL/6 mice. *Clin Diagn Lab Immunol* **8**: 1003-11.

Swindell, W.R. 2008. Comparative analysis of microarray data identifies common responses to caloric restriction among mouse tissues. *Mech Ageing Dev* **129**: 138-53.

Takeda, R., H. Nishimatsu, E. Suzuki, H. Satonaka, D. Nagata, S. Oba, M. Sata, M. Takahashi, Y. Yamamoto, Y. Terauchi, T. Kadowaki, K. Kangawa, T. Kitamura, R. Nagai, and Y. Hirata. 2006. Ghrelin improves renal function in mice with ischemic acute renal failure. *J Am Soc Nephrol* **17**: 113-21.

Tatar, M., A. Bartke, and A. Antebi. 2003. The endocrine regulation of aging by insulin-like signals. *Science* **299**: 1346-51.

Varady, K.A. and M.K. Hellerstein. 2007. Alternate-day fasting and chronic disease prevention: a review of human and animal trials. *Am J Clin Nutr* **86**: 7-13.

Weindruch, R., R.L. Walford, S. Fligiel, and D. Guthrie. 1986. The retardation of ageing in mice by dietary restriction: longevity, cancer, immunity and lifetime energy intake. *Journal of Nutrition* **116**: 641–654.

Weiss, E.P., S.B. Racette, D.T. Villareal, L. Fontana, K. Steger-May, K.B. Schechtman, S. Klein, and J.O. Holloszy. 2006. Improvements in glucose tolerance and insulin action induced by increasing energy expenditure or decreasing energy intake: a randomized controlled trial. *Am J Clin Nutr* **84**: 1033-42.

Yu, Z.F. and M.P. Mattson. 1999. Dietary restriction and 2-deoxyglucose administration reduce focal ischemic brain damage and improve behavioral outcome: evidence for a preconditioning mechanism. *J Neurosci Res* **57**: 830-9.

A II

&

SUMMARY

The daily rotation of the Earth about its own axis and annually around the sun exposes life to profound variation in environmental conditions. This variation results in predictable changes of light, temperature and consequently food availability and predation. Most organisms have evolved a circadian (from *circa dies*, Latin for 'about a day') time keeping mechanism which generates, co-ordinates and synchronizes internal processes with the local time. This circadian clock maintains approximately 24 hour rhythms in behavior, physiology and metabolism, even in the absence of timing cues. In mammals the locus of the circadian clock is the suprachiasmatic nucleus (SCN) which is located in the anterior hypothalamus and receives its timing cue, light, directly from intrinsically photoreceptive retinal ganglion cells of the eye. The SCN is composed of two hemispheres each containing ~10,000 coupled neurons, most of which contribute a ~24 hour rhythm in electrical discharge and neuropeptide secretion which is responsible for communicating the external time cue to other brain regions and peripheral organs. This ~24 hour rhythm in output is generated by a self sustained intracellular oscillator consisting of a transcription-translation feedback loop of a set of core clock genes which produces daily rhythms in individual SCN neurons and virtually all cells. Animals in which the SCN has been surgically ablated, or core clock genes genetically disrupted, immediately alter or lose behavioral and endocrine rhythms underscoring the importance of the SCN and molecular clock. Although most neurons of the SCN are intrinsically rhythmic, differences in retinal innervation, neuropeptide content and molecular clock phasing of neurons between different regions reveal a tissue of striking diversity and heterogeneity. Unique roles have been ascribed to different regions based on the aforementioned characteristics, where the ventral (SCNv) functions in light reception, the dorsal (SCNd) in rhythm maintenance and the central (SCNce) in gating the communication of light signals from SCNv to SCNd. Daylength (photoperiod) is believed to be the principle cue for driving seasonal adaptations in organisms. A role in photoperiod encoding has been posited for rostral and caudal SCN regions (R-SCN; C-SCN), in which these subregions appear to house morning (*M*) and evening (*E*) daily oscillators, independently phased to dawn to dusk.

Although there is a body of evidence supporting the unique functions localized within these SCN subregions, there is a lack of global, top-down understanding how these functions are performed at the molecular level. To this end we developed an approach to interrogate the transcriptome of these SCN subregions, presented in **Chapter 2**. We combined laser catapult microdissection with an efficient, single cycle amplification protocol to generate sufficient quantities of transcripts for microarray analysis. The success of our approach is demonstrated in the recapitulation of known regional markers, ie. *Avp*, *Vip* and *Grp*. 481 unique transcripts show subregion enriched expression between ventral, dorsal and central SCN. These transcripts were assessed for over-representation of their respective biological functions, i.e. gene ontology. We identified novel overrepresented terms enriching understanding of these regions as well as terms which support their putative functions and thus further strengthen confidence in the veracity, sensitivity and power of our approach. Furthermore, the novel candidate species we identified represent a resource for characterizing regionally enriched markers and which allow further insight into the mechanisms underlying the function of these subregions.

The model describing the dependence of a seasonal timer on circadian *M* and *E* oscillators for encoding photoperiod preceded characterization of both the molecular clock and the SCN, both requisite for maintaining daily rhythms. However this model has been vindicated in several model organisms and finds support in rodents from the observation of differential responses by R-SCN and C-SCN in electrophysiology and core-clock phasing under different photoperiods. The R-SCN and C-SCN thus represent candidate *E* and *M* components respectively. We applied the method described in Chapter 2 to explore global transcription levels of R-SCN and C-SCN in mice entrained under short (6 hours light/day), equinoxal (12 hours light/day) and long (18 hours light/day) photoperiods as presented in **Chapter 3**. High density sampling of R-SCN and C-SCN over a complete circadian combined with flexible, robust bioinformatics allowed us to identify photoperiodically regulated, rhythmic transcripts. Our results support previous studies on the response of core-clock gene expression in mice to different photoperiods and we reveal photoperiodic regulation of the entire rhythmic genome identified in rostral and caudal SCN. Strikingly, the temporal profile of rhythmic transcripts overall show photoperiodic regulation in both subregions and to a greater extent in R-SCN. We also find the peak expression of rhythmic transcripts clusters around dawn or dusk, with several transcripts specifically tracking dawn or dusk across all photoperiods. These transcripts represent novel, photoperiodically regulated transcripts and warrant further characterization for their role in encoding or driving seasonal adaptation. Finally, we identified photoperiodic regulation of rhythmic transcripts previously associated with seasonal affective disorder (SAD) highlighting the need for further investigation of these genes in SAD and other cognitive pathologies with circadian and/or seasonal etiology.

Besides applying the approach described in Chapter 2 to deepen understanding of the of R-SCN and C-SCNM in photoperiod encoding we also used these methods for several related applications. We present preliminary results of our examination of the transcriptional response by the ventral, dorsal and central SCN subregions during re-entrainment to a phase-advance light stimulus delivered at CT22. These results, a list of transcripts induced in each of these subregions four hours after a light pulse, is available online (http://bioinf-quad07.erasmusmc.nl/scn/). Notably, we find an abundance of transcripts known for their function in modulating glutamatergic synapse efficacy. This suggests that a modulation of synaptic strength occurs in the SCN during re-entrainment. **Appendix I** shows the use of precise LCM capture of the SCN to verify the expression of a rat kangaroo photolyase transgene in the SCN of transgenic mice. With this confirmation, we support the possibility of the novel circadian phenotype observed in these animals arising from the expression of the cryptochrome-like photolyase transgene in the SCN. In **Appendix II**, we use similar statistical methods as those in Chapters 2 and 3 to identify over-represented biological themes amongst differentially expressed genes from fasted and dietary restricted mice. Critically, this analysis revealed strikingly similar biological responses in both short-term fasted and long term caloric restricted mice. Moreover these data show strong similarity with a core set of genes believed to be consistently differentially regulated across many transcriptome studies in diverse tissue types obtained from caloric restricted animals.

SAMENVATTING

De rotatie van de aarde om haar eigen as in één dag en jaarlijks om de zon stelt het leven bloot aan een grote variatie in omgevingsfactoren. Onder deze variatie vallen voorspelbare veranderingen in zonlicht, temperatuur en als gevolg hiervan de beschikbaarheid van voedsel en de mogelijkheid tot jagen. De meeste organismen hebben een circadiaan (van *circa dies*, Latijn voor 'ongeveer een dag') mechanisme voor het bijhouden van tijd geëvolueerd, dat interne processen genereert en synchroniseert met de actuele tijd. Deze circadiane klok zorgt voor een ongeveer 24 uur durend ritme in gedrag, fysiologie en metabolisme, zelfs in afwezigheid van indicaties van tijd. In zoogdieren bevindt de kern van de circadiane klok zich in de suprachiamatische nucleus (SCN). Deze is gelokaliseerd in de anteriële hypothalamus en krijgt tijdsindicaties van buiten het organisme door iddel van signalen die door retinale ganglia cellen van het oog worden doorgegeven nadat licht op deze lichtgevoelige cellen is gevallen. De SCN bestaat uit twee hemisferen die ieder uit ongeveer 10.000 met elkaar verbonden neuronen bestaan. De meeste van deze neuronen dragen bij aan een elektrische ontlading en vrijzetting van neuropeptiden in een 24 uur ritme, dat ervoor zorgt dat de externe tijdsindicaties worden doorgegeven naar andere gebieden van de hersenen en de perifere organen. Deze ritmische output wordt gegenereerd door een zich zelf instaand houdende intracellulaire oscillator die bestaat uit een terugkoppeling tussen transcriptie en translatie van een set kern-klok genen dat dagelijkse ritmes produceert in individuele SCN neuronen en vrijwel alle andere cellen van het lichaam. Dieren waarbij de SCN chirurgisch is verwijderd of waarvan kern-klok genen genetisch veranderd of verwijderd zijn, verliezen onmiddellijk hun ritmiek in gedrag, fysiologie en metabolisme, wat het belang onderstreept van de SCN en de moleculaire klok. Hoewel de meeste neuronen van de SCN intrinsiek ritmisch zijn, is de SCN opvallend divers en heterogeen, wat blijkt uit verschillen tussen neuronen wat betreft de innervatie van neuronen verbonden met de retina, het voorkomen van verschillende neuropeptiden en de fasering van de moleculaire klok in deze neuronen. Op basis van bovengenoemde kenmerken zijn er unieke rollen aan de verschillende regio's in de SCN toe te schrijven, zoals de functie van lichtopname door de ventrale SCN (SCNv), het onderhouden van de ritmiek door de dorsale SCN (SCNd) en het gecontroleerd doorlaten van signalen tussen de SCNv en SCNd door de centrale SCN (SCNce). Men is van mening dat de lengte van de dag (fotoperiode) de belangrijkste indiatie is voor het sturen van seizoensgebonden aanpassingen in organismen. Een rol van de fotoperiode codering is geponeerd voor de rostrale en caudale delen van de SCN (R-SCN; C-SCN), waarbij in deze subregio's ochtend (O) en avond (A) oscillatoren lijken te bevatten, onafhankelijk gefaseerd tot zonsopgang en zonsondergang. Hoewel er een bulk van bewijs is ter ondersteuning van de unieke functies die zijn gelokaliseerd binnen deze SCN subregio's, is er een gebrek aan een globaal, volledig begrip hoe deze functies plaatsvinden op moleculair niveau.

Daartoe ontwikkelden wij een aanpak om het transcriptoom van deze SCN subregio's te achterhalen, gepresenteerd in **hoofdstuk 2**. We combineerden laser katapult microdissectie met een efficiënt, single-cyclus amplificatieprotocol om voldoende hoeveelheden

transcripten voor microarray-analyse te genereren. Het succes van onze aanpak blijkt uit het aantonen van reeds bekende regionale markers als, AVP, Vip en GRP. 481 uniek aanwezige transcripten laten een verrijking zien per subregio tussen de ventrale, dorsale en de centrale SCN. Deze transcripten werden vervolgens beoordeeld op oververtegenwoordiging van hun respectieve biologische functies. Wij hebben oververtegenwoordigde biologische functies gevonden die een verder begrip van deze subregio's bewerkstelligen alsmede biologische functies die overeenkomen met de vermeende functies van de verschillende subregio's zoals hierboven beschreven. Hiermee ondersteunen en versterken wij het vertrouwen in de juistheid, de gevoeligheid en de kracht van onze aanpak. De nieuwe kandidaatgenen die wij hebben geïdentificeerd vormen een bron voor het karakteriseren van markers die regionaal zijn verrijkt en die meer inzicht geven in het mechanisme achter de functie van deze subregio's. Het model dat de afhankelijkheid van een seizoensgebonden wekker op circadiane O en A oscillatoren voor het coderen van de fotoperiode beschrijft, ging vooraf aan de karakterisering van zowel de moleculaire klok en de SCN, die beide zijn vereist voor het behoud van dagelijkse ritmes. Ondanks dat is dit model gerechtvaardigd in verschillende modelorganismen zoals in knaagdieren waar men differentiële reacties van de R-SCN en C-SCN in elektrofysiologie en kern-clock fasering onder verschillende fotoperiodes heeft geobserveerd. De R-SCN en C-SCN vertegenwoordigen dus respectievelijk kandidaat O en A componenten. We hebben de methode beschreven in **hoofdstuk 2** toegepast om de globale transcriptieniveaus in de R-SCN en C-SCN van muizen die werden gehouden onder korte (6 uur licht per dag), equatoriale (12 uur licht per dag) en lange (18 uur licht per dag) fotoperiodes. Dit is gepresenteerd in **hoofdstuk 3**. Door middel van het nemen van veel monsters van de R-SCN en C-SCN gedurende een volledige circadiane periode te combineren met flexibele, robuuste bio-informatica konden wij ritmische transcripten identificeren die worden gestuurd door de fotoperiode. Onze resultaten ondersteunen eerdere studies over de reactie van klokgenexpressie in muizen op de verschillende fotoperiodes en wij laten de regulatie zien van het gehele ritmische genoom in de rostrale en caudale SCN door de fotoperiode. Opvallend is dat het tijdsprofiel van ritmische transcripten in het algemeen een regulatie door de fotoperiode laat zien in beide subregio's en in grotere mate in de R-SCN. Wij hebben ook gevonden dat de expressie van clusters van ritmische transcripten piekt rond zonsopgang of zonsondergang, met verschillende transcripten die specifiek zonsopgang of zonsondergang volgen over alle fotoperiodes. Deze clusters vertegenwoordigen nieuwe, door de fotoperiode gereguleerde transcripten en vraagt om een verdere karakterisering van hun rol in de regulatie van seizoensgebonden aanpassing. Ten slotte hebben wij door de fotoperiode gereguleerde ritmische transcripten, die eerder geassocieerd zijn met seizoensgebonden affectieve stoornis (SAD, winterdepressie), geïdentificeerd. Dit benadrukt de noodzaak van verder onderzoek van deze genen met betrekking tot SAD en andere cognitieve aandoeningen met een circadiane en / of seizoensgebonden etiologie. Naast het toepassen van de aanpak beschreven in **hoofdstuk 2** om het begrip van de R-SCN en C-SCN in het coderen van de fotoperiode te verbreden, hebben wij deze methoden ook gebruikt voor diverse gerelateerde toepassingen. Wij presenteren voorlopige resultaten van ons onderzoek naar de

transcriptionele responsie door de ventrale, dorsale en centrale SCN subregio's gedurende de aanpassing aan een fase-vervroegende lichtstimulus toegediend op het tijdstip CT22. Deze resultaten, zijnde een lijst van transcripten geïnduceerd in elk van deze subregio's vier uur na de lichtstimulus, is te vinden op het internet (http://bioinf-quad07.erasmusmc.nl/scn/). Vermeldenswaardig is het feit dat wij veel transcripten hebben gevonden waarvan bekend is dat de eiwitprodukten glutamaterge neurotransmisie moduleren. Dit suggereert dat een modulatie van synaptische sterkte optreedt in de SCN gedurende aanpassinge van het ritme door licht. **Bijlage I** toont het gebruik van nauwkeurige LCM micro dissectie van de SCN om de expressie van een rat-kangaroo transgen, fotolyase, te verifiëren in de SCN van transgene muizen. Met deze bevestigingondersteunen wij het nieuwe circadiane fenotype dat is waargenomen bij deze dieren als gevolg van de expressie van het fotolyase transgen in de SCN. In **Bijlage II** hebben wij soortgelijke statistische methoden als die in de hoofdstukken 2 en 3 zijn gebruikt om oververtegenwoordigde biologische functies te identificeren onder differentieel tot expressie komende genen in muizen die hadden gevast en toegang hadden tot beperkte voeding. Belangrijk is dat deze analyse opvallend veel gelijke biologische reacties in zowel de korte termijn als de lange termijn calorie-beperkte muizen liet zien. Bovendien tonen deze gegevens aan dat er een sterke gelijkenis is met een set van genen, waarvan verondersteld wordt dat zij consequent differentieel zijn gereguleerd zoals aangetoond is in vele transcriptoomstudies uitgevoerd in diverse soorten weefsel van calorie-beperkte dieren.

&

ACKNOWLEDGMENTS

To Bert and Jan, my scientific father's: you have successfully launched another scientist into the world. You have profoundly shaped my perception of our world and wo/mans place in it. What you've taught me will be expressed in every choice I make, every action I take, in this lab we call life. Always. Thank you.

Countless people contributed to this thesis. But several defined its trajectory and a few may claim responsibility for its existence. These people are Antonio Carvalho da Silva, Ed Jacobs, Erik Engelen, Eugin Destici, Filippo Tamanini, Frank Grosveld, Gosia Oklejewicz, George Garinis, Inês Chaves, Jay Mitchell, Justine Peeters, Karen Basoalto, Lars Vahlkamp, Peter van der Spek, Rolf Brand, Romana Nijman and Xavier Bonnefont.

Nicole Kohlmann: your sacrifice for this thesis can not be measured nor the dept fully repaid. *But I will try like hell.*

To those I did count below, thank you. To those countless I did not, thank you.

Agnes Boer	Ce15 murine mum
Agnes Hahn	TFBS analysis, parenting
Albert Kloosterman	mouse database untangler
Alex Maas	mouse travel agent
Alireza Ghamari	piano accompaniment to tenor
Ambra Giglia-Mari	xmas dinner, believer
Ana Janicijevic	Serbian network access, coffee, winks
André Eker	photon quantity and quality assay
Andreas Kremer	Germanic sentence structure empathy
Andrew Stubbs	Antwerp accommodation, iCock
Angelika Zotter	jamond, chocolate
Anieta Sieuwerts	qPCR fingerspitzengefühl
Annelieke de Wit	focusing concentration
Annemarie Verzijl	breeding with care as well
Arthur van der Kamp	salary & employee contract
Astrid Lalai	bread, coffee, shoe shopping
Audrey Gourdin	je ne sais quoi
Bas Hulsof	ribo-spia delivery yesterday
Benno Arentsen	three degrees for the visit of one
Bianca Hollander	breeding with care too
Bjorn Schumacher	safest driving speed: 200km/h
Bonnie van Wilgenburg	impassioned NMDA thesis

Branko Misovic	limma deep factorial design
Calinda Middelkoop	Ce15 murine aunt
Carol Quayle	genotyping in mezzo-soprano
Caspar Hoogenraad	neurons don't change shape
Catherine Robin	understands man::cryostat lovin
Celine Baldeyron	Vogue, Numéro, Reblochon, La Haine
Charlotte Soler-Andrieu	skype microphone, conference insight
Chris de Zeeuw	SCN review
Chris Dinant	flat screen TV poker master
Christina Lim	coffee, green tea, heat packs, chocolate ad lib.
Claudia	Gaspar
Crystal Kockx	hybridized my precious
Danielle Zondervan	Ce15, B-unit grand aunt
David Ferster	acotgrams from Belgium wheels
Dennis Meulder	Ce15 Papa
Densheng Xu	NP1/2/R Abs, genotyping and protocols
Dies Meijer	synaptic remodeling gene lists
Dimitris Rizopoulos	splines and knots in R
Dolf Segers	Apple, limma and RocknRolla
Dominic Kupier	ethical reflection
Don De Lange	iClock
Dorota Kurek	artists, exposés and second hand
Dubi Drabek	dramatic inspiration, Greece
Ed Landsberger	Ce Grandpapa
Edo Schraa	dissection lamps
Edwin Romme	Ce15 uncle, retailing USA immigrants
Elizabeth McClellan	apply(), M&M cookies
Esther Fijnman	Ce15 aunty
Farzin Pourfarzad	Jurriaanse grant
Fiona de Bruin	kind breeding
Frank van Fliet	course organization and mediation
Frans Meijers	ethical adherence
Gosia Jaremko	LCM proteomics
Hanspeter Herzel	TFBS analysis, Berlin hospitality
Henk Dronk	tolerated the black vinyl sauna
Hugh Piggins	believer of an extraordinary SCN
Ineke Maas	Ce15 niece

Inge Geerts	Ce15 cousin
Ingeborg van den Berg	one off breedings
Iris Janssen	pool mouse mum
Jan Gietema	Nugen logisticizer
Jan Voetan	running wheel mechanic
Jan-Olle Andresso	vodka, sauna, Tailin mob, natural selection
Jasperina Erades	mortar
Jean-Marc Neefs	Excel power
Jessica Brakshoofen	breeding with flair
Joey Riepsamme	mutha uckers
John Hogenesch	ANOVA not COSOPT/JTK_cycle
John van der Voort	navigating the welfare system
Joke Meijer	last piece in my puzzle
Jopie Bolman	LB bits
Joris Pothof	miRNA explanation of ageing
Karin Kwikkers	running wheel Madonna
Karine Bollerot	5:55
Kaye Ballantyne	Spot and Harry
Kim Grolle	breeding triples
Koos Smit	La Perla undies
Laura Gutierrez	you tube faux par forgiveness
Leo Scheek	PC bits and bytes
Leo van Kempen	all your reagents yesterday
Lieneke Uittenboogaard	order from chaos, phone
Maarten Bijl	bioinfoRmatic man
Magda Biernat	great taste in music, fashion and westerns
Marcel Boersma	Ce17 breeding brother
Marcel de Jeu	SCN synaptic plasticity
Marian Comas	Brains, pizza without rucola
Marike van Geest	glue
Mario Redeker	PC back end, solar panel role model
Marjolein van Riel	administrative chaos compensator
Marlot Pieper	breeding with care
Martha Merrow	lines show connectedness
Martijn Dekkers	Sint
Mathieu Sommers	ethical oversight
Mathijs Jonker	significance of overlap

&

Melle van der Kamp	logistics queen
Michael Hughes	COSOPT, JTK_cycle
Michael Moorhouse	vennology, beavers by roots
Michael	A bit to the left
Michiel Swank	para-formaldehyde under dim red light, errands
Mieke Blijenberg	Reimbursal, coffee
Mirjam van Vroonhoven	Unix
Mohamed Ibrahim	Ch. 1 and 2 Fig. 1 Laser!
Monika Bajek	promovendi role model
Myriam Pleijser	breeding carefully
Niels Galjart	GFAP Abs, protocol, reflections
Nils Wijgers	-80 superintendant
Nuran Tuzen	crèche benefits, desk with a window
Patricia	murine Dutch hospitality
Patrick Molenbeek	breeding stable overseer
Paul Murrell	decomplicating R graphics
Paul Worley	NP, Homer1a, mutants, Abs and discourse
Peter Riegman	tissue arrayer, PALM mikroscope
Petros Papadopoulos	donuts
Pierre-Oliver Mari	iPod
Pim Drinkenberg	running wheels, dual proc. PC
Pim Schalkwijk	genotyping in baritone
Pim Visser	old PCs, new support, fever insight
Raoul Tan	royal company
Raymond Poot	apartment hunting translation
Renata Brandt	miscellaneous mice
Renee Menzes	time as a factor
Rini de Crom	shear stress model
Rob Willemsen	cryostat superintendent and zebra fish
Roel Janssens	Tax translation
Roelof Hut	light pulse box, CircWave, photoperiod analyses
Ron de Bruin	fasting, calorie and dietary restriction
Sahar Bassal	Beerse agent
Sander Barnhoorn	movie night
Sander Botter	R array QC script
Serge Daan	photoperiod experimental design
Sigrid Swagemakers	bioinformatic beachhead, PDF homologue

&

Sjaak Philipsen	pantomime banter, thesis guidance
Sjozef van Baal	64bit, custom searches, slugs, TB drives
Stefanie Vester	mouse database entry and enlightenment
Steven Bergink	vodka, HR23a
Surya Reis	bench top collaboration
Suzette de Groot	re-deriving the PHD
Sytske Brinksma	Ce17 special breeding
Theo Stijnan	Friedman test
Thomas Girke	'The' R bioinformatics referance
Tiago Brazao	Leuven pub stats
Till Roenneberg	glutamate mediates photic input
Ton Verkerk	new windows & linux PCs
Wendy Toussaint	DS
Wilfred Ijcken	chip summary
Yara Hofman	breeding as well
Ype Elgersma	CaMKinase
Yuri Mochine	unstack(), covMcd(), cov.mve()
Yvonne Rijksen	IHC, perfusion and breeding

&

PUBLICATIONS

Peer Reviewed

Mitchell J.R., Verweij M., **Brand K.**, van de Ven M., Goemaere N., van den Engel S., Chu T., Forrer F., Müller C., de Jong M., van Ijcken W, Ijzermans J.N., Hoeijmakers J.H., de Bruin R.W. Short-term dietary restriction and fasting precondition against ischemia reperfusion injury in mice. *Aging Cell*. 2010 Feb;9(1):40-53.

Garinis G.A., Mitchell J.R., Moorhouse M.J., Hanada K., de Waard H., Vandeputte D., Jans J., **Brand K.**, Smid M., van der Spek P.J., Hoeijmakers J.H., Kanaar R., van der Horst G.T.. Transcriptome analysis reveals cyclobutane pyrimidine dimers as a major source of UV-induced DNA breaks. *EMBO J.* 2005 Nov 16;24(22):3952-62.

Bassal S., Nomura N., Venter D., **Brand K.**, McKay M.J., van der Spek P.J. Characterization of a novel human cell-cycle-regulated homologue of Drosophila dlg1. *Genomics* Sep;77(1-2):5-7, 2001.

Book Chapters

Sambrook, J. and Bowtell, D. (editors). Section 8: Tissue Microarrays. **Brand K.**, Hostetter G., Kallioniemi O.P., Kononen J., Sauter G., Trivett M. In *DNA Microarrays: A molecular Cloning Manual*. Cold Spring Harbor Laboratory Press. Section 7. 2003.

Conferences & Symposia

Oral communication
4th EUCLOCK Annual Meeting, Frauenchiemsee, Germany 2010
4th Center for Timing Research meeting, Rotterdam, Holland, 2009
2nd EUCLOCK Annual Meeting, Frauenchiemsee, Germany 2008
14th MGC PhD Student Workshop, Maastricht, Holland, 2007

Poster communication
XI. Congress of the European Biological Rhythms Society, Strasbourg, France, 2009
3rd EUCLOCK Annual Meeting, Frauenchiemsee, Germany 2009
10th Meeting Society for Research on Biological rhythms, Sandestin, USA, 2006
13th MGC PhD Student Workshop, Oxford, UK, 2006
11th MGC PhD Student Workshop, Leuven, Belgium, 2004

Abstracts
10th MGC PhD Student Workshop, Lille, France, 2004

CURRICULUM VITAE

Name:	Karl Brand
Birth date:	26th December, 1973
Birth place:	Hanover ON, Canada

2002 – 2011   Ph.D. Student, Dept. of Cell Biology and Genetics, Erasmus MC
Thesis: "Transcripts from the Circadian Clock: Telling Time and Season"
Promotors: Prof. Dr. Jan H.J. Hoeijmakers & Prof. Dr. Gijsbertus T.G.
van der Horst

2001 – 2002   Research Associate, Eos Biotechnology, Sth San Francisco, USA

2000 – 2001   Research Assistant, PMCI, Melbourne, Australia

1999 – 2000   Research Assistant, The Peter MacCallum Cancer Institute (PMCI) &
Eos Biotechnology Inc. Melbourne, Australia

1998 – 1999   Sales Team Coordinator, GKR Karate International, Melbourne, Australia

1997 – 1998   Technician, Faculty of Biomedical and Health Science, RMIT,
Melbourne, Australia

1996 – 1997   Honours student, B. Sci. (Honours), Dept of Pediatrics,
University of Melbourne, Australia

1992 – 1995   Undergraduate, B. App. Sci., Applied Biology and Biotechnology
Royal Melbourne Institute of Technology (RMIT), Melbourne, Australia

&

"I don't know enough to be incompetent" Woody Allen, Shadows and Fog 1991